First International Workshop on Sediment Bypass Tunnels

Conference Proceedings

Author(s):
Sumi, Tetsuya; Morris, G.; Kantoush, S.; Fernandes, J.; Auel, Christian; Albayrak, Ismail (iD); De Cesare, Giovanni; Manso, P.; Oertli, C.; Facchini, M.; Felix, D.; Hagmann, M.; Lutz, N.; Boes, Robert (iD)

April 27-29
ETH Zurich
2015

International Workshop on
Sediment Bypass Tunnels

First International Workshop on Sediment Bypass Tunnels

Organizer

ETH *zürich*

Laboratory of Hydraulics, Hydrology and Glaciology, ETH Zurich

In collaboration with:

ewz
Die Energie

Electric Power Company of Zurich

Water Resources Research Center, Disaster Prevention Research Institute, Kyoto University

Copyright

Proposed citation:

Author, M. (2015). Title of the contribution. *Proc. First International Workshop on Sediment Bypass Tunnels*, VAW-Mitteilungen 232 (R. M. Boes ed.), Laboratory of Hydraulics, Hydrology and Glaciology (VAW), ETH Zurich, Switzerland.

Member of the scientific committee

Prof. Dr. R.M. Boes	Laboratory of Hydraulics, Hydrology and Glaciology, ETH Zurich
Prof. Dr. T. Sumi	Water Resources Research Center, Disaster Prevention Research Institute, Kyoto University
Dr. G. Morris	GLM Engineering Coop, Puerto Rico
Assoc. Prof. Dr. S. Kantoush	Water Resources Research Center, Disaster Prevention Research Institute, Kyoto University
Dr. C. Auel	Water Resources Research Center, Disaster Prevention Research Institute, Kyoto University
Dr. I. Albayrak	Laboratory of Hydraulics, Hydrology and Glaciology, ETH Zurich
Dr. J. Fernandes	Laboratory of Hydraulics, Hydrology and Glaciology, ETH Zurich
Dr. G. De Cesare	Laboratoire de constructions hydrauliques, Ecole polytechnique fédérale de Lausanne
Dr. P. Manso	Laboratoire de constructions hydrauliques, Ecole polytechnique fédérale de Lausanne
C. Oertli	Electric Power Company of Zurich (ewz)
M. Facchini	Laboratory of Hydraulics, Hydrology and Glaciology, ETH Zurich
D. Felix	Laboratory of Hydraulics, Hydrology and Glaciology, ETH Zurich
M. Hagmann	Laboratory of Hydraulics, Hydrology and Glaciology, ETH Zurich
N. Lutz	Laboratory of Hydraulics, Hydrology and Glaciology, ETH Zurich

Member of the organization committee

Prof. Dr. R.M. Boes — Laboratory of Hydraulics, Hydrology and Glaciology, ETH Zurich

Prof. Dr. T. Sumi — Water Resources Research Center, Disaster Prevention Research Institute, Kyoto University

Dr. C. Auel — Water Resources Research Center, Disaster Prevention Research Institute, Kyoto University

C. Oertli — Electric Power Company of Zurich (ewz)

Dr. I. Albayrak — Laboratory of Hydraulics, Hydrology and Glaciology, ETH Zurich

M. Hagmann — Laboratory of Hydraulics, Hydrology and Glaciology, ETH Zurich

Editor

Preface

Sediment Bypass Tunnels (SBTs) are hydraulic structures that gain in importance as a measure to counter reservoir sedimentation in view of the growing problem of rapid filling of worldwide storage basins and reservoirs with sediments. An SBT is an effective means to pass sediments around a dam to the tailwater reach, thereby reducing sediment aggradation in the reservoir on the one hand, and allowing for re-establishing sediment continuity on the other. The latter is more and more aimed at from an ecological point of view, since river bed erosion downstream of the dam may be stopped or at least significantly decelerated, along with an increase of the morphological variability. Only sediments provided from the upstream river reach are conveyed through an SBT, but no removal of already accumulated sediments in the reservoir occurs. The sediment concentration in the tailwater of the dam is therefore not affected by the reservoir itself and of natural character.

Despite these pros, the number of realized SBTs in the world is limited primarily due to high investment and maintenance cost. The latter is often caused by pronounced invert abrasion as a result of significant sediment transport at high velocities, putting the sustainable operation of these tunnels at risk. Major SBTs in operation are located e.g. both in Switzerland and Japan, and a number of projects have also been realized recently or are at the planning stage in France, South America and Taiwan, amongst others. China with its pronounced hydropower construction activities and high sediment loads is likely to feature a number of SBTs, but the situation is hardly known to the editor as there seems to be no English literature available so far.

Because general design guidelines on how to optimize a SBT to minimize maintenance cost were missing until recently, research was started at VAW some years ago to gain knowledge on the hydraulic processes and the hydroabrasion phenomena in SBTs as well as on the morphological consequences in the downstream river stretches. From these projects arose the idea to exchange the knowledge and the experience on SBT design and operation gained internationally, both from academia and engineering practice, in the frame of an international workshop. This communication booklet summarizes the topics presented and discussed at this workshop held at the Laboratory of Hydraulics, Hydrology and Glaciology of ETH Zurich from April 27 to 28, 2015. The workshop was organized in cooperation with the Disaster Prevention Research Institute of Kyoto University, Japan, and ewz, the electric utility of the city of Zurich, both of which are gratefully acknowledged here.

My sincere thanks also go to the Swiss Federal Office for the Environment (FOEN), the Swiss Association for Water Resources Management (SWV), the Swiss hydroelectric utilities ewz, KWO and OFIMA, the Swiss Federal Railways (SBB), the engineering consultant company Lombardi SA, and the industrial wear protection company Kalenborn, who financially or logistically supported this workshop including a 1.5-day post-workshop field trip to three Swiss SBTs from April 28 to 29, 2015.

Zurich, April 2015   Prof. Dr. Robert M. Boes

Supported by:

Federal Office for the Environment FOEN

KWO
GRIMSELSTROM

Schweizerischer Wasserwirtschaftsverband
Association suisse pour l'aménagement des eaux
Associazione svizzera di economia delle acque

Lombardi

Kalenborn
Wear Protection Solutions

Ofima

SBB CFF FFS

VI

Content

Comprehensive reservoir sedimentation countermeasures in Japan

Tetsuya Sumi

Abstract

Currently, the reservoir sedimentation management strategy in Japan is changing drastically from just receiving and depositing to releasing and supplying to downstream river channels. In contrast to the emergent and local conventional countermeasures such as dredging and excavation, sediment bypassing and sediment flushing measures which aim at radically reducing the sediment inflowing and deposition are implemented. Unazuki and Dashidaira dams in the Kurobe River, Miwa, Koshibu and Matsukawa dams in the Tenryu River and Asahi dam in the Shingu River are well known as advanced examples. Regarding after conventional excavation, sediment replenishment (augmentation) has been conducted for river restoration below dams in many cases. This paper introduces these present state of the art methodologies of reservoir sedimentation in Japan. Additionally, latest study on sediment bypass system such as how to select this technique among several other options and how to optimize its design.

1   Introduction

Reservoir sedimentation is one of the most crucial issue for reservoir sustainability in the world. Current gross storage capacity in the world is 6,000 km^3 with 45,000 large dams and total storage loss and annual sedimentation rate are about 570km^3 (12%) and 31km^3-year (0.52%-year) respectively. If additional new development projects are not considered, total capacity will be decreased even to less than half by 2100. In many countries, various countermeasures have been implemented to decrease sediment accumulation and loss of storage capacity. They are (i) reduce sediment inflow by erosion control and upstream sediment trapping, (ii) route sediments by sediment bypass, off stream reservoirs, sediment sluicing (drawdown routing) and venting of turbid density currents, and (iii) sediment removal by mechanical dry excavation, dredging, drawdown/pressure flushing and HSRS (Hydro-suction Sediment Removal System). These are summarized in Figure1 (Kondolf et al. (2014)). Current reservoir sedimentation management measures in Japan are also illustrated in Figure 2.
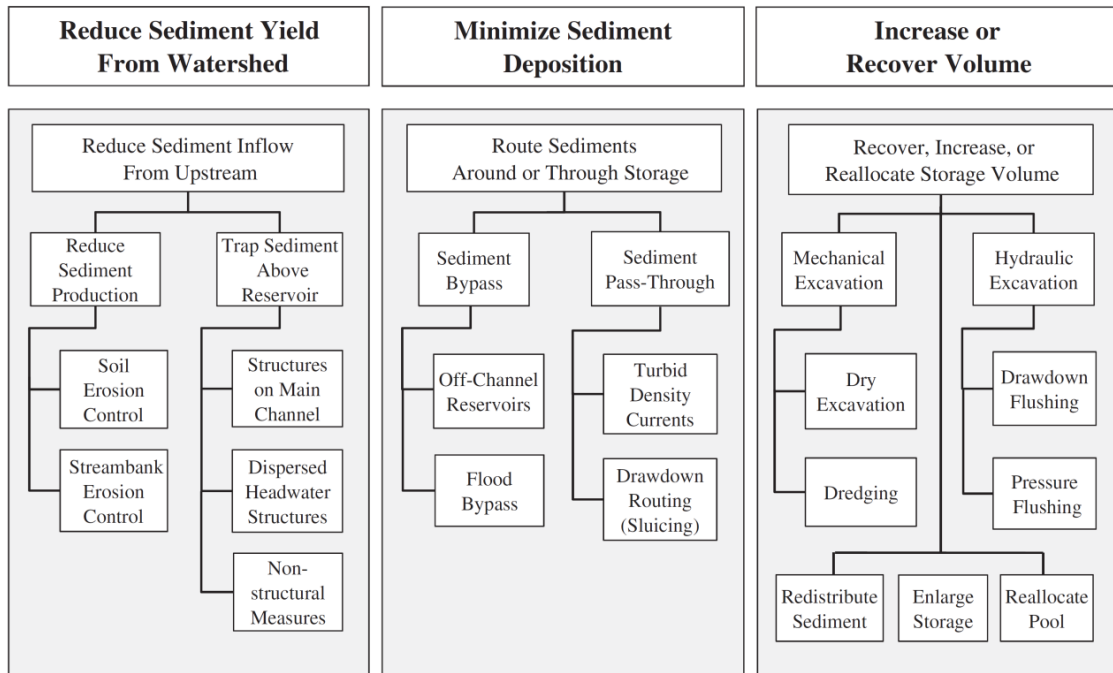
Figure 1: Classification of strategies for sediment management from the perspective of sustaining reservoir capacity (Kondolf et al. 2014)
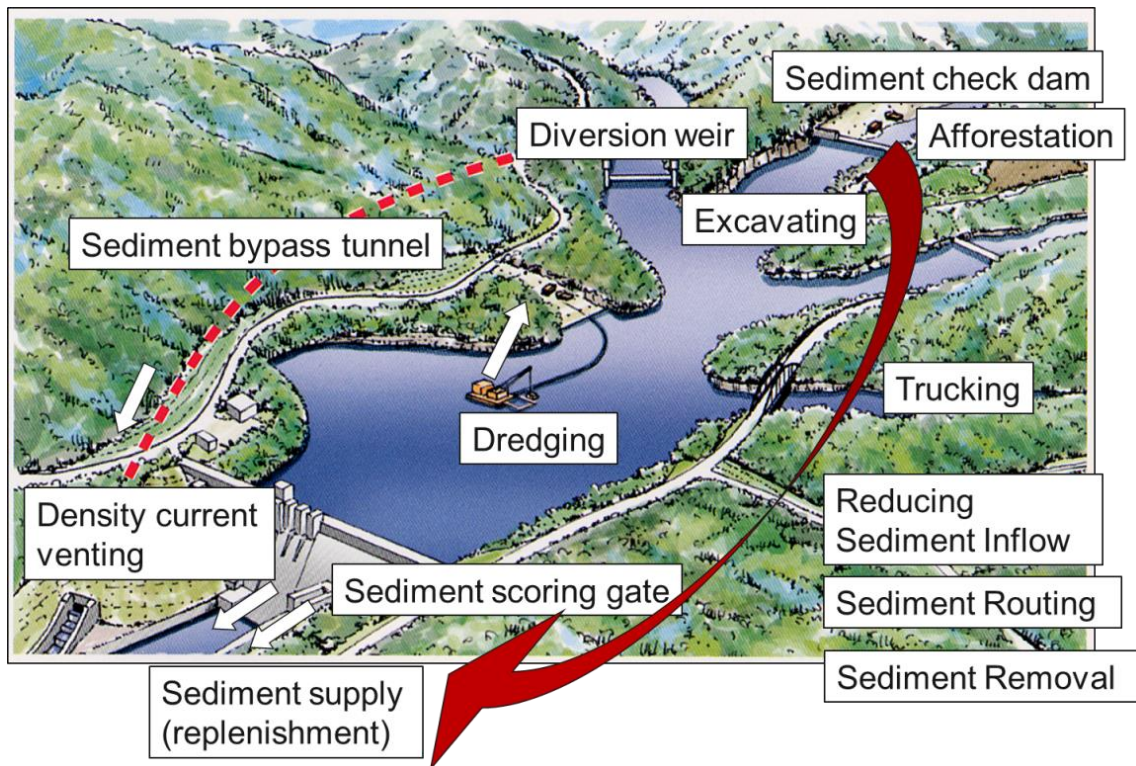

Figure 2: Reservoir sediment management measures in Japan

Among these methodologies, sediment bypassing and flushing are considered to be as permanent remedial measures. Worldwide, limited numbers of sediment bypass tunnels

have been constructed because of topographical, hydrological or economic conditions. Bypass tunnels, however, have many advantages such that they can be constructed even at existing dams and prevents a loss of stored reservoir water caused by the lowering of the reservoir water level. They are also considered to have a relatively small impact on the environment downstream because inflow discharge can be passed through tunnels naturally during flood time.

In this paper, current overview of reservoir sedimentation management in Japan is presented. Additionally, design criteria and future challenges as well as a case study on sediment bypass will be discussed.

2   Present state of reservoir sedimentation in Japan

2.1   Reservoir storage loss

As of 2013, from 971 dams accounting for approximately 1/3 of 3,000 dams over 15 meters in height, annual changes in sedimentation volume and the shape of accumulated sediment were reported. It is probably only Japan that established such a nationwide survey system, and such accumulated data is regarded as considerably valuable records on a global basis. Figure 3 shows reservoir storage losses by sedimentation depend on regions and categories based on purposes.

2.2   Comprehensive sediment management in the sediment routing system

Nowadays, new concept of sediment management is discussed in Japan. River fluvial system is composed of 6 segments which are headwater, mountain, valley, alluvial fun, flood plane and delta. The amount of sediment supplied from rivers to coasts was radically reduced with construction of many check dams and storage reservoirs in mountain areas and acceleration of the aggregate excavation from riverbed after World War II in Japan. As a result, various problems rose up including riverbed degradation at downstream channel, fixing of river channel and beach erosion as well as severe environmental changes in river and coastal areas. Environmental changes are largely depending on armoring of river bed and lack of sediment transport. These are causing too much vegetation growth in the river channel and losing suitable habitats for native spices.

Following a recommendation by the River Council of Japan in 1997, comprehensive sediment management in order to recover a sound sediment transport regarding not only quantity but also quality point of view in 'the Sediment Routing System' has been proposed as shown in Figure 4. The Sediment Routing System is including 6 segments plus coastal segment where sediment has been transported from mountains to the coast. For storage dams, sediment supply to the downstream river is strongly requested in order to reduce storage loss for reservoir sustainability and mitigate adverse environmental impacts as much as possible for river restoration. In that regards, both flow and sediment management should be considered at the same time. A new concept of river restoration

by flow and sediment management considering relationship between geomorphic and habitat measures is proposed as shown in Figure 5.
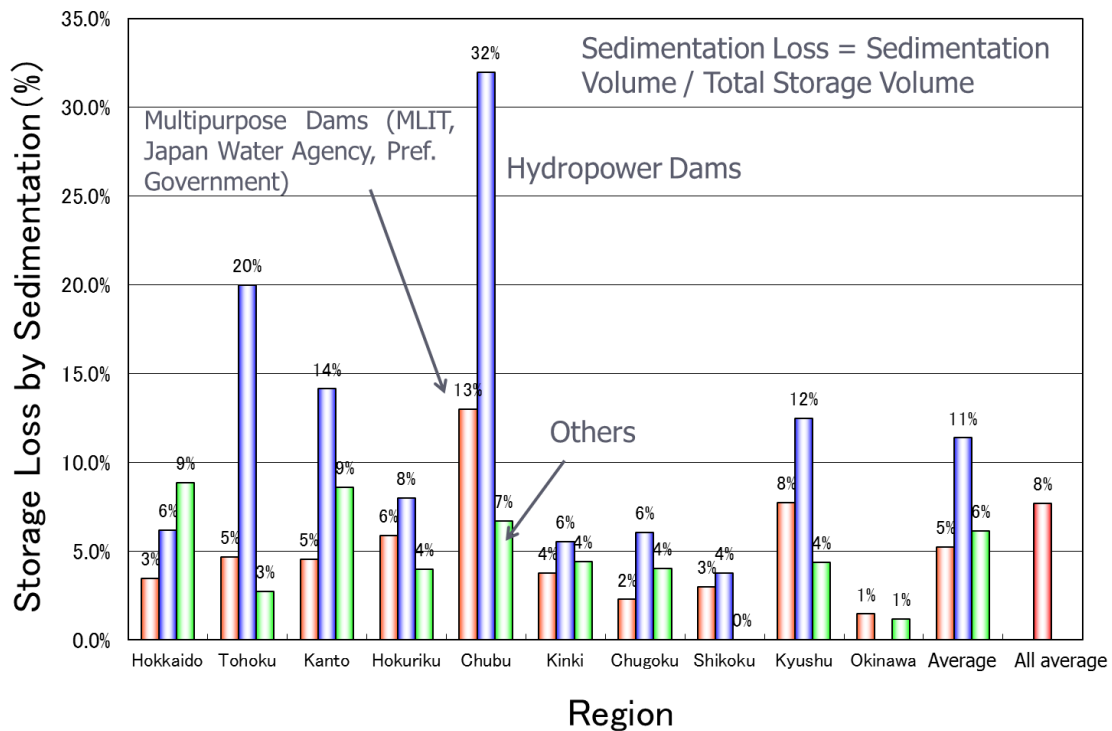
Figure 3: Reservoir storage loss by sedimentation in all regions in Japan and sediment yield potential map
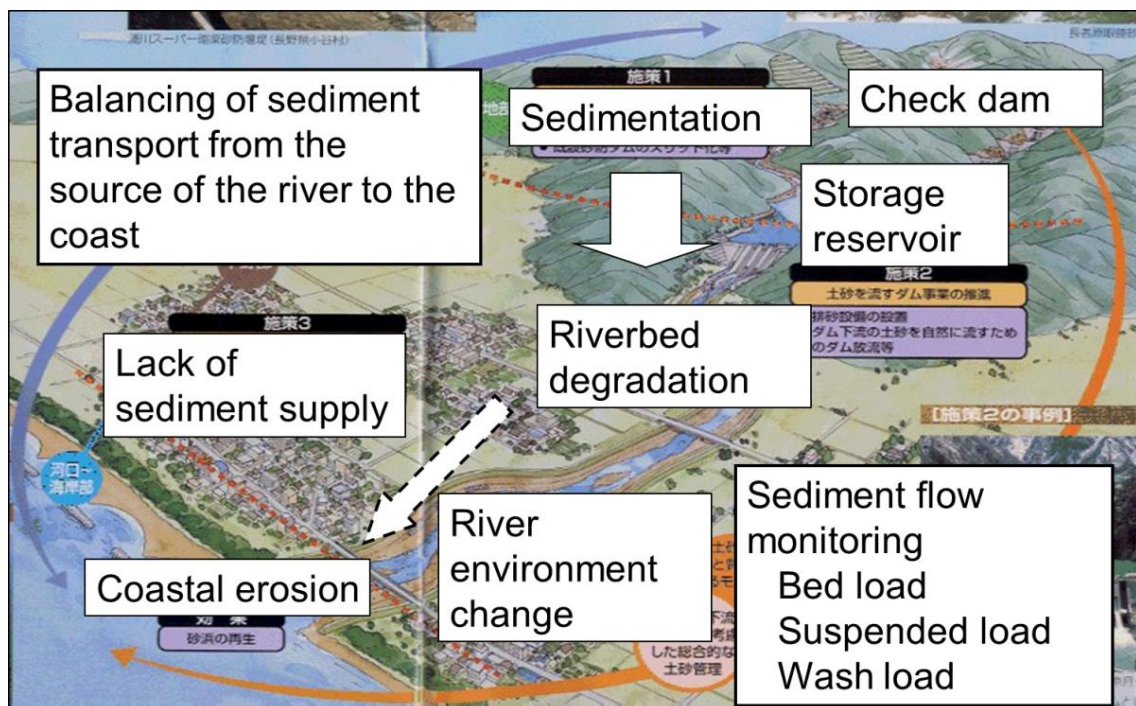
Figure 4: Comprehensive sediment management in the sediment routing system
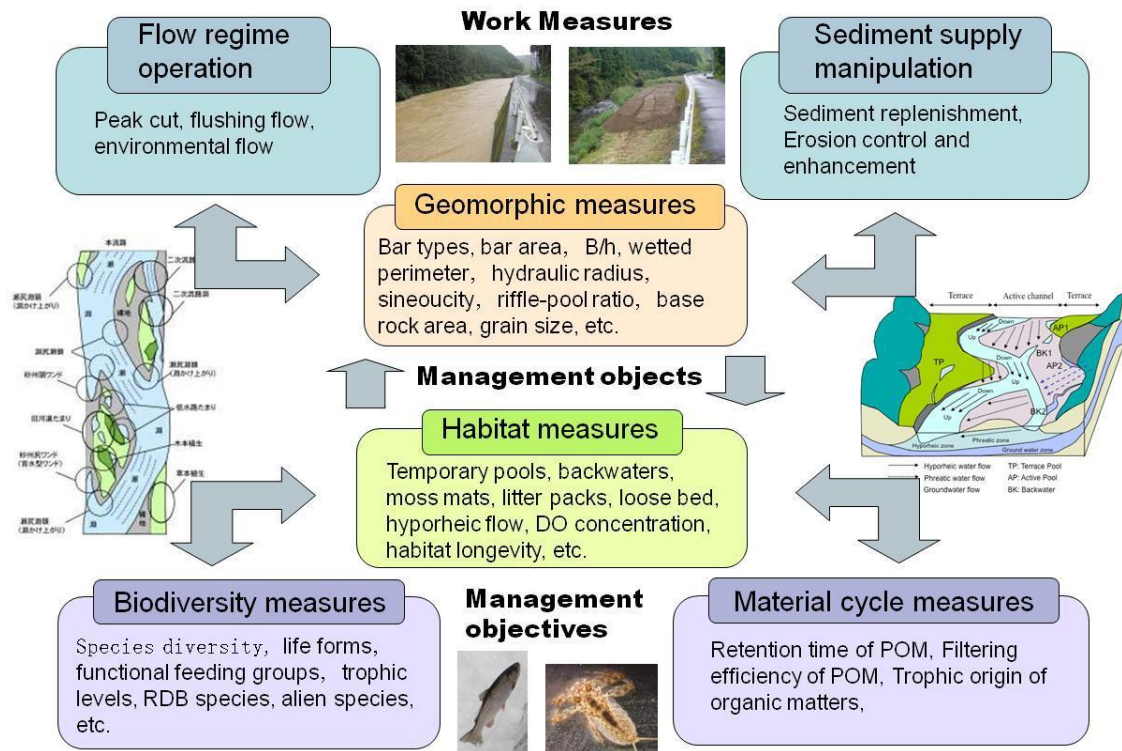
Figure 5: Concept of river restoration by flow and sediment management considering relationship between geomorphic and habitat measures

3 Selecting suitable sediment management options

Sediment management in reservoirs is largely classified into the three approaches: 1) to reduce sediment inflow to reservoirs, 2) to route sediment inflow so as not to accumulate in reservoirs and 3) to remove sediment accumulated in reservoirs. Sumi and Kantoush (2011b) have classified selected examples in Japan and Europe to these methodologies (Figure 6).

3.1 Reduction of sediment inflow into reservoirs

There are two techniques to reduce the amount of transported sediment: 1) countermeasure to control sediment discharge which covers entire basin including the construction of erosion control dams; and 2) countermeasure to forcibly trap sediment by constructing check dams at the end of reservoirs. Although the catchment areas of dams have high forest cover rates, a remarkable amount of sediment is produced in the watershed where landslides frequently occur due to the topographical and geological conditions.

Since an attempt to trap sediment using check dams is found effective for the reservoirs where bed load of relatively coarse grain size accounts for a large percentage of sediment inflow, many dams have proceeded in constructing them recently. In this technique, a low dam is constructed at the end of reservoir to trap transported sediment, and then the deposited sediment is regularly removed.

Classification | Timing | Place | Methods and details of sediment control measures | Examples of dams in Japan | Examples of dams in Europe

Sediment Management Strategies

- Sediment yield Reduction
- Sediment Routing
- Sediment Removal

Timing: Non-seasonal, Seasonal, Non-seasonal

Place: Catchment, River US of reservoir; End of reservoir; Inside of reservoir; Inside reservoir; End of reservoir; Inside reservoir — Mechanically, Hydraulically, Dry excavation, Dredging

Methods and details of sediment control measures:
- Afforestation and Vegetation practices
- Settling and off-stream storage basins
- Slope and bank protection, River regulation
- Sediment check dams
- Sediment bypass
- Gated outlets
- Gatless outlets
- Sediment sluicing
- Bottom outlet
- None-gate & curtain wall
- Selective withdraw inlets
- Submerged dam, groynes
- Turbidity current venting
- flushing outlet
- Drawdown flushing
- Sediment scouring gate
- Sediment scouring pipe
- Partial flushing
- Sediment Replenishment
- Recycling for concrete aggregate
- Sediment siphoning
- Sediment redistribution

Examples of dams in Japan:
- Sabo Area, Changing from sediment check dams to sediment control dams
- Miwa, Koshibu, Nagashima
- Asahi, Miwa, Koshibu, Yokoyama,
- Sabaishigawa, Dashidaira, Unazuki
- Masudagawa
- Koshibu, Futase, Kigawa
- Katagiri
- Yahagi
- Dashidaira, Unazuki
- Senzu, Yasuoka
- Ikawa
- Nunome, Akiba, Futase, Murou
- Miwa, Yasuoka, Hirao ka
- Miwa, Yanase
- Sakuma
- Sakuma

Examples of dams in Europe:
- Changing from sediment check dams to sediment control dams
- Beninar
- Egschi, Rempen, Pala gnedra
- Luzzone, Livigno
- Orden, Ligistbach
- Luzzone
- Glockner-Kaprun
- Tourtemagne
- Grimsel
- Bodendorf, Gebidem, Verbois
- Feistritz, Edling
- Annabrucke
- Margaritze, Emosson
- Bodendorf, Genissiat
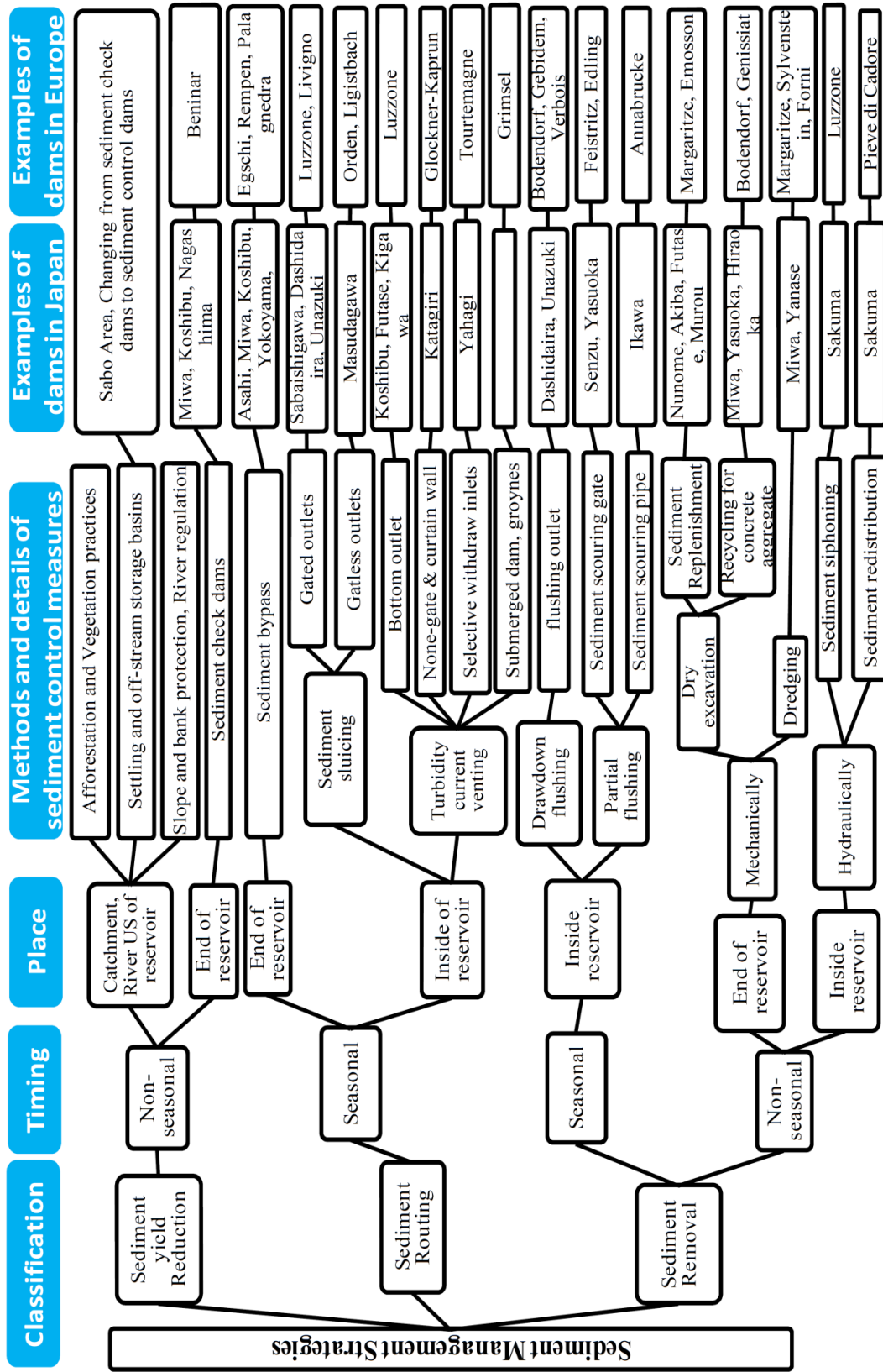- Margaritze, Sylvenstein, Forni
- Luzzone
- Pieve di Cadore

Figure 6: Sediment management strategies in Japanese and European reservoirs (Sumi and Kantoush (2011b))

The accumulated sediment can be excavated on land except for flood time, and the removed sediment is utilized effectively as concrete aggregate. As of 2013, the check dams have been constructed at 57 out of the dams under jurisdiction of MLIT.

Recently, sediment augmentation, or replenishment, has been carried out in some dams in Japan (Okano et al.(2004), Kantoush et al. (2010b), Kantoush et al. (2011a, b). Trapped sediments in the sediment check dam upstream of the reservoir are excavated and transported to the downstream of the dam. These sediments are put on the downstream river channel temporarily and washed out by the natural flood flows. Ock et al. (2013) summarized sediment replenishment methodologies as shown in Figure 7. They are classified into (a) In-channel stockpile, (b) High-flow stockpile, (c) Point bar stockpile and (d) high-flow direct injection. In Japan, high-flow stockpile is commonly used in order to avoid artificial turbid flow release by side bank erosion even in low flow rate. They are summarized in Figure 8 (Sakurai et al. (2013).

3.2　Routing of Sediment Inflow into Reservoirs

Another possible approach to sediment management, next to the reduction of sediment inflow itself, is to route sediment inflow so as not to allow it to accumulate in reservoirs. In Japan, the following techniques are adopted: 1) sediment bypass by directly diverting sediment transport flow, and 2) density current venting by using a nature of high-concentration sediment transport flow. In Japan, sediment bypass tunnels have been studied most exhaustively. History and current approaches on sediment bypass tunnels are shown in the next chapter. Density current venting, on the other hand, is a technique to use a nature of high-concentration sediment transport flow, which runs through relatively deep reservoir with original channel bed of steep slope as a density current with less diffusion, and to discharge it effectively through outlets in timing of reaching dam. In this technique, the main target is fine-grained sediment such as suspended sediment and wash load. In multiple-purpose dams in Japan that usually have high-pressure bottom outlets for flood control, the effective operation of these facilities during flood season can increase a chance to actively discharge fine-grained sediment.

3.3　Removal of sediment accumulated in reservoirs

This approach is regarded as the last measure in case sediment is accumulated in reservoirs in spite of various efforts being done: 1) mechanically excavating sediment accumulated in the upstream region of reservoirs, 2) dredging sediment accumulated at the middle and downstream regions, and 3) flushing out sediment with tractive force.

As for excavation and dredging techniques, it is important that the removed sediment should be treated properly and reused. On the other hand, sediment flushing is a technique to restore tractive force in a reservoir beyond its critical force by means of drawdown of reservoir level, and flush the deposits through bottom outlets mainly in an open channel flow condition, to the downstream of dam.
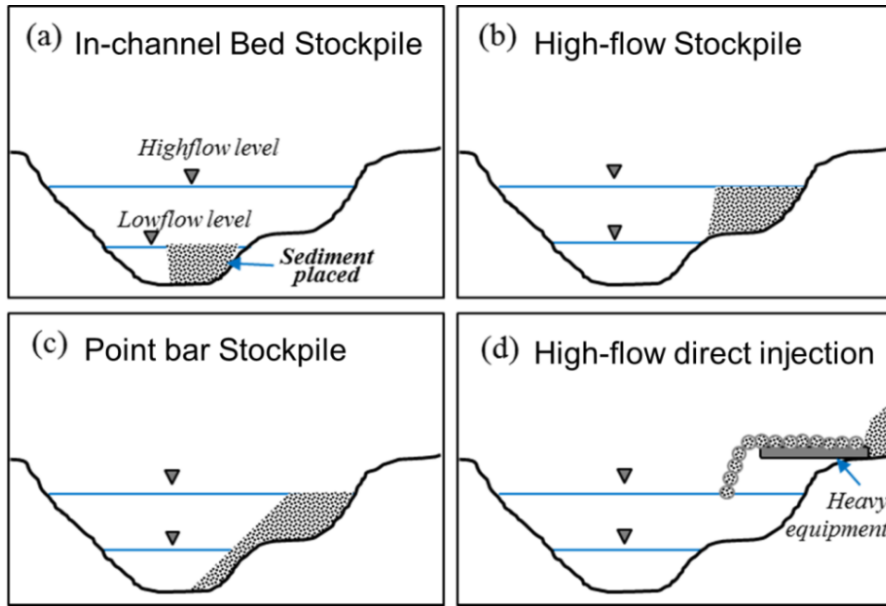
Figure 7: Sediment replenishment (augmentation) methodologies (Ock et al. (2013))
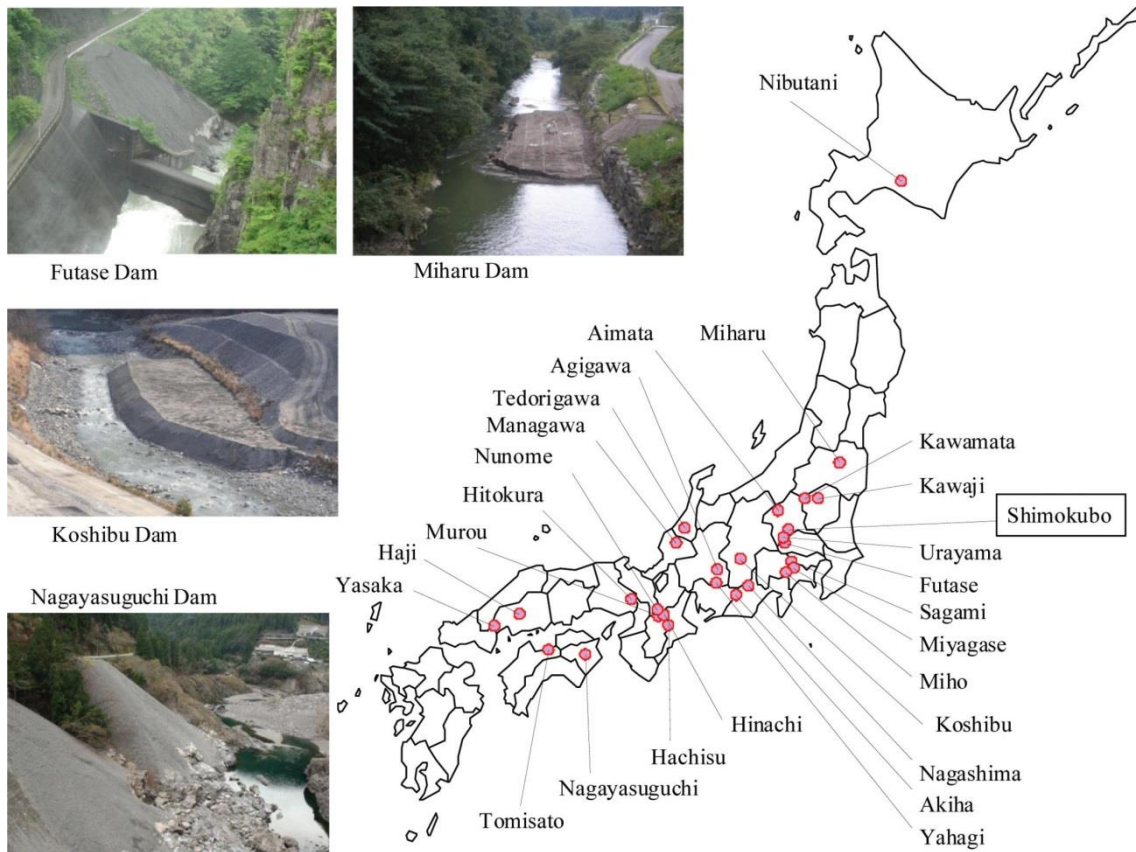

Figure 8: Location map of sediment replenishment (augmentation) dams in Japan (Sakurai et al. (2013))

Traditionally in Japan, sediment flushing facilities such as flushing sluices and outlets were installed at small-scale hydroelectric dams. In contrast, drawdown flushing at Dashidaira and Unazuki dams in the Kurobe river (e.g. Sumi et al. (2006), Sumi et al.

(2009), Kantoush et al. (2010a)) has been implemented in coordination of upstream and downstream dams from 2004. Sediment flushing is performed at many dams all over the world. Sediment flushing is considered as an extremely effective technique for discharging sediment. However, when this technique is introduced, an extensive study is required from the planning stages considering water and sediment inflow, storage capacity, grain size distribution and reservoir operation. At the same time, it is also required to minimize environmental impacts under sediment flushing process.

Moreover, HSRS (Hydro-suction Sediment Removal System) which can intake and discharge sediment using only the water level differences without the mechanical force is developed in some types in recent years. In Japan, several HSRS systems have been developed in the laboratory and fields (e.g. Sakurai et al. (2011), Miyakawa et al. (2014)). New ejector pump system has been also tested which has advantage to create strong suction power which can intake large gravels and stones, and directly transport through the pipe line (Temmyo et al.(2011)).

3.4　Promotion strategy of reservoir sedimentation management

In order to increase number of good examples for reservoir sediment management, it is important to establish selection measures of appropriate sediment management measures. Sumi (2004) has analyzed Japanese dams based on the parameter of the turnover rate of water (CAP/MAR=Total capacity/Mean annual runoff) and sediment (CAP/MAS=Total capacity/Mean annual inflow sediment) as shown in Figure 9. It is thought that the selected sediment management measures can be classified by these two parameters. It is understood that measures actually selected have changed in the order of the sediment flushing, the sediment bypass, sediment check dam and excavating, and dredging as CAP/MAR increases (decrease in the turnover rate). This is because of greatly depending on the volume of water to be able to use the sediment management measure that can be selected for the sediment transport. This chart has been converted to the one including worldwide examples by Annandale (2013) as shown in Figure 10.

4　Design guidelines for sediment bypass

4.1　Suitable selection of sediment bypass options

In Japan, sediment bypass tunnels have been studied for a long time. Although this technique involves high cost caused by tunnel construction, there are many advantages such that it is applicable to existing dams; it does not involve drawdown of reservoir level and therefore no storage capacity loss; and it has relatively small impact on environment because sediment is discharged during natural flood events compared to sediment flushing which discharge accumulated sediment in a short period.

CAP: Original total storage capacity volume, MAR: Mean annual runoff, MAS: Mean annual sediment inflow

Reservoir Life=CAP/MAS

Capacity−inflow ratio=CAP/MAR

No measures (from inner factors)

Sakuma
Miwa
Koshibu
Matsukawa
Unazuki
Dashidaira

Sediment check dam, Sediment replenishment
Sediment bypass, Sluicing
Sediment flushing, Sediment scoring gate

○ Check dam
■ Flushing
▲ Scoring gate
● Scoring pipe
◆ Bypassing
■ Excavating
● Dredging

1 大井　　　　　Oi　　　　　　　D, SP
2 千頭　　　　　Senzu　　　　　SG
3 泰阜　　　　　Yasuoka　　　　SG, D, PF
4 笠置　　　　　Kasagi　　　　　SG, PF
5 大間　　　　　Ooma　　　　　　SG, PF
6 常盤　　　　　Tokiwa　　　　　SG
7 三浦　　　　　Miura　　　　　　SP
8 平岡　　　　　Hiraoka　　　　　D, PF
9 佐久間　　　　Sakuma　　　　　B, D
10 八久和　　　　Hakuwa　　　　　E, D
11 井川　　　　　Ikawa　　　　　　SP, E, D, PF
12 山口　　　　　Yamaguchi　　　SG, PF
13 秋葉　　　　　Akiba　　　　　　E, D, PF
14 美和　　　　　Miwa　　　　　　B, E, D, CD
15 牧尾　　　　　Makio　　　　　　E, D, CD
16 小渋　　　　　Koshibu　　　　　B, E, CD
17 松川　　　　　Matsukawa　　　B, E, CD
18 旭　　　　　　Asahi　　　　　　B
19 出し平　　　　Dashidaira　　　　F
20 宇奈月　　　　Unazuki　　　　　F

CD : Check dam
F : Flushing (Draw down)
PF : Flushing (Partial draw down)
SG : Scoring gate
SP : Scoring pipe
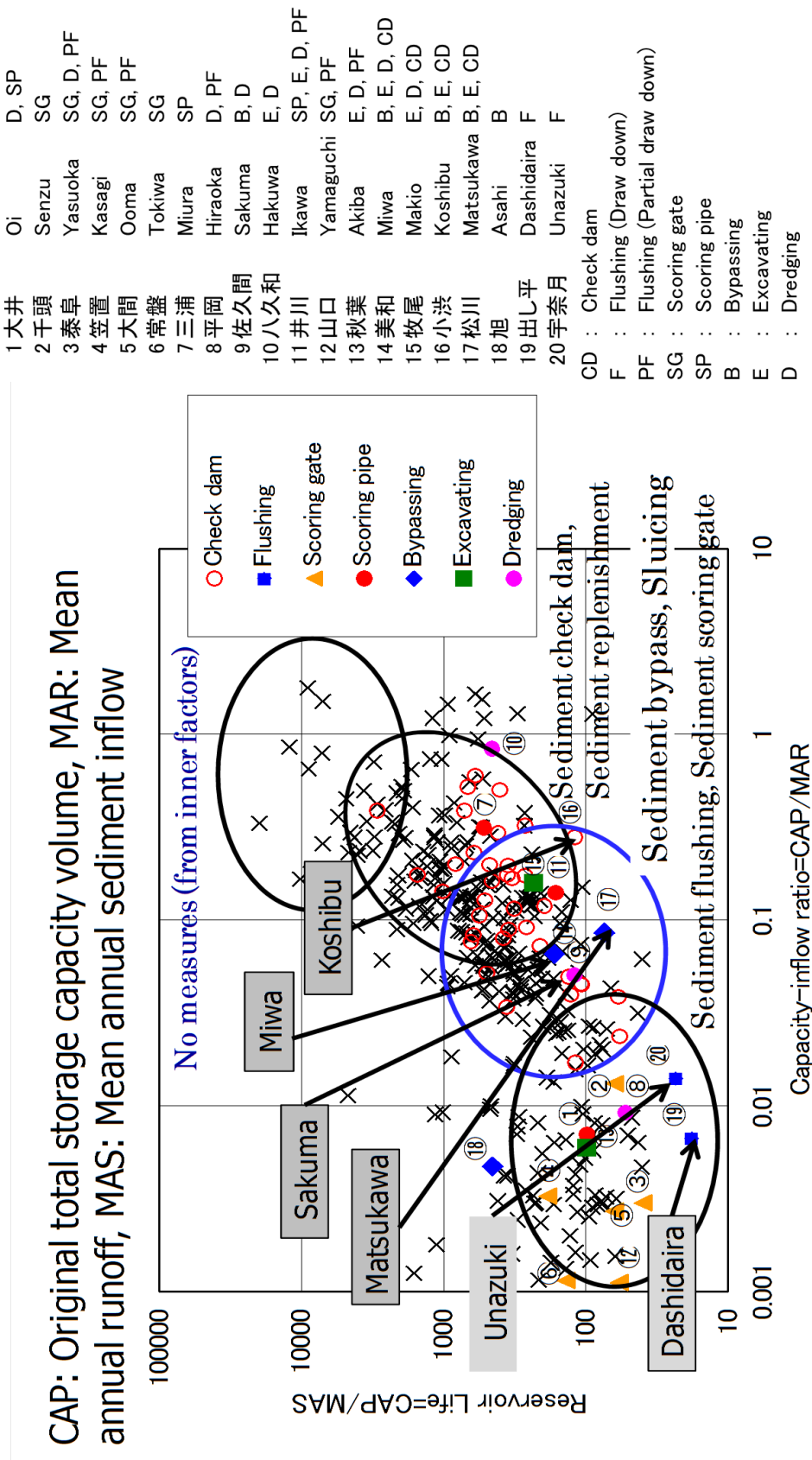B : Bypassing
E : Excavating
D : Dredging

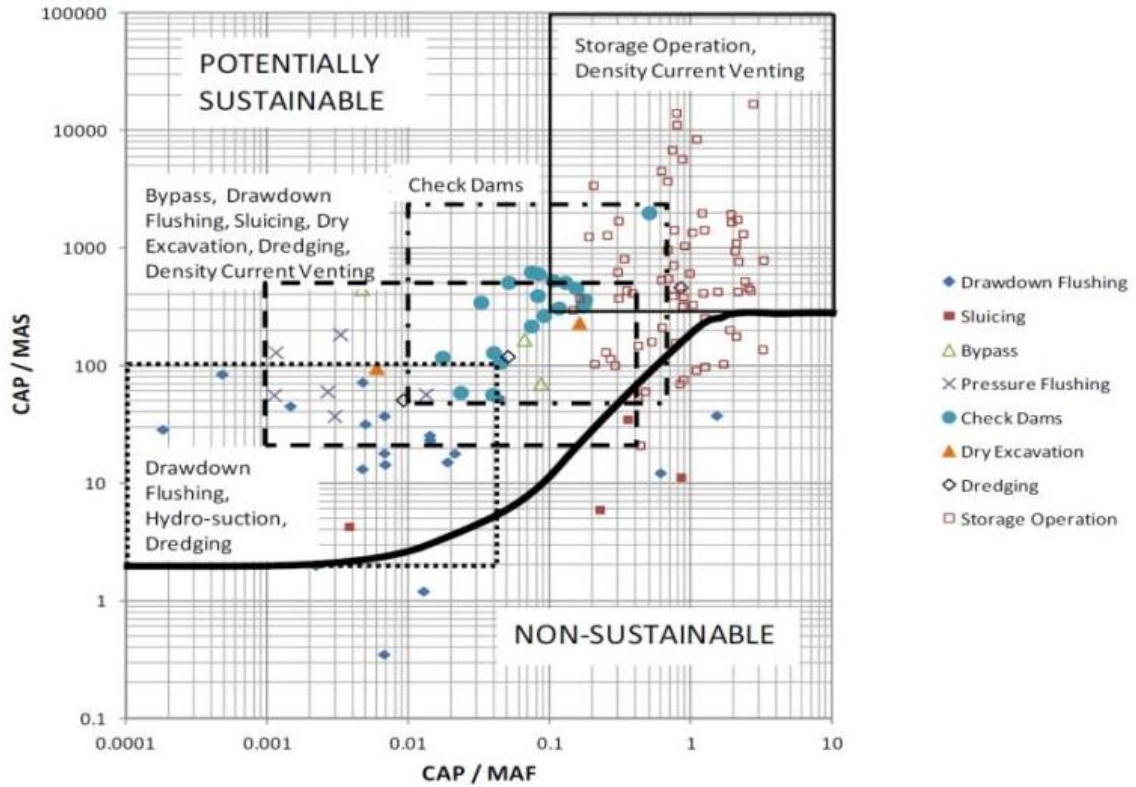Figure 9: Representative sediment management dams in Japan

Figure 10: Categorizing of reservoir sedimentation measures (Annandale (2013))

Table 1: Characteristics of successful sediment bypass tunnels in Japan and Switzerland

Name of Dam	Cou ntry	Date constr	Tunnel shape	Tunnel cross section (BxH) (m)	Tunnel length (m)	General slope (%)	Design Q (m³s⁻¹)	Design velocity (ms⁻¹)	Annual operation frequency (days/a)
Nunobiki	JP	1908	Archway	2.9 x 2.9	258	1.3	39	7	-
Asahi	JP	1998	Archway	3.8 x 3.8	2350	2.9	140	12	13
Miwa	JP	2004	Horseshoe	2r = 7.8	4300	1	300	10	2-3
Matsukawa	JP	2015	Archway	5.2 x 5.2	1417	4	200	15	-
Koshibu	JP	2016	Horseshoe	2r = 7.9	3982	2	370	9	-
Egshi	CH	1976	Circular	R = 2.8	360	2.6	74	10	10
Palagnedra	CH	1974	Circular	2r = 6.2	1800	2	110	13	2-5
Pffaffensprung	CH	1922	Horseshoe	A = 21 m²	280	3	220	14	ca. 200
Rempen	CH	1983	Horseshoe	3.5 x 3,3	450	4	80	12	1-5
Runcahez	CH	1961	Archway	3.8 x 4.5	572	1.4	110	9	4
Solis	CH	2012	Archway	4.4 x 4.68	968	1.8	170	11	1-10

Notes: JP = Japan, CH = Switzerland, Q = discharge

Table 1 shows examples of existing sediment bypass tunnels in Japan and Switzerland. Sediment bypass in the Nunobiki dam, the first example in Japan, was constructed in 1908 just after 8 years from dam completion in 1900 (Figure 11). Because of this sediment bypass, it is estimated that reservoir life has been extended from just only 25 years to over 1,000 years. Recently, the bypassing effect is clarified after completion of Asahi (Sumi et al. (2005), Kataoka (2003), Mitsuzumi (2009)) and Miwa (Suzuki (2009), Sumi et al.(2011a), Sumi et al.(2012)) dams. The bypass tunnels in Koshibu and Matsu-

kawa (Figure 12) dams are under construction. For the purpose of designing these by-pass systems, hydraulic characteristics of tunnel and diversion weir have been studied (Ando et al. (1994), Kashiwai et al. (1997), Harada et al. (1997)).

Figure 9 shows all Japanese dams based on CAP/MAR and CAP/MAS. Typical sediment bypassing dams are located around CAP/MAR = 0.02 - 0.2 and CAP/MAS = 50 – 500. These ratios indicate that sediment bypass is suitable for medium size reservoirs. The medium size meant not only that of reservoir, but also a hydrological size related to the catchment as well. For instance, smaller reservoirs are easier to drawdown and refill comparing with the medium size. Therefore, sediment flushing may be more suitable such as Unazuki and Dashidaira dams in Kurobe River since temporal draw-down operation is much easier and more cost effective to discharge sediment from all reservoir area (Sumi et al. (2009), Kantoush et al. (2010)). On the other hand, sediment bypass tunnels are more efficient and saving water resources for medium size reservoirs as the new bypass tunnels in Koshibu and Matsukawa dams.
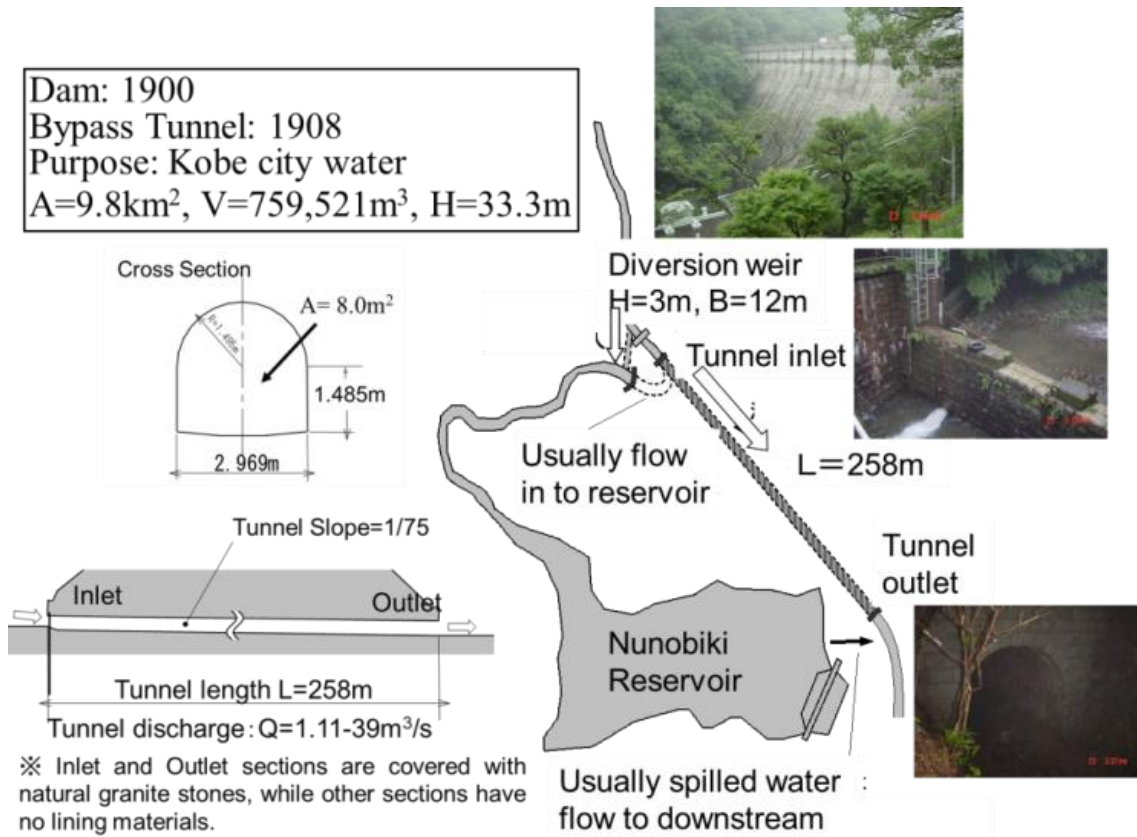

Figure 11: Sediment bypass tunnel in the Nunobiki dam
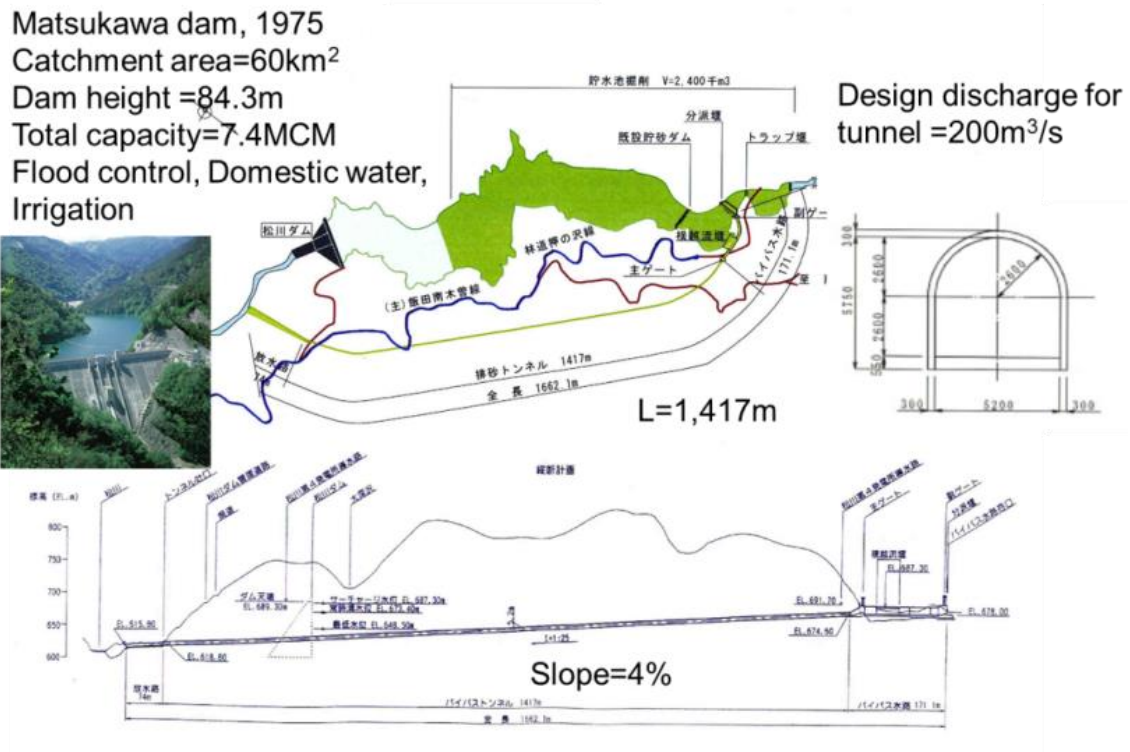
Figure 12: Sediment bypass tunnel in the Matsukawa dam. Design and operational considerations of sediment bypass

Study committee on reservoir sediment management conducted by the Water Resources Research Center (WEC) has studied several aspects on reservoir sedimentation management including sediment bypass. This committee summarized several aspects for design and operational consideration on sediment bypass system as shown in Figure 13 and Table 2.

Figure 13: Planning, designing and management considerations of sediment bypass tunnels

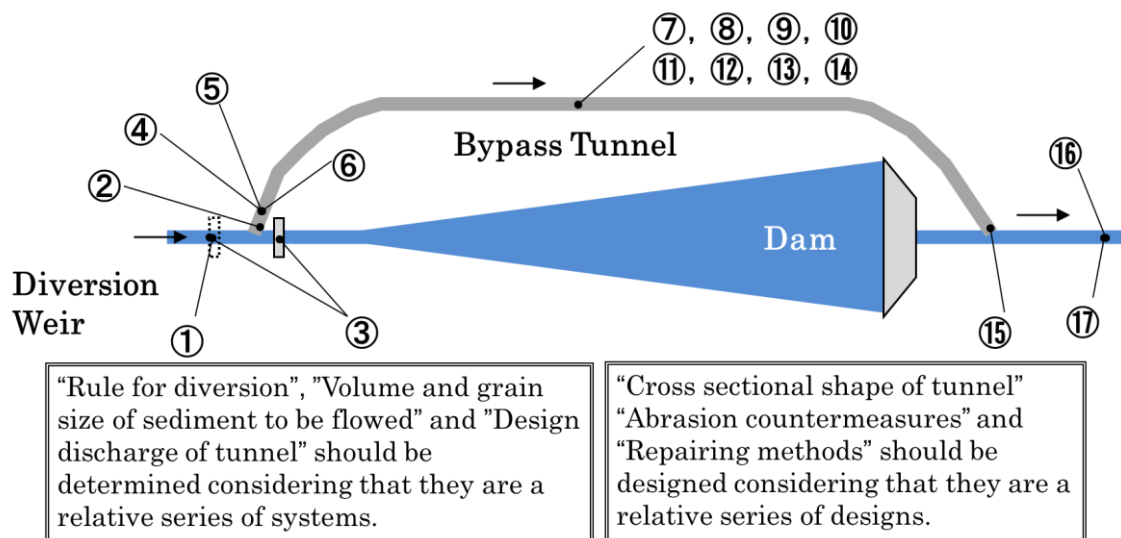Table 2: Planning, designing and management considerations of sediment bypass tunnels

	Items	Considerations
1	Facilities for trapping gravel and woody debris	・Large gravels and woody debris should be trapped upstream side of the diversion weir in order to prevent them flow into the tunnel.
2	Determination of the diversion rule (In case of multipurpose dams including flood control)	・The diversion weir should be operated during floods. ・Design discharge of the tunnel should be determined without avoiding the flood control operation. Diversion rule with suitable design of the inlet structure should meet the necessary operation.
3	Construction of the diversion weir and sediment trap weir	・The necessary scale of the diversion weir (or the sediment trap weir) should be determined from the result of numerical analysis. ・Diversion weir (or sediment trap weir) basically consists of concrete structures. ・From the viewpoint of effective utilization of river bed materials, adopting double steel sheet piles can be selected.
4	Measurement of inflow discharge	・Inflow discharge to the tunnel (relationship between water level at diversion weir and inflow) should be measured in order to control flood discharge.
5	Construction of the tunnel inlet section	・The channelized section from inlet to the tunnel should be designed to be chute type in order to control sediment. ・Curtain walls should be installed in order to control gravel and woody debris flowing into the tunnel.
6	Abrasion countermeasures of the tunnel inlet section	・Inlet section basically should be covered by steel lining.
7	Design discharge of the tunnel	・Design discharge of the tunnel should be determined without avoiding the flood control operation. ・Several design discharges of the tunnel should be carefully studied and compared because this is the key parameter to define the project cost.
8	Horizontal alignment	・The route should be selected as it can take a shortcut.
9	Vertical alignment	・Bypass tunnel should be designed based on the design standard of the waterway tunnel. ・Bypass tunnel should be designed from the comprehensive viewpoint of safety and life cycle costs by considering design discharge, and volume and grain size of sediment to be transported.
10	Volume and grain size of sediment to be transported	・Bypass tunnel is designed basically to transport all grain sizes (from wash load to bed load).
11	Cross sectional shape of the tunnel	・Bypass tunnel should be designed based on the design standard of waterway tunnel. ・From the viewpoint of maintenance, flat invert should be designed in order to disperse abrasion damages. ・In the case of long tunnel length, bypass tunnel should be designed so as to be inspected and repaired with vehicles.
12	Abrasion countermeasures of the tunnel	・Bypass tunnel basically consists of high-strength concrete. ・It should be considered to use stone lining, steel-fiber concrete, polymer concrete and so on, as necessary.
13	Inspection methods	・It should be considered to be inspected by 3D Laser Scanning etc.
14	Repairing methods	・Bypass tunnel basically should be repaired with high-strength concrete. ・It should be considered to be repaired with stone lining, steel-fiber concrete, polymer concrete and so on, as necessary.

14

15	Construction of the outlet section	・Free-fall type, step type and so on can be selected considering the river topography and the alignment etc.. ・If there are some facilities to be protected, energy dissipater should be considered.
16	Monitoring methods for the downstream river	・Water quality, physical and biological environments should be monitored at the downstream river. It is recommended to compare with upstream of the dam and several points downstream from the tunnel outlet.
17	Dealing with increased sediment loading	・In case of increasing downstream sediment discharge, it is needed to control rising of river bed level and preventing intake facilities from being buried and so on.

They are divided into diversion and inlet structures, tunnel main section, tunnel outlet structure and downstream river channel. There are several issues of sediment bypass technique to be resolved in the future as follows:

Hydrology: In order to improve the bypass operation, prediction of upstream rainfall and runoff by distributed hydrological modelling and monitoring techniques is needed. Moreover, prediction of sediment inflow to the reservoir during flood events and real time monitoring are important in order to optimize sediment bypass operation.

Hydraulics: Clarification of the hydraulic behavior of flow and sediment in tunnels is needed for the purpose of designing safe and economical sediment tunnels (i.e., cross section, velocity, curvature, invert, slope and material design), as well as the establishment of countermeasures for abrasion damages on channel bed surface. The main problem of sediment bypass tunnels is abrasion along the invert. To counter abrasion, selecting high strength concrete and preparing enough abrasion depth on top of necessary tunnel invert depth are recommended from the viewpoints of initial construction cost and easy maintenance. In order to increase diversion effect, hydraulic design of diversion weir is one of key point of hydraulic design issue (Kashiwai et al. (1997)).

Environment: Sediment bypass has a possibility to improve downstream river channel by supplying sediments. It is needed to establish measures how to assess these positive effects spatiotemporally. Case Studies of Sediment Bypass Tunnel

As an example, the committee has started to compare several layout of sediment bypass tunnel for the Futase dam completed in 1961 as shown in Figure 14. Present accumulated sedimentation volume in 2012 is 4.7MCM where annual average accumulated sediment is 92,000m^3/yr and storage loss is 17.4% of the total capacity of 26.9MCM. This value is up to 92% of 100 yrs design sedimentation volume of 5.1 MCM.

In the Futase dam, there are two major tributaries whose catchment areas are 108km^2 and 61km^2 respectively. Important question is how to select target tributary and design inlet point for sediment bypass tunnel. If we will select A-1 sediment bypass option with the design discharge of 500m^3/s, total sediment of 47,000m^3/yr including coarse sediment of 24,000m^3/yr can be diverted by assuming diversion rate of coarse sediment is 100%. Figure 15 shows estimated construction and maintenance costs for A-1 sedi-

ment bypass option where direct tunnel construction costs are accounted for 62% of the total cost. Inflow sediment to the reservoir is occupied by the coarse sediment more than 50%. To reduce the construction cost of the tunnel, it is important to reduce the tunnel design discharge and the cross-section by guiding this coarse sediment to the tunnel effectively with suitable design of diversion weir.
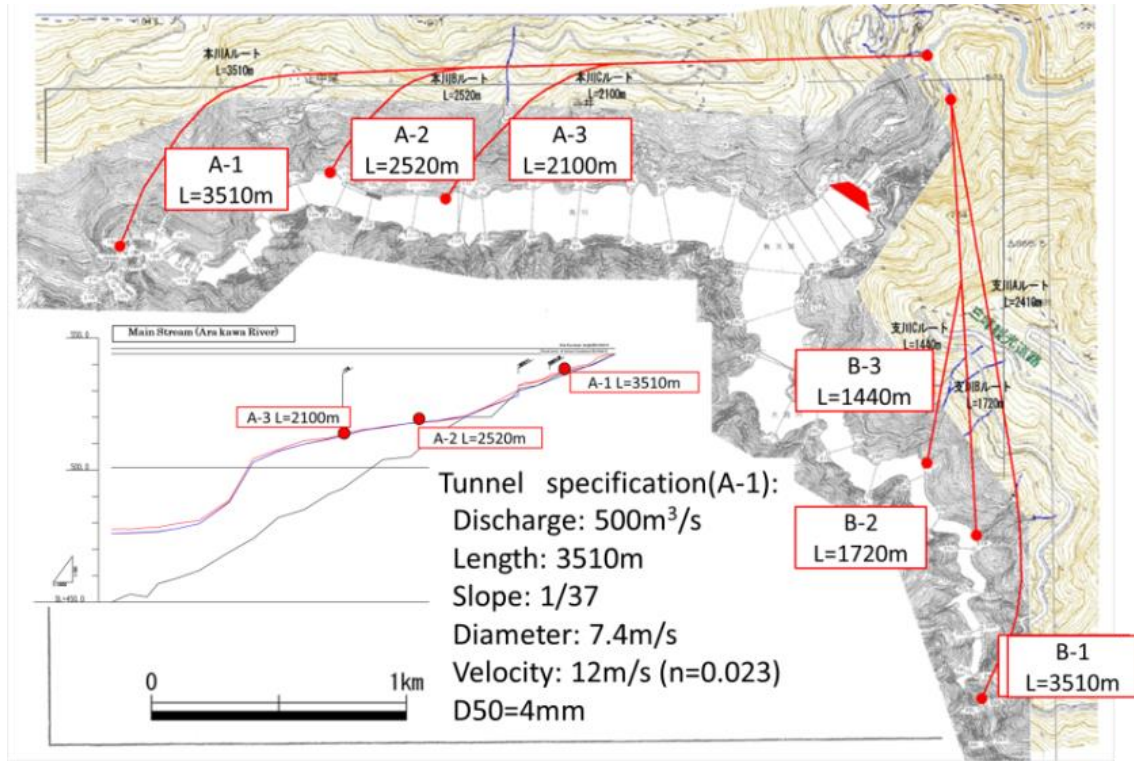
Figure 14: Several options of sediment bypass tunnels for Futase dam

Sensitivity analysis on the design discharge of the tunnel has been shown in Figure 16. If we increase the design discharge, both bypassing sediment volume and bypassing efficiency which is defined by bypassing sediment via total incoming sediment are increase whereas necessary cost for bypass construction will increase at the same time. Thus, we can find optimum design discharge with respect to sediment removal rate which is defined by bypassing sediment volume via necessary construction cost. After these analyses, we should select appropriate tunnel size based on bypassing sediment volume, bypassing efficiency and tunnel construction cost.

16

Figure15: Trial cost estimations of sediment bypass tunnel (In case of A-1)

Figure16: Sensitivity analysis of sediment removal cost by changing tunnel design discharge
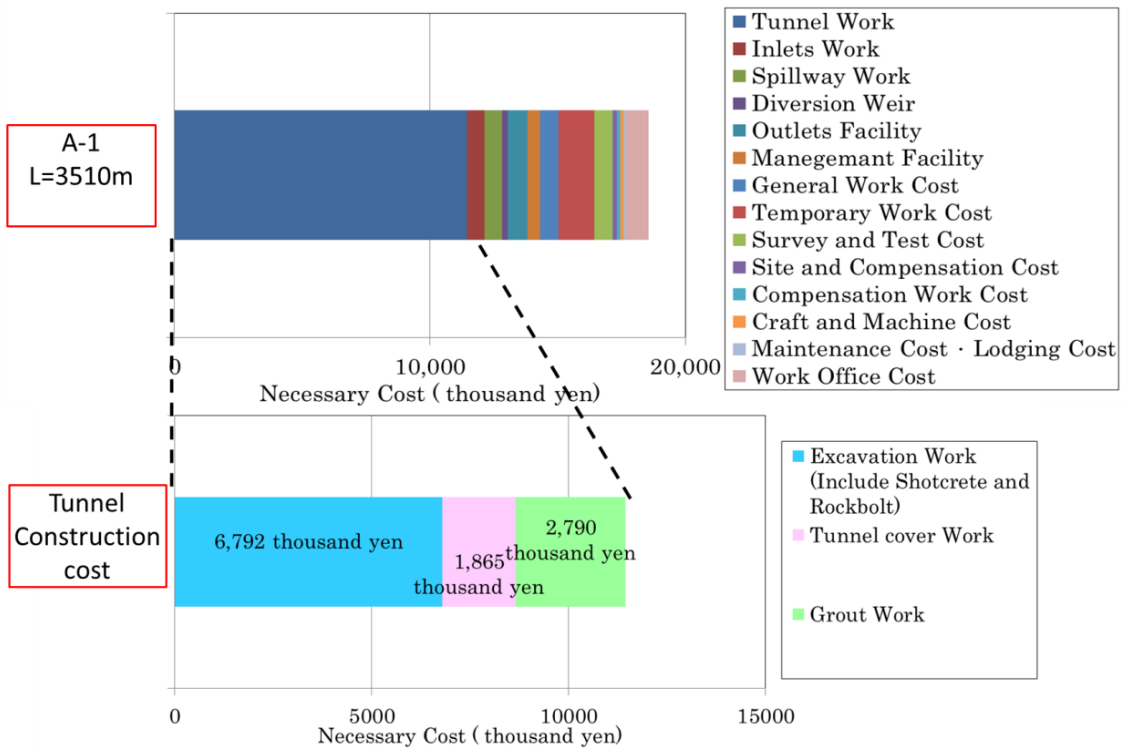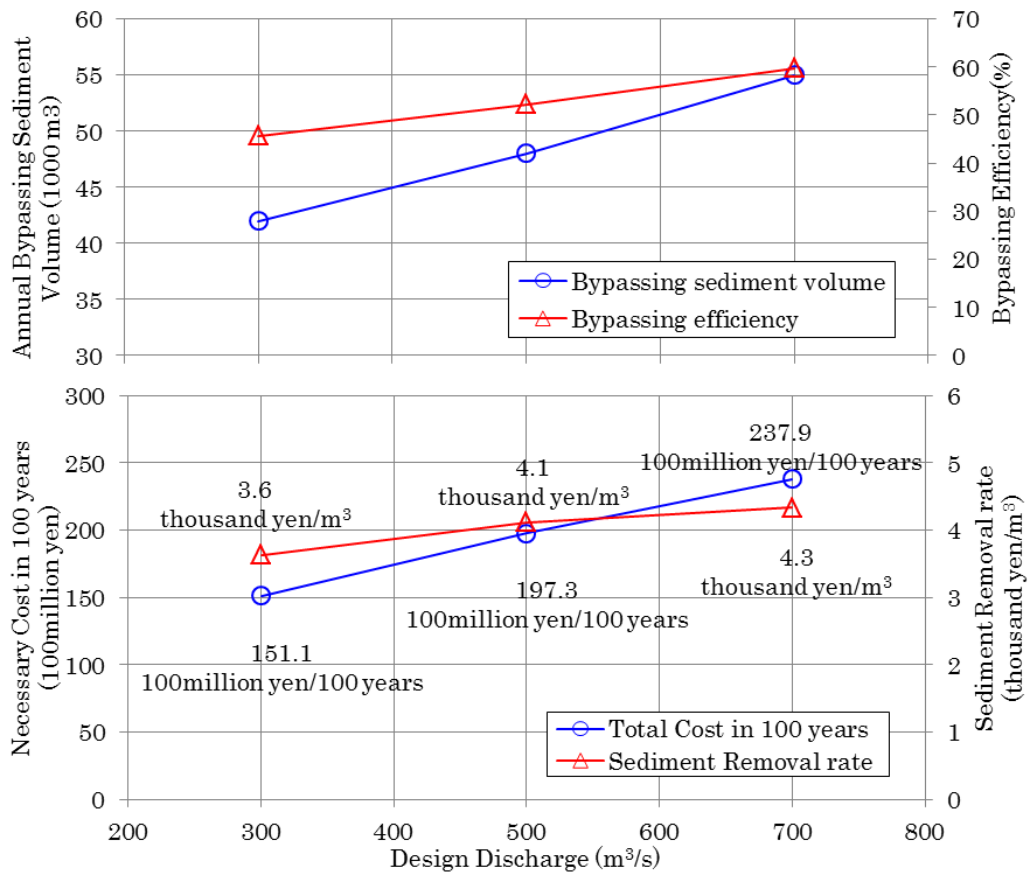
5 Conclusions

Reservoir sedimentation management is entering a new era worldwide. Although there are still technical problems to be solved, we believe that the importance of sediment management will increase for reservoir sustainability. Since several sediment management measures have been proposed, it is important to select suitable options for each reservoir considering both reservoir size and river basin scale. In order to enhance our challenges, we should also study comprehensive approach on sustainable management of sediment routing system. Sediment flushing, bypassing and replenishment are current important case studies in Japan. Through implementing these leading projects, we should clarify remaining unknown factors on planning, designing and operational issues for suitable selections and optimization of these options. Among them, sediment bypassing measure is really unique approach fitting mountain reservoirs by contributing both for increasing reservoir life and contributing downstream river restoration. In order to increase number of applying this sediment bypass technique, we should collect actual filed data as much as possible and establish its design guideline. Based on these data, it is required to minimize construction and maintenance costs of sediment bypass tunnel without increasing any operational risks. Since Japan and Swiss are leading countries on this matter historically, exchanging lessons learned and networking related institutes will be beneficial not only for both countries but also worldwide.

Acknowledgments

References

Annandale, G. (2013). Quenching the Thirst: Sustainable Water Supply and Climate Change, Createspace, ISBN-10: 1480265152.

Ando, N., Terazono, K. and Kitazume, R. (1994). Sediment removal project at Miwa dam, The 18th Congress of ICOLD, Durban, Q.69, R.27, pp.421-441.

Auel C. and Boes R. (2011). Sediment bypass tunnel design – review and outlook. *Proc. 79th Annual Meeting of ICOLD "Dams and Reservoirs under Changing Challenges"*. Lucerne, Switzerland. Taylor & Francis, London. 403-412.

Fukuroi, H. (2012). Damage from Typhoon Talas to Civil Engineering Structures for Hydropower and the Effect of the Sediment Bypass System at Asahi Dam, *Proc. International Symposium on Dams for a Changing World*, The 80th Annual Meeting of ICOLD, Kyoto.

Harada, M., Terada, M. and Kokubo, T. (1997). Planning and hydraulic design of bypass tunnel for sluicing sediments past Asahi reservoir, *Proc. 19th Congress of ICOLD*, Florence, C.9, pp.509-539.

Kantoush, S. A., Sumi, T., Suzuki, T. and Murasaki, M. (2010a). Impacts of sediment flushing on channel evolution and morphological processes: Case study of the Kurobe River, Japan", *International Conference on Fluvial Hydraulics*, River Flow 2010 Braunschweig, Germany, pp. 1165-1173.

Kantoush, S. A., Sumi, T. and Kubota, A. (2010b). Geomorphic response of rivers below dams by sediment replenishment technique", *International Conference on Fluvial Hydraulics*, River Flow 2010 Braunschweig, Germany, pp. 1155-1163.

Kantoush, S. A., Sumi, T., and Takemon, Y. (2011a). Lighten the load, *International Water Power & Dam Construction*, May, 38-45.

Kantoush, S. A. and Sumi, T. (2011b). Sediment Replenishing Measures for Revitalization of Japanese Rivers below Dams, *Proc. 34th IAHR World Congress*, 2838-2846.

Kataoka, K. (2003). Sedimentation management at Asahi dam, *3rd world water forum*, Kyoto-Shiga, pp. 197-207.

Kashiwai, J., Sumi, T. and Honda, T. (1997). Hydraulic study on diversion facilities required for sediment bypass systems, *19th Congress of ICOLD*, Florence, Q.74, R.59, pp.957-976.

Kondolf G.M., Gao Y., Annandale G.W., Morris G.L., Jiang E., Zhang J., Cao Y., Carling P., Fu K., Guo Q., Hotchkiss R., Peteuil P., Sumi T., Wang H.-W., Wang Z., Wei Z., Wu B., Wu C. and Yang C.T. (2014). Sustainable sediment management in reservoirs and regulated rivers: Experiences from five continents, *Earth's Future*, 2, 256–280, doi:10.1002/2013EF000184.

Mitsuzumi, A., Kato, M. and Omoto, Y. (2009). Effect of sediment bypass system as a measure against long-term turbidity and sedimentation in dam reservoir, *ICOLD, 23rd Congress*, Brasilia, Q89-R8.

Miyakawa M., Hakoishi N. and Sakurai T. (2014). Development of the Sediment Removal Suction Pipe by Laboratory and Field Experiments, *International Symposium on Dams in a Global Environmental Challenges, 82nd Annual Meeting of ICOLD*, V-15-24.

Okano M., Kikui H., Ishida H. and Sumi T. (2004). Reservoir Sedimentation Management by Coarse Sediment Replenishment below Dams, ISRS, *9th International Symposium on River Sedimentation*, II, 1070-1078.

Ock G., Sumi T. and Takemon Y. (2013). Sediment replenishment to downstream reaches below dams: implementation perspectives, *Hydrological Research Letters*, Vol. 7, No. 3 p. 54-59, doi: http://dx.doi.org/10.3178/hrl.7.54.

Sakurai T. and Hakoishi N. (2011). Burrowing-type sediment removal suction pipe for a sediment supply from reservoirs, Proc. of the International symposium on Dams and Reservoirs under Changing Challenges – Schleiss & Boes (Eds). Annual Meeting of ICOLD, Lucerne, 371-378.

Sakurai T. and Hakoishi N. (2013). Numerical simulation of sediment supply from dam reservoirs to downstream by the placed sediment, Advances in River Sediment Research – Fukuoka et al. (eds), 1193-1199, Taylor & Francis Group, ISBN 978-1-138-00062-9.

Sumi, T., Okano, M. and Takata, Y. (2005). Reservoir Sedimentation Management with Bypass Tunnels in Japan, *9th International Symposium on River Sedimentation*, II, pp. 1036-1043.

Sumi, T. and Kanazawa. H. (2006). Environmental study on sediment flushing in the Kurobe River, *22nd international congress on large dams ICOLD*, Barcelona, Q.85-R.16, 219-242.

Sumi, T., Nakamura, S. and Hayashi K. (2009). The Effect of Sediment Flushing and Environmental Mitigation Measures in the Kurobe River, *23rd ICOLD Congress*, Brasilia, Q89-R6.

Sumi, T. and Kantoush, S. A. (2011a). Comprehensive Sediment Management Strategies in Japan: Sediment bypass tunnels, *Proc. 34th IAHR World Congress*, 1803-1810.

Sumi, T. and Kantoush, S. A. (2011b). Sediment management strategies for sustainable reservoir, Proc. of the International Symposium on Dams and Reservoirs under Changing Challenges, *79th Annual Meeting of ICOLD*, 353-362.

Sumi, T., Kantoush, S. A. and Suzuki, S., (2012). Performance of Miwa Dam Sediment Bypass Tunnel : Evaluation of Upstream and Downstream State and Bypassing Efficiency, *Proc. 24th ICOLD Congress*, Kyoto, Q92-R38, pp.576-596.

Suzuki, M. (2009). Outline and Effects of Permanent Sediment Management measures for Miwa Dam, *23rd ICOLD Congress*, Brasilia, Q.90-R.1.

Temmyo T., Miura N., Okabe T., Kaku M., Kammera T., Yamagami Y. and Sumi T. (2011). Trial dredging by a new ejector-pump system for the reservoir sedimentation, *Proc. International symposium on Dams and Reservoirs under Changing Challenges*, Schleiss & Boes (Eds). Annual Meeting of ICOLD, Lucerne, CD-ROM.

Authors

Prof. Dr. Tetsuya Sumi (corresponding Author)
Water Resources Research Center, Disaster Prevention Research Institute, Kyoto University, Japan
Email: sumi.tetsuya.2s@kyoto-u.ac.jp

Abrasion and corrective measures of a sediment bypass system at Asahi Dam

Hiroshi Nakajima, Yusuke Otsubo, Yuji Omoto

Abstract

At the Asahi Dam of Kansai Electric Power Co., Inc., a sediment bypass system was built to take a fundamental measure to control prolonged water turbidity and the progress of rapid sedimentation ascribable to the collapse of mountain slopes caused by a great flood of 1990 and has been operated since 1998. The effectiveness of the bypass system was verified after the commencement of system operation for controlling prolonged water turbidity and the progress of sedimentation in the reservoir. In the meantime, the tunnel invert has been worn notably and how to increase the efficiency of periodical repair is an issue.

This paper describes the abrasion of the tunnel invert of the sediment bypass system at the Asahi Dam that has been in service for approximately 15 years, and considers efficient tunnel maintenance methods in the future.

1 Outline of Asahi Dam

The Asahi Dam is on the lower regulating reservoir of the Oku-yoshino Power Plant, a pure pumped-storage power plant. The operation was commenced in 1978. The location of the power plant is shown in Figure 1 and the specifications are listed in Table 1.
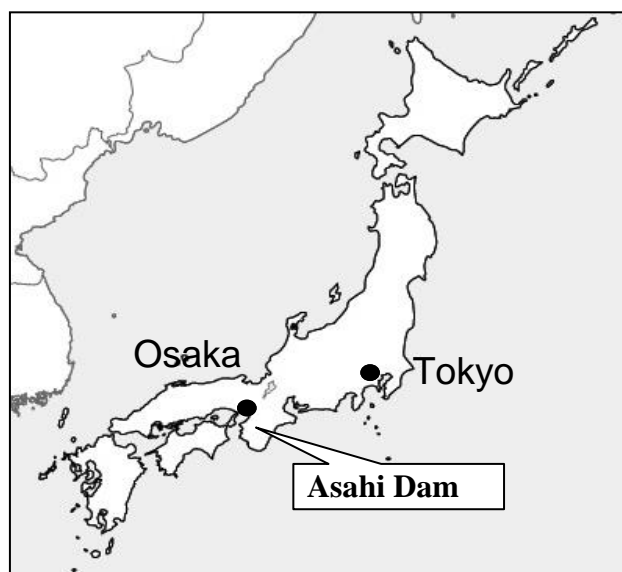

Figure 1: Location of Asahi Dam

Table 1: Specifications for Asahi Dam and Oku-yoshino Power Plant

Catchment area	39.2km^2		Dam	Type	Arch
Design flood	1,200m^3/s			Height	86.1m
Power plant	Name	Oku-yoshino		Crest length	199.41m
	Max. output	1,206MW	Reservoir	Gross storage	15.47×10^{6}m^3
	Max discharge	288m^3/s		Effective storage	12.63×10^{6}m^3
	Effective head	505m		Available depth	32m

2 Plan and design of sediment bypass system

The sediment bypass system at the Asahi Dam was designed to treat bed load and suspended load besides wash load from the purposes of mitigating both prolonged turbidity and sedimentation. There were two requirements for the bypass system. One was to eliminate most of the prolonged turbidity when the peak inflow was 200m^3/s, which is the 1-year return period inflow at the Asahi Dam. The other was to flush all of bed load from the upstream when the peak inflow was 660m^3/s (50-year flood in sediment bypass design) which is the maximum inflow in sediment bypass design, or when 1,200m^3/s (100-year flood in dam design) which is the design flood, at the Asahi Dam. The capacity of the bypass system was determined as 140m^3/s by performing simulations.

Based on the uniform flow calculation, the cross-section of the bypass tunnel was planned so that the tunnel could pass the flow with the water depth of 80% of the tunnel height. D-shape cross section was adopted because of cost performance and ease of maintenance. The entrance of the tunnel was composed of a diversion weir and an orifice intake, which would be desirable for flushing bed load. With these structures, the volume of water and sediment into the tunnel could be naturally regulated (Table 2 and Figure 2).

Table 2: Specifications for sediment bypass system

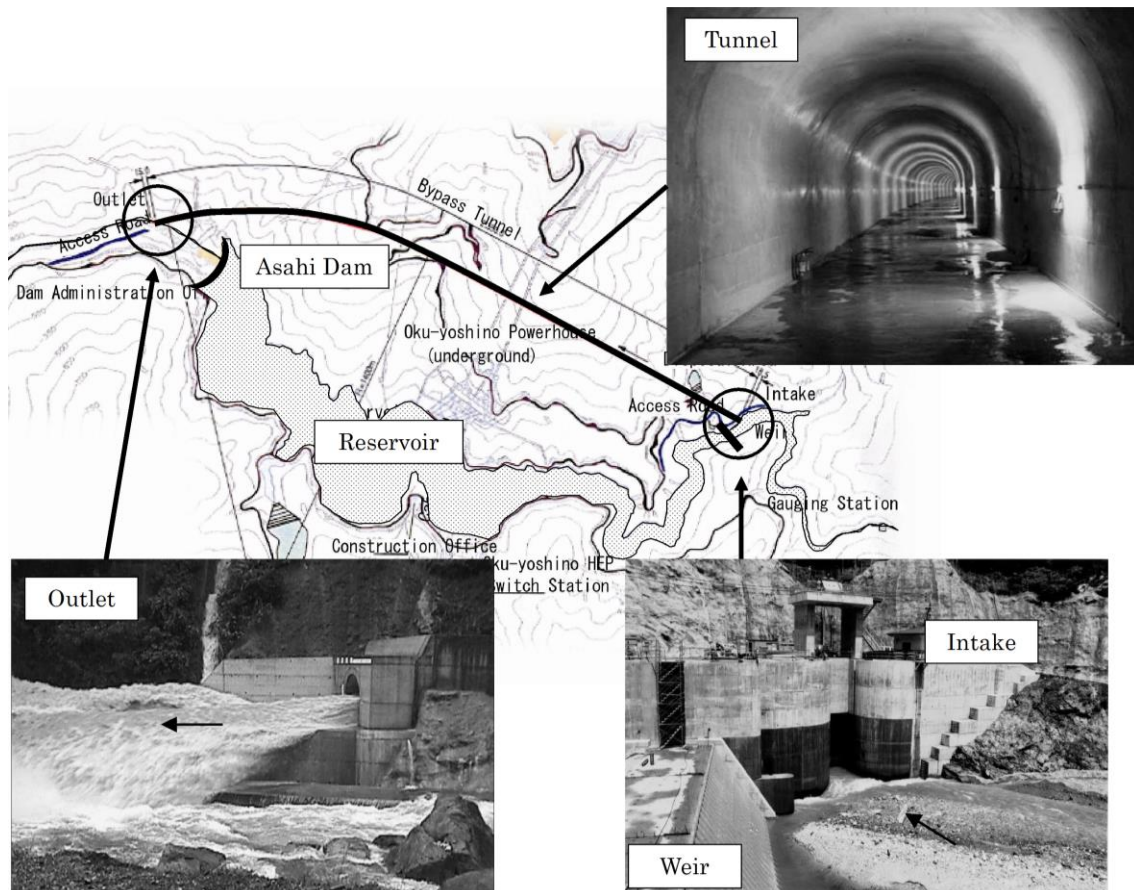| Weir	Height	13.5m		Bypass tunnel	Length	2,350m
	Crest Length	45.0m			Height×Width	3.8m×3.8m
Intake	Height	14.5m			Shape	D-shape
	Width	3.8m			Gradient	Approx. 1/35
	Crest Length	18.5m			Max. discharge	140m^3
	Type	Reinforced Concrete and steel lining		Outlet	Width	8.0～5.0m
					Length	15.0m
	Gate	1			Type	Reinforced concrete

Figure 2: Plan view of the bypass system at the Asahi Dam

3   Performance and effect of sediment bypass system

3.1   Performance of sediment bypass system

Figure 3 shows the annual total inflow into the reservoir and bypass tunnel since the start of operation. Fifty to eighty percent of total inflow flowed downstream via the bypass tunnel every year. A peak flow of 895m^3/s, highest since the start of operation, was recorded at the Asahi Dam in September 2011 (Figure 4).

3.2   Effects of sediment bypass system

Water was turbid for 50 to 130 days during the year on the average depending on the scale of flooding before the commencement of sediment bypass operation. The average number of days of prolonged turbidity was reduced to about ten after the start of operation. The bypass system was found to be effective for mitigating water turbidity on a long-term basis.
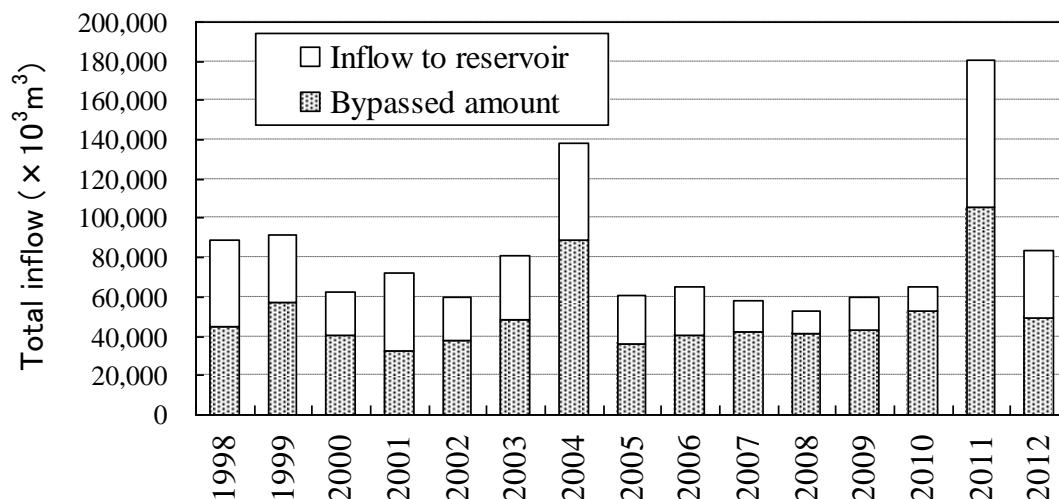
Figure 3: Annual total inflow
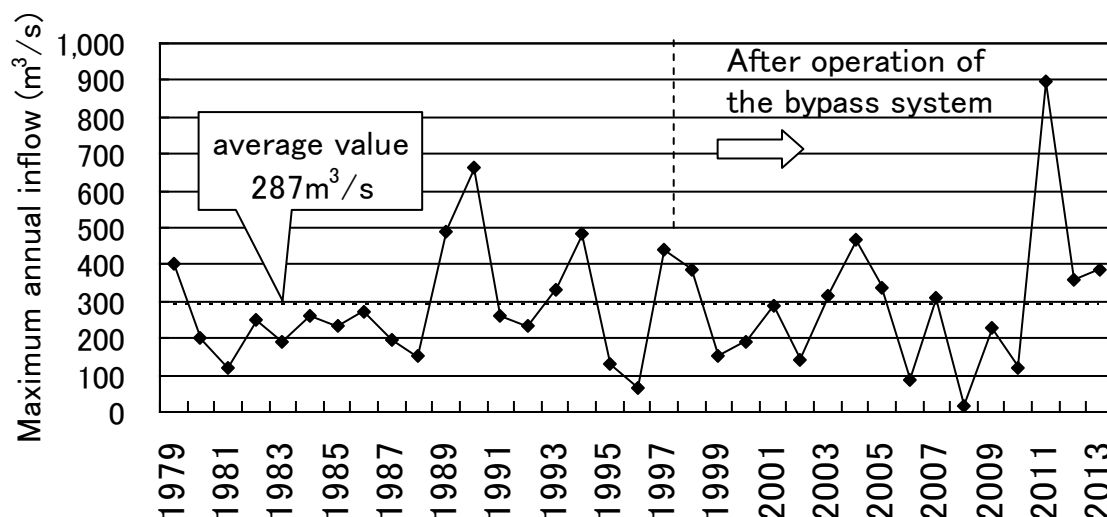
Figure 4: Maximum annual inflow at the Asahi Dam

In the meantime, it was estimated that 80% of the total sediment at the Asahi Dam that would have deposited without the bypass system was bypassed downstream. Thus, sedimentation was reduced. The estimate was made by calculating the volume of bed load that reached the diversion weir using a bed load equation (Ashida-Michiue Formula) and assuming that the total volume would be bypassed. For details, refer to Harada *et al.* (1997), Kataoka (2000), Doi (2005) and Fukuroi (2012).

Figure5 shows changes in sedimentation volume (bed elevation) and in bed material grain size distribution downstream of the reservoir in order to indicate changes in rivers downstream of the reservoir owing to the operation of the bypass system.

The changes in downstream sedimentation volume (bed elevation) show that bed elevations in downstream channels had repeatedly increased or decreased and basically

24

stabilized but that sedimentation volume increased to approximately 200,000 m^3 due to landslides caused by a flood of 2011.

Focus was placed on the changes in grain size distribution downstream of the reservoir. Fine grained fractions increased since the commencement of bypass operation. It is thus assumed that sediment was supplied downstream of the reservoir by the bypass system and river condition is becoming close to that before the construction of the dam.
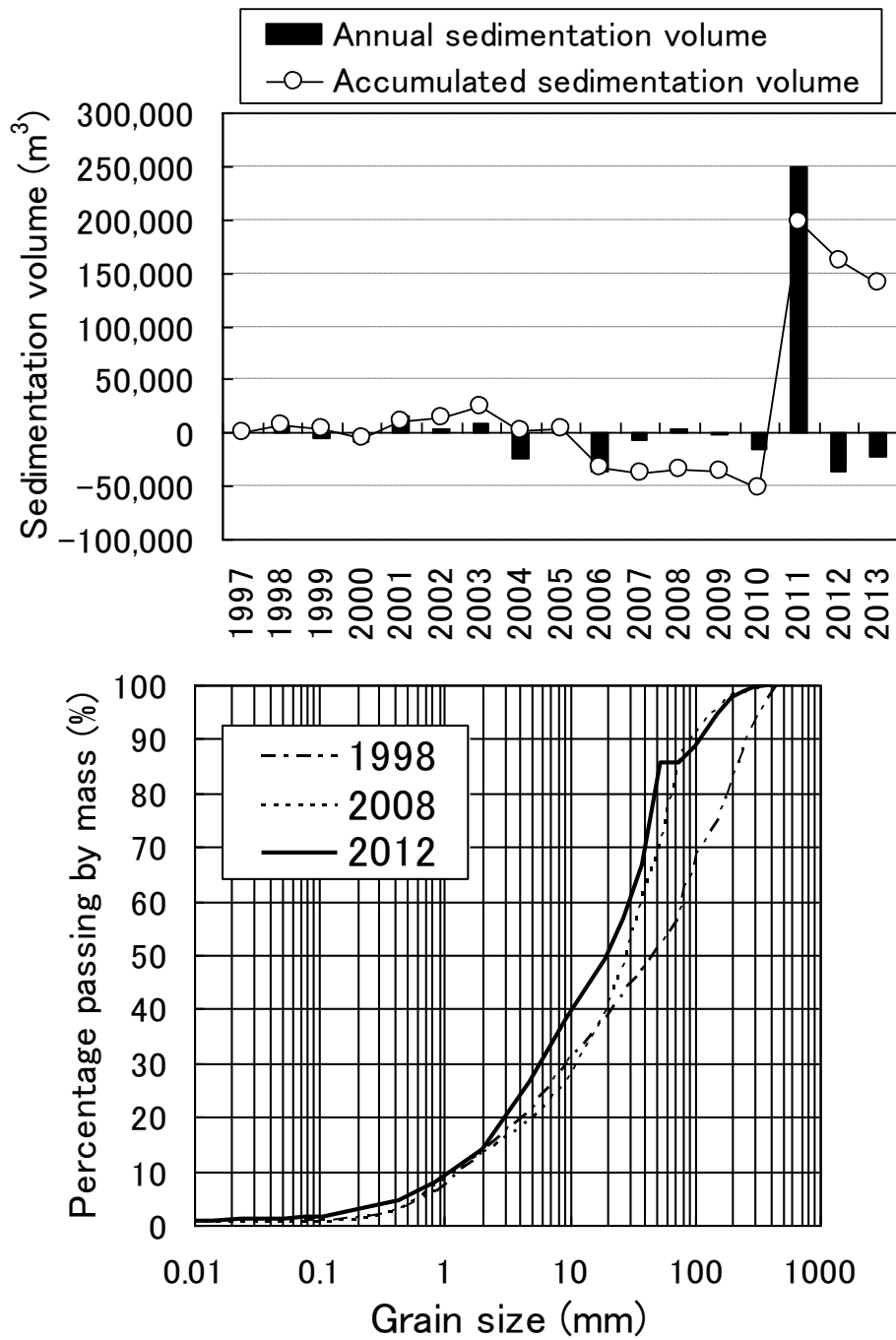
Figure 5: Changes in rivers downstream of Asahi Dam

4 Abrasion of sediment bypass

When designing a bypass tunnel, concrete strength and abrasion allowance are determined based on the results of abrasion prediction and considering the scale of repair. The objective is to reflect the influences of sediment transport on abrasion. In reality, however, predicting the distribution and volume of abrasion is difficult because they vary from place to place. First, the intake where severe abrasion was evidently expected to occur was reinforced with steel plates. The tunnel section was constructed using the concrete of a uniform strength throughout except at part of the downstream end.

It has been known through repeated repair during 15 years of service that the distribution of abrasion tends to show a particular pattern. In addition, knowledge important to the control of abrasion was also obtained based on the results of monitoring of reinforcing materials in trial constructions. These were used to develop efficient measures to control the abrasion of the bypass tunnel.

4.1 Prediction of abrasion in the design phase

In the area upstream of the Asahi Dam, granites are distributed and granite boulders have deposited on the river bed. The bed materials at the bypass intake had a mean grain diameter of 50 mm and a maximum diameter of 300 mm. It was assumed that the sediment of the size flowed through the tunnel.

For predicting abrasion in the design phase, an Ishibashi's formula shown below (Ishibashi (1983)) was used.

$$V = C_1 \times E_t + C_2 \times W_t \qquad\qquad [1]$$

Where, V is the volume of abrasion (damage) (m^3), C_1 is the coefficient of damage by impact (m^2/N), C_2 is the coefficient of abrasion due to friction (m^2/N), E_t is the total kinetic energy of gravel acting on the channel bed (N x m), and W_t is the total work done by abrasive force. (N x m).

The mean thicknesses of annual abrasion of concrete and steel were estimated at 40 to 50 mm/year and 0.2 mm/year, respectively. As a result, the volume of abrasion of invert concrete was sufficient for repair. The tunnel invert was therefore lined with concrete (design strength: 36 N/mm^2 and lining thickness: 40 cm) to incorporate abrasion allowance.

4.2 Actual abrasion and abrasion phenomenon

Described below are the results of observation of actual abrasion at the steel-plate-applied intake and in the tunnel section since the commencement of bypass system operation.

4.2.1 Steel plates at intake

The intake of the bypass tunnel was lined with steel plates because the severest abrasion was expected. Damage was predominant on the right bank side in the steel-plate-applied area. Repair has been made three times in this area since the commencement of operation. Damage was predominant in this repaired area because the slope changed from sharp to moderate (Figure 6) and sediment likely flowed on the right bank side. After the flood of 2011, repair was made in a wide area mainly on the right bank side. Frequency of repair has, however, been much less than in the tunnel section since the commencement of bypass operation.
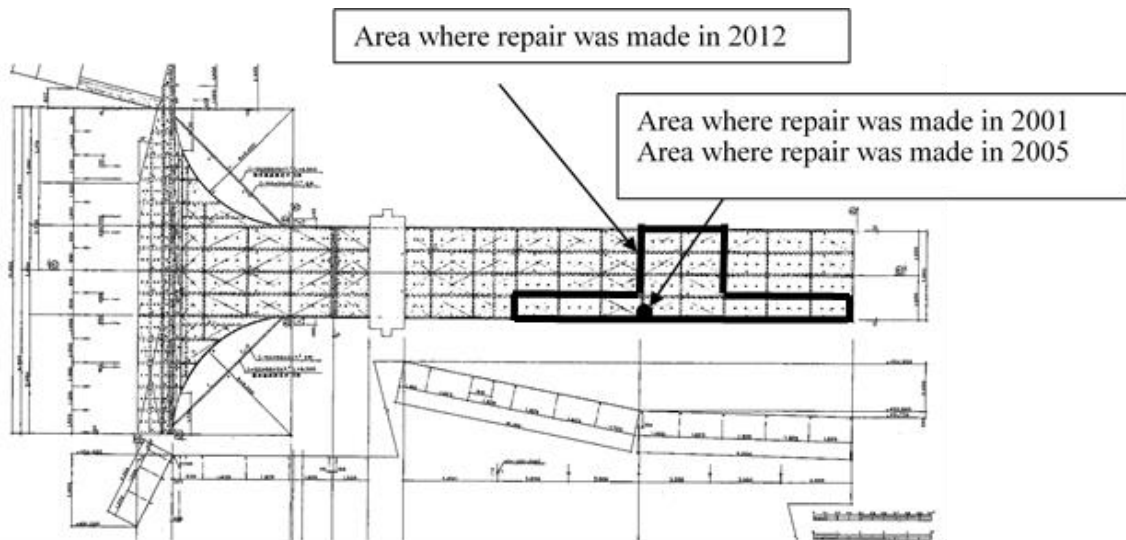

Figure 6: Areas repaired with steel plates at the intake

4.2.2 Tunnel section

Abrasion was observed nearly throughout the invert in the tunnel section. Repair was made periodically using high-strength concrete (design strength: 70 N/mm^2). From a viewpoint of tunnel structure, fracture of reinforcement in the invert was allowed. The invert was repaired before the rock was exposed to prevent adverse effects on the sidewalls and arch. Repair was, however, made on a priority basis before the fracture of reinforcement over a length of approximately 100 m from the intake and because the invert was important to tunnel structure.

Sidewalls were worn slightly in areas at low elevations. In the arch, long-term cracking and exposure of reinforcement were observed in some areas. Because it was unlikely that sediment of the grain size contributing to abrasion reached the arch, these phenomena were attributed to the effects of ordinary deterioration.

The distribution and volume of abrasion in the invert were identified as abrasion was predominant in the invert. The cumulative abrasion since the commencement of bypass operation is shown using contours to verify the tendency of planar distribution of

abrasion (Figure 7). The cumulative abrasion is the accumulation of abrasion calculated based on the measurement results. In the places where repair was made, however, abrasion of concrete that was additionally placed by repair was accumulated. The distribution of cumulative abrasion shows a certain planar tendency. The depth of abrasion is locally larger near the tunnel outlet than near the tunnel intake. In the transverse direction, abrasion was predominant on the right bank side at the intake and on the left bank side at the outlet. The maximum cumulative abrasion depth on the left bank side at the outlet was largest at 1272 mm. The tendency shows that the sediment does not flow uniformly in the transverse direction but flows in a certain pattern because the tunnel has a channel alignment that bends leftward from the midpoint. In other words, bed load concentrate on the right bank side at the intake and then on the left bank side downstream of the bend owing to the secondary flow created by bending, resulting in increase in abrasion volume. Abrasion depth was larger at the outlet than at the intake also because secondary flow was more likely to develop in the bend than at the intake and consequently the points of passing sediment flow were concentrated more.
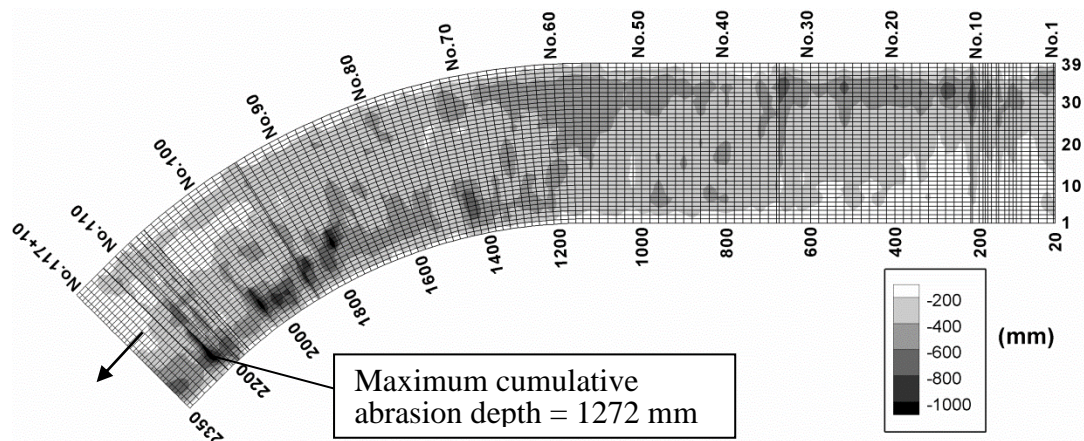

Figure 7: Cumulative abrasion in the tunnel invert (sum of abrasion between the start of bypass operation and November 2011)

In order to quantitatively evaluate abrasion, the results of measurement of the volume of sediment that passed the bypass tunnel, volume of abrasion in the tunnel invert and the volume of materials used for repair are shown in Figure 8.

28
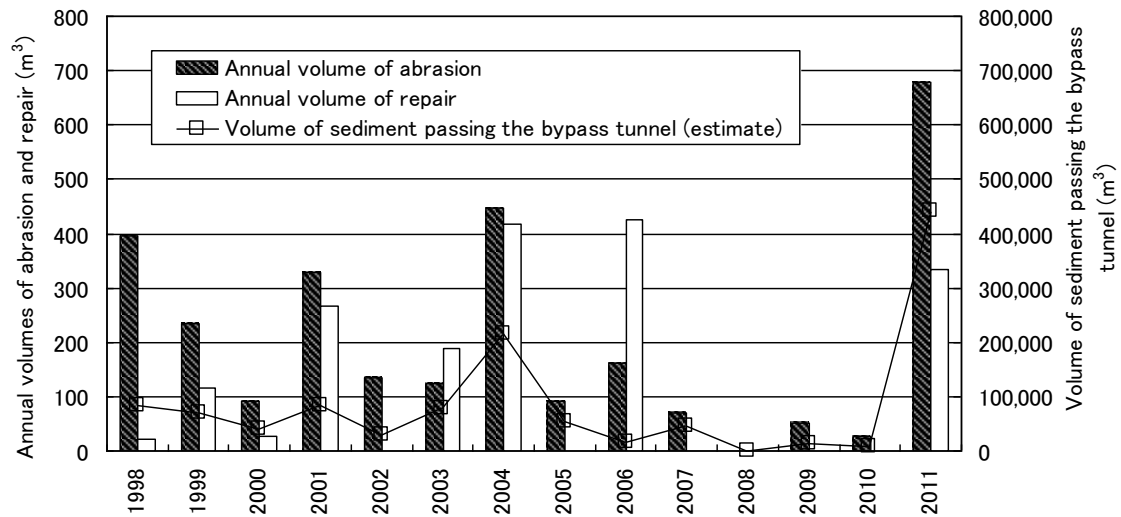
Figure 8: Annual volumes of abrasion and repair

The changes in abrasion volume affected by the volume of sediment passing the bypass tunnel were indicated by the relation between annual volume of abrasion and sediment load in the bypass tunnel (annual abrasion volume (m³/year)/sediment load in the bypass tunnel (m³/year) (Figure 9).
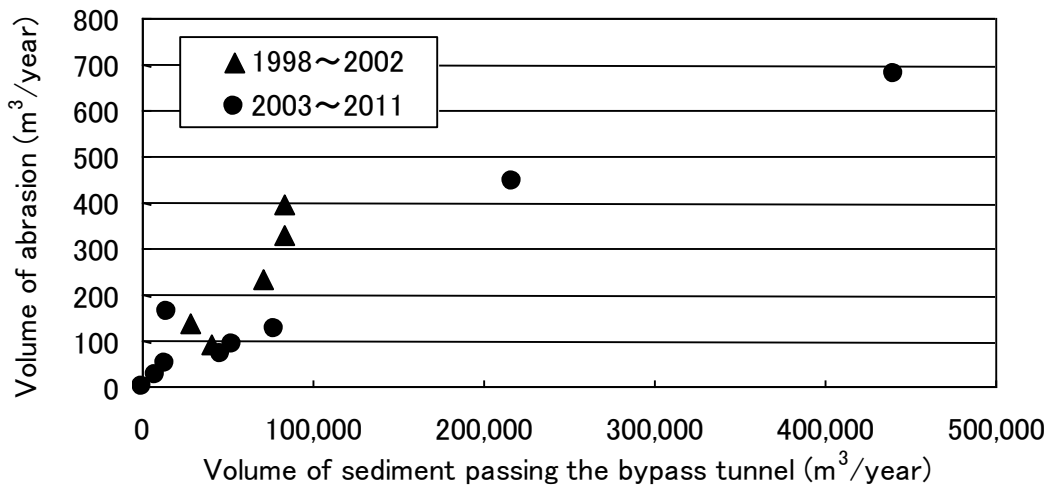
Figure 9: Relationship between the volumes of abrasion and sediment passing the bypass tunnel

The volume of abrasion tends to increase nearly in proportion to the volume of sediment that passed the bypass tunnel. The volume of abrasion was highest in 2011 when the maximum flow was recorded. The percentage of high-strength concrete increased on the invert surface of the bypass tunnel owing to periodical repair (Figure 10). Figure 9 shows that the volume of abrasion decreased relative to the volume of sediment that passed the bypass tunnel in 2003 when the percentage of high-strength concrete exceeded 70% and in subsequent years. In addition, the planar distribution of abrasion

was not affected by the volume of passing sediment, and abrasion was predominant in the convex bend in 2011 as well.
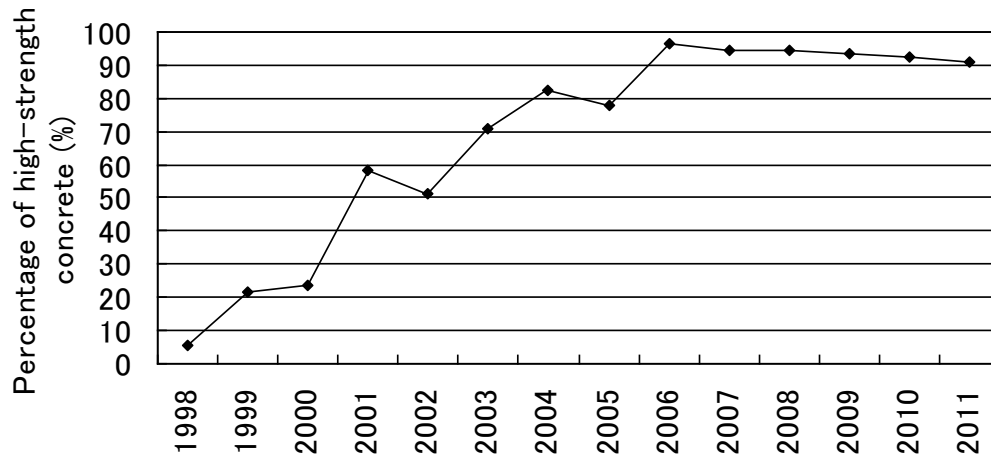
Figure 10: Percentage of high-strength concrete

4.3 Trial construction

Other materials than concrete have also been applied in the invert. Figure 11 shows how they were arranged. As the reinforcing materials, high-strength precast panels, steel plates and stones, which had a good record as materials highly resistant to abrasion, and resins with a low modulus of elasticity were selected. The abrasion resistance of respective materials was tested. Nearly all of the materials were greatly worn or delaminated in a few years after construction. It was assumed that abrasion progressed from the joint of the material, creating a weak point and that abrasion rapidly progressed to the reinforcing material or the material was delaminate at once owing to the impact of gravel or for other reasons. In 2013, an abrasion-resistant protective material made of rubber was applied on a trial basis. The condition was verified ten months after construction. As a result, it was found that the volume of abrasion was greater in the bypass tunnel than in Sabo Dams as the mean abrasion volume was 0.7 to 1.1 mm/year in the bypass tunnel while actual mean abrasion volume in Sabo Dams was 0.1 to 0.3 mm/year.

Figure 11: Locations of materials applied in trial construction

4.4 Abrasion control measures

Concrete has been adopted to control abrasion because of the availability of repair materials and ease of construction. In order to increase the efficiency of repair that was repeated periodically, new repair methods were examined based on the results of past abrasion control. In this study, repair methods wer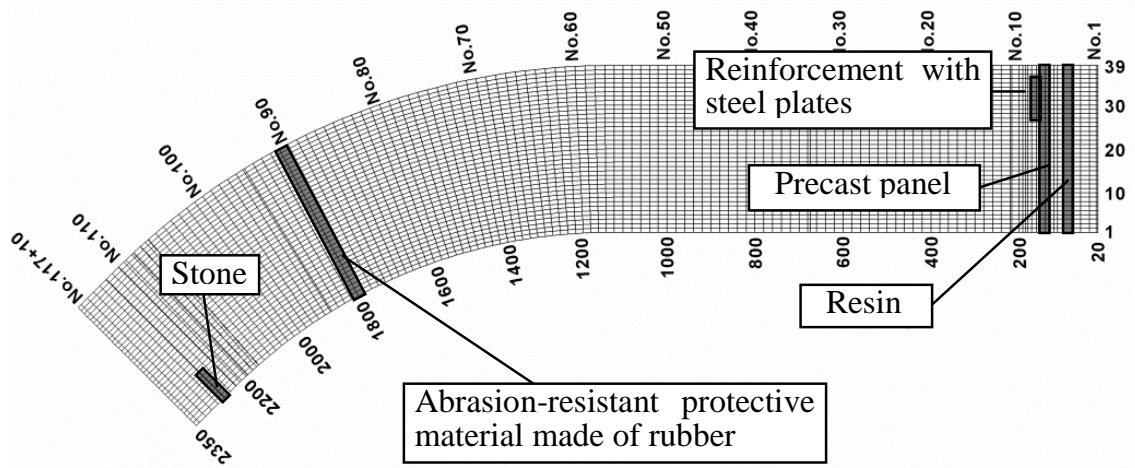e selected on the assumption that the design cross section should be maintained inasmuch as possible as in the past because the hydraulic stability of cross section that changed with the progress of abrasion was unknown.

The abrasion control methods are selected from the trial construction proven to be useful in preventing abrasion at Sabo Dams or other structures as described above. These methods were compared with one another in terms of life-cycle cost. Combinations of repair methods were examined that were fit for the location considering the distribution and volume of abrasion at areas currently subjected to abrasion, using the ease of construction, cost and the frequency of repair as parameters. It is important to consider that the volume of abrasion is larger in the tunnel than the actual volume in other places such as Sabo Dams and to apply careful treatment at the joint in view of the past damage to materials.

5 Conclusions

This paper, aimed at increasing the efficiency of abrasion control that is repeated periodically, described the distribution and volume of abrasion in a bypass tunnel. As a result, it was found that efficient measures could be taken by selecting separate methods in the areas with predominant abrasion and in other areas. The results of trial construction could serve as basic data for determining the types of repair materials and the frequency of repair because they showed the importance of treatment at the joint a

31

weak point in abrasion control, and that the bypass tunnel had larger volume of abrasion than Sabo Dams and was placed under a severe condition.

In the future, efficient repair methods will be selected for maintenance using the life-cycle cost as a parameter after due consideration to abrasion phenomenon.

References

Doi, H. (2005). Reservoir sedimentation management at the Dashidaira and Asahi Dams. *International Workshop on Sediment Management for Hydro Projects*.

Fukuroi, H. (2012). Damage from Typhoon Talas to Civil Engineering Structures for Hydropower Stations and the Effect of the Sediment Bypass System at Asahi Dam. *24th ICOLD Congress*.

Harada, M., Terada, M., Kokubo, J. (1997). Planning and hydraulic design of bypass tunnel for sluicing sediments past Asahi reservoir. *19th ICOLD Congress*.

Ishibashi, T. (1983). A hydraulic study on protection for erosion of sediment flush equipment of dams. *Journal of Hydraulic,* No.334.

Kataoka, K. (2000). An overview of sediment bypassing operation in Asahi reservoir. *An overview of sediment bypassing operation in Asahi reservoir*.

Authors

Hiroshi Nakajima (corresponding Author)
Division of operation and maintenance, Centers for civil engineering and architectures, Kansai Electric Power Co., Inc.
Email: nakajima.hiroshi@c3.kepco.co.jp

Yusuke Otsubo
Division of operation and maintenance, Centers for civil engineering and architectures, Kansai Electric Power Co., Inc.

Yuji Omoto
River Eng. Group, Newjec, Inc.

Operations of the sediment bypass tunnel and examination of the auxiliary sedimentation measure facility at Miwa Dam

Toshiyuki Sakurai, Keiji Kobayashi

Abstract

After construction of Miwa dam, sedimentation due to a large amount of sediment inflow during floods was a continuing problem. In order to cope with this sedimentation problem, a redevelopment project has been implemented. Sedimentation measures consist of the sediment bypass, sediment excavation and auxiliary sedimentation measure. Construction of the sediment bypass facility and sediment excavation were already completed. Examination of auxiliary sedimentation measure facility, a new approach to complement functions of sediment bypass, is in progress. Sediment accumulated in Miwa dam reservoir is characterized by a large proportion of fine particle diameter components. Therefore, the sediment bypass facility has been specifically designed to bypass only the fine sediment (wash load). In this paper, we explain an overview of the sediment bypass facility and report the results of the operations of the facility. In addition, we also report about the examination situation of the auxiliary facility.

1   Introduction

Miwa Dam is a multipurpose dam that the Ministry of Land, Infrastructure and Transport managed, built at Mibu River, the largest tributary of the Tenryu River water system, in 1959. The purposes of Miwa dam are power generation, irrigation water supply and flood control. The location and specifications of Miwa dam are shown in Figure 1 and Table 1.

Tenryu River flows near the Median Tectonic Line, so its sediment production volume is very large. In particular, during floods, a large amount of sediment discharge occurs. In the sediment management plan that was made at the time of construction of Miwa dam, sedimentation capacity of 6.59 million m^3 has been kept in the reservoir. This amount corresponds to 40 times the predicted annual sedimentation amount at that time. However, as shown in Figure 2, a large amount of sedimentation had occurred often, especially between 1982 and 1983, when large-scale floods occurred for two consecutive years, and about 6 million m^3 of sediment was deposited in two years. From the results of the previous boring survey, the percentage of clay and silt occupied in the

Miwa dam reservoir was estimated to be about 90%. An important characteristic of Miwa dam sedimentation is its large proportion of fine sediment. Excavation of sediment has been implemented since 1966, but large amounts of sediment have been difficult to deal with. Therefore, fundamental sedimentation measures were required.
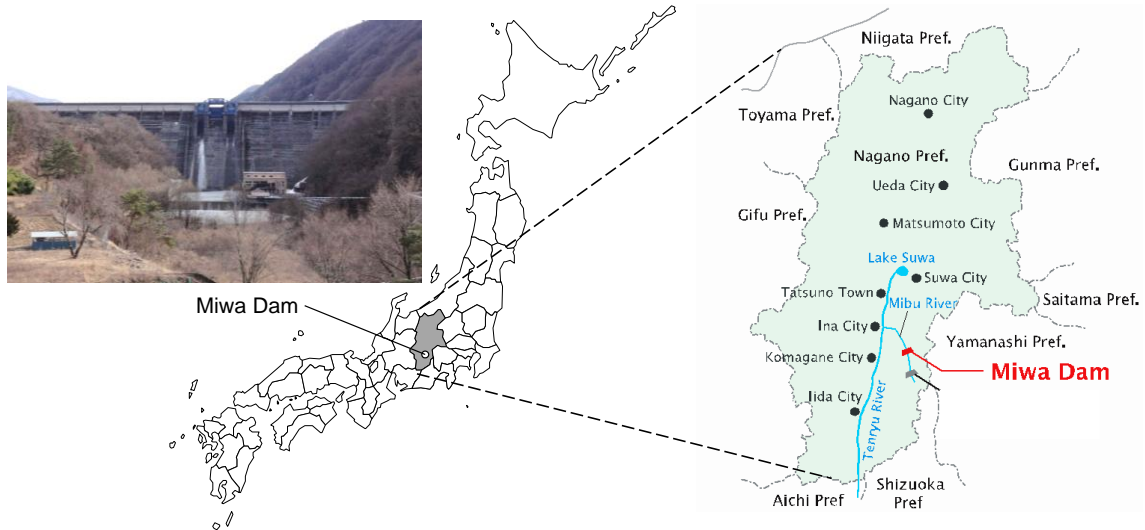
Figure 1: Location of Miwa dam

Table 1: Specifications of Miwa Dam

Reservoir		Dam	
Catchment area	311.1km^2	Type	Concrete gravity dam
Total storage capacity	29,952,000m^3	Height	69.1m
Effective storage capacity	20,745,000m^3	Crest length	367.5m
Dead storage capacity	2,621,000m^3	Emergency Spillway	Crest radial gate: 1
Storage capacity for sedimentation	6,586,000m^3	Flood control spillway	Orifice radial gates: 2
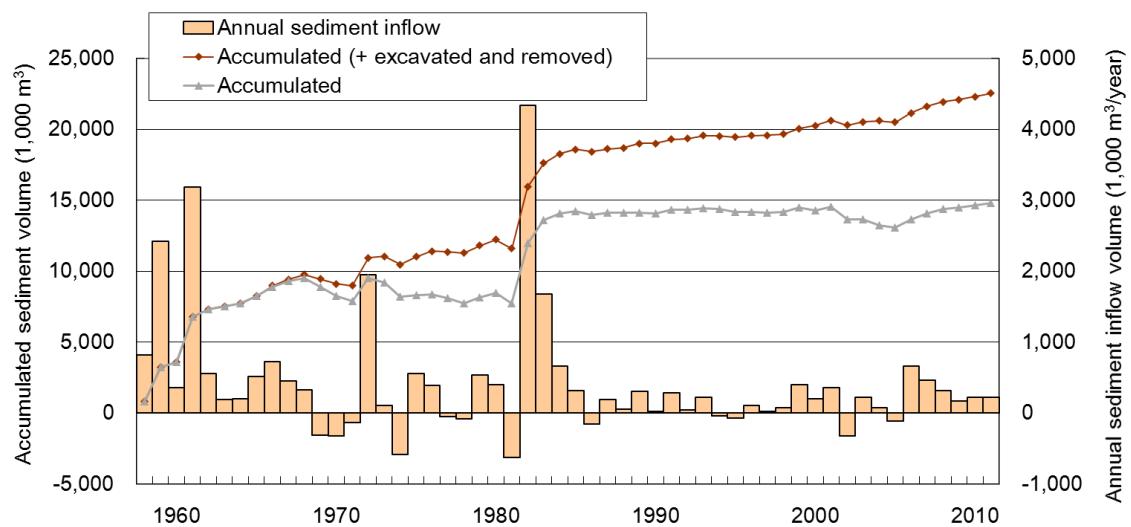
Figure 2: Time series of the annual sediment inflow volume and sediment deposit volume in Miwa dam

For the purpose of sedimentation problem solving and flood control enhancements of Miwa dam, redevelopment projects have been implemented since 1989. These redevelopment projects are composed of three measures: "sediment bypass", "sediment excavation" and "auxiliary sedimentation measure". The sediment management plans of Miwa dam have been reviewed several times, and the planned average annual sediment budget at the present time is shown in Figure 3. Sediment bypass is planned to bypass 43% of the inflow sediment to downstream and has been constructed in 2005. Sediment excavation was completed in 2005. The removal of sediment volume was about 2 million m^3. The auxiliary sedimentation measure is a method for discharging sediment deposited in the reservoir by passing it through the bypass facility to the downstream river. It is currently under examination. In this paper, we report the operational situation of the completed sediment bypass facility (Sumi *et al.* (2011, 2012), Kantoush *et al.* (2011) and Nohara *et al.* (2013)) as well as the progress of examination for the auxiliary sedimentation measure facility.
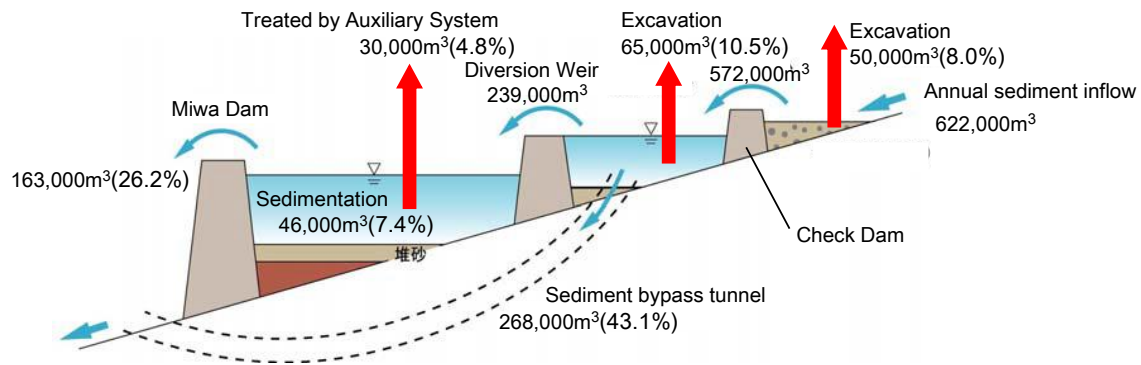
Figure 3: Average annual sediment budget in the sediment management plan of Miwa Dam

2   Operation of the sediment bypass tunnel

2.1   Overview of the sediment bypass tunnel

An overview of the Miwa dam's sediment bypass tunnel is shown in Figure 4 and Figure 5. The facility consists of the following elements: check dam (height: 10.2 m, sedimentation capacity: 200,000 m^3), diversion weir (height: 20.5 m, sedimentation capacity: 520,000 m^3), inflow facility, tunnel (length: 4,308 m, maximum flow rate: 300 m^3/s) and outflow facility. Because the sediments of Miwa dam contains such large amounts of fine sediment, in order to prevent abrasion and damage to the bypass tunnel facility, a plan to bypass only the fine sediment was made.

The coarse sediment is firstly captured in the check dam. The sediment exceeding the check dam, is captured by the trap weir (submerged weir) which is installed in the inflow facility upstream. Captured sediment is excavated and is effectively utilized as concrete aggregates, banking material and so on or conveyed to disposal yard.

Upstream of the inlet, in order to prevent driftwood from flowing into the tunnel, log boom consisting of steel pipe in an arc shape is installed. Two gates were installed to control the flow rate in the inflow facility. The side overflow weir was installed at the gate downstream to simplify gate operations in the case of a large flood. The weir is used to control the bypass flow rate to 300 m^3/s, with the gates fully open situation. Cross-sectional shape of the tunnel is a horseshoe shape with 7 m height and 7.8 m width. Its longitudinal slope is 1/100. At the time of flow rate of 300 m^3/s, the tunnel is designed to make an open channel flow with a velocity of 10.8 m/s. In order to prevent scouring of downstream rivers from bypass water, semi-circular pool type energy dissipator was installed at the outflow facility.

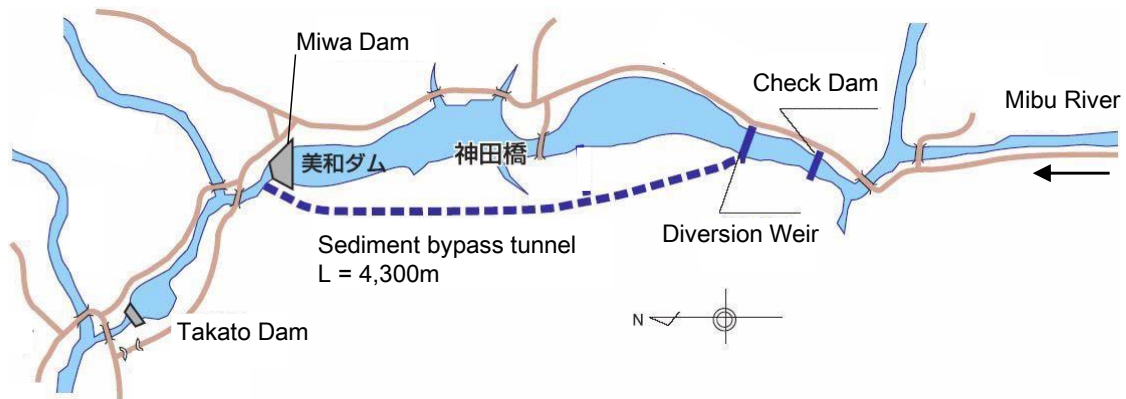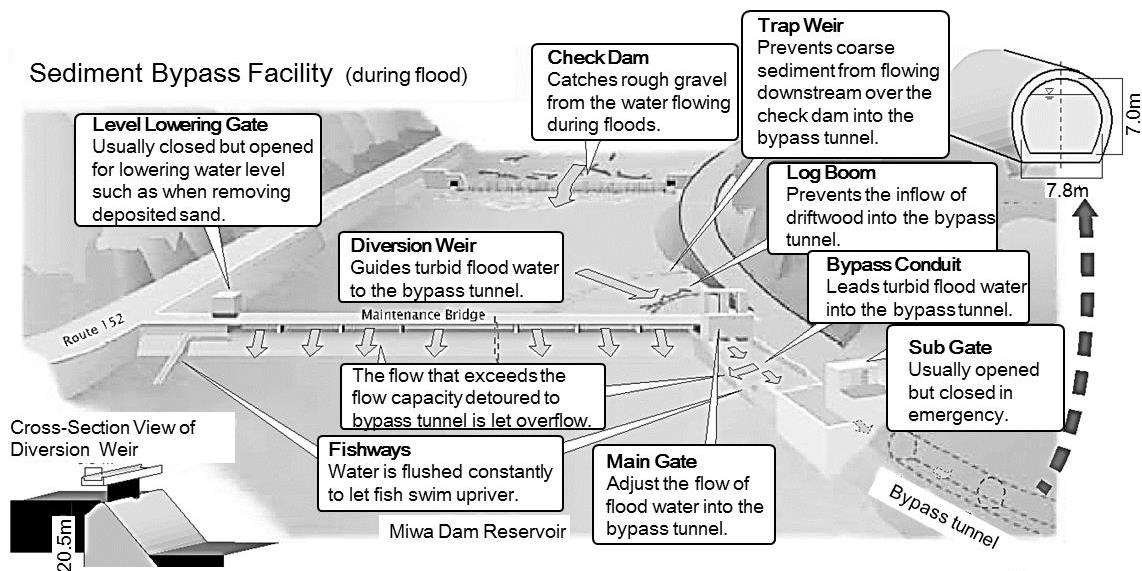Figure 4: Outline of the sediment bypass facility (plain view)

Figure 5: Outline of sediment bypass facility (detail image of each element)

Operations of sediment bypass tunnel are performed in conjunction with the flood control and water utilization operations. Specifically, the bypass operation starts when the inflow is expected to exceed 100 m^3/s. The maximum bypass discharge is 300 m^3/s

36

(Figure 6). Bypass discharge is finished when the inflow is beyond the peak and is less than 100 m^3/s. During bypass discharge, a power generation discharge of 25 m^3/s is also performed. As for operation methods, appropriate methods are determined through the reviewing of feedback results from the monitoring research.

2.2 Operation situation of the sediment bypass tunnel and research methods

The reservoir water level and inflow discharge rate of Miwa dam from 2006 to 2008 is shown in Figure 7. During this time, the sediment bypass tunnel was in operation four times, for which the monitoring research was carried out.

Elements of the monitoring research were flow rate, water quality (Suspended Solids (SS) concentration, particle size distribution, and other water quality items), sedimentation, bed material, biological research and the situation of the riverbed.
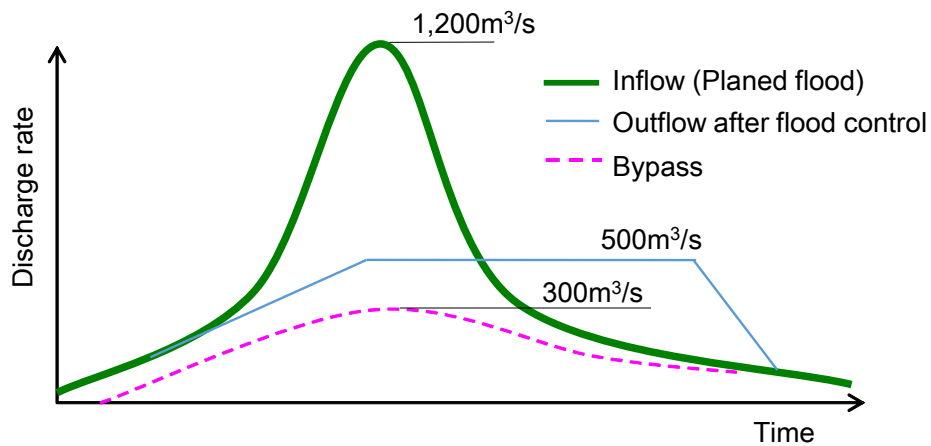
Figure 6: Image of flood control and bypass discharge

A summary of the four bypass discharges is shown in Table 2. Variation of the discharge rate and the SS concentration over time during the flood of September 2007 which was the largest flood for three years, is indicated in Figure 8.

All bypass discharges were carried out during a flood, however the floods of July 2007 and June 2008 were relatively small scale. Especially during the flood in June 2008, in order to recover the water utilization capacity, the bypass discharge amount was small and the bypass discharge time was short. Figure 8 shows that the SS concentration of inflow during peak time is a fairly large value of 25,000 mg/L. The SS concentration of bypass discharge shows a value similar to that of the inflow water, and is greater than the value of the spillway discharge and the power generation discharge at the dam site. Miwa dam's bypass facility is considered to be able to discharge sediment at approximately the same proportion of flow rate of water.
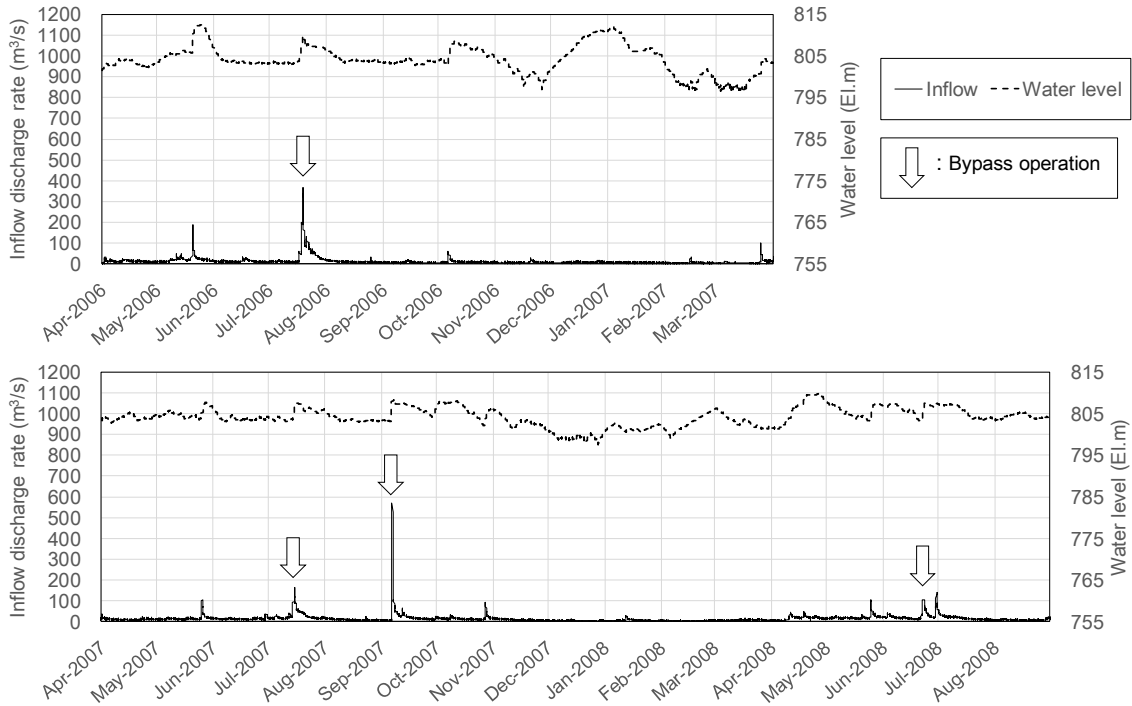
Figure 7: Time series of inflow discharge rate and reservoir water level

Table 2: Summary of bypass discharges during floods

Flood	Basin precipitation	Max. inflow discharge	Return period of flood	Max. bypass discharge	Duration of bypass operation
Jul. 2006	253mm	366m^3/s	5 year	242m^3/s	47 hours
Jul. 2007	117mm	166m^3/s	1 year	136m^3/s	35 hours
Sept. 2007	254mm	568m^3/s	11 year	262m^3/s	48 hours
Jun. 2008	144mm	107m^3/s	1 year	30m^3/s	7 hours
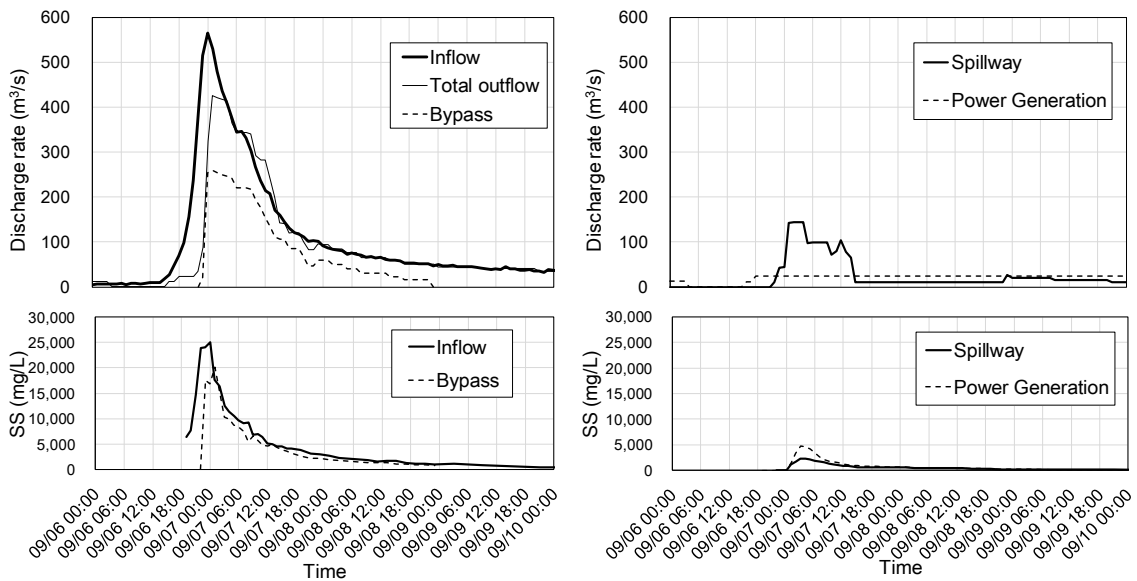
Figure 8: Time variation of inflow and outflow discharge of each facility and SS concentration during the flood of September 2007

38

2.3 Research results of sediment bypass operation

For 4 floods, the sediment budget and the percentage of wash load (sediment contained in the sample collected from surface water of flood flow, average particle size: about 0.017mm), which was calculated on the basis of observed results of flow rate and SS concentration, is shown in Table 3. Except for the flood in June 2008, in which the bypass discharge rate was very small, approximately 40 percent of the inflow wash load was bypassed. In fact, the storage operation was carried out to recover capacity for water utilization during the early terms of flood, but if it is assumed the operations for recovering water utilization capacity are carried out during the late term of the flood and also do not generate power, it has been estimated through simulations that it is possible to bypass about 70% of the inflow wash load.

Table 3: Sediment budget of wash load during a flood (void included)

| Flood	Inflow sediment volume during flood (m^3)	Deposit volume upstream of Diversion weir (m^3)		Bypassed sediment volume (m^3)		Deposit volume in the reservoir (m^3)		Discharged volume form the dam (m^3)	
Jul. 2006	325,650	58,120	18%	150,330	46%	96,750	30%	20,450	6%
Jul. 2007	36,990	5,050	14%	14,120	38%	13,690	37%	4,130	11%
Sept. 2007	461,600	57,270	12%	154,910	34%	230,800	50%	18,620	4%
Jun. 2008	12,630	2,600	21%	310	2%	6,810	54%	2,910	23%

The annual sediment budget including all particle sizes is shown in Table 4. It was calculated from the observation results of discharge rates and SS concentrations as well as sedimentation survey results. Bypass percentage in the actual operation was about 20%. This is a small value when compared to the planed bypass percentage of 43%, but about 320,000 m^3 of sediment was bypassed for three years. The sediment bypass facility has the ability to reduce the inflow sediment to the reservoir. The sediment trapped in the diversion weir upstream was approximately 630,000 m^3 for 3 years, and combined with a bypass, about 950,000 m^3 of the reservoir sediment inflow was prevented.

Table 4: Annual sediment budget including all particle sizes (void included)

Year	Annual inflow sediment volume (m^3)	Deposit volume upstream of Check dam (m^3)		Bypassed sediment volume (m^3)		Deposit volume in the reservoir (m^3)		Discharged volume form the dam (m^3)	
2006	705,000	200,000	28%	150,000	21%	324,000	46%	31,000	4%
2007	763,000	295,000	39%	169,000	22%	264,000	35%	35,000	5%
2008	384,000	137,000	36%	300	0%	230,000	60%	17,000	4%

Focusing on the function of the facility, the results of the investigation after bypass operations showed the effectiveness of the check dam and the trap weir upstream of bypass inlet, since coarse sediment was confirmed to not flow into the tunnel as designed. The log boom was able to prevent the entry of driftwood (Figure 9). Moreover,

in the bypass tunnel inner wall and energy dissipator, it was confirmed there was no abrasion or damage (Figure 9).

Considering the space of this paper, research results about water quality, biological research and downstream riverbed situation were not described in detail. From the research results however, no significant impact has been established. In the future, it is planned that investigations will be continued in order to confirm the long-term effects of sediment bypass.

Figure 9: Situation of each facility in sediment bypass, a) log boom during flood, b) inner wall of tunnel after flood, c) energy dissipator during flood

3 Examination of the auxiliary sedimentation measure facility

3.1 Overview of the auxiliary sedimentation measure facility

The function of the auxiliary sedimentation measure facility is to discharge sediment after the deposition of the sediment flowing into the reservoir beyond the diversion weir during sediment bypass operations.

Many alternative proposals have been examined as a draft of the auxiliary sedimentation measure. For example, there was a plan of dredging and soil improvement and transport it to the dumping, or discharging sediment via a suction pump to the dam downstream at the time of flood. According to the result from comparing these plans, at the present time, in terms of the cost, ease of operation and mechanical troubles risk during floods, a proposal to install the sediment stockyard upstream of the bypass tunnel inlet was judged advantageous. Examination of the stockyard plan has been carried out.

Specific details of the plan are as follows. First, a stockyard for storing the sediment is built at the diversion weir upstream. During normal times, sediment that had been dredged in the reservoir would be transported to the stockyard. Then, when performing the bypass discharge during floods, the sediment in the stockyards is eroded and flushed to the bypass tunnel by the tractive force of the water. The image of the facility is shown in Figure 10.
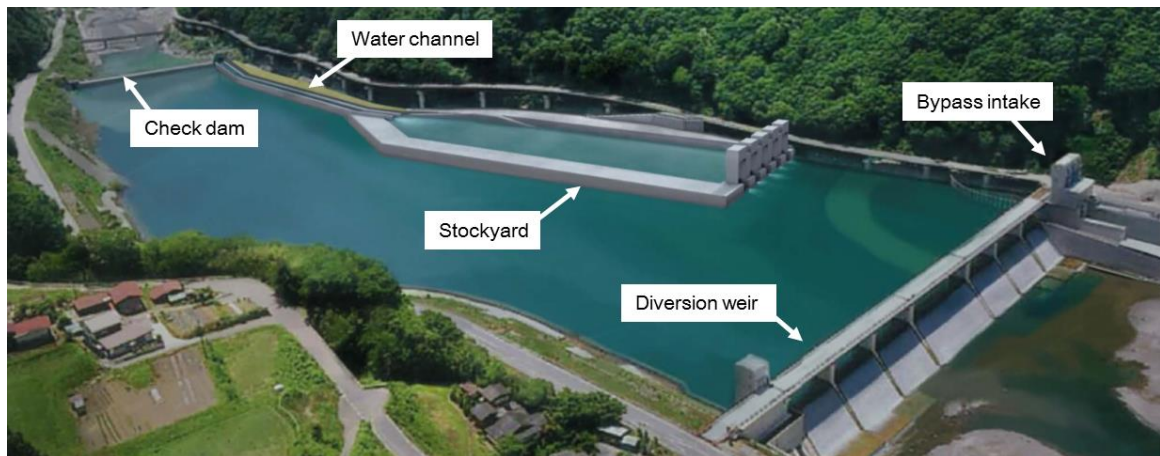
Figure 10: Image of the auxiliary sedimentation measure facility

3.2 Challenges and examination methods of the auxiliary sedimentation measure facility

The above-mentioned auxiliary sedimentation measure is an unprecedented new approach in Japan, the following challenges can be listed in order to put this technique into practical use.

- The shape of the stockyard should not affect the flow situation of the diversion weir upstream area.

- The bypass tunnel was designed to not transport the coarse sediment, so the coarse sediment stored in the stockyard should not flow down into the tunnel.

- Most of a sediment stored in the stockyard is assumed to be fine sediment with a viscosity, so it is necessary to understand the erosion condition of the sediment.

To examine the above challenges, hydraulic model experiments and numerical simulations using a plain two-dimensional model were carried out. The three-dimensional model of the upstream area of the diversion weir was scaled 1/50, the three-dimensional model of the stockyard was scaled 1/25, two-dimensional models for sediment erosion tests were scaled 1/15 and 1/5 in the experiments.

3.3 Results of the experiments

In this paper, we report the main examination results obtained in the experiments. Comparisons of the proposals for the shape of the stockyards have been examined by hydraulic experiments using a 1/50 scale model (Figure 11). As a result, the shape and the placement of the stockyard as shown in Figure 12 (width 40 m, length 220 m, height 5.5 m and installation of the central partition wall) was proposed.

a)

b)
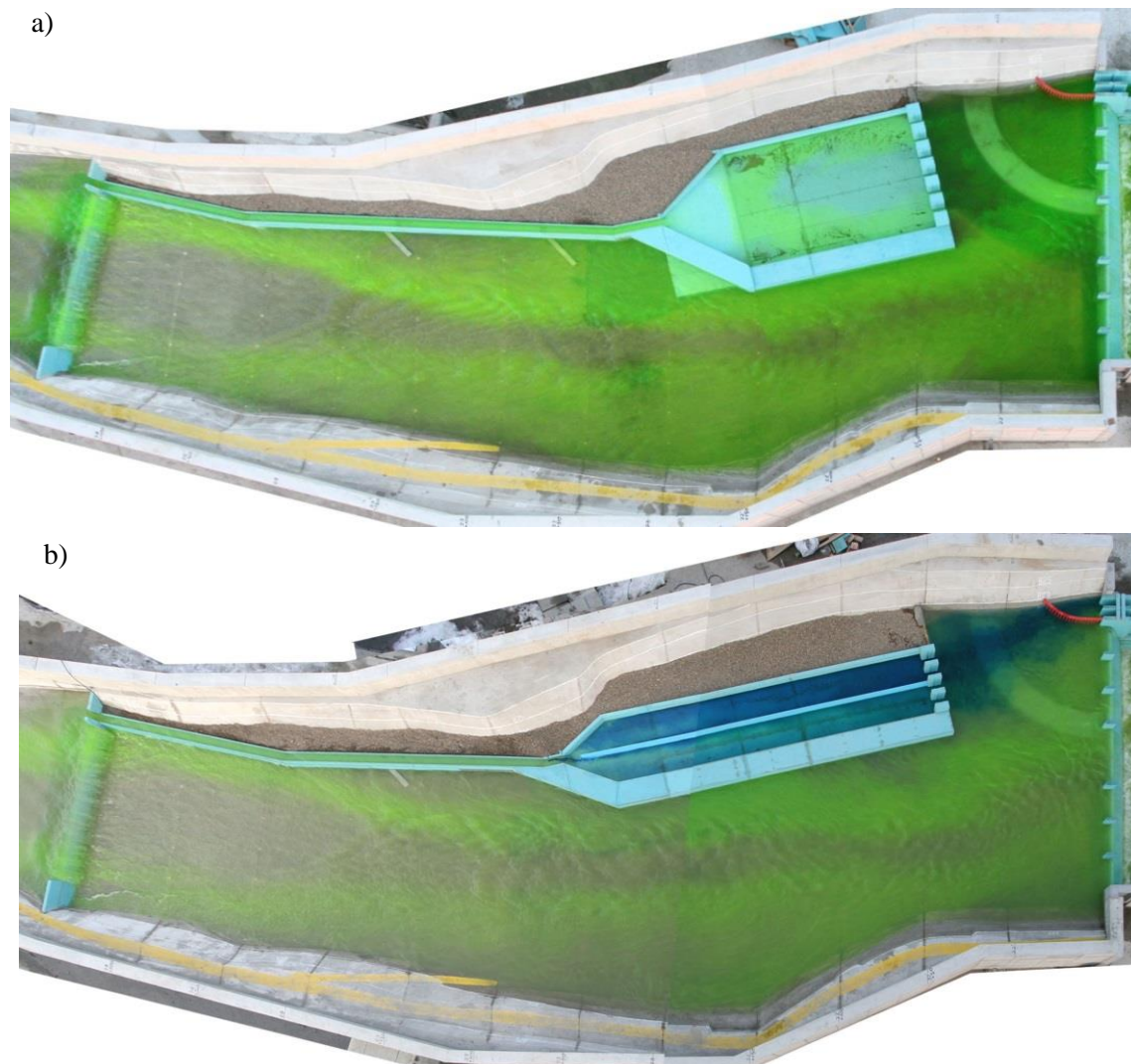
Figure 11: Examples of the experimental flow situation of the three-dimensional model of the scale 1/50
    a) draft shape of width 80 m, b) draft shape of width 40 m
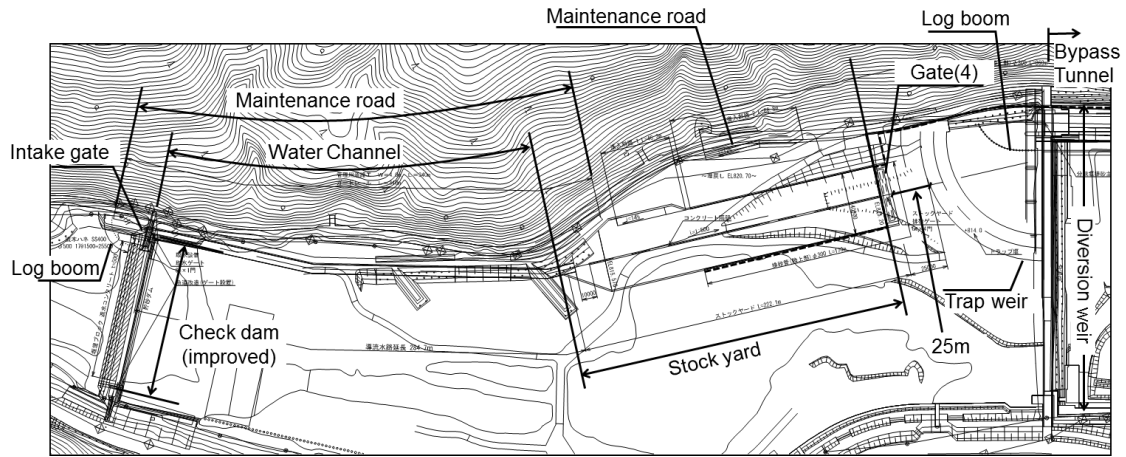
Figure 12: Proposal shape of the auxiliary sedimentation measure facility (plain view)

Figure 13: Situation of sediment erosion experiments a) scale 1/25, b) scale 1/15, c) scale 1/5

Through the sediment erosion experiments (Figure 13), it was confirmed that the erosion rate of the viscous sediment becomes larger as the model scale becomes larger, and progress states of viscous sediment differ (close to the mud flow state, step erosion, sheet erosion) depending on the state of the particle size distribution and consolidation. Information required for predicting erosion states of sediment was obtained. Assuming the sediment in the Miwa dam reservoir, from the resulting knowledge, it is considered to be possible to flush the sediment stored in stockyard to the bypass tunnel. In the future, examinations for detailed designs of gate equipment or operational methods of the facility and so on will be carried out.

4 Conclusion

Miwa Dam sediment bypass facility was built in 2005. As a result of the subsequent operation, it was confirmed that each facility functions almost as planned. It was also confirmed that it is possible to reduce the inflow volume of fine sediment to the dam reservoir.

The auxiliary sediment measure considered at Miwa dam is a new approach to complement the functions of sediment bypass. Particular facility specifications have been proposed by the experiments. For practical use of the facility, it is scheduled to examine the challenges remained.

References

Kantoush, S.A., Sumi T. and Murasaki, M. (2011). Evaluation of Sediment Bypass Efficiency by Flow Field and Sediment Concentration Monitoring Techniques, *Annual Journal of Hydraulic Engineering*, JSCE, Vol.55, S169-S174.

Nohara, D., Sumi, T. and Kantoush, S.A. (2013). Real-time sediment inflow prediction for sediment bypass operation at Miwa Dam in Japan, *Proceeding of the 12th International Symposium on River Sedimentation*, Advances in River Sediment Research, pp. 1211-1217

Sumi, T. and Kantoush, S.A. (2011). Comprehensive Sediment Management Strategies in Japan: Sediment bypass tunnels, *Proceedings of the 34th IAHR World Congress*, 1803-1810.

Sumi, T., Kantoush, S.A. and Suzuki, S. (2012). Performance of Miwa Dam Sediment Bypass Tunnel: Evaluation of Upstream and Downstream State and Bypassing Efficiency, *24th ICOLD Congress*, Kyoto, Q92-R38, pp.576-596.

Authors

Toshiyuki Sakurai (corresponding Author)
Senior Researcher of River and Dam Hydraulic Engineering Research Team,
Hydraulic Engineering Research Group,
Public Works Research Institute, Japan
Email: t-sakurai@pwri.go.jp

Keiji Kobayashi
Director, Mibugawa River Comprehensive Development Office,
Ministry of Land, Infrastructure, Transport and Tourism, Japan

Hydraulic examination of Koshibu dam's intake facilities for sediment bypass

Josuke Kashiwai, Shuji Kimura

Abstract

Koshibu dam's reservoir has been suffering from large amount of sediment inflow since the completion of the dam. Sediment bypass project was examined and employed as one of the main countermeasures to keep reservoir capacity against sedimentation. Since Koshibu dam has the purpose of flood control, outflow from the bypass tunnel should be controlled with a certain level of accuracy even in the flow down condition of sediment and driftwood. Hydraulic design of the bypass facilities was carefully carried out using hydraulic model tests especially for discharge related facilities. This paper introduces the outline of the project, the hydraulic design of discharge related facilities and the experimental way of hydraulic model tests to obtain the results. Bypass facilities of Koshibu dam are under construction toward the first operation at 2016.

1 Introduction

Koshibu dam is an arch type dam completed in 1969. Height of the dam is 105 m and the total capacity of reservoir is 58 million m^3, which is used for power generation, irrigation and flood control. Sedimentation capacity of 20 million m^3 is also included in the total capacity. 100 years sedimentation capacity is usually planned for sedimentation in Japan. Koshibu dam's capacity, however, has 50 years sedimentation, a half of the usual term.

Koshibu dam is located in Nagano prefecture, center part of Japan, known as the high mountainous and the large sediment yield country. Figure 1 shows the history of sedimentation volume of Koshibu dam. Excavation history is also shown in the figure. Excavation has been executed to cope with the requirement of construction materials and reduce the sedimentation progress. Two check dams were constructed at upstream areas in the reservoir to trap sand and gravel for easier removal. They were completed in 1977, and 1989.

Because of the consecutive hitting of strong typhoons, large amount of deposits were recorded in 1982 and 1983. Sediments of 240 million m^3 were accumulated in these years. In spite of efforts of removal, sedimentation has been gradually progressed in other years and reached to 85.5% of the sedimentation capacity. Sediment bypass method was examined in this situation to reduce sediment inflow to the reservoir.

45
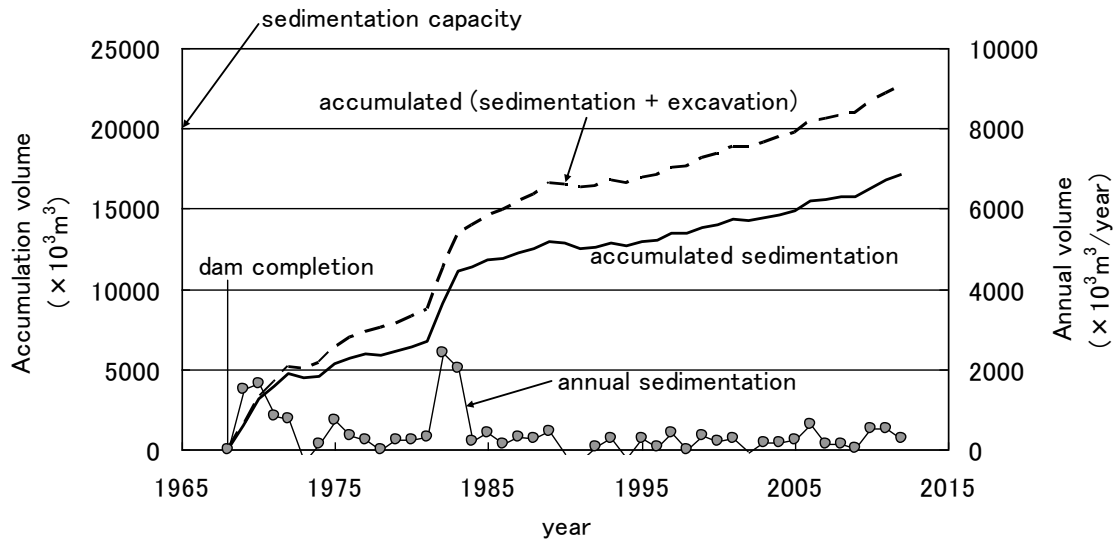
Figure 1: Histories of sedimentation and excavation volume at Koshibu dam

Since Koshibu dam has the purpose of flood control, outflow from the bypass tunnel is restricted by flood control operation. Also, outflow from the bypass tunnel should be controlled with a certain level of accuracy even in flow down condition of sediment and driftwood. This was considered one of the main subjects of the hydraulic design of Koshibu dam's sediment bypass facilities, especially for the intake structure. This paper will introduce the outline of the sediment bypass project and the hydraulic design of discharge related facilities of Koshibu dam, including intake structure. Examination of the design was carried out using hydraulic model tests.

2   Outline of sediment bypass facilities

Figure 2 shows the outline of Koshibu dam's sediment bypass facilities. Maximum discharge rate of 370 m³/s with sediments will flow down the bypass tunnel. Tunnel Length is about 4 km and slope is 1/50. Horseshoe arc with horizontal bottom is employed for the tunnel structure. Outflow from the tunnel outlet is spread by horizontal floor to reduce the energy concentration and falls into the river from the side slope.

Intake structure is located between the diversion weir and the check dam. The check dam is newly constructed for trapping relatively large sediments to use structural materials as used to be. One of the existing check dams is remodeled and used for a diversion weir to control water level at the intake. Design of surrounding intake structures includes some special technological considerations explained below.

46
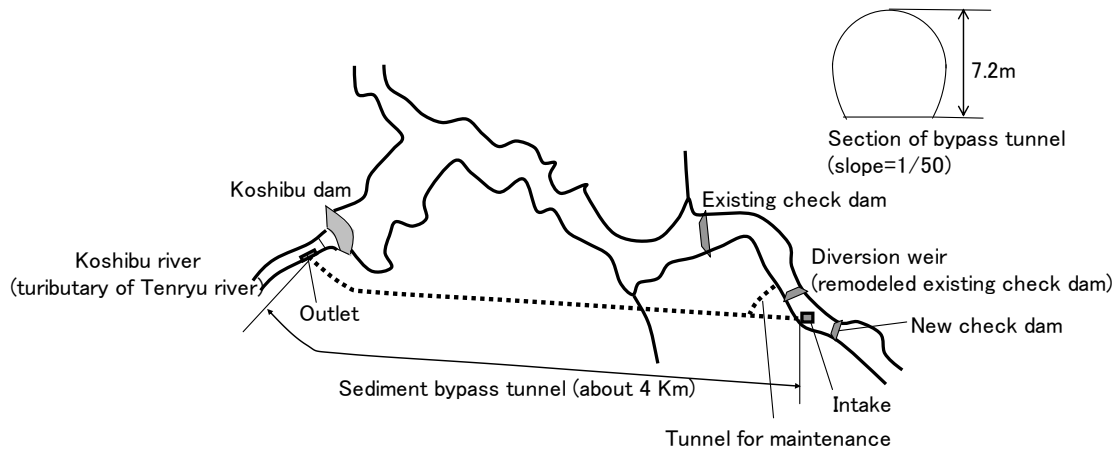
Figure 2: Outline of sediment bypass facilities of Koshibu dam

3 Discharge control and required design

3.1 Flood control method and bypass discharge

Flood control method of Koshibu dam is called constant ratio-constant discharge method. Before a peak inflow, increase of outflow is controlled in direct ratio to the discharge difference between inflow and flood control starting discharge rate (constant ratio operation). Then, outflow at the peak inflow is kept after the peak (constant discharge operation).

Figure 3 shows planning flood control (inflow and outflow) hydrographs of Koshibu dam's sediment bypass project. The flood was obtained through the examination for the river improvement principle of areas downstream. Return period of 100 years is employed in the principle. Flood control starting discharge rate is 200 m^3/s and maximum outflow is 370 m^3/s. Since the sediment bypass tunnel releases water to just downstream of the dam, outflow from the tunnel should be smaller than that of the flood control.
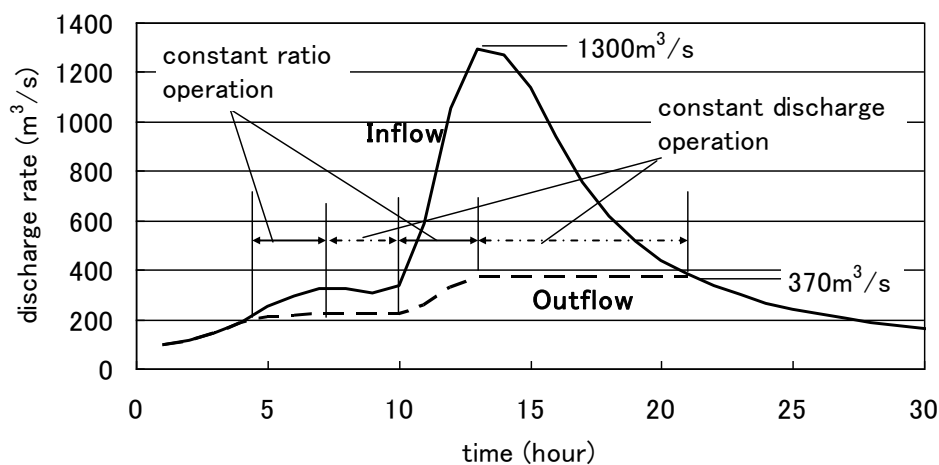
Figure 3: Planning hydrographs of Koshibu dam's sediment bypass project

Greater amount of sediments can be bypassed by larger bypass water discharge. Too much water flow bypassing, however, requires uneconomical costs for the facility construction. Economical examination was executed to find out the most effective design discharge of bypass facilities.
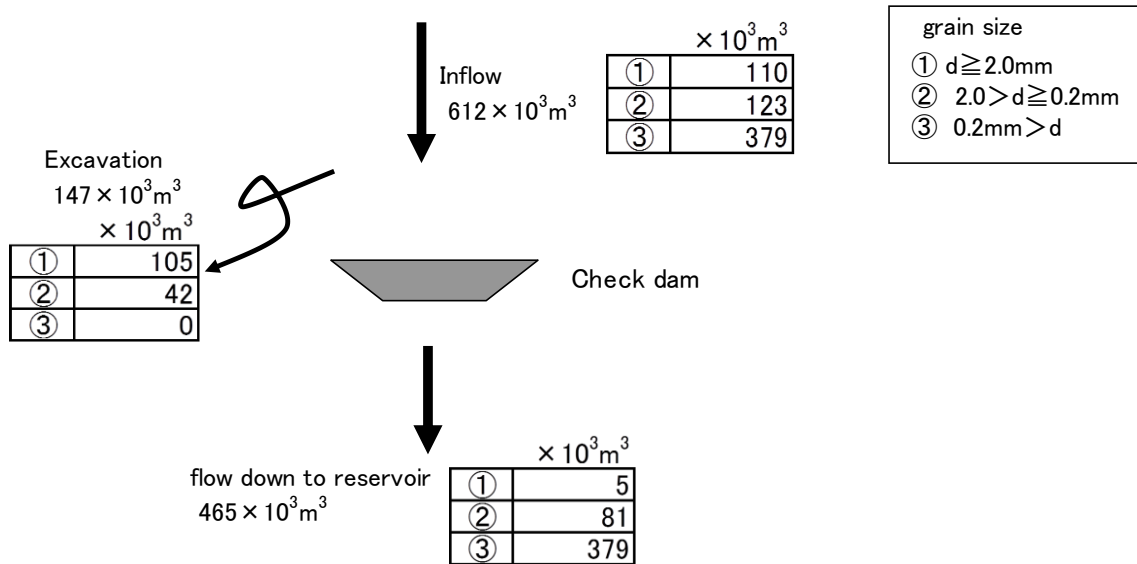
(a) without bypass facilities
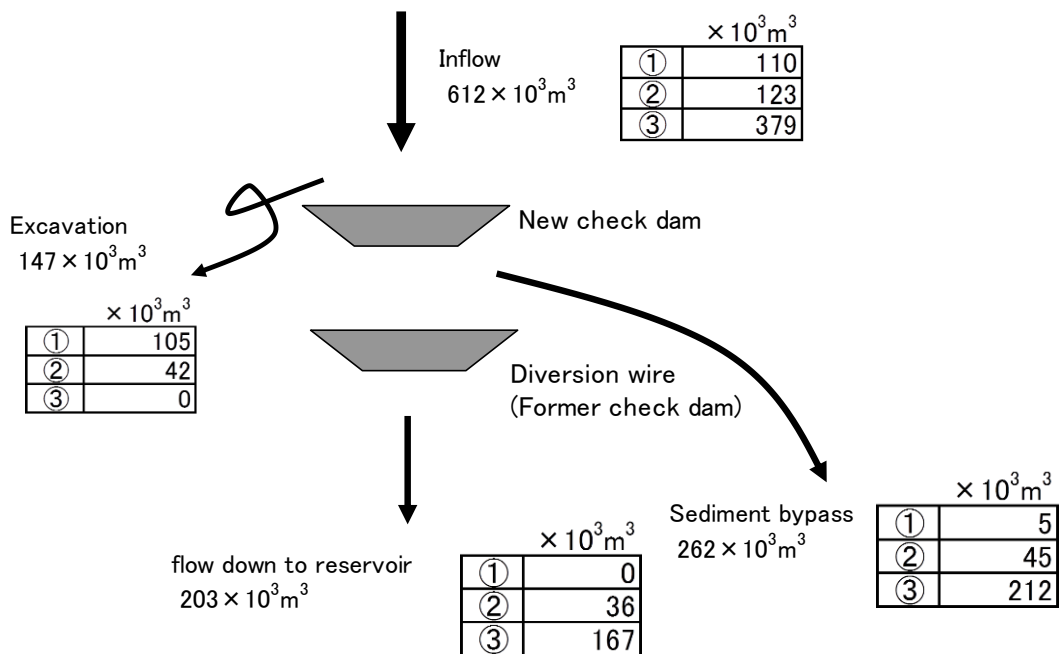
(b) with bypass facilities

Figure 4: Sediment flow with and without bypass facilities

Results of the examination showed that the most effective design discharge is same as the maximum outflow of planning flood control. Results were obtained through statistical analyses of water and sediments inflow, and hydraulic considerations about sediment diversion phenomena. In the examination, it was assumed that bypassed water discharge is decided in the same way of the constant ratio operation of the flood control, in the limitation that assumed design discharge rate is the maximum. Bypass starting water discharge of 80 m^3/s was also assumed. Discharge of fine sediments becomes to a certain level at 80 m^3/s, and correlation between water and sediment discharge becomes clear at the discharge.

Figure 4 shows the estimation results of sediment flow with and without bypass facilities. Annual average volumes of sediment flow are shown with grain size classification. Bypass sediment volume is expected to reach 0.31×10^6 m^3/year, which brings sediment inflow reduction of 70%, by above mentioned bypassing conditions. Since most of the large sediments, greater than sand, are trapped by new check dam and removed, bypassed sediments are mostly fine sediment. Sediment flow map of Figure 4 was obtained through boring survey, analysis for capture rate of fine sediments, 1D simulation of river bed variation which includes bed load, suspended load and wash load model, etc.

3.2 Hydraulic design of intake structure

As mentioned before, outflow of flood control includes bypass water discharge. Outflow should be controlled by both of bypass intake and dam's outlet facilities. It is somewhat hard to control gates of both facilities for the dam's office manager (dam's gates should be always controlled because some catchment area remains at areas downstream of the bypass intake). Office manager may feel great stress in flood control situation especially at the constant ratio operation. Since both of inflow and outflow are in increasing situation at the constant ratio operation, office staffs have several important works at that situation such as gathering information about weather and flooding situation of related areas, deciding future outflow plan, informing the decided plan to related organization including national and local governments and so on. It is necessary to control bypass water discharge without gate operation.

In order to approximate the flood control outflow of constant ratio operation, both of discharge characteristics of orifice and crest weir are required and combined. Since the site space is limited, both facilities cannot be arranged side by side. Orifices and crest weirs are designed as two-story structure (Figure 5). Two crest weirs are arranged on two orifices. Separate walls with air pipes are located at crests downstream to keep each facility's discharge characteristics. Air pipes are attached to side walls respectively, beneath the upstream end of separate walls, to supply air between flow jets from orifices and crests. There are two one leaf gates to control discharge through each pair of an orifice and a crest weir. These gates will be fully opened from fully closed position at

the beginning of sediment bypass operation. Also, these gates will be operated in the case that the residents of areas downstream requires outflow reduction in flooding situations. Maintenance gates are installed upstream side of orifices and crest weir.

Hydraulic model tests were carried out to check flow conditions including discharge characteristics and find final design shape of the intake structure. Influence of roughness change was also examined by the model tests. Discharge control parts of the intake structure should be lined against flow down sediments by durable and less worn material. Same lining is also required at the channel downstream of the intake for preventing back water influence caused by roughness increase by abrasion. Required lining area was examined through the model tests by changing area, assuming the roughness increase at normal concrete surface. Obtained lining area is also shown in Figure 5. Regarding the lining materials, abrasion resistant rubber with steel is employed for the intake lining and steel is for the tunnel lining. They were selected by referring to recent actual lining results of river related structures in Japan.
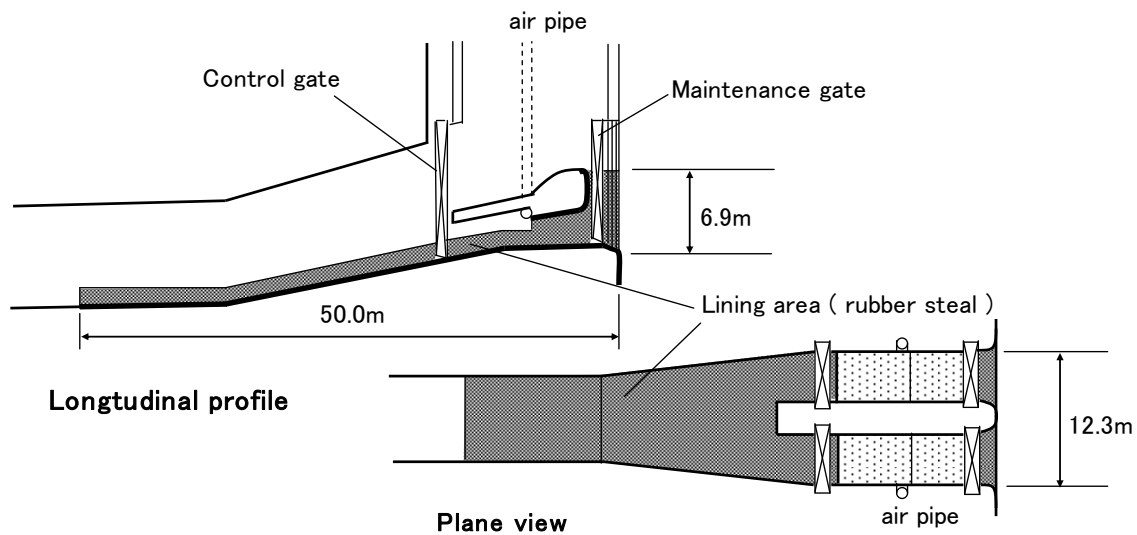
Figure 5: Intake of Koshibu dam

3.3 Countermeasures against change factors of bypass discharge

From the experiences of Koshibu dam management, large amount of driftwood possibly flow down to the reservoir during flood. Bypass intake should be defended against the influence of driftwood to keep discharge control and sediment bypass functions. Guard piles fence against driftwood was chosen as the countermeasure and its alignment, fundamental dimensions of the piles etc. were examined through hydraulic model tests. Since sediments accumulation at the surrounding area of the intake also possibly influences bypass discharge and flow situation within the intake, model tests were basically carried out in sediment supply conditions.

Results of the examinations are shown in Figure 6. The alignment of guard piles encloses the intake structure and the road for intake maintenance; piles are located 10 m apart from the intake structure. Diameter of piles is 0.9 m and clear span of each pile is 1.5 m. Since flow from new check dam toward the intake becomes stronger in sedimentation condition, bypass discharge increases more than 15% at the maximum inflow of the planning hydrograph only by above piles. Plate bar, height of 1m, is attached nearly the crest elevation for reducing bypass discharge in sedimentation condition. Also two strings of vertical wire rope are fixed between piles. Although most of driftwood flows down to reservoir without trapping by guard piles, a large number of pieces stay at the front of guard piles and some of them pass through (Figure 7). Pieces of trees are possibly trapped in flow areas of the intake. For example, they are easily trapped at nearby areas of gate slots. Guard function of piles against driftwood is strengthened by wire ropes; nearly 50% of pieces, which flow down to the intake, can be reduced.

In the hydraulic model tests, influences of sediments accumulation were examined in quasi-steady flow conditions. Constant water discharge with constant sediment discharge, which was decided by water discharge, was continuously supplied at the upstream end of the model to keep the condition that the sum of overflow sediment discharge of the diversion weir and bypass sediment discharge approximates the sediment supply discharge. Influences of sediments accumulation on the bypass water discharge were checked in this condition at some water discharge rates.

Behavior of driftwood was observed in above sediment condition using sticks of several dimensions as the model. Sticks were supplied at areas upstream to cover water surface from the new check dam to the diversion weir once in a water discharge condition. The total volume of sticks of this condition is about three times of the maximum driftwood inflow among past floods. Preliminary tests cleared that the largest number of trapped sticks and bypassed sticks occurred at maximum inflow condition of 1300 m^3/s, examinations concerning driftwood were carried out in the maximum inflow condition.
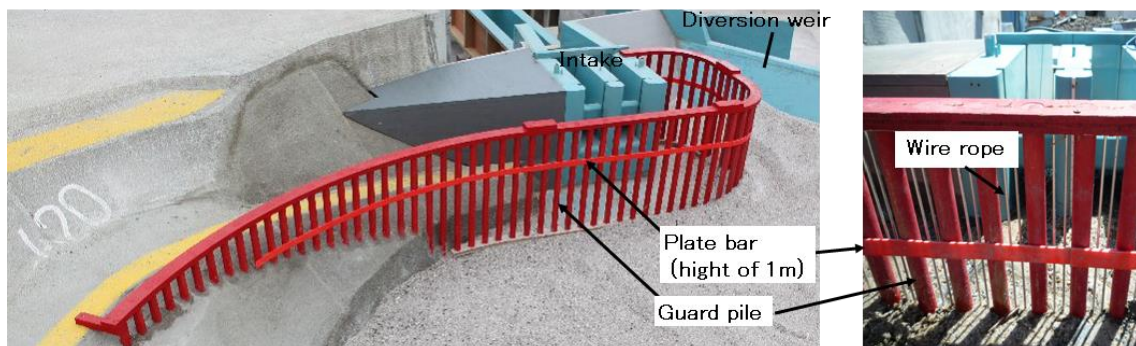
Figure 6: Surrounding facilities for the intake

Figure 7: Trapping situation of drift wood (1300m^3/s)

As for the final design of guard piles, influence of trapped sticks to bypass water discharge was observed not only the maximum inflow but some inflows less than the maximum by reducing water discharge from the maximum. Trapped sticks at the maximum inflow remained in reducing water discharge condition. Experiments repeated three times by the same way, it was known that bypass water discharge decreases at most about 10% by trapped sticks.

Measurement of bypass water discharge is important for actual management. Measuring point of water surface level, where the level was unchanged by surrounding sedimentation of the intake, was searched for. Water surface at 5 m upstream from the center of the intake face was found out for the measuring point. Water surface will be measured by micro wave sensors.

4   Construction situation

Koshibu dam's sediment bypass facilities are under construction now. Construction of bypass tunnel was started in 2009 and completed in 2013. Main structure of the intake was also completed in 2013 (Figure 8). The project has been strenuously advanced toward the first operation of sediment bypass at 2016.

Figure 8: Construction situation of the intake structure

5 Conclusions

Koshibu dam's reservoir has been suffered from large amount of sediment inflow since the completion of the dam in 1969. Sediment bypass project was examined and employed as one of the main countermeasures to keep reservoir capacity against sedimentation. Since Koshibu dam has the purpose of flood control, sediment bypass facilities should be able to control discharge like outlets facilities installed in the dam body. Hydraulic design of the bypass facilities was carefully carried out using hydraulic model tests. Special features of the design are shown around the intake structure. Main features are as follows,

- two-story structure of orifices and crest weirs considering non-gate operation during constant ratio operation and small site

- lining by abrasion resistant rubber with steal and steal considering appropriate areas to prevent discharge change caused by concrete abrasion

- guard piles with plate bar and wire ropes to prevent harmful bypass discharge change caused by sedimentation and driftwood

This paper introduces the meaning of above designs and experimental way of hydraulic model tests to obtain the results.

Authors

Josuke Kashiwai (corresponding Author)
Director, Research Department 1, Japan Dam Engineering Center
Email: kashiwai@jdec.or.jp

Dr. Shuji Kimura
Director, Integrate Dam Management Office of Tenryu River, Chubu Regional Development Bureau, Ministry of Land, Infrastructure, Transport and Tourism

Sediment bypass tunnels of the Shihmen Reservoir in Taiwan

Jihn-Sung Lai, Fong-Zuo Lee, Ching-Hsien Wu, Yih-Chi Tan, Tetsuya Sumi

Abstract

Owing to high turbid water usually generated from upstream watershed during typhoon events, inflow sediments have resulted in serious sedimentation problem in Shihmen reservoir, Taiwan. One of two penstocks at powerhouse was modified in 2012, which was a first major project undertaken to improve sediment sluicing capacity. The modified penstock as a venting tunnel was operated to release high turbid water during the typhoon event in 2013. In this study, two of the four proposed sediment bypass tunnel design plans (C and D) are selected to investigate sediment sluicing efficiency in typhoon floods. Based on the experimental results from physical model, the sediment sluicing efficiency of Plans C and D are 66.89% and 48.12%, respectively. Comparing the outflow sediment ratio between Plan C and Plan D, Plan C is much better than Plan D due to the effects of lower intake elevation and muddy lake consolidation. A two-dimensional numerical mobile bed model is adopted to simulate suspended sediment transport and bed variation in the downstream river. Based on simulated results for Plan D by using Typhoon Aere hydrological conditions, one flood event and long-term simulation are adopted to investigate aggradation and degradation changes of river bed around the junction reach of two tributaries. The simulated bed variation ranges from 1 m for one flood event to 3 m for long-term hydrological conditions, which provides useful information for management of navigation, wetland or levee safety.

1 Introduction

In recent years, the issues related to sustainable operation and storage reservation of existing reservoirs are essentially important. The loss of active reservoir volumedue to sedimentation was higher than the increase of reservoir capacity by construction, according to the report by Oehy (2007). Useful desiltation strategies and effective countermeasures have been investigated in relative researches (Morris and Fan 1998; Lee *et al*. 2010a; Sumi *et al*. 2011; Lee *et al*. 2012). Taiwan is an island situated at a geographical location with special climatic condition that brings 3~4 typhoons to this island per year on the average. On the one hand, these typhoons often result in flood disasters that can cause serious damage to properties and sometimes with severe casualties. On the other hand, when typhoon or heavy rain fall occurs, the watershed may generate great amount of sediment yield. Land development in the watershed could

also accelerate soil erosion. In addition, earthquake-triggered landslides in mountainous areas could supply large amount of sediment from upstream river basin. Sediment produced in upper basins may not be immediately delivered to lower basin owing to river aggradations. However, still great part of sediment can be transported and deposited in downstream river particularly during extreme rainfall events, which could generate turbidity current into a reservoir (Lee *et al*. 2014). As sediment is transported into a reservoir, deposition occurs due to flow velocity decrease. In general, the large size sediment may deposit quickly to form delta near the backwater region tail. The hydraulic phenomenon of delta area is similar to the shallow water in open channel flow. The sediment-laden inflow consists of two parts, bed load and suspended load. The bed load may deposit at the front set of delta, and the suspended load may flow through the delta and deposit by sorting. When turbid inflow with finer suspended load continues to move, the turbulence energy decreases by resistance. The inflow may plunge into the reservoir to develop turbidity current and move toward downstream. On the downstream side of the plunge point, the water near the surface in the reservoir can flow toward upstream due to continuity behavior of the flow. Figure 1 illustrates the phenomenon of a density current with trapped debris (Lee *et al*. 2014).
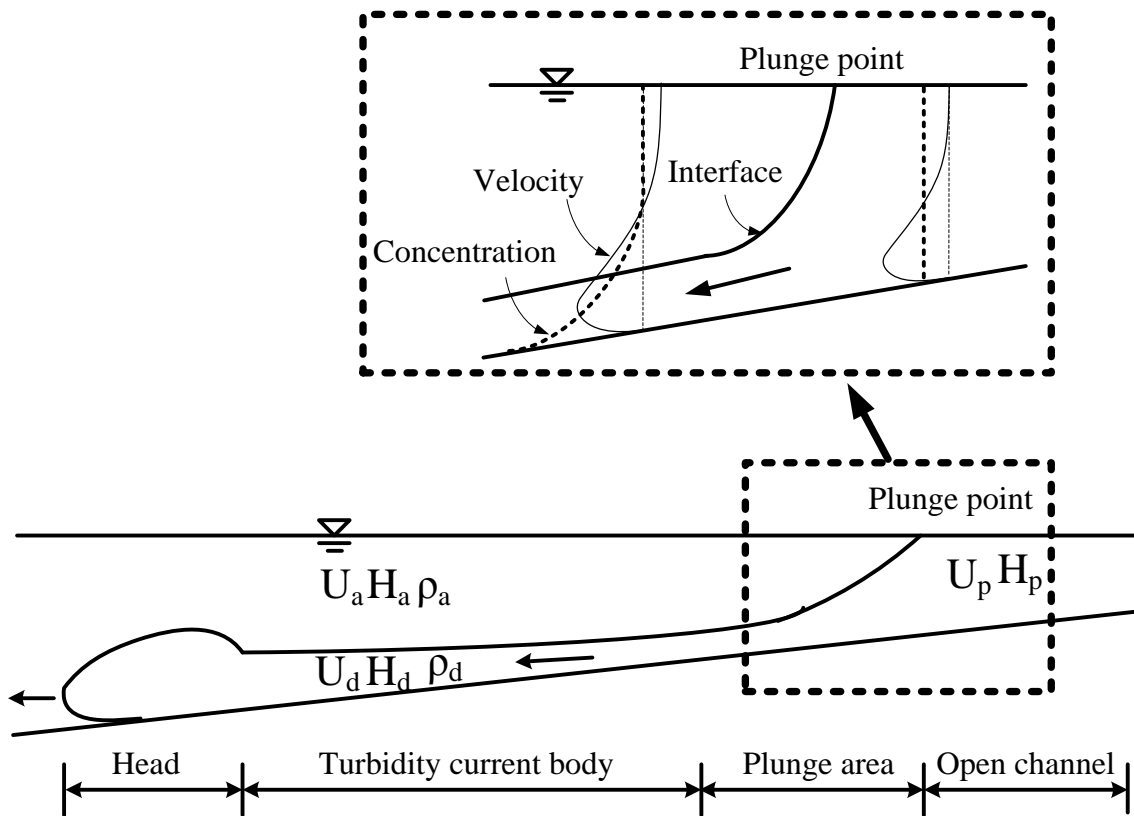
Figure 1: Sketch of turbidity current plunging with velocity and concentration distribution

Flume and field measurements have shown that the occurrence of the turbidity current at plunge point can be related to flow velocity, water depth and fluid density before

plunge point (Graf 1983). In fact, after the severe Chi-Chi earthquake happened in 1999, Typhoon Aerein 2004 attacked northern Taiwan and generated more than 973 mm rainfall within 4 days in the catchment of the Shihmen reservoir. Highly turbid inflows affected the water supply system seriously and the water supply suffered from a shortage for 14 days. Sediment concentration of the inflow discharge during Typhoon Aere rose to 242,000 Nephelometric Turbidity Unit (NTU) and was far-exceeded water treatment capacity which can only deal with 6,000 NTU (Tan *et al*. 2011). In another case, Typhoon Sinlaku in 2008 attacked the Wushe reservoir located in central Taiwan, which reduced reservoir capacity down to 36.3% of its original effective storage. Besides, the reservoir bed level near the Wushe dam site became 30 m higher than that of the power plant intake entrance. Fortunately, the function of generate electric power was still working because of only fine sediment deposits near the intake entrance area. However, coarse materials in delta reach have still moved toward the dam and threatened operation and safety of the Wushe dam in the following years. In order to preserve the storage of Wushe reservoir and ensure sustainable operation of power plant, the Taiwan Electric Power Company has been expected to deal with sedimentation problem. A feasibility study of hydraulic flushing was conducted to investigate sedimentation problem on short-term or long-term bases (Taiwan Electric Power Company 2013). In the case of 2009 Typhoon Morakot attacked southern Taiwan, the inflow sediment concentration was more than 0.2×10^6 ppm during peak flow and caused about $90 \times 10^6 \, \mathrm{m}^3$ sediment deposited in the Tsengwen reservoir. Total amount of the deposition in this event was more than 20 times the annual value. The accumulative rainfall was more than 3,000 mm within 3 days (South Region Water Resources Office 2013). To deal with serious sedimentation in the Shihmen and Tsengwen reservoirs, specific budgets were granted by the central government of which the Water Resources Agency has been appointed to execute desiltation projects since 2006. The desiltation strategies were urgently needed for sedimentation problems.

This study presents several desiltation strategies for sustainable operation of the Shihmen reservoir. The watershed of the Shihmen reservoir is shown in Figure 2. Figure 3(a) shows the floating woody debris distribution near the dam site after Typhoon Aere in 2004. In the figure, massive woody debris got trapped in front of the dam. The extraction volume of woody debris was about 5.4×10^5 m^3. According to investigation after typhoon, the turbine was damaged by woody debris carried by flow through the hydroelectric power intake (Figure 3(b)). The modification of the existing powerhouse penstock as a venting tunnel for venting the turbid water was a major project task to improve the sluicing capacity. One of the two penstocks at the powerhouse was modified in 2012. It was operated for the first time during Typhoon Soulik in 2013 to release abundant sediments to the downstream river. Moreover, four sediment bypass tunnel plans (Plan A, B, C and D) were proposed to reduce sediment deposition in Shihmen reservoir. With the tunnel lengths of 8.1 km and 14.4 km in Plan
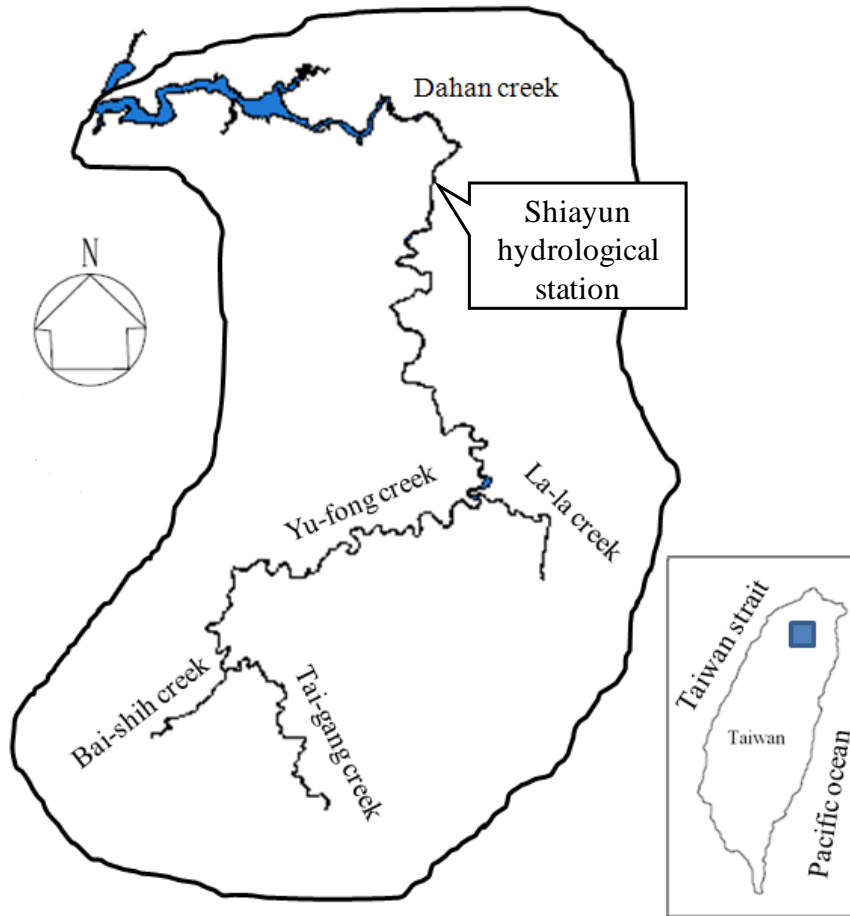
Figure 2: Watershed area of the Shihmen reservoir

A and Plan B, respectively, were investigated. However, Plan A and Plan B did not have efficient sediment releasing efficiency and besides their construction were costly. Therefore, Plan D and Plan C have been considered as two effective strategies for sediment releasing in Shihmen reservoir (Water Resources Planning Institute 2012). In design stage, Plan C mainly releases venting turbidity current, and Plan D is designed to cooperate with downstream sediment replenishment. In Plan D, tunnel is also designed to serve flood control purpose and provide discharge to flush sediment disposal in the settling basin located at the outlet of Plan D tunnel for sediment disposal. The settling basin consists of one main channel, lateral floodplain and two overflow weirs at sides. Based on the experimental results, sediment removal by lateral erosion can be achieved with relatively low discharge by supplying overflow water from two side weirs. (Morris and Fan 1998; Lai and Chang 2001; Northern Region Water Resources Office 2014). A developed two-dimensional layer-averaged turbidity current model is adapted to estimate outflow sediment discharges and to compare with the results obtained from the hydraulic physical model. Downstream impact of Plan D tunnel releasing sediment during typhoon event is also investigated in this study.

(a)

(b)

Figure 3: Floating woody debris in Typhoon Aere (a) near dam site (b) turbine clogged by woody debris

2 Site description

The Shihmen reservoir is a multi-functional reservoir and its functions include irrigation, water supply, power generation, flood control and tourism. The irrigation area covers Taoyuan, Hsinchu and Taipei areas in the northern Taiwan for a total of $3.65 \times 10^8 \, \text{m}^2$. It is a major contributor in helping the agriculture in these areas. The reservoir supplies water to 28 districts and 3.4 million people, which provides major water resources for the livelihood of the people in the northern Taiwan. Making use of the water impoundment at Shihmen dam, the Shihmen Power Plant annually generates 2.3 hundred million KWH (kilowatt per hour) vitally contributing electric power demand and industrial development at peak hours. Another function of the reservoir is to mitigate flood damage on the downstream areas during typhoons and heavy rain seasons by reducing flood peak discharge.

The Shihmen reservoir has a natural drainage area of 762.4 km^2. It is formed by the Shihmen dam located at the upstream reach of the Dahan River flowing westward to the Taiwan Strait. The Shihmen dam completed in 1963 is a 133 m high embankment dam with six spillways, one bottom outlet, two power plant intakes and two flood diversion

tunnels. The elevations of the spillway crest, bottom outlet, power plant intake and flood diversion tunnel are EL.235 m, EL.169.5 m, EL.173 m and EL.220 m, respectively. The design discharge of six spillways, one bottom outlet, two power plant intakes and two flood diversion tunnels are 11,400 m^3/s, 34 m^3/s, 137.2 m^3/s and 2,400 m^3/s, respectively. With a design water level of EL.245 m, the reservoir pool has 16.5 km in length and the surface area of the water has 8.15 km^2. The initial storage capacity was 0.31×10^9 m^3, and the active storage was 0.25×10^9 m^3. Due to a lack of desilting works, most of the incoming sediment particles had settled down rapidly along the reservoir since the dam was commissioned. Based on the survey data, the longitudinal bed profile along the reservoir had accumulated a significant amount of sediment after dam completion. The depositional pattern has become wedge-shaped since 2000. From recent survey data in 2013, the storage capacity was estimated to be 67% of its initial capacity. Based on particle size distribution sampled from outflow discharge in 2013 Typhoon Soulik, the sediment deposition was classified as silt or clay (Figure 4).
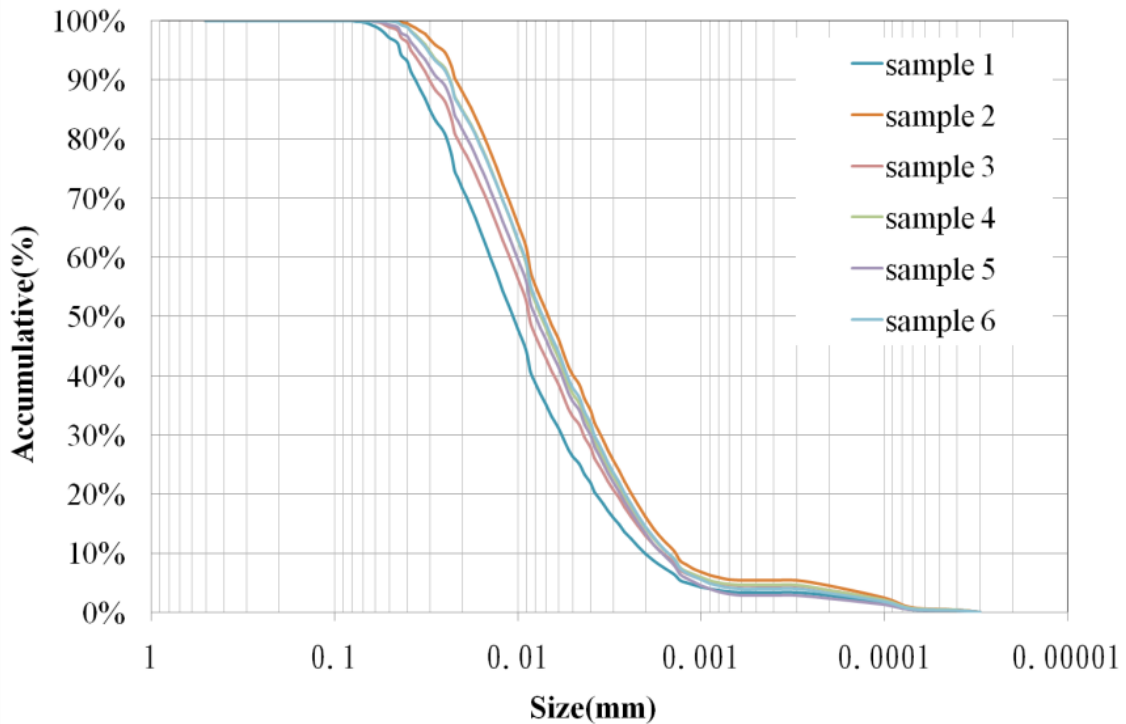
Figure 4: Outflow sediment size sampled in Typhoon Soulik

Due to serious deposition problem in 2004 induced by Typhoon Aere, the stratified withdrawal facility was built beside the dam site in 2009 to ensure water supply capacity (Figure 5(a) and Figure 6) and one of the penstocks of power plant was modified in 2012 to vent turbidity current (Figure 5 (b) and Figure 6). The stratified withdraw facility with three intakes (at EL.220 m, EL.228 m, EL.236 m) was finished in Dec. 2009. In addition, the Jhongjhuang pond at downstream reach near the

60

Yuanshanyan water intake for backup water resources during typhoon flood event has been constructed, which is expected to be completed in 2016.

(a)

(b)
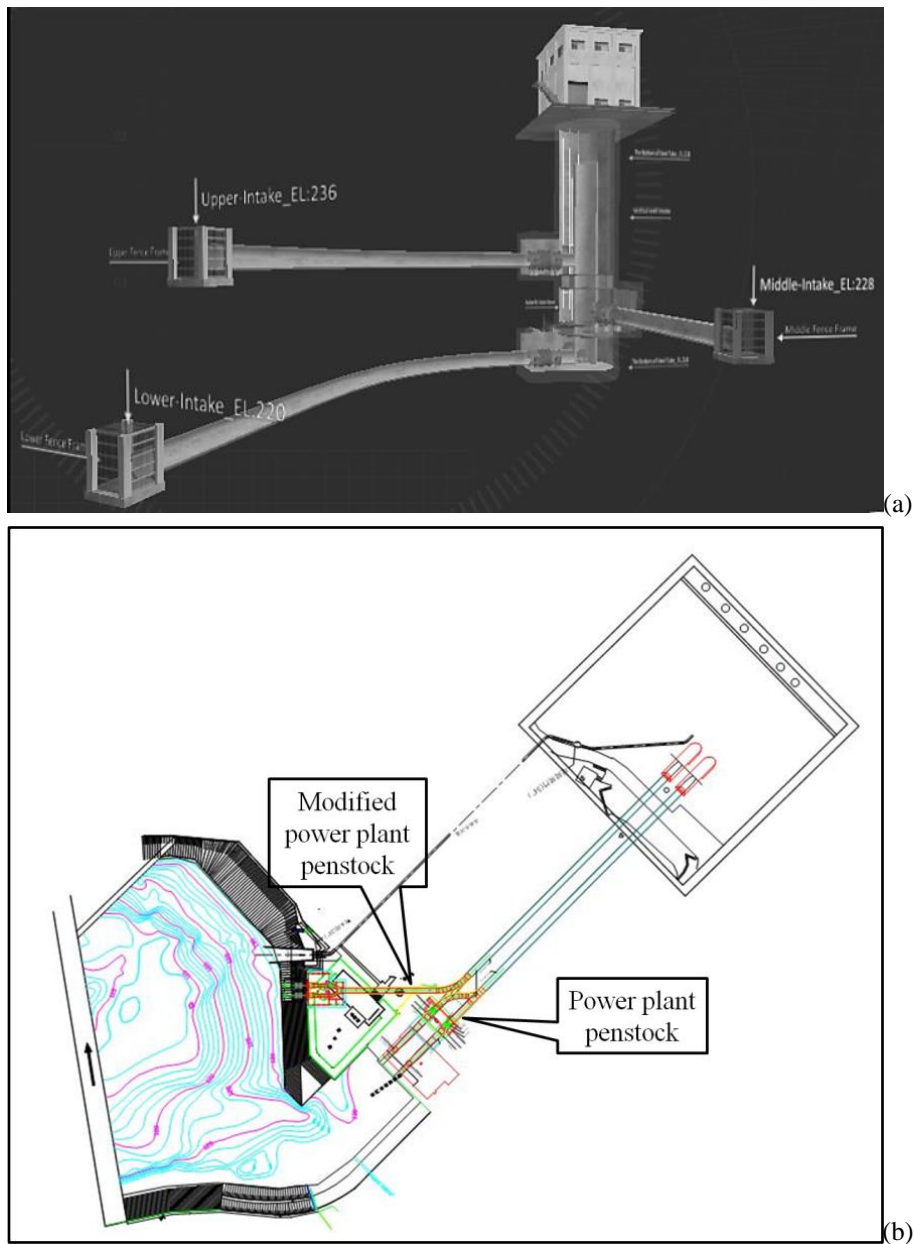
Figure 5: Sketches of a) withdrawal facility and b) layout of the modified power plant penstock in physical model

3 Physical model study

The physical model study of the Shihmen reservoir was conducted by using a 1/100 undistorted scale model (Figure 6). It covered 15.5 km longitudinal length of the reservoir with its upstream boundary located between reservoir cross section 30 and 31. The model needed a lab space of 120 m by 20 m. The physical model topography was based on the field bathymetrical survey data. The model was built to study the turbidity

current movement from 2007 to now using hydrological condition of Typhoon Aere in August, 2004. The Froude number similarity was adopted for the model scale ratio, 1/100, of the physical model. The sediment used in the physical model study was taken from those deposited near the powerhouse intake. The medium diameter d_{50} of the deposited sediment was 4 ~ 8 μ m. Its size distribution is close to those plotted in Figure 4. This sediment size chosen was based on several primarily tests. From experimental results, the turbidity current moving speed and sediment vertical concentration distribution could be reproduced in the physical model if the sediment concentration is above 35 kilograms per cubic meters (i.e. the concentration limit for flocculation). The sediment concentration during Typhoon Aere was estimated to be 43 kg/m^3 on average which is above the flocculation limit. However, it was expected that the experimental results of the outflow sediment concentration could be underestimated during the falling limb of the outflow discharge hydrograph. The particle fall velocity could be faster in the model than that of the prototype when the concentration was below 35 kg/m^3 during the falling limb period.
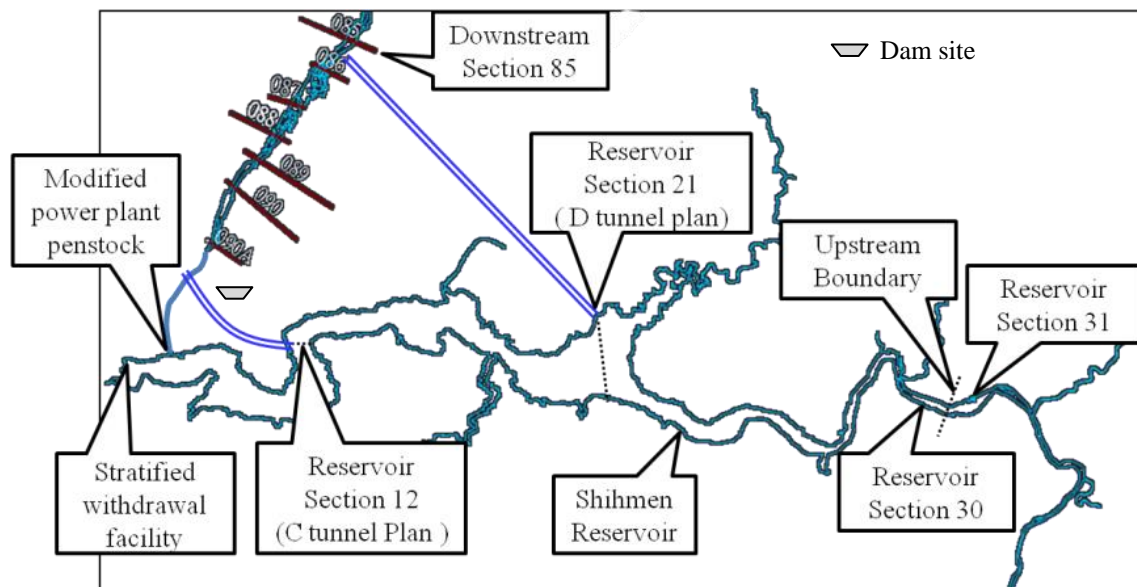
Figure 6: Study area in the physical model layout

There are a number of scenarios tested in the physical model with the flow conditions in Typhoon Aere: (a) modified existing facilities, (b) two sediment bypass tunnel scenarios named sediment bypass tunnel Plan C and Plan D. A description of each scenario is described below (Water Resources Planning Institute 2012).

3.1 Modified existing facilities

The modified existing condition scenario corresponded to modifications of several outlets to increase the sediment sluicing capacity during typhoon events. The powerhouse penstock modification was a major project work to improve the sluicing

capacity (completed in June, 2012). Figures 7(a) and 7(b) show photos of the powerhouse intakes in prototype when the dam was constructed and in the physical model. There were originally two intake openings with penstocks. In the modified project, the second penstock was modified as a venting tunnel and dedicated for venting sediment only (not for power generation). The sluicing capacity increased from 137 to 380 m^3/s. Based on the hydrological condition of Typhoon Aere (Q_{peak}=8,594 m^3/s), the experimental results of outflow sediment quantity was about 29% of total inflow sediment volume. The experimental results show the outflow sediment ratio of spillway with a flood diversion tunnel, bottom outlet and water supply intake were 13.1%, 2.4% and 0.4%, respectively. In 2013, the venting tunnel at the powerhouse was operated for the first time during Typhoon Soulik (Q_{peak}=5,458 m^3/s). Abundant sediment was released by desiltation operation through the outlet of the venting tunnel to the downstream river (Figure 7(c)). The outflow sediment volume through the outlet of the venting tunnel was about 24% of total inflow volume in this flood event.

Figure 7: Photos of powerhouse (a) intake in the physical model (b) intake in the field (c) outlet of the venting tunnel during Typhoon Soulik

3.2 Sediment bypass tunnel Plan C

The location of the sediment bypass tunnel Plan C (C tunnel plan) is shown in Figure 6. A two-dimensional layer-averaged turbidity current model developed by Lai and Huang (2012) was adapted to estimate outflow sediment discharge and compared with the experimental re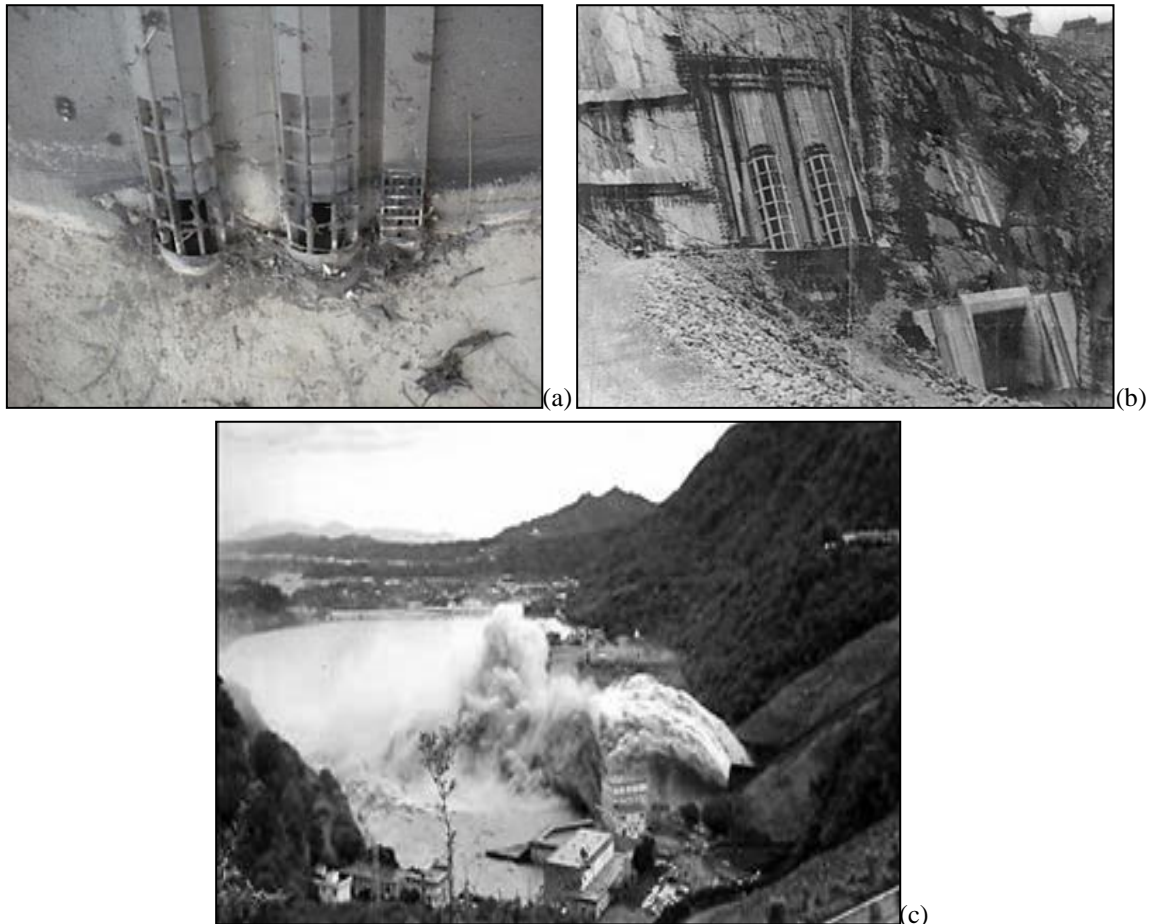sults from the physical model (Water Resources Planning Institute, 2012). In the numerical model the intake opening was at the bottom elevation at EL.200 m with the height of 10 m and width of 10 m. The measurements from the physical model for the Typhoon Aere case were incomplete since no discharge data was available at the flood diversion tunnel and spillway outlets. Therefore, another case load in the physical model was numerically simulated with the bottom elevation of the tunnel intake lowered to EL.195 m. The outflow sediment quantity was compared between numerical model and physical model. In Plan C case, the data obtained from physical model test were used to verify the numerical model. The predicted and measured sediments through all outlets are compared in Table 1 for the Plan C case. In Plan C case, the inflow water and sediment discharges at the upstream boundary were used for the physical model test. The total inflow sediment volume was 10.74×10^6 m^3. The boundary condition at the entrance of the intake has a constant design capacity discharge through the Plan C tunnel and the discharge capacity of Plan C tunnel is 1,200 m^3/s. In Table 1, the sediment sluicing efficiencies obtained from the physical model and the numerical model are 66.89% and 71.36%, respectively. The model results are in good agreement with the measured data. Both the magnitudes and trends were captured by the numerical model at all outlets. The discrepancy occurred in the simulated sediment sluicing efficiency through the venting tunnel, which was numerically over estimated comparing with the field data (Water Resources Planning Institute 2013).

Table1: Summary of outflow sediment volume at various outlets in Typhoon Aere case under sediment bypass tunnel Plan C

Outflow sediment volume	Plan C tunnel	Venting tunnel at powerhouse	Spillway & flood diversion tunnel	Bottom outlet	Water supply intake
Measured x10^{6}m^3/(%)	3.41/ (31.6%)	2.02/ (18.8%)	1.59/ (14.7%)	0.152/ (1.41%)	0.041/ (0.38%)
Simulated x10^{6}m^3/(%)	3.36/ (31.4%)	2.72/ (25.3%)	1.30/ (12.1%)	0.226/ (2.1%)	0.045/ (0.46%)

3.3 Sediment bypass tunnel Plan D

The location of the sediment bypass tunnel plan D (D tunnel plan) is shown in Figure 6. The intake in the model was at the bottom elevation of 210 m, and12 m high and 75 m wide. The total inflow sediment volume was 10.92×10^6 m^3. The measured sediment sluicing efficiency through all outlets is listed in Table 2 for the tunnel plan D. Note that, the boundary conditions at Plan D tunnel intake had a constant full-capacity discharge

600 m³/s at water level 245 m. the experimental results showed that total sediment volume passed through the reservoir was 48.12% of the inflow sediment volume. Comparing the outflow sediment ratio between two sediment bypass tunnels, Plan C tunnel was better than Plan D tunnel on the sediment outflow ratio owing to the effects of intake elevation and muddy lake consolidation. Additionally, the Plan D tunnel is also planned to serve flood control purpose and provide discharge to flush sediment disposal in the settling basin. The settling basin will be constructed at the outlet of Plan D tunnel for sediment deposition in the field (Figure 8) with the maximum disposal volume of 165 x10³m³. The settling basin consists of one main channel, lateral floodplain and two overflow weirs at sides. Based on the experimental results, with slope 1/20 on floodplain, sediment removal by lateral erosion was achieved with relatively low discharge by supplying overflow water from two side weirs. The discharges of overflow weir and main channel were 40m³/s and 520m³/s, respectively. The overall maximum flushing efficiency of the settling basin was about 97.5% (Northern Region Water Resources Office 2014).
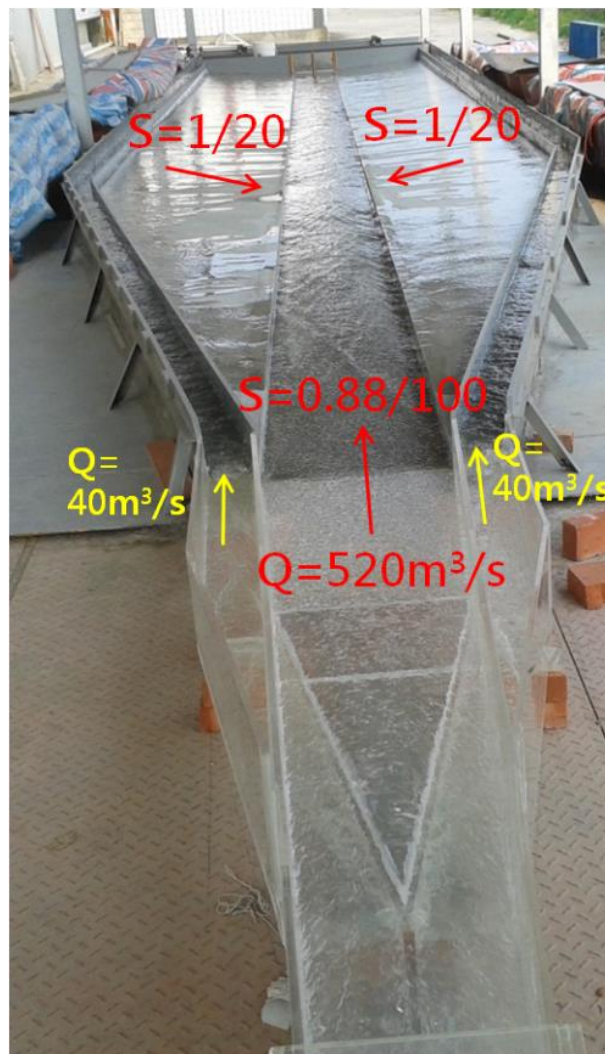

Figure 8: Model of the settling basin at the outlet of Plan D tunnel

Table 2: Summary of outflow sediment volume at various outlets in Typhoon Aere case under sediment bypass tunnel Plan D

Outflow sediment volume	Plan D tunnel	Venting tunnel at powerhouse	Spillway & flood diversion tunnel	Bottom outlet	Water supply intake
Measured x10^{6}m^3/(%)	1.34/ (12.3%)	2.78/ (25.5%)	0.926/ (8.48%)	0.137/ (1.26%)	0.063/ (0.58%)

4 Downstream impact

The venting tunnel at the powerhouse was operated for the first time during Typhoon Soulik in 2013. Abundant sediment was released by desiltation operation to the downstream river. A two-dimensional numerical mobile bed model was adopted to simulate suspended sediment transport and river bed variation for investigation of morphological changes in the downstream river reach at Jiangzicui area (Huang *et al.* 2014). Downstream river bed elevation changes resulted from desiltation operation may cause the important issues in this study area, such as wetland, the entrance of Erchung Floodway and the ferry routes. Figure 9 shows the simulated result of bed elevation changes in one flood event, Typhoon Aere, in 2004 with desiltation operation under the Plan D condition. Imposing same hydrological conditions of Typhoon Aere for ten times, Figure 10 shows the simulated result of long-term (10 years period) bed elevation changes. The results indicate that the primary impact on morphological change occurs in the ferry routes. The bed elevation variation ranges from 1 m for one flood event to 3 m for long-term hydrological conditions providing useful information for downstream river management such as navigation, wetland management and levee safety (Lai et al. 2014; Lee et al. 2014).

5 Conclusions

The Shihmen reservoir is a multi-functional reservoir providing water resource for irrigation and water supply over 28 districts to serve 3.4 million people in the northern Taiwan. Modification of several existing outlets to increase the sediment sluicing capacity was an important task after Typhoon Aere in 2004. The powerhouse penstock modification was a major project undertaken to improve the sluicing capacity, which was completed in June, 2012. According to the experimental results of the physical model, the venting tunnel at powerhouse resulted in the effective sluicing efficiency with higher outflow sediment concentration than those by other hydraulic facilities. It indicated that the lower outflow elevation the higher outflow sediment concentration owing to sediment settlement near the reservoir bottom.
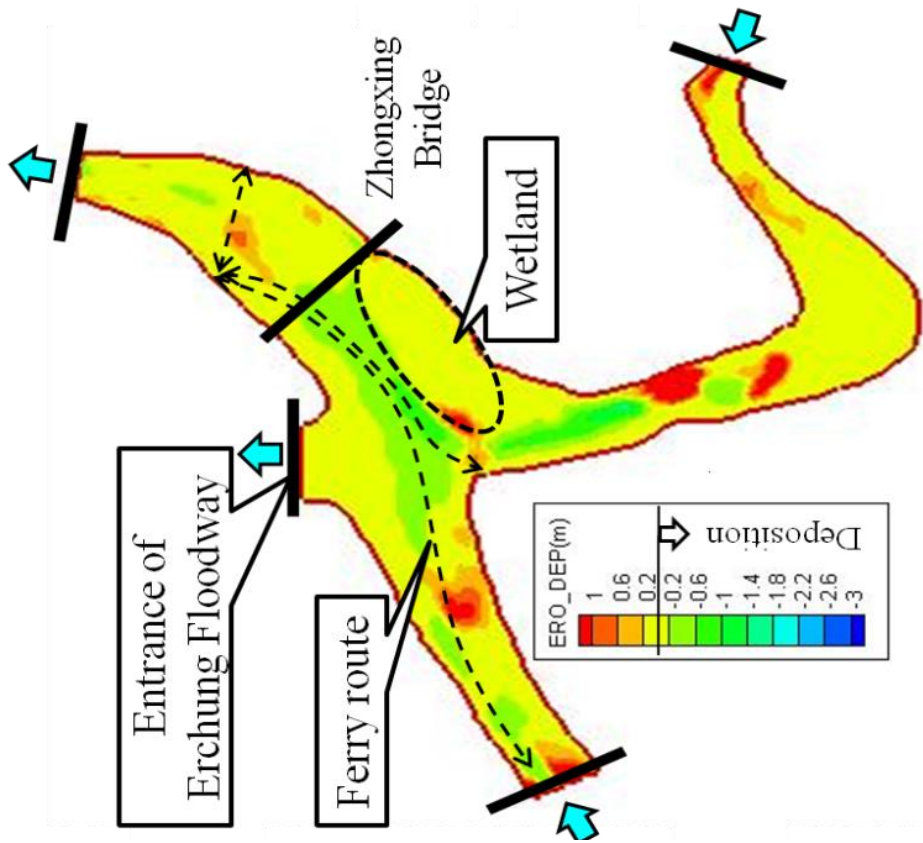
Figure 9: Simulated bed elevation changes in one flood event
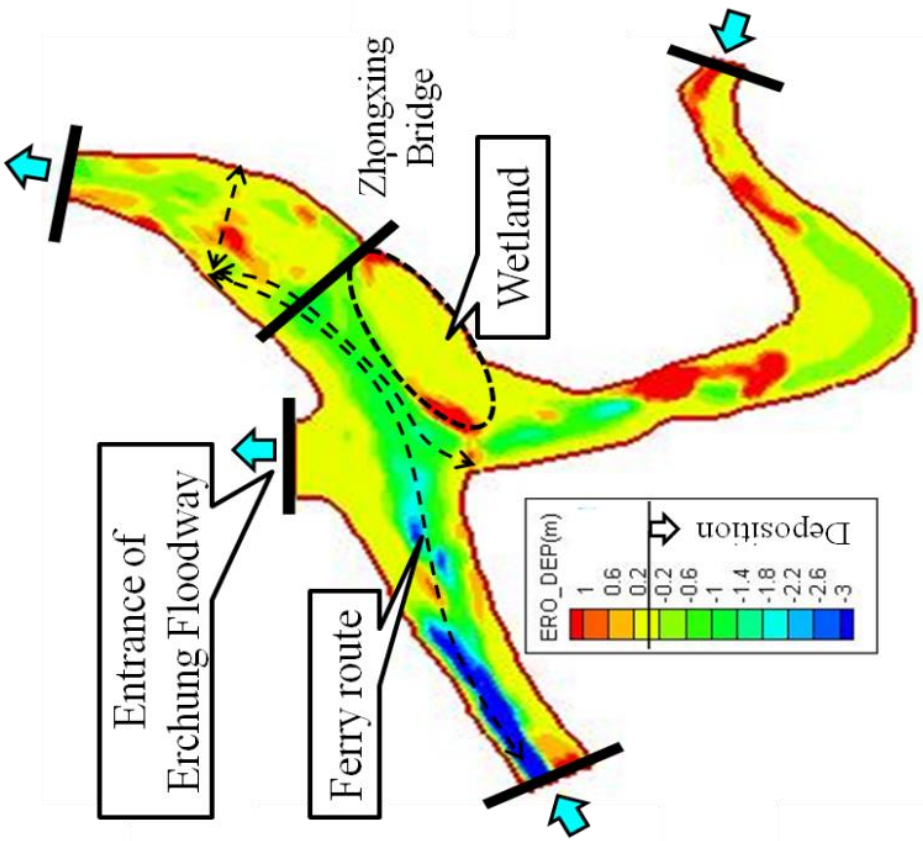
Figure 10: Simulated bed elevation changes in long-term variations

67

The physical model study was conducted by using a 1/100 undistorted model scale ratio. The model was built to investigate the turbidity current movement. The Froude number similarity was adopted for the scale ratio of the physical model. Scenarios of sediment bypass tunnels were tested in the physical model with the flow conditions in Typhoon Aere, which were evaluated for sediment sluicing efficiency. Two sediment bypass tunnel design cases, named Plan C and Plan D, were mainly tested in the physical model. In Plan C case, a developed two-dimensional layer-averaged turbidity current model was adapted to simulate outflow sediment discharge. With good agreement, the sediment sluicing efficiency listed in Table 1 from the physical model and the numerical model was 66.89% and 71.36%, respectively. The discrepancy of sluicing efficiency occurs in the venting tunnel at powerhouse.

In Plan D case, the measured sediment sluicing efficiency through all outlets listed in Table 2 indicates that the overall outflow sluicing efficiency is 48.12%. Comparing the outflow sediment ratio between two sediment bypass tunnels, Plan C tunnel is better than Plan D tunnel owing to the effects of intake elevation and muddy lake consolidation. Plan D tunnel also serves flood control and provides discharge to flush sediment disposal in the settling basin. The settling basin constructed at the outlet of Plan D tunnel for sediment deposition, consisting of one main channel, lateral floodplain and two overflow weirs at sides. With slope 1/20 on floodplain, sediment removal by lateral erosion was achieved with relatively low discharge by supplying overflow water from two side weirs. Based on the experimental results, the maximum flushing efficiency of the settling basin is about 97.5%

Downstream river impact due to releasing sediment by the sediment bypass tunnel during a typhoon event was also studied in this research. One flood event and long-term simulation by using Typhoon Aere hydrological conditions were adopted to investigate aggradations and degradation changes of river bed around Jiangzicui reach. The simulated bed elevation variation ranges from 1 m for one flood event to 3 m for long-term hydrological conditions providing useful information for management of navigation, wetland and levee safety.

Acknowledgement

References

Graf, W.H. (1983). The Behavior of Silt-laden Current. *Water power and dam construction*, 35(9), 33-38.

Huang, C.C., Lai, J.S., Lee, F.Z., Kang, S.Y. Shih, S.S., Hwang, G.W., Lin, G.F. (2014). Long-term Effects of River Bed Variations Downstream of the Shihmen Reservoir Due to Climate Change. *11th International Conference on Hydroinformatics*, HIC, New York City, USA.

Lai, J.S., Chang F.J. (2001). Physical Modeling of Hydraulic Desiltation in Tapu Reservoir. *Intl. Jour. of Sediment Research*, 16(3), 363-379.

Lai, J.S., Lee, F.Z., Huang, C.C., Hwang, G.W., Shih, S.S., and Tan, Y.C. (2014). Effect of Sediment Releasing Operation from Reservoir Outlets on the Water Treatment Plant Downstream. *11th International Conference on Hydroinformatics*, HIC, New York City, USA.

Lai, Y.G., Huang, J.V. (2012). A Two-dimensional Layer-averaged Turbidity Current Model. Technical Report SRH-2013-05, Technical Service Center, Bureau of Reclamation, Denver, Colorado.

Lee, F.Z., Lai, J.S., Tan, Y.C., Lee, L.C., Lin, Y.J. (2010a). Experiment and Simulation for the Movementof Density Current in a Flume. *Journal of Taiwan Water Conservancy*, 58(4), 1-12.

Lee, F.Z., Lai, J.S., Tan, Y.C., Lee, H.Y., Lin, T.J. (2010b). Research of Density Current Movement by Variant Slopes of the Dam. *Journal of Taiwan Water Conservancy*, 58(2), 11-21.

Lee, F.Z., Sumi, T., Lai, J.S., Tan, Y.C., Huang, C.C. (2012). Sustainable Countermeasure Using Frequency Analysis and Desiltation Strategy in a Reservoir. *2012 IAHR-APD*, Jeju Island, Korea.

Lee, F.Z., Lai, J.S., Tan, Y.C., Sung, C.C. (2014). Turbid Density Current Venting through Reservoir Outlets. *KSCE Journal of Civil Engineering*, 18(2), 694-705.

Morris, G.L. and Fan, J. (1998). Reservoir Sedimentation Handbook, McGraw-Hill Book Co., New York.

Northern Region Water Resources Office (2014). Evaluation of Morphological Mffects in Downstream River due to Sediment Venting and Replenishment from the Shihmen Reservoir, Technical report, National Taiwan University, Taipei.

Oehy, C., Schleiss, A. (2007). Control of Turbidity Currents in Reservoirs by Solid and Permeable Obstacles. *J. Hydraul. Eng.*, 133(6), 637-648.

South Region Water Resources Office(2013). Establishment of Sediment Concentration Monitoring System andDecision Analysis from Measurement in Tsengwen Reservoir, Technical report, National Taiwan University.

Sumi, T., Kantoush, S.A. (2011). Comprehensive Sediment Management Strategies in Japan: Sediment bypass tunnels. *34th IAHR World Congress*, 1803-1810, Brisbane, Australia.

Taiwan Electric Power Company (2013). Feasibility Study of Rational Control of the Sediment in Wushe Reservoir, Technical report, National Taiwan University, Taipei.

Tan, Y. C., Lee, F. Z. and Lai, J. S. (2011). Complex disaster damaged to water resources in Taiwan. *21st International Congress on Irrigation and Drainage*, Question 56: Water and Land Productivity Challenges Sub-Topic 56.5: Irrigation and Drainage Management Improvements.

Water Resources Planning Institute (2012). Hydraulic Model Studies for Sediment Sluicing and Flood Diversion Engineering of Shihman Reservoir, Technical report, Water Resources Agency, Taipei.

Water Resources Planning Institute (2013). A Two-Dimensional Layer-Averaged Turbidity Current Model, Technical report, Water Resources Agency, Taipei.

Authors

Dr. Jihn-Sung Lai (Corresponding author)
Hydrotech Research Institute, National Taiwan University, Taipei, Taiwan, R.O.C.
Email: jslai525@ntu.edu.tw

Dr. Fong-Zuo Lee
Prof. Dr. Yih-Chi Tan
Center for Weather Climate and Disaster Research, National Taiwan University; Department of Bioenvironmental Systems Engineering, National Taiwan University, Taipei, Taiwan, R.O.C.

Dr. Ching-Hsien Wu
Hydro-Tech Research Section, Water Resources Planning Institute, Water Resources Agency, MOEA, Taichung County, Taiwan, R.O.C.

Prof. Dr. Tetsuya Sumi
Water Resources Research Center, Disaster Prevention Research Institute, Kyoto University, Kyoto, Japan.

Sediment sluicing tunnel at Nanhua Reservoir in Taiwan

Chen-Shan Kung, Min-Yi Tsai, Yi-Liang Chen, Shih-Wei Huang, Ming-Yang Liao

Abstract

In recent years, severe silting problem has affected Nanhua Reservoir. After the impact of typhoon Kalmaegi (2008) and typhoon Morakot (2009), 38% of the effective storage volume of Nanhua reservoir was silt. A sediment sluicing tunnel is designed to flush the incoming sediment from upstream of the reservoir to the downstream of the Nanhua dam in the future. The design is based on the numerical hydraulic analyses and hydraulic model tests. An overview of the sluicing tunnel, hydraulic analyses, model tests, and cofferdam is presented in this paper.

1 Project overview

1.1 Project background

Nanhua reservoir, located at Nanhua district in Tainan City, was built to provide municipal water for Tainan and Kaohsiung Cites. The dam impounds the water from Houjue River with the catchment area of 108.3 km^2. The design storage volume is $1.58 \times 10^8 \text{ m}^3$ and the assumed sediment discharge is $1.56 \times 10^6 \text{ m}^3/\text{yr}$.

Due to the climate change, extreme hydrology events have occurred frequently in recent years. Large amount of sediment is flushed into the reservoir by rainstorm thus silts up the reservoir. In 2008 and 2009, typhoon Kalmaegi and typhoon Morakot brought $2 \times 10^7 \text{ m}^3$ and $1.708 \times 10^7 \text{ m}^3$ amount of sediment into Nanhua reservoir and the silt level was increased 8.5m. According to the silt survey in 2012, the effective storage volume was $9.943 \times 10^7 \text{ m}^3$, which was 62.9% of its design storage volume.

Three major issues arise from the reservoir siltation: First, the decrease of the effective storage volume; second, the blockage of the intake; third, the decrease of the water supply capability. To enhance the silt sluicing and flood-discharge capabilities, a sediment sluicing tunnel with the design discharge of $1,000 \text{ m}^3/\text{s}$ and sediment sluicing efficiency of 24% was proposed in the basic design stage.

The basic design has been completed in 2013. The following detail design and construction have been started in 2014. The construction will be completed in 2018.

1.2 Sluicing tunnel elements

The sediment sluicing tunnel consists of the intake, sluicing tunnel, and outlet work. The length of the sluicing tunnel is 1,287 m with a constant slope of 1.847%. (Figure 1). A new access road with tunnel is designed for the transportation during the construction period and future maintenance. The intake structure locates at the upstream of the Nanhua dam on the right bank. The outlet work is at the downstream of the Nanhua dam with the distance of 400 m from the dam. A vertical shaft connects the operating room and the control chamber with an elevator installed inside (Figure 2). The typical cross section of the sluicing tunnel is horse shoe shape with a clearance width and height of 9.5 m (Figure 3).
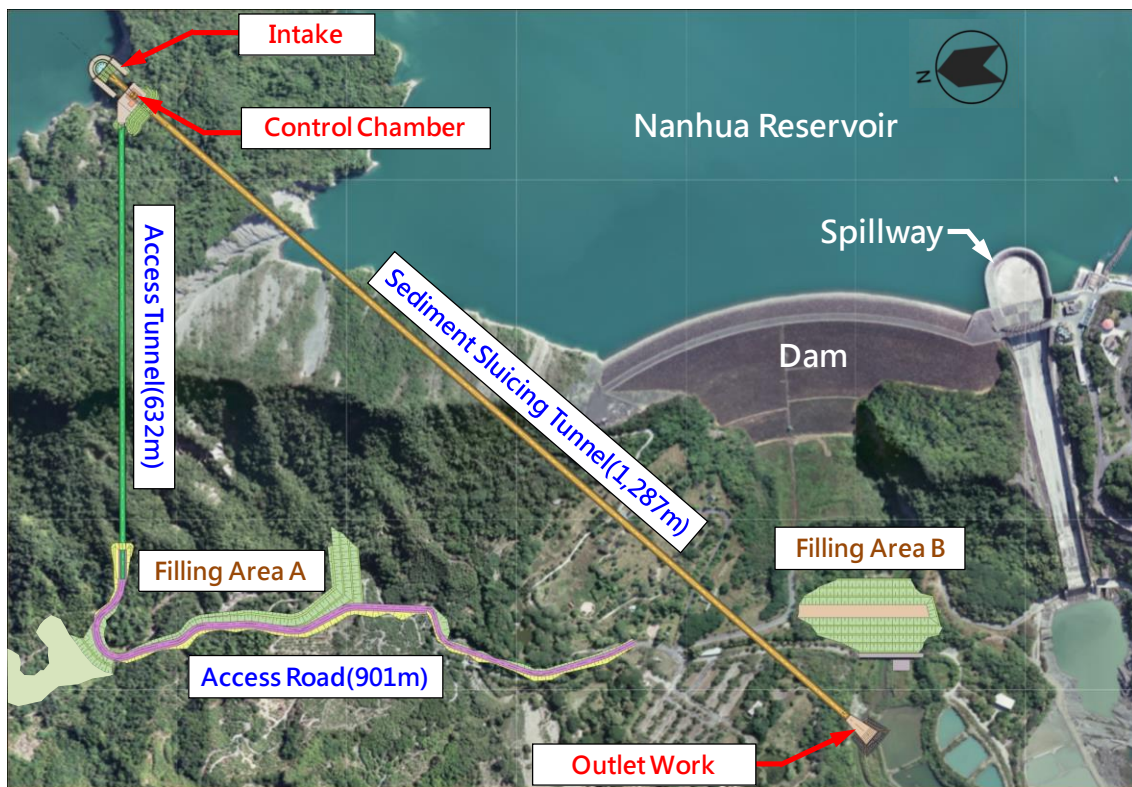
Figure 1: General arrangement of the sediment sluicing tunnel at Nanhua Reservoir

2 Hydraulic analysis

Flow 3D was adopted to simulate the hydraulic conditions (Figure 4). The boundary conditions for the simulation at the sediment sluicing tunnel were the reservoir level at elevation (E.L.) of 180 m, tainter gate fully opened, and Manning coefficient n = 0.015. For the simulation at outlet work, scenarios of high discharge (Q $\geqq$ 250 m^3/s) and low discharge (Q < 250 m^3/s) were simulated to observe the flow condition at outlet work.
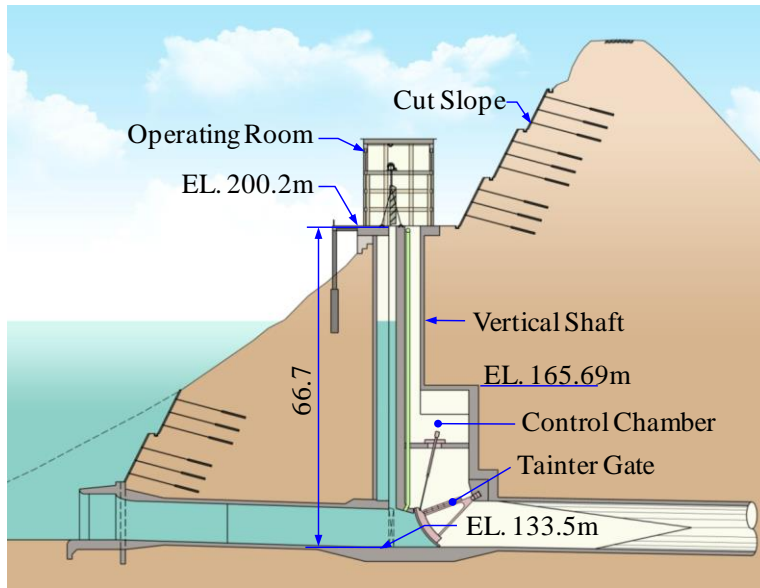
Figure 2: Vertical shaft and control chamber
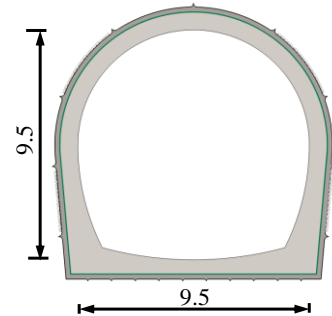
Figure 3: Typical sluicing tunnel cross section
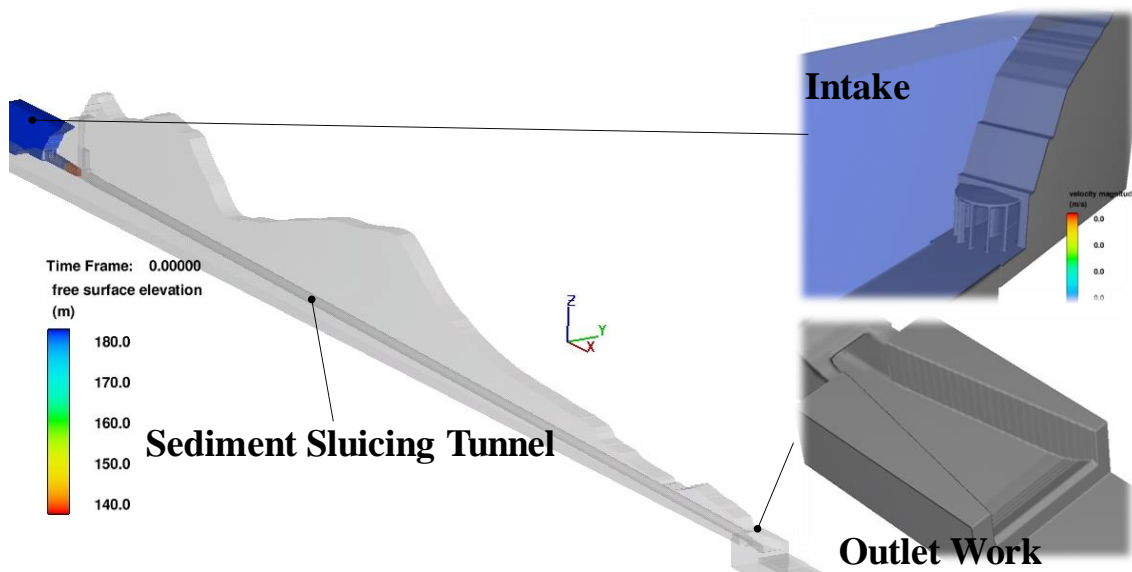
Figure 4: Flow 3D model for the sediment sluicing tunnel

2.1 Flow conditions in the sluicing tunnel

The results show that the flow in the sluicing tunnel is supercritical flow with the discharge of 998 m^3/s. The flow depth of each tested tunnel section is smaller than 0.75 times the tunnel diameter. The average flow velocity is around 18.0 ~ 27.0 m/s and the flow type is gravity flow. Overall, at Station (Sta.) 0K+000 ~ 0K+200, the water surface is unstable due to the flow development; the water surface becomes steady at Sta. 0K+200 ~ 1K+287.
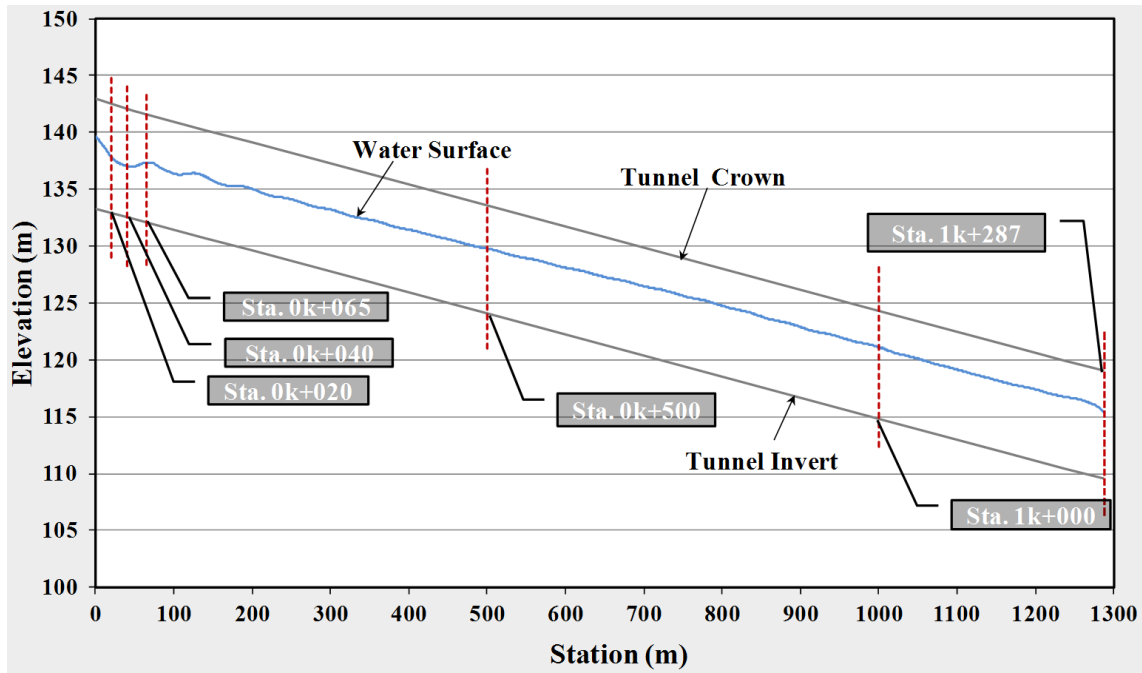
Figure 5: Water surface along the tunnel station

2.2 Abrasion analysis

The maximum shear velocity occurs at different locations with different types of water surface.

- Concave or convex water surface: the maximum shear velocity occurs at the lower part of the tunnel walls due to the secondary flow.

- Horizontal water surface: the maximum shear velocity occurs at the center of the tunnel invert due to the tunnel shape effect (horse shoe shape)

As a result, in the secondary flow developed area, the abrasion will occur at the tunnel walls; if the flow is fully developed, the abrasion will concentrate at the center of the tunnel invert. The diagrams are listed in Table 1.

74

Table 1: Water surface, flow velocity and shear velocity at the tunnel sections

Station [m]	*Velocity* [m/s]	*Shear Velocity* [m/s]
Sta. 0K+040		
Sta. 0K+065		
Sta. 0K+500		
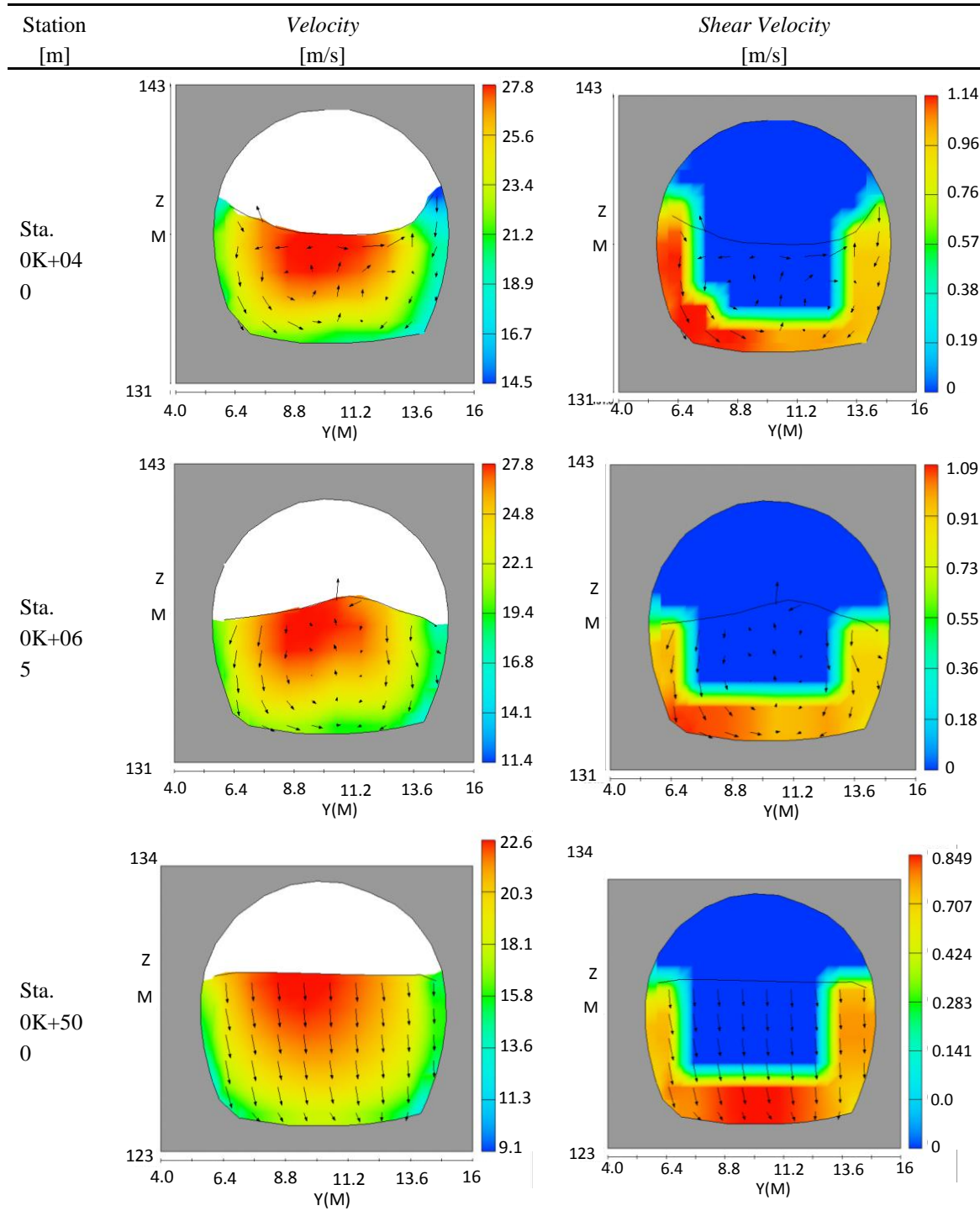
2.3   Flow condition at the outlet work

At the design discharge $Q_d = 1000 \text{m}^3/\text{s}$, the jump flow velocity is 17.6 m/s with the length of 40m. However, at the low discharge conditions ($Q < 250 \text{ m}^3/\text{s}$), no jet flow occur and the flow will jump to the downstream close to the outlet work. As a result, foundation scouring at outlet work may occur (Figure 6).

Q=1,000m³/s
Jet Flow Length = 40m

Q=250m³/s
Jet Flow Length = 12m

Q=200m³/s
No Jet Flow

Q=150m³/s
No Jet Flow
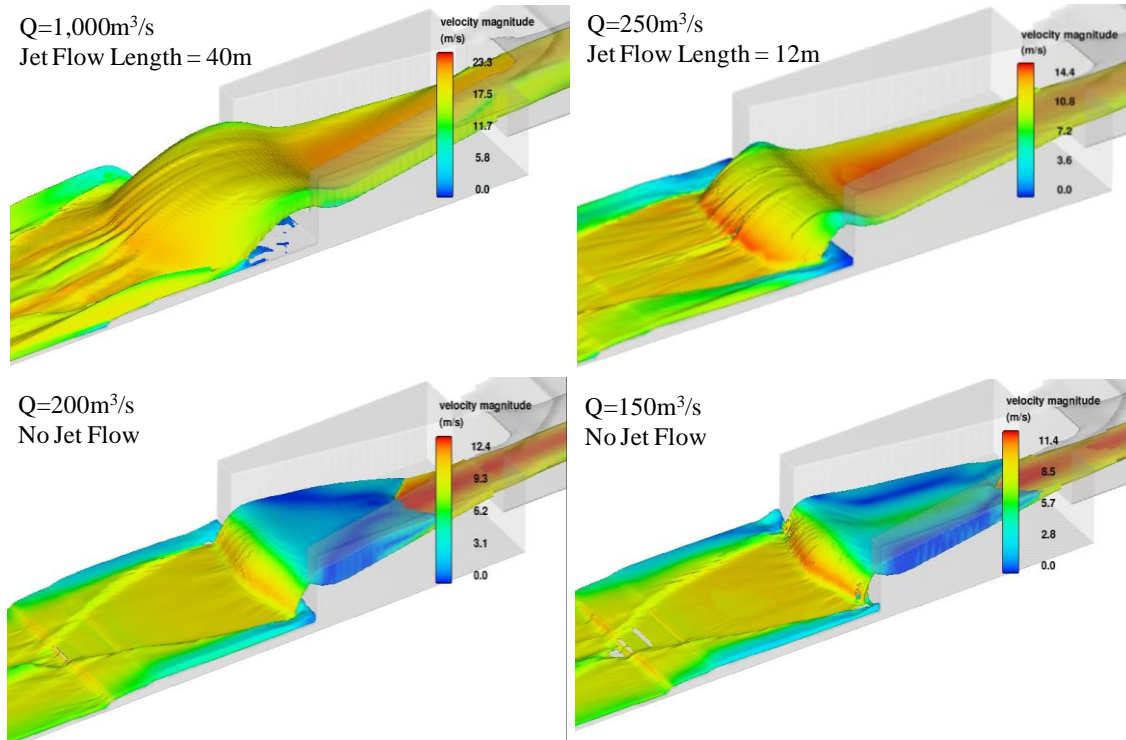
Figure 6: Jet flow at different discharge

3 Hydraulic model test

A 1/81 whole-field model and a 1/40 local model were constructed. The main objectives of the hydraulic model tests were specifying the sediment sluicing efficiency, hydrodynamics of the flow in the sediment sluicing tunnel, and flow conditions at the intake. The experimental setup is shown in Figure 7, 8 and Figure 9.

Figure 7: 1/81 whole-field model
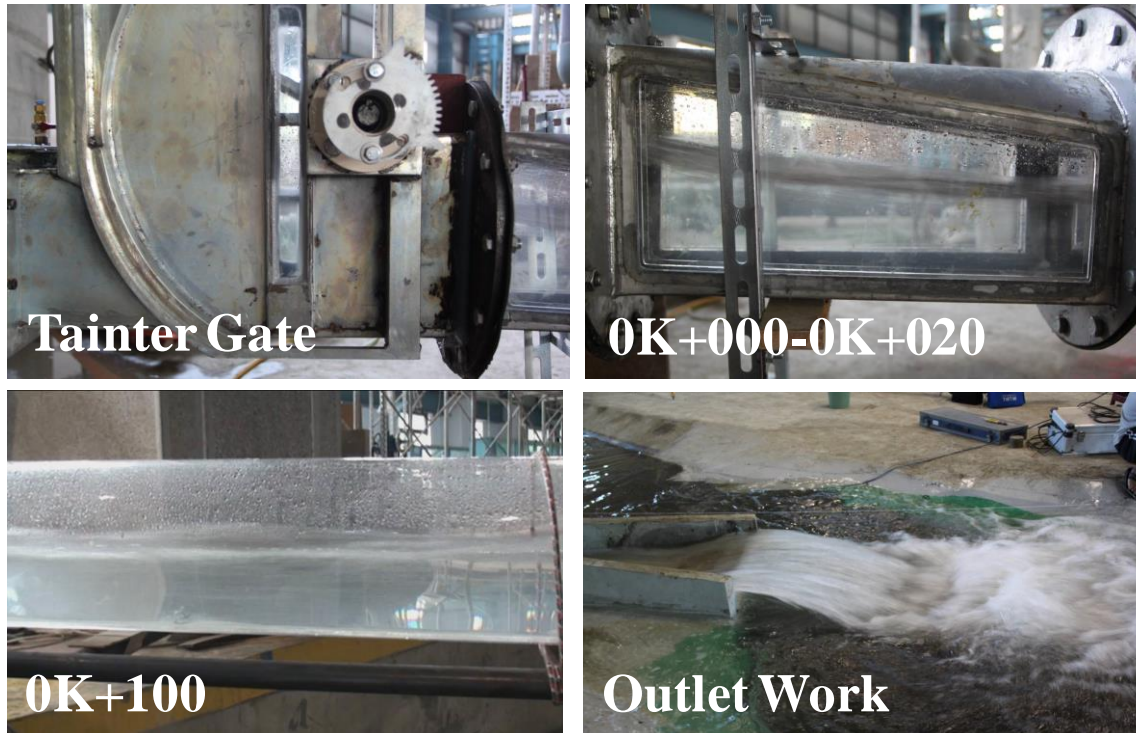
Figure 8: 1/40 local model
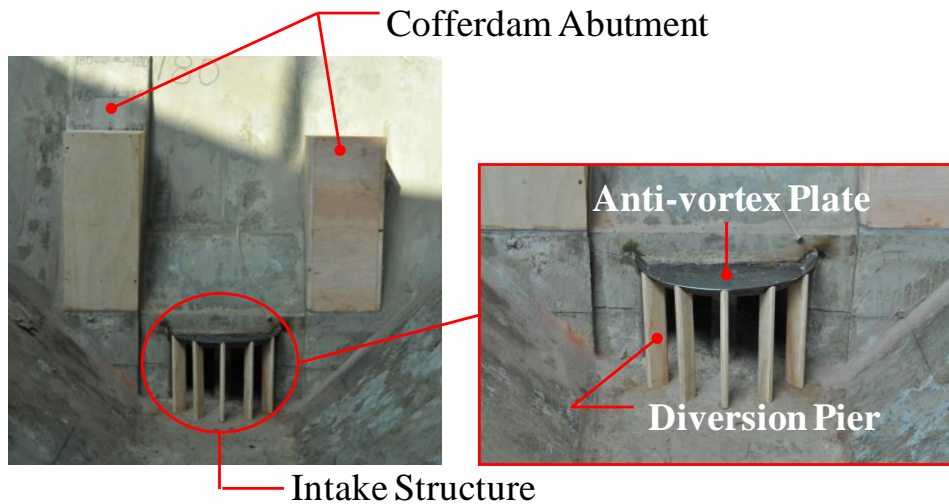
Figure 9: 1/40 local model at the intake area

3.1 Test results of 1/81 whole-field model

With the inflow $Q_{in} = 2{,}540$ m³/s (Typhoon Kalmaegi, 2008), flow concentration of 70,000ppm, and the outflow discharge $Q_{out} = 1{,}000$ m³/s the sediment sluicing efficiency was 32.3%, which was above the design efficiency of 24%. The chart for the flow concentration with regards to the time is shown in Figure 10.
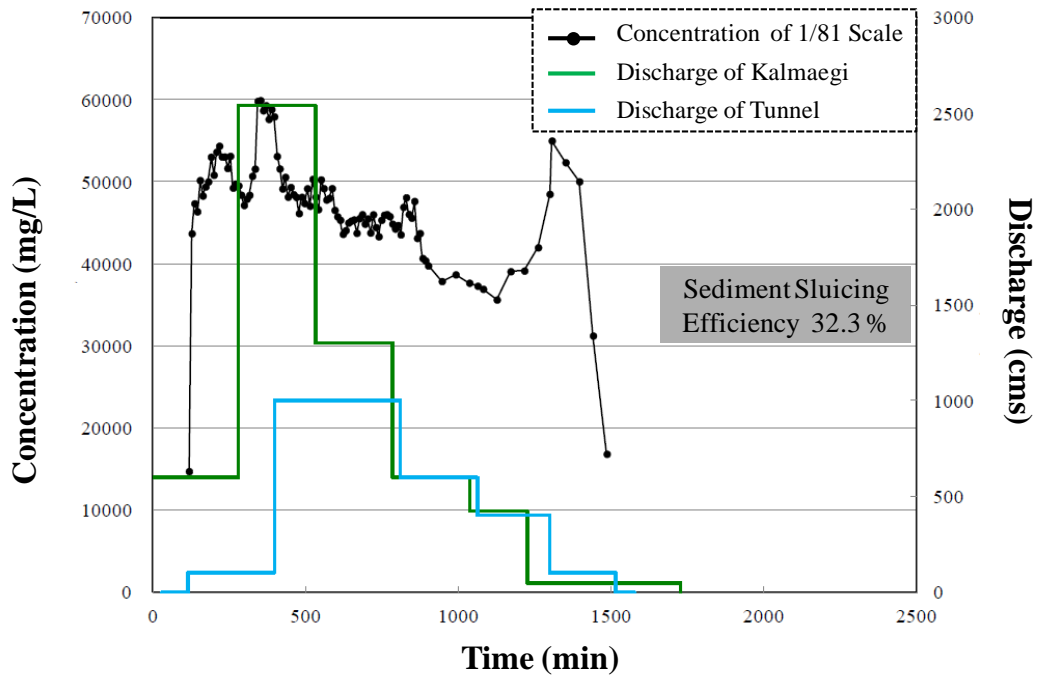
Figure 10: chart for the flow concentration with regards to the time

3.2 Test results of 1/40 local model

For the reservoir level of EL.180 m, the flow depth in the tunnel was less than 0.75D, and the flow discharge in the tunnel was 990 m^3/s close to the design discharge of 1000 m^3/s. The depth of the scour pit at the downstream of the outlet work was about 16.3m. The distance between the edge of the outlet work and the bottom of the scour pit was about 80 m (Figure 11).
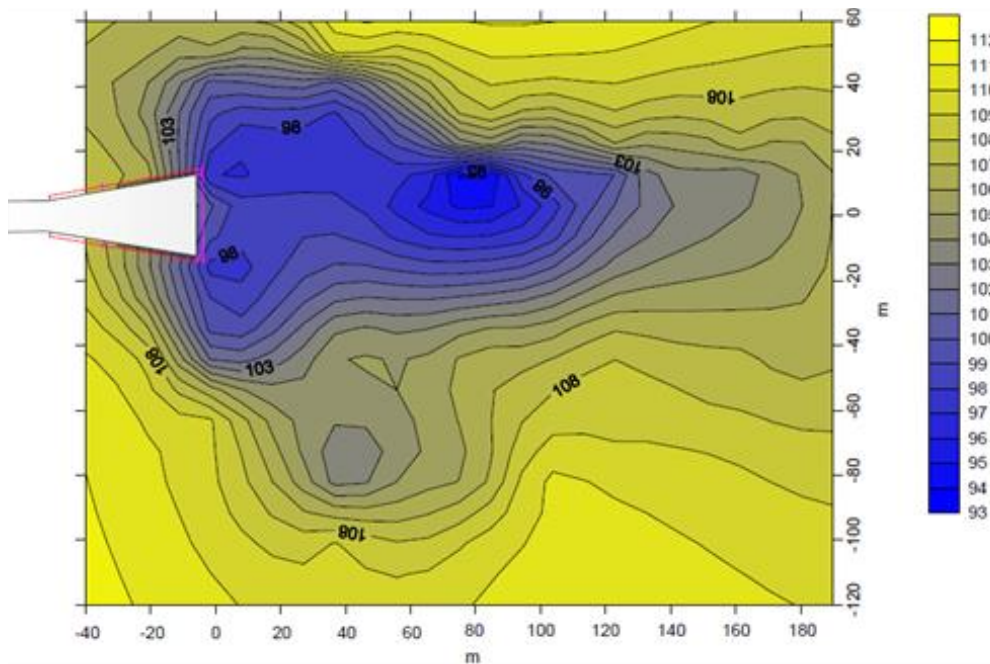
Figure 11: Depth contour of the scour pit at the outlet work

3.3 Test results of 1/40 local model at intake

Models with and without diversion piers and abutments were setup to check the effects on the flow conditions at intake. The definition of free surface vortices type follows ANSI Hi index-2012.

3.3.1 Surface Vortex Observation

For the reservoir level of EL.180 m, type 6 vortex didn't occur, the occurrence of type 5 vortex was 1.4%, and the occurrence of type 4 vortex decreased at the model with diversion piers and abutments (Figure 12). No type 5 and 6 vortices occurred at the reservoir level of EL.175m and EL.170m, but the occurrence of type 3 and 4 vortices increased slightly at lower reservoir level at the model with diversion piers and abutments (Figure 13).

It was concluded that the abutments protruded from the ground surface and were close to the water surface, acting like an anti-vortex structure and reducing the surface vortex.
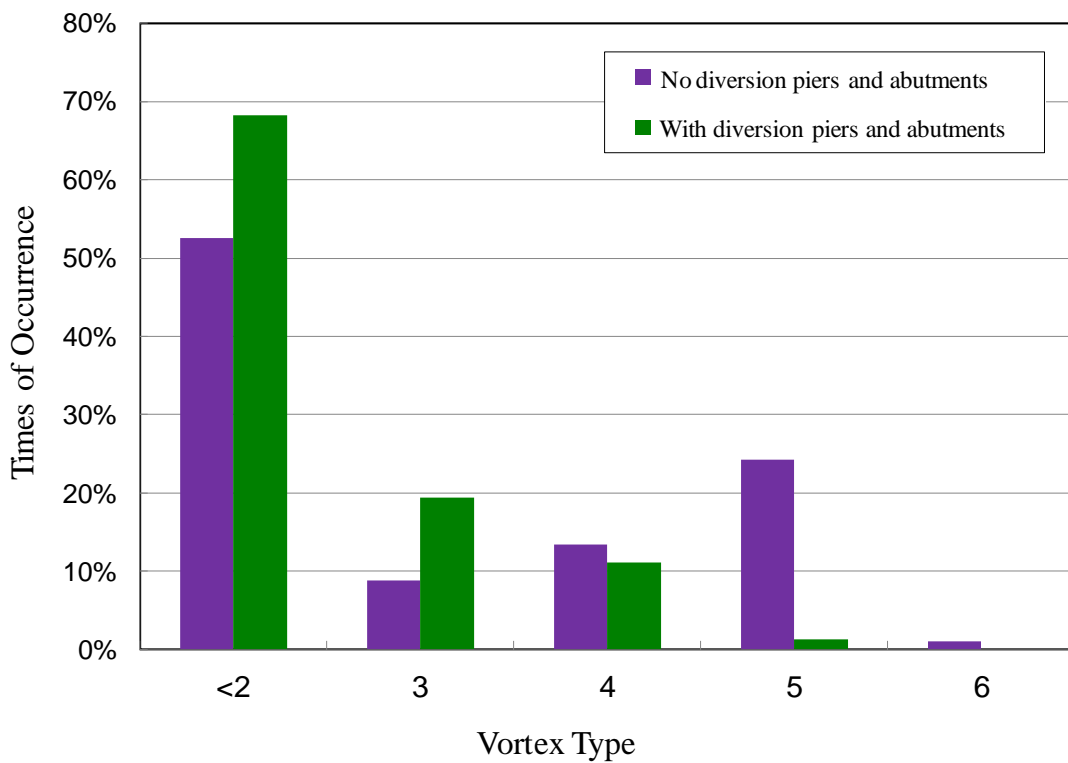
Figure 12: Vortex occurrence at model with and without diversion piers and abutments
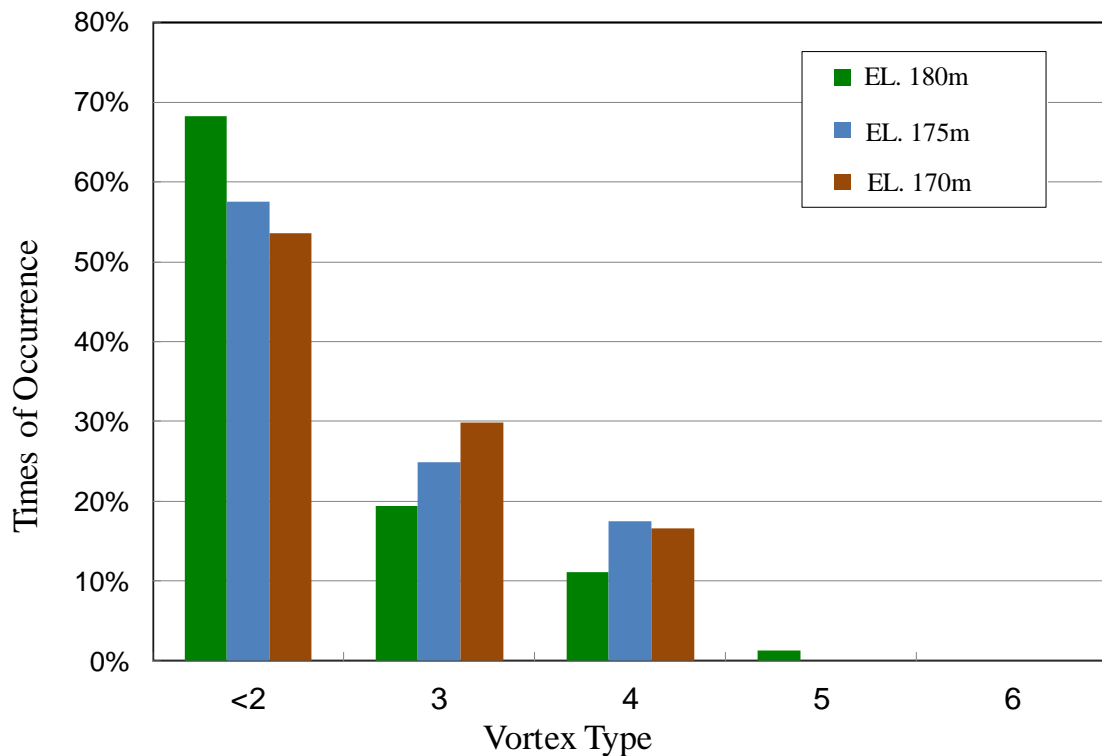
Figure 13: Vortex occurrence between different reservoir levels at model with diversion piers and abutments

3.3.2   *Pressure head and flow discharge*

Pressure head was measured at the intake, the middle of the intake tunnel, and the front of the tainter gate. The data showed that the head loss didn't occur at the model with the diversion piers and abutments, thus, the diversion piers wouldn't cause any effect on the inflow discharge (Figure 14).

During the test, the discharge difference between the model with and without diversion piers was in the range of ±5%. The tunnel discharge was still 990 m^3/s at reservoir level of E.L. 180 m, and it indicated that the effects by the diversion piers were very small and hence negligible.

80
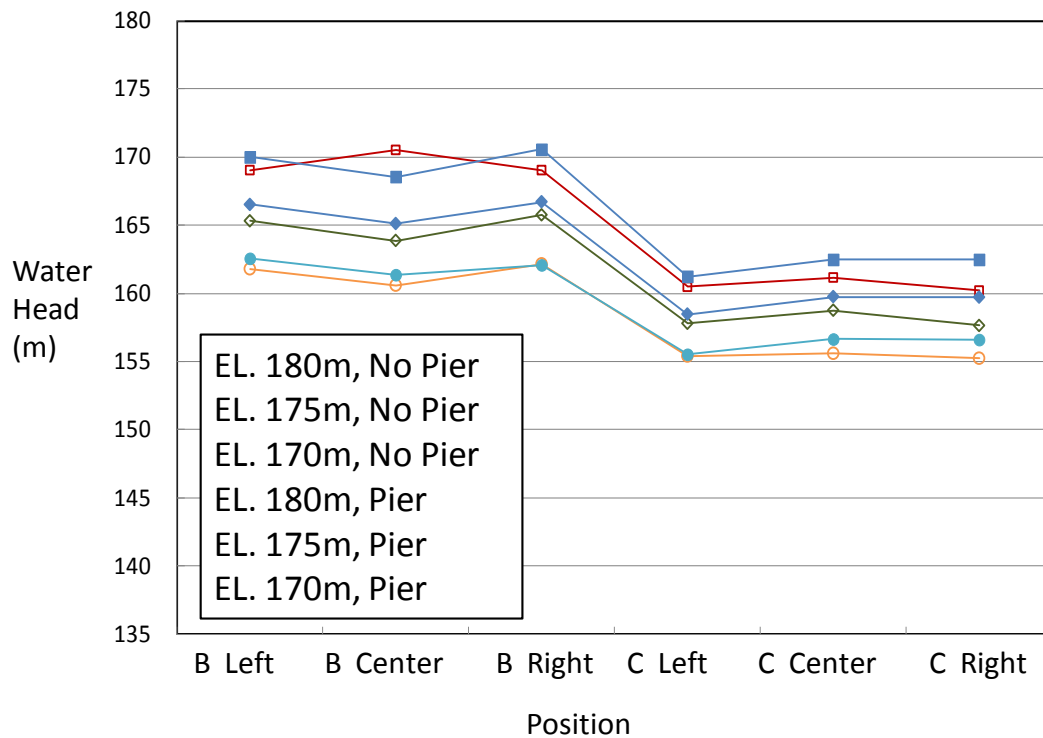
Figure 14: The pressure head differences at the intake with and without diversion piers and abutments

4   Cofferdam

A 47.5 m cofferdam is designed to retain water during the intake construction. The cofferdam consists of a semicircle weir and two abutments (Figure 15). The thickness of the semicircle weir is varies from 4m at center to 5m at sides, and the thickness of the abutments is 7 m. 1.25 m thick steel pipe piles are installed as formwork for concrete placing.
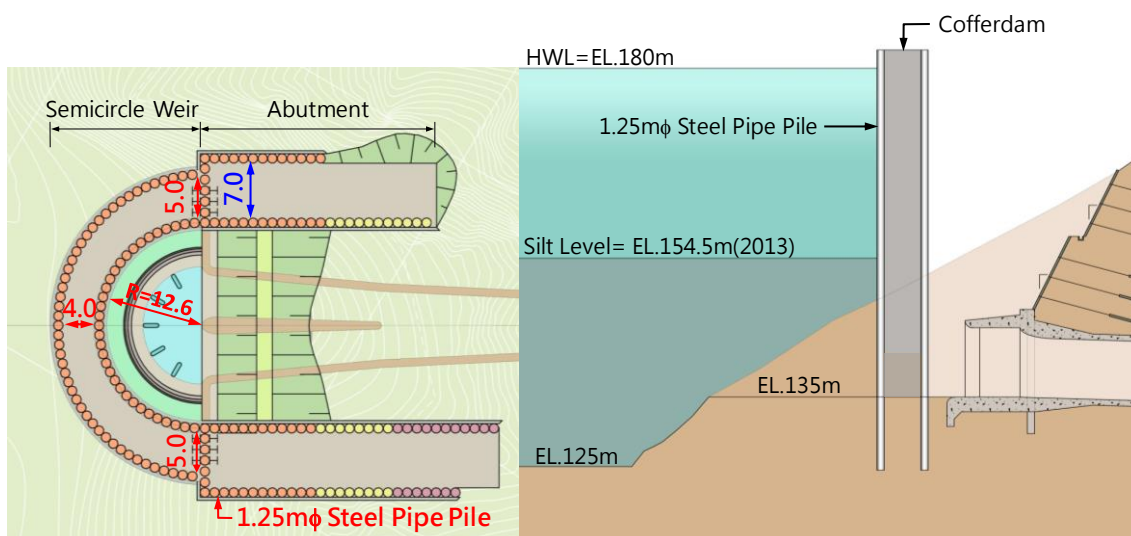
Figure 15: Plan view and profile of the cofferdam

Issues during the cofferdam construction and the proposed solutions are listed in the Table 2

Table 2: The important issues for the cofferdam construction

Item	Issues during the construction	Solutions
1	Cold joints and honeycomb in the concrete	Continuous concrete pouring with high-flow concrete
2	Hydration heat in the massive concrete	Temperature control during concrete pouring (<32°C during concrete pouring; <36°C initial setting of concrete)
3	Problems with construction tolerance	tolerance control during the construction
4	Water leakage at the cofferdam	Water glass filling in the connection of the steel pipe pile

5 Conclusions

In recent years, severe siltation has affected Nanhua reservoir adversely. According to the silt survey in 2012, the effective storage volume of Nanhua reservoir decreased to 62.9% of its design storage volume. A sediment sluicing tunnel was proposed to flush the incoming sediment to the downstream of the Nanhua dam during the flood season.

Comprehensive numerical hydraulic analyses and hydraulic model tests had been conducted to testify the efficiency of the sediment sluicing tunnel. The results showed that the sluicing efficiency was 32.3% and satisfied with the design requirement of 24%. The flow conditions at the tunnel, intake and outlet work were acceptable, but foundation scouring may occur at outlet work at low discharge conditions.

A Cofferdam with 47.5m in height will be constructed to retain the water during the construction. Quality of the cofferdam concrete and the precision of the installation of the steel pipe piles are the key issues of the cofferdam construction.

References

South Region Water Resources Office, WRA, MOEA (2013). The Hydraulic Model Test Report for the Sediment Sluicing Tunnel Project of Nanhua Reservoir.

South Region Water Resources Office, WRA, MOEA (2013). The Basic Design Report of the Sediment Sluicing Tunnel Project of Nanhua Reservoir.

Hydraulic Institute Standards (2012). Pump Intake Design. *American National Standards Institute,Inc.*, 37.

Authors

Min-Yi Tsai (Corresponding Author)
Sinotech Engineering Consultants Limited
Email: yellyo1839@mail,.sinotech.com.tw.

Dr. Chen-Shan Kung
Mr. Yi-Liang Chen
Sinotech Engineering Consultants Limited

Dr. Shih-Wei Huang
Southern Region Water Resources Office, WRA, MOEA

Ming-Yang Liao
RSEA Engineering Corporation

Sediment management in Andean Region: Chespí-Palma Real project

Carmelo Grimaldi, Fabio Micheli, Roger Bremen

Abstract

The 470 MW Chespí-Palma Real project is a hydroelectric power plant with a 63 m high double curvature arch dam on the Guayllabamba River, in the North-Western part of Ecuador. Sediment management is a key aspect for the project. In fact, a high inflow sediment rate has been estimated, as typical for the Andean water courses, where high sediment production is due to the presence of volcanoes, in combination with scarce vegetation resulting in very high flood discharges with high sediment transport rates.

Sediment management is achieved by means of a 2.24 km long bypass tunnel located at the inlet of the reservoir, where a weir is also located in order to trap the sediments before they enter into the reservoir.

The bypass tunnel behavior has been checked through laboratory tests on physical model, which confirmed high efficiency in sediment evacuation and a satisfactory hydraulic behavior according to the design conditions.

Zusammenfassung

Die 470 MW Wasserkraftanlage Chespí-Palma Real nutzt die Gewässer des Flusses Guayllabamba, im nordwestlichen Teil von Ecuador und ist geprägt durch eine 63 m-hohe, doppelgekrümmte Bogenstaumauer. Die im Einzugsgebiet liegenden Vulkane führen zu einem hohen Sedimentvorkommen.

Um Verlandungsprobleme zu beseitigen, ist im Oberwasser eine Schwelle geplant, welche die Sedimente vor dem Speicher auffangen wird und in einem 2.24 km langen Sedimentumleitstollen (6.6 m x 6.6 m) unterhalb der Stauhaltung leiten soll.

Die Bypass-Effizienz wurde durch Versuche an einem physikalischen Modell untersucht, welches eine effiziente Sedimentumleitung mit gutem hydraulischen Verhalten gemäss den Projektbedingungen bestätigt.

1   Focus on the general problem

Reservoir sedimentation is object of several studies and research since many years and is considered worldwide one of the most significant problems affecting the capacity for water supply, flood control and energy production regulation (*e.g.*, Mahmood 1987, Hotchkiss 1990, Lai and Shen 1996, Morris and Fan 1997, Sumi 2000, Morris 2003).

ICOLD (2009) recently assessed the gross storage capacity in the world equal to 7'000 km^3 (6'100 km^3 based on the ICOLD Register of Dams, but if smaller of 15m dams are included, 7'000 km^3 could be the current total storage), of which 3'000 km^3 is dead storage for hydropower dams. The total storage loss and annual sedimentation rate are estimated of 570 km^3 (12%) and 31 km^3/year (0.52%/year) respectively; the existing total storage capacity is expected to decreased to less than half by 2'100 (Sumi *et al.* 2004).

Indeed, dams create discontinuity in a river system by affecting both the water discharges and natural sediment transport. Sediments retained upstream to the dam tend to accumulate with consequences on the reservoir itself, by impairing reservoir operation and decreasing storage, and the downstream reaches of the river, with effects on the morphology and the ecosystem.

Sediment management is mainly achieved in three ways:

- by reducing the sediment inflow rate: structural and non-structural measures in the catchment area (soil conservation works) and along the river (river training works)

- by routing sediment around or through the reservoir: *i.e.*, by means of sediment bypass and sediment pass-through structures;

- by recovering the reservoir volume: removing sediments accumulated in the reservoir, *e.g.*, by flushing (hydraulic removal) or by dredging/excavating (mechanical removal); enlarging the reservoir capacity with the dam heightening;

Each approach has advantages and disadvantages. The choice of the right one, is mainly depending on the specific features of the site.

Sediment bypass structures have not been a commonly used measure in the past due to topographical, hydrological and economical conditions. In the last decades the interest for this kind of structure is growing. In fact, bypass tunnels allow achieving several advantages: *e.g.*, they can be constructed even at existing dams; they have a relatively small impact on the downstream environment because inflow discharge can be passed through tunnels very naturally during flood time (Sumi *et al.* (2004)). Nevertheless, this kind of structure may suffer of abrasion problems and nowadays research is focused to test new materials or define effective measures to prevent tunnel damages (*e.g.* Auel (2014)).

Some effective examples of bypass tunnels are in Switzerland (Vischer *et al.* 1997, Auel *et al.* 2010) and in Japan (Ando *et al*. 1994, Kashiwai *et al.* 1997, Harada *et al*. 1997).

2   Chespí-Palma Real Project: The main features

Chespí-Palma Real project includes a 63 m high double curvature arch dam, located on the Guayllabamba River, in the North-Western part of Ecuador, about 30 km north from Quito.
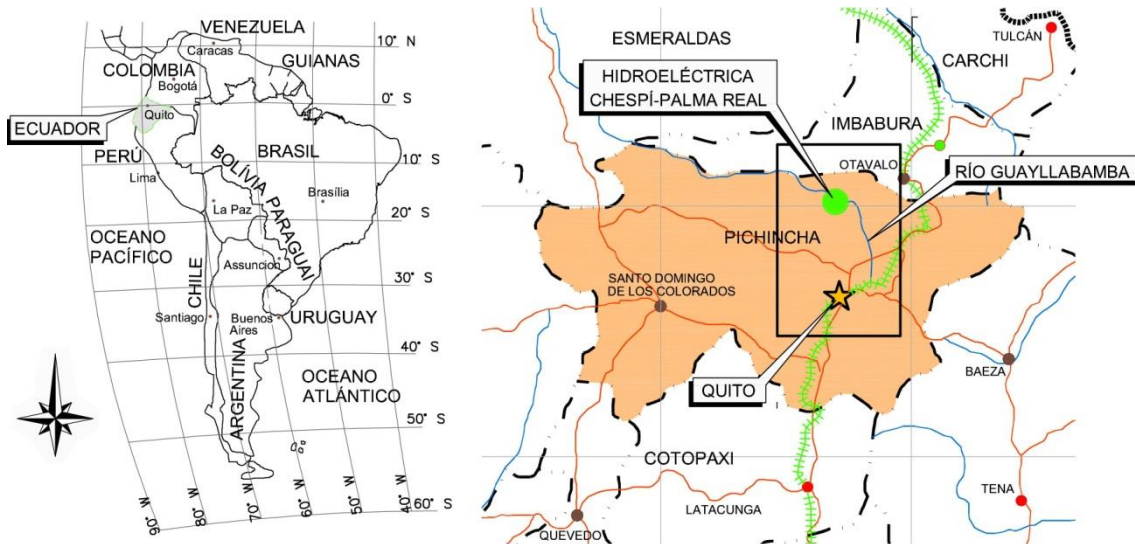
Figure 1: Geographical project location

The catchment basin is about 4'500 km^2. The reservoir capacity is of only 4.4 x 10^6 m^3 and covers 22.2 ha extending 3.2 km upstream to the dam.

As preliminary work, 2 diversion tunnels (6.60 m x 6.90 m) are designed in order to divert flows during the dam construction and protect the area from floods; after the works completion, both tunnels will be used as bottom outlets (each one with a final section of 6.0 m x 6.0 m).

The project of the powerplant includes the following structures: the power intake (Q=80 m^3/s); the headrace tunnel (L=18.29 km; D=5.40 m); the surge shaft (upper part D=15 m; H=123 m; lower part D=3.50 m; H=58 m); the penstock (L≈1000 m; D=4÷3.40 m); the powerhouse equipped with 4 Pelton turbines (P=468 MW); the tailrace tunnel (L=6.3 km; D=6.40 m).

The total cost of the project is estimated approx. of about 750 mio US$.
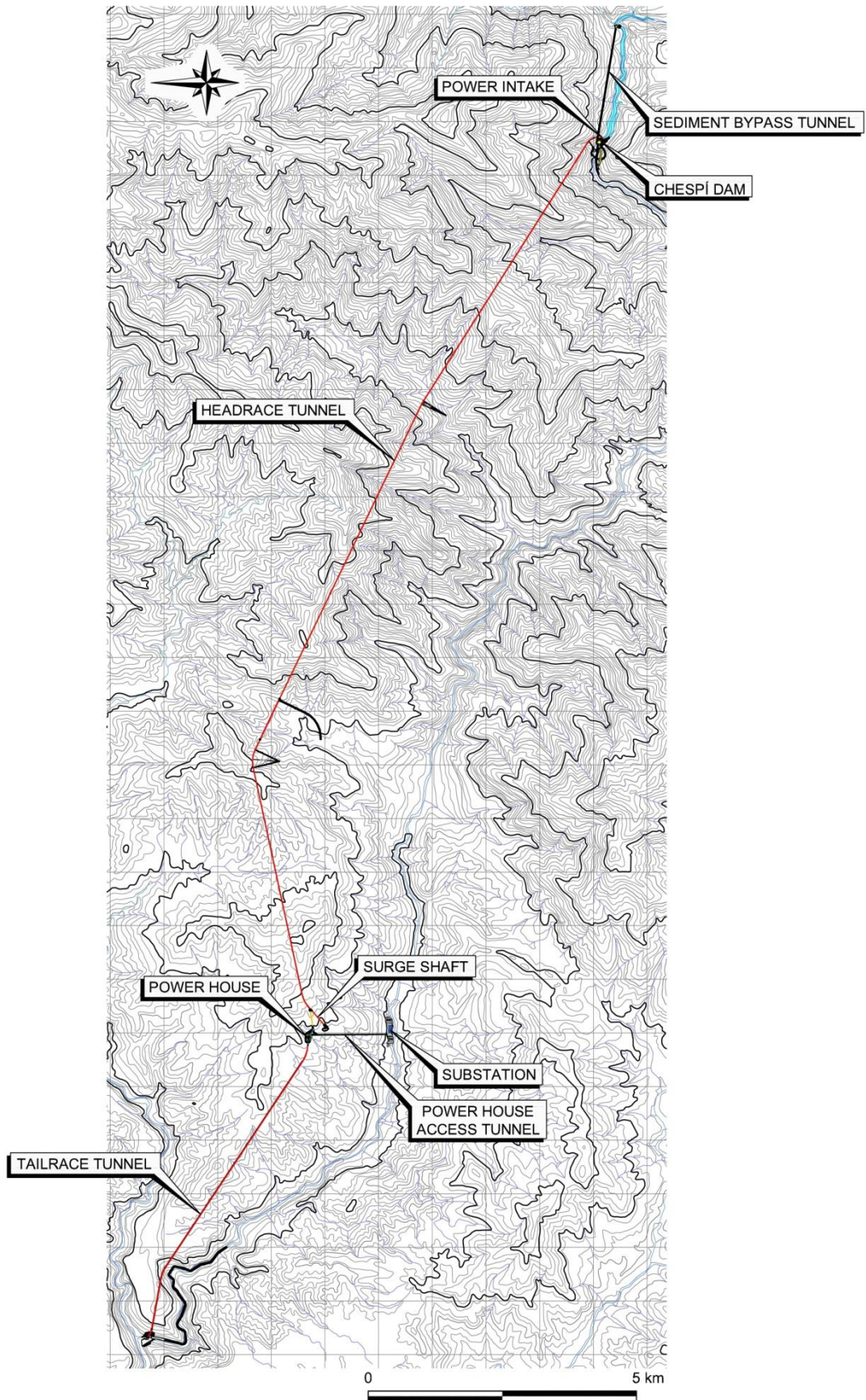
Figure 2: General layout of the Chespí-Palma Real project

3   The sediment management

Sediment management is a crucial issue because of the high sediment transport rate of the Guayllabamba river.

The annual sediment runoff is estimated of 820'000 m^3., corresponding approx. to 20% of the reservoir storage capacity. Sediment carried out during a extreme floods may reach and overcome 250 mm size; the suspended transport is generally characterised by a mixuture of fine sand and silt. Without any appropriate measure, the live storage of the reservoir would thus be rapidly affected by sediments.

Sediment management is achieved by means of a 2.24 km long sediment bypass tunnel (6.6 m x 6.6 m) located on the right bank of the reservoir. The bypass behavior takes advantages from the reservoir morphology. In fact the river curves at the reservoir upstream end – just downstream of the confluence of the Perlabi and the Guayllabamba Rivers – and the bypass tunnel develops with a straight alignment.

The tunnel is concrete lined and is designed to convey a flood of 400 m^3/s, corresponding to a 5-years return period. The intake is regulated by two radial gates (width of 4 m and H=5 m) separated by a 1.5 m wide wall. The plan view and the longitudinal profile of the tunnel are illustrated in Figure 4. A detailed section of the tunnel inlet is showed in Figure 6.

At the upstream end of the reservoir, just downstream of the bypass inlet, a rectangular notch weir is located to trap the sediments and avoid they enter into the reservoir. The weir crest is designed with a double height/elevation: H=5.5 on the right side – elevation 1444 masl; H=3.50 m on the left side – elevation 1442 masl, allowing a regulation of the discharge. Figure 5 shows the bypass tunnel inlet and the weir location.
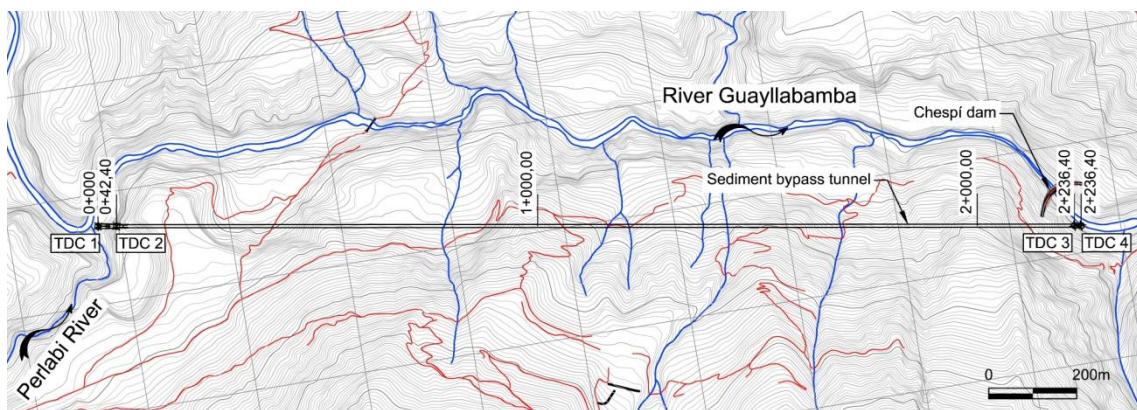
Figure 3: Plan view of the sediment bypass tunnel
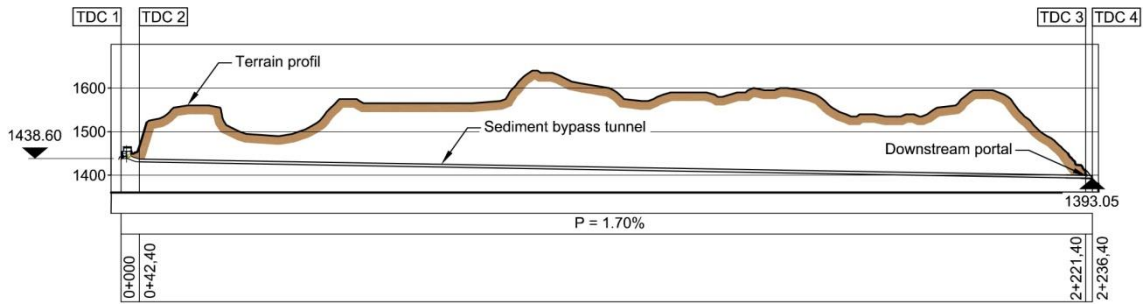
Figure 4: Longitudinal profile of the sediment bypass tunnel
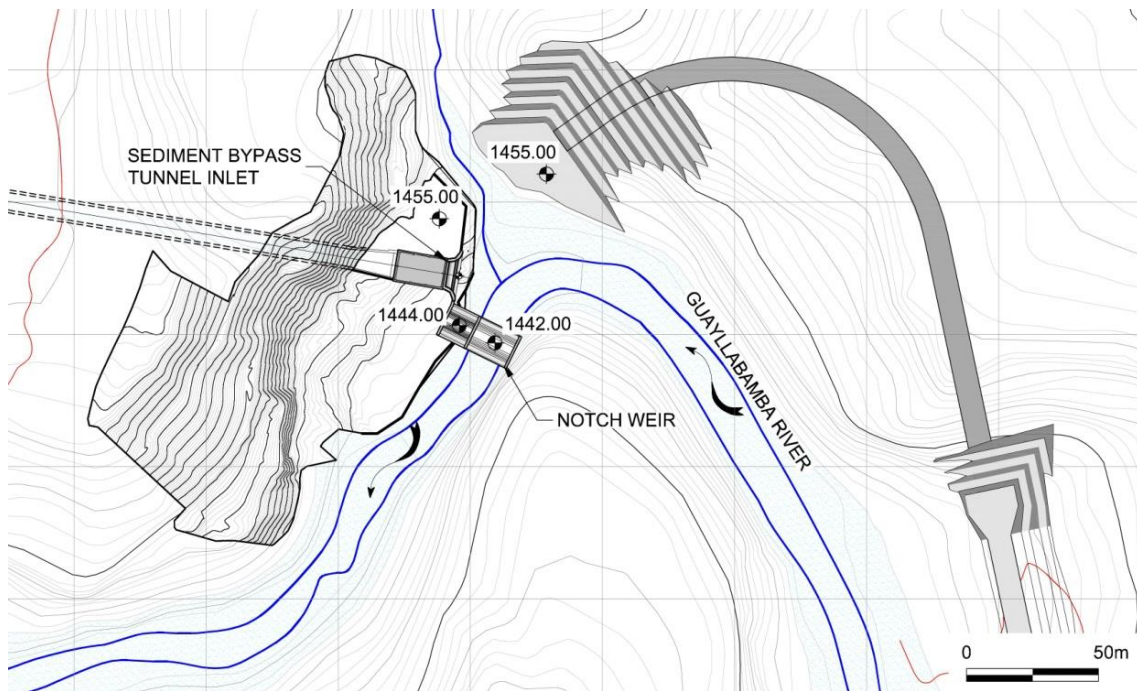
Figure 5: Plan view of the sediment bypass tunnel intake and the downstream notch weir

4 Hydraulic design of the sediment bypass tunnel

The tunnel has been designed in order to allow the evacuation of the sediments with the purpose to avoid regular flushing of the reservoir and subsequently the plant shutdown. Therefore it has been designed to operate in free surface supercritical regime, with sufficiently high flow velocities.

The hydraulic design of sediment bypass tunnels is rather complex due to the necessity to consider not only the hydraulics but also the sediment transport capacity. Particularly delicate is the appropriate selection of the tunnel slope, since low slopes may cause sediments deposits resulting in a complete clogging of the tunnel.

The bottom is shaped with a Creager profile, reaching the maximum slope of 42.3%, allowing the flow to achieve supercritical regime in about 30 meters. The tunnel section and the slope (length of 2'183 m, with a longitudinal slope of 1.71%) have been set in order the flow is achieving the uniform supercritical regime at the tunnel inlet with a

90

sediment transport capacity similar to the river. Uniform supercritical flow starting from the tunnel inlet allows is essential to limit the risk of sediments deposits inside the tunnel.
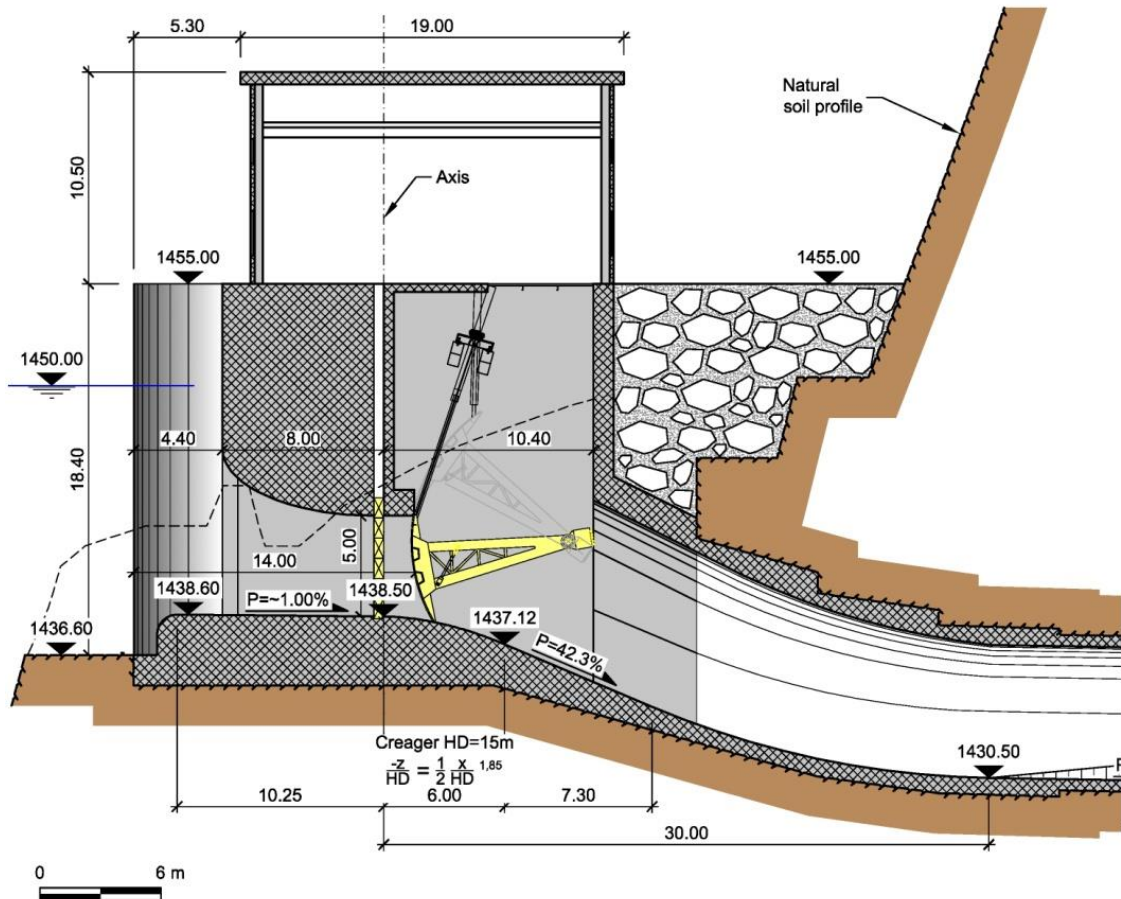
Figure 6: Detailed section of the sediment bypass tunnel intake

The preliminary design discharge have been set to 158 m³/s, leading to a water level at the inlet at elevation 1444 masl (equal to the highest sill crest elevation). In this condition the estimated flow velocity is about 4 m/s at the initial bypass reach, leading to an adequate sediment transport capacity.

The design criterion is based on the energy balance: the hydraulic head at the inlet, subtracted the local and continuous head losses along the initial reach, has to lead to a specific energy of uniform flow regime at the beginning of the tunnel, for the design tunnel slope and discharge. Both parameters have been chosen in order to have the tunnel outlet at higher elevation than the water level of Guayllabamba River and avoid its influence on the bypass flow regime.

Final calculations has been aimed to check the standing waves formation inside the tunnel because of the cross section contraction at the tunnel inlet. In fact, low waves have been estimated and no cross section plug occurrence has been assessed.

4.1 Physical model tests

A physical model (scale 1:38; Froude Similitude) of the river, sediment bypass, weir and the reservoir has been built at the Ecole Polytechnique Féderale de Lausanne, Switzerland. The hydraulic model tests aimed to verify and optimize the following aspects:

- the hydraulic performance of the bypass in the established configuration;
- the identification of potential deposit zones in the river;
- the proper sediment evacuation during floods (sediment flushing procedure).

Figure 7: General view of the physical model (from LCH, 2011)

Tests were carried out in two major phases, in clear water conditions and with sediment, for various flood return periods. Water profile, approach condition through the inlet, sediment deposition and evacuation process as well as flow velocity in the bypass tunnel and over the weir's vicinity were measured for the different scenarios.

Preliminary tests (bypass tunnel inlet closed and absence of weir) showed a significant sediment transport capacity with minor deposits at the inner bank of the river bend. In the case of lower reservoir level all sediments flowed into the reservoir and filled it over

a short period of time (LCH, 2011). Further tests with weir and bypass tunnel in operation showed high efficiency in sediment evacuation.

In particular, almost 100% of the incoming sediment volume was bypassed inside the tunnel during test with simulated flood of 100 m^3/s; more than 70% in tests with simulated flood of 200 m^3/s; for flood of 400 m^3/s the best performance was achieved with reservoir at elevation 1450 masl, in order to increase the bypass discharges and achieve improved evacuation of the suspended sediment load.

The inlet structure resulted well designed and able to bypass the required discharges and the transition from the gated section to the free flow tunnel led to a correct acceleration and smooth evolution of the flow. The inlet structure resulted working well for all the tested scenarios, with variable reservoir water surface elevation, weir position and elevation.

5 Conclusions

The present paper briefly present Chespí-Palma Real project and its sediment bypass tunnel, designed in order to manage sediment transport and avoid the sediment reservoir filling.

The tunnel has been designed taking into account the actual river morphology; in order to optimize the hydraulic behavior.

Tests carried out in laboratory on physical model confirmed the design behavior and the bypass effectiveness to prevent sediment accumulation upstream to the weir as well the sediment entrance inside the reservoir.

References

Ando, N. *et al.* (1994). Sediment removal project at Miwa dam. *18th Congress of ICOLD*, Durban, Q.69, R.27, pp.421-441.

Auel, C. *et al.* (2010) Sediment Management in the Solis Reservoir using a bypass tunnel. *8th ICOLD European Club Symposium*. 22nd - 23rd September 2010 Innsbruck, Austria.

Auel, C. (2014). Flow characteristics, particle motion and invert abrasion in sediment bypass tunnels. Diss., Eidgenössische Technische Hochschule ETH Zürich, Nr. 22008.

LCH (2011). Chespi-Palma Real, Ecuador. Physical hydraulic model tests for flood and sediment bypass. LCH report 09/2011. EPFL, Lausanne (unpublished project report).

Harada, M. *et al.* (1997). Planning and hydraulic design of bypass tunnel for sluicing sediments past Asahi reservoir, *19th Congress of ICOLD*, Florence, C.9, pp.509-539.

Hotchkiss, R.H. (1990). Reservoir sedimentation and sediment sluicing: experimental and numerical analysis. Project Report No. 304, St. Anthony Falls Hydraulic Laboratory, University of Minnesota, Minneapolis, Minnesota, USA.

ICOLD (2009) Sedimentation and Sustainable Use of Reservoirs and River Systems, ICOLD Bulletin.

Kashiwai, J. *et al.* (1997). Hydraulic study on diversion facilities required for sediment bypass systems. *19th Congress of ICOLD*, Florence, Q.74, R.59, pp.957-976.

Lai, J.-S. Shen, H. W. (1996). Flushing sediment through reservoirs. *Journal of Hydraulic Research*, Volume 34, No. 2-1996, pp. 237-255.

Mahmood, K. (1987). Reservoir sedimentation: impact, extent, and mitigation. World Bank Technical Paper Number 71.

Morris, G.L. & Fan, J. (1997). Reservoir sedimentation handbook, McGraw-Hill, New York.

Morris, G.L. (2003). Reservoir sedimentation management: world wide status and prospects, Session "Challenges to the sedimentation management for reservoir sustainability", *3rd world water forum*, Kyoto-Shiga, pp. 97-108.

Sloff C. J. (1991). Reservoir sedimentation: a literature survey. Communications on hydraulic and geotechnical engineering, Report No. 91-2, Delft University of Technology, The Netherlands.

Sumi, T. 2000, Future perspective of reservoir sediment management, *International workshop on reservoir sedimentation management*, Toyama, pp. 145-156.

Sumi, T *et. al.* (2004). Reservoir sedimentation management with bypass tunnels in japan. *Proc. of the Ninth International Symposium on River Sedimentation*, October 18 – 21, 2004, Yichang, China.

Vischer, D. *et al.* (1997). Bypass tunnels to prevent reservoir sedimentation. Q. 74 R. 37. *Proc. of the 19th Congress of ICOLD*, Florence, Italy.

Authors

Dr. Carmelo Grimaldi (corresponding Author)
Lombardi Engineering Limited, Minusio, Switzerland
(Email: carmelo.grimaldi@lombardi.ch)

Mr. Fabio Micheli
Dr. Roger Bremen
Lombardi Engineering Limited, Minusio, Switzerland

Rizzanese sediment bypass tunnel

Eric Laperrousaz, Pierre Carlioz

1   Introduction

The integration of environmental issues, as well as recent changes in the legislation - "Law on Water and the Aquatic Environment" - led the owner to decide to install a system that could offer the largest possible effectiveness with respect to sediment continuity. It was decided to convert the temporary diversion tunnel, used during the construction phase, into a permanent structure used for sediment-flushing operations during floods called Sediment Bypass Tunnel (SBT).

Herein the previous studies linked to this SBT are presented:

- The feedback from a similar scheme,

- The hydraulic and hydro-sedimentary physical model implemented.

The paper focuses on operating conditions today defined for the operation of this SBT.

2   Main features of the work

The Rizzanese scheme includes a 40 m high roller compacted concrete (RCC) dam, a headrace tunnel and a penstock. The powerhouse (2 vertical-shaft Pelton units) has a rated capacity of 2 * 27.5 MW. The design flow is 15 m^3/s (7.5 m^3/s per unit), for a head of 418 m. The net capacity of the reservoir is 1 hm^3. The Full Supply Level (FSL) is 541.0 m.a.s.l. and the Maximum Water Level (MWL) is 545.7 m.a.s.l. The dam is equipped with a mid-level outlet gate and an overflow spillway set at the FSL (Creager-type).

This Sediment Bypass Tunnel includes:

- A rough intake that houses a stoplog to isolate the conduit from the reservoir, and four orifices of approximate dimensions 3.25 m x 2.3 m (HxL) to prevent large floating debris from entering. The integrated stoplog can be controlled from a platform located at level 529.5 m.a.s.l. (i.e. 50 cm above the minimum water level) by means of a lifting beam and a mobile crane (Figure 1a and 1b).

- A circular steel lining, inside the tunnel, with an inner diameter of 4.2 m and a length of 133 m, which can withstand the abrasion of sediments. Upstream from the conduit, two vent pipes 600 mm diameter supply the tunnel with air and thereby facilitate the transitions between pressurized and free surface flows.

- A fixed-wheel gate (dimensions 3.60 m x 3.60 m), and a radial gate (dimensions 3.60 m x 3.80 m) on the downstream side ensure controlling the released flow rate (Figure 1a).
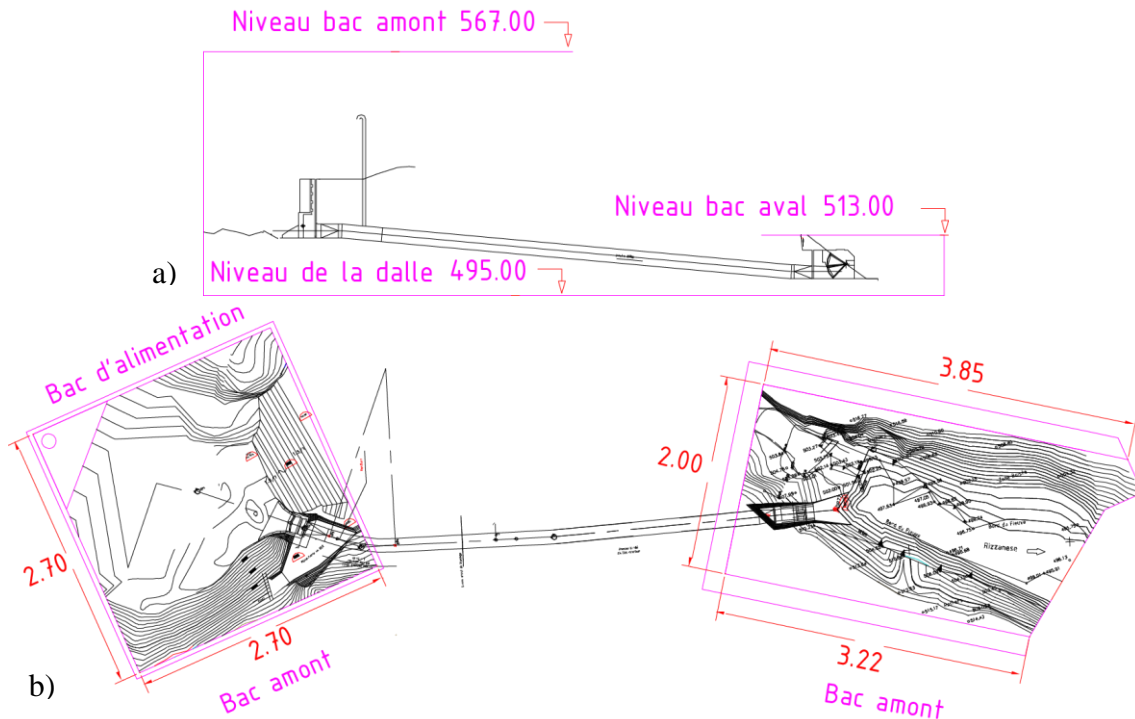
Figure 1: The Rizzanese SBT: a) longitudinal profile and b) plan view

3   Feedback from the Jotty Dam

One of the early key stages of the design consisted of searching for similar existing structures and collecting information. The experience gained by EDF operator of the Jotty dam (50 m high) over the last forty years provided useful information on how such schemes can be efficiently operated.

According to the operator, the main difficulty consists of making the decision to launch the sediment flushing operation, firstly due to flash-flood type events (requiring only 2 and 3 hours to reach their peak), and secondly due to the 4-hour authorization request constraints. However, only one of the six sediment-flushing operations performed in the last 12 years was a failure. During these flushing operations, the majority of the sediment accumulated in the reservoir was satisfactorily flushed out downstream.

4   Physical modeling

A 1/30 scale physical model was carried out for the Rizzanese, designed and constructed by the University of Liège (Belgium). It was divided into two stages: (1) the study of the hydraulic behavior; (2) the study of the hydro-sedimentary behavior (Figure 2).

Figure 2: Physical model designed and constructed by the University of Liège (Belgium).

4.1 Hydraulic study

The hydraulic studies showed that depending on the reservoir level and the opening of the radial control gate, the SBT is subject to pressurized flows, free surface flows, or mixed flows (Figure 3).
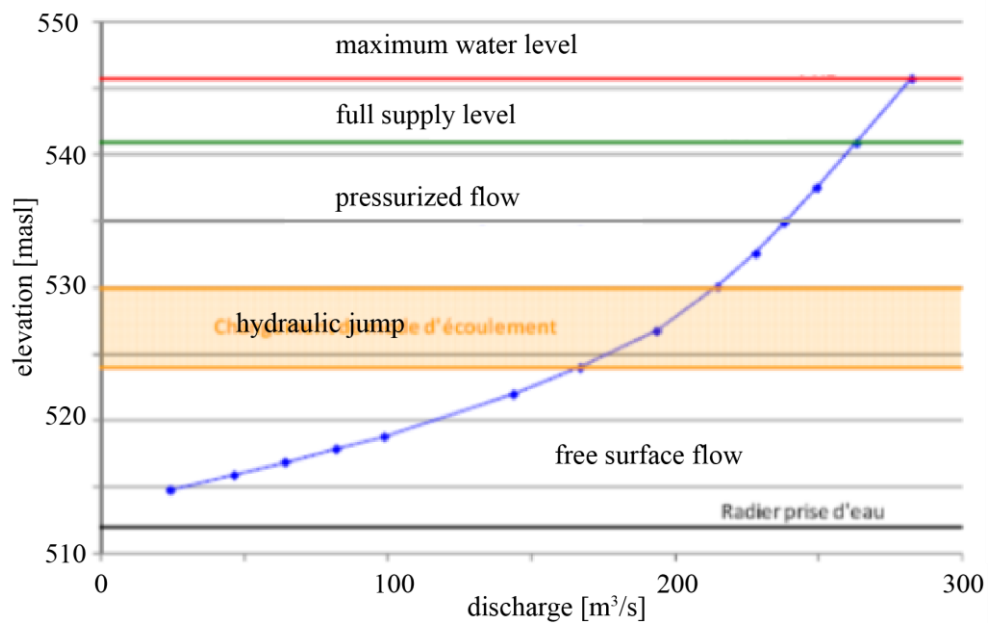
Figure 3: Flow conditions in the Rizzanese SBT

4.2 Hydro-sedimentary Study

The hydro-sedimentary study was carried out using two crushed limestone sands 0-2 mm and 0-6 mm, modeling sediment transported by the river, and showed the main characteristics of the sediment discharge through the SBT, and the effect that could be expected in the reservoir (Figure 4, 5 and 6).
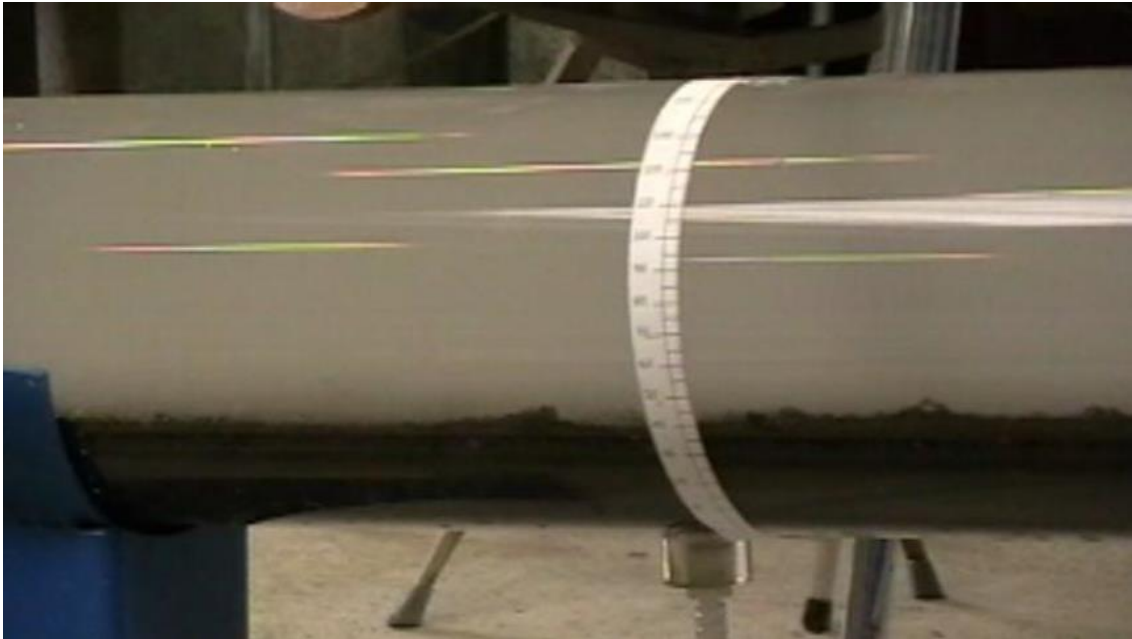
Figure 4: Sediment transport through the SBT

Figure 5: Residual deposits at the end of one of the hydro-sedimentary test

98

Figure 6: Deposit in the SBT at the end of one of the hydro-sedimentary test

5 The SBT operating

The paper will focus on the various elements taken into account in the instructions of operation of the SBT, among which:

- Hydro-meteorological forecast: The regional weather forecasts are completed by the local measures of rainy precipitation and flows; flow hydrographs of the main floods recorded over the past 25 years and characteristics of the riverbed sediment (mainly composed of medium/coarse sand and gravel) compute by ETRM, a consultant firm specialized in mountain river studies showed that the total sediment discharge rate through the SBT should allow to control deposits in the reservoir.

- Water level management: Operation for hydropower production requires maintaining the pool at high level all around the year. As the prediction of the floods is only some tens of hours, the first objective of the operating staff will be to lower the reservoir level while checking, for safety reasons, the increase of the flows downstream of the dam.

- The time request to get the data to identify the feasibility of a sediment flushing operation and to make the decision to launch this operation. The main difficulties are related to flash-flood type events requiring only few hours to

reach their peak knowing that the efficiency of the operation depends on the time spent in supercritical flow conditions.

- Downstream safety: The gradients of flow in downstream the dam, especially in the section which is short-circuited by the works must be checked.

- Environmental requirements: Constraints concerning the reserved flow in the section which is short-circuited by the work, the rate of suspension materials…

- Risk of obstruction of the tunnel: as the physical model showed a risk of obstruction of the Sediment Bypass Tunnel if its closure happens under some conditions which have been identified in laboratory, these conditions must be prevented.

- Re-filling of the reservoir by the end of the operation.

- Discharging clear water to avoid any significant deposit of fine materials downstream the reservoir.

References

Garcia, M. (2008). Sedimentation engineering, processes, measurements, modeling and practice, ASCE.

Graf, W., Altinakar, M. (1993). Hydraulique fluviale Tome 2, écoulements non permanents et phénomènes de transport, Presses polytechniques et universitaires romandes, Suisse.

Koulinski, V. (2009). Rizzanese, détermination des apports solides. ETRM. France.

Koulinski, V. (2009). Rizzanese, étude des chasses solides de la retenue. ETRM. France.

Malavoi, J.R., Bravard, J.P. (2011). Elements d'hydromorphologie fluviale, ONEMA, France.

Morris, G.L., Fan, J. (1997). *Reservoir sedimentation Handbook,* Mc Graw-Hill, USA.

Orvain, F., Laperrousaz, E. (2012). Laboratory measurements and sand/mud sediment erodability in the Longefan EDF retention basin, *6th International Conference on Scour and Erosion*, Paris.

Partheniades, E. (1965). Erosion and Deposition of Cohesive Soils. *Journal of Hydraulices Division*, (91): 105-139.

Sogreah (2008). Rizzanese, expertise sur l'efficacité de la vanne sédimentaire. France.

Authors

Eric Laperrousaz (corresponding author)
EDF-CIH
Le Bourget du Lac, France
Email: eric.laperrousaz@edf.fr

Pierre Carlioz
EDF-CIH
Le Bourget du Lac, France

Saltation-abrasion model for hydraulic structures

Christian Auel, Ismail Albayrak, Tetsuya Sumi, Robert M. Boes

Abstract

The derivation of an abrasion prediction model for concrete hydraulic structures valid in supercritical flows is presented herein. The *state of the art* saltation-abrasion model from Sklar and Dietrich (2004) is modified using the findings of a recent research project on the design and layout of sediment bypass tunnels. The model correlates the impacting parameters with the invert material properties by an abrasion coefficient k_v. The value of this coefficient is verified by a similarity analysis to bedrock abrasion in river systems applying a correlation between the abrasion rate and the bed material strength. A sensitivity analysis reveals that the saltation-abrasion model is highly dependent on an adequate estimation of k_v. However, as a first order estimate the proposed model enables the practical engineer to estimate abrasion at hydraulic structures prone to supercritical flows.

Zusammenfassung

In diesem Beitrag wird ein Abrasionsvorhersagemodell für wasserbauliche Anlagen vorgestellt, die hohen Fliessgeschwindigkeiten ausgesetzt sind. Das Modell beruht auf dem Ansatz von Sklar und Dietrich (2004) und beinhaltet neue Erkenntnisse über die Partikeltrajektorien und Aufprallgeschwindigkeiten in schiessendem Abfluss. Das Modell verbindet die Einwirkungs- mit den Materialwiderstandsparametern der Sohle mit Hilfe des Abrasionskoeffizienten k_v. Der Wert dieses Koeffizienten wurde anhand einer Ähnlichkeitsanalyse zur Flusssohlenabrasion durch eine Korrelation der Abrasionsrate mit der Sohlmaterialfestigkeit verifiziert. Eine Sensivitätsanalyse zeigt den grossen Einfluss dieses Parameters auf die Abrasion auf. Dennoch ist das vorgeschlagene Modell als praktische Hilfe für den Ingenieur in der Praxis geeignet, um die Abrasion an wasserbaulichen Anlagen abzuschätzen.

1 Introduction

Abrasion is a wear phenomenon involving progressive material loss due to hard particles forced against and moving along a solid surface. In bedrock rivers, abrasion is the driving process for bed incision (Sklar and Dietrich 2004, 2006, Lamb *et al.* 2008, Turowski 2009), while in hydraulic structures such as spillways, weirs, flushing channels and sediment bypass tunnels abrasion causes severe damage of the concrete invert

surface (Jacobs *et al.* 2001, Auel and Boes 2011, Helbig *et al.* 2012, Boes *et al.* 2014). In general, abrasive damage can always be expected when particle bedload transport takes place. Particles are transported in sliding, rolling or saltation motion depending on the flow conditions causing grinding, rolling or saltating impact stress on the bed. According to Bitter (1963a, b) and Sklar and Dietrich (2001, 2004) the governing process causing abrasion is saltation, whereas sliding and rolling do not cause significant wear. A number of models exist to predict the abrasion rate. While the models for prediction of bedrock incision rate (Sklar and Dietrich 2004, Lamb *et al.* 2008) focus on typical flow conditions in river systems in the sub- and low supercritical flow regime, the others for prediction of abrasion rate on concrete surfaces (Ishibashi 1983, Helbig and Horlacher 2007) have to account for highly supercritical flows. So far, the latter are either only locally applied or only valid in a limited parameter range.

In this research paper, the widely applied *state of the art* saltation-abrasion model of Sklar and Dietrich (2004) is described and modified using results of Auel (2014) to develop a new abrasion prediction model valid for concrete abrasion in sediment-laden supercritical flows.

2　Parameter definitions

2.1　Abrasion rate

The abrasion rate is expressed either as a vertical abrasion rate, an abrasion mass or a volume. These correlations have to be conscientiously taken into account when comparing different models. The abrasion depth h_a is related to the vertical abrasion rate A_r by

$$A_r = \frac{h_a}{t} \qquad\qquad \text{[m/s]} \qquad [1]$$

where t = time. The volumetric abrasion rate A_{rv} is related to A_r by

$$A_{rv} = A_r b \qquad\qquad \text{[m}^3\text{/(sm')]} \qquad [2]$$

where b = decisive width. The gravimetric abrasion rate A_{rg} is related to A_{rv} by

$$A_{rg} = A_{rv}\rho_c \qquad\qquad \text{[kg/(sm')]} \qquad [3]$$

where ρ_c = invert material density. The gravimetric and volumetric abrasion rates are expressed per meter length [m'] of the abraded section.

2.2　Tensile and compression strength

Depending on the research field different parameters are used to describe the bed material strength in literature. In geomorphological research the bedrock abrasion is correlated to the tensile strength f_t (Sklar and Dietrich 2001, Lamb *et al.* 2008, Turowski *et al.* 2013, Scheingross *et al.* 2014), whereas in civil engineering the concrete abrasion is mostly related to the compression strength f_c (Jacobs *et al.* 2001, Mechtcherine *et al.*

2012, Helbig *et al.* 2012). In order to compare the data, the material strength parameters have to be clarified and a suitable transformation has to be done.

Three types of tensile strength tests are commonly used in engineering science: direct f_t, flexure f_{tf}, and splitting tension f_{tsp} (Arioglu *et al.* 2006). Direct tension strength is accepted as the genuine value. However, the simplest and mostly applied method is the splitting tension test. In this test, a cylindrical sample is placed between two plates in a test machine and loaded. This loading generates almost uniform tensile stress along the diameter causing the sample to fail by splitting along a vertical plane (Arioglu *et al.* 2006). The splitting tensile strength f_{tsp} is a function of the direct tensile strength f_t as

$$f_t = \alpha f_{tsp} \qquad \text{[MPa]} \qquad [4]$$

where α = correlation coefficient. The value of α is basically not constant. However, an average value of $\alpha = 0.9$ is given by Hannant *et al.* (1973) and is applied in engineering practice (CEB-FIB 1991, Arioglu *et al.* 2006).

Arioglu *et al.* (2006) found a correlation between the tensile and the compression strength based on a sound regression analysis using 30 data sets valid for $4 < f_{c,cyl} < 120$ MPa:

$$f_{tsp} = 0.387 f_{c,cyl}^{0.63} \qquad \text{[MPa]} \qquad [5]$$

Similar to the tensile strength tests, the compression strength is also derived from different test procedures. Samples are either cubed or cylindrical, and the relationship between them is given as

$$f_{c,cyl} = \beta f_{c,cube} \qquad \text{[MPa]} \qquad [6]$$

where $\beta = 0.8$ = correlation coefficient according to EN 1992-1-1.

3 Saltation-abrasion model

Sklar and Dietrich (2004) published an outstanding work by analyzing a wide range of research data sets on particle motion and abrasion and proposed a saltation-abrasion model to predict bedrock abrasion in river systems. The magnitude of abrasion is expressed as a vertical abrasion rate A_r in the following form

$$A_r = \frac{q_s W_{im}^2 Y_M}{L_p k_v f_{tsp}^2}\left(1 - \frac{q_s}{q_s^*}\right) \qquad \text{[m/s]} \qquad [7]$$

where W_{im} = mean vertical particle impact velocity [m/s], Y_M = Young's Modulus of elasticity [Pa], L_p = particle saltation length, k_v = rock resistance coefficient [-], q_s = specific gravimetric bedload rate [kg/(sm)], and q_s^* = specific gravimetric bedload transport capacity [kg/(sm)]. Note that all parameters have to be applied in SI units, thus the units of Y_M and f_{tsp} are in [Pa], not in [MPa].

The last term on the right in Eq. (1) is related to the cover effect occurring at high bed-load transport rates partly or totally covering the bed, leading to a decrease in particle impact energy (Sklar and Dietrich 1998, Turowski 2009). The coefficient k_v describes the correlation between bed material and sediment properties and abrasion rate (further explanation in Section 3.3).

Sklar and Dietrich (2004) applied correlations obtained for the hop length, hop height, and particle velocity to Eq. (7) and proposed the saltation abrasion model for bedrock river abrasion in the following form:

$$A_r = \left(\frac{0.08(s-1)gY_m}{k_v f_{tsp}^2} \right) q_s \left(\frac{\theta}{\theta_c} - 1 \right)^{-0.5} \left(1 - \frac{q_s}{q_s^*} \right) \left(1 - \left(\frac{U_*}{V_s} \right)^2 \right)^{1.5} \qquad \text{[m/s]} \qquad [8]$$

where θ = Shields parameter calculated as $\theta = U_*^2/[(s\text{-}1)gD]$, where $s = \rho_s/\rho$, ρ_s = particle density, ρ = fluid density, D = particle diameter, $U_* = (gR_hS)^{0.5}$ = friction velocity, g = gravitational acceleration, R_h = hydraulic radius, S = energy line slope, and θ_c = critical Shields parameter and V_S = particle settling velocity.

3.1 Modified saltation-abrasion model

The work of Sklar and Dietrich (2004) focuses on bedrock river systems with moderate flow velocities in the sub- or slightly supercritical range. Concrete abrasion processes at hydraulic structures such as weirs, spillways, outlets and sediment bypass tunnels are often exposed to highly supercritical flows (Jacobs *et al.* 2001, Helbig and Horlacher 2007, Auel 2014). Especially sediment bypass tunnels are exposed to severe abrasion of the tunnel invert due to high flow velocities in combination with high bedload transport (Sumi *et al.* 2004, Auel and Boes 2011).

To apply the saltation-abrasion model to such conditions, Auel (2014) conducted a scaled hydraulic model study in a 13.50 m long straight laboratory flume to analyze the flow characteristics, particle motion and invert abrasion in supercritical flows. The results of flow mean and turbulence characteristics and the particle motion analysis are published in Auel *et al.* (2014a, b) and Auel (2014), respectively. The latter implies the determination of the transport mode, particle velocities and saltation trajectories for a wide range of flow velocity, flow depth, bed slope, and particle diameter. It is found that the particle saltation velocity and trajectory strongly correlate with both Froude number $\mathsf{F} = U/(gh)^{0.5}$, where U = flow velocity and h = flow depth, and Shields parameter θ.

Furthermore, Auel (2014) conducted experiments to investigate the spatial and temporal invert abrasion development using weak mortar as bed material in the hydraulic model under a range of hydraulic and particle parameters (Table 1). The compression and flexure tensile strengths were obtained from direct load tests in the laboratory and the

Young's modulus was estimated applying a formulation by Noguchi *et al.* (2009) based on more than 3000 data sets valid for a range from f_c = 40 to 160 MPa:

$$Y_M = k_1 k_2 \cdot 33500 \left(\frac{f_c}{60}\right)^{(1/3)} \left(\frac{\rho_c}{2400}\right)^2 \qquad \text{[MPa]} \qquad [9]$$

where k_1 and k_2 are correction factors accounting for the type of coarse aggregate and admixtures, respectively. In Auel (2014), $k_1 = k_2 = 1.0$ is chosen due to small sand aggregates (D = 1-1.4 mm) and no admixtures. Although the mortar properties were about an order of magnitude lower compared to standard concrete, they showed similar behavior in terms of curing times and material collapse characteristics at the conducted load tests.

Table 1: Mortar properties (Auel 2014)

		Hard mixture	Samples n	Soft mixture	Samples n
Water/cement ratio	[-]	0.6		0.6	
Sand/cement ratio	[-]	10		15	
$f_{c,cube}$	[MPa]	6.81 ±1.21	33	3.67 ±0.60	34
f_{tf}	[MPa]	0.84 ±0.18	14	0.56 ±0.11	13
ρ_c	[kg/m^3]	1773 ±0.58	17	1692 ±45	16
Y_M	[MPa]	9061 ±657		6723 ±454	

Based on the findings of Auel (2014) a modified saltation-abrasion model applicable for hydraulic structures prone to supercritical flows is proposed in the following form similar to Sklar and Dietrich (2004):

$$A_r = \frac{Y_M}{k_v f_{tsp}^2} W_{im}^2 \cdot I \cdot q_s \qquad \text{[m/s]} \qquad [10]$$

where I = number of particle impacts per unit length [1/m]. Note that similar to Eq. (7), Y_M and f_{tsp} have to be applied in [Pa]. The cover effect term in Eq. (7) is dropped due to the fact that Auel (2014) did not observe any cover tendencies in his experiments for the parameter range tested. Sklar and Dietrich (2004) developed equations for the estimation of W_{im} and L_p in Eq. (7) and implemented in Eq. (8). However, they are not applicable for saltating particles in highly supercritical flows (Auel 2014). Therefore, new equations for these terms based on Auel (2014) are introduced below for Eq. (10).

The number of impacts per unit length is defined as the reciprocal value of the hop length L_p as:

$$I = \frac{\left(1 - \left(U_*/V_s\right)^2\right)^{0.5}}{L_p} \left(1 - P_R\right) \qquad \text{[1/m]} \qquad [11]$$

where P_R = rolling probability. The numerator of the first term on the right hand side is proposed by Sklar and Dietrich (2004) and accounts for the mode shift from saltation to suspension. V_s may be calculated using the equation developed by either Dietrich (1982) or Ferguson and Church (2004). The rolling probability P_R and hop length L_p are given in Auel (2014).

The following further assumptions are proposed:

- $f_{tsp} = 0.387 f_{c,cyl}^{0.63}$ (Eq. 5)

- $W_{im} = U_*$

- $k_v = 10^6$

In the following, the two latter assumptions will be explained in detail.

3.2 Estimation of particle impact velocity

Motion of a saltating particle in water stream is described with a saltation trajectory of length L_p and height H_p, and particle impact velocity V_{im} at an impact angle γ_{im} (Figure 1). The vertical velocity component is given by $W_{im} = V_{im} \sin(\gamma_{im})$. As direct measurements of W_{im} or γ_{im} are scarce, Sklar and Dietrich (2004) approximate W_{im} as follows:

$$W_{im} = \frac{3H_p V_p}{L_p} \qquad \text{[m/s]} \qquad [12]$$

where V_p = average particle velocity. Sklar and Dietrich (2004) analyzed a number of particle saltation research studies in sub- and slightly supercritical flow and proposed correlations to express L_p, H_p and V_p as functions of the transport stage $T^* = \theta/\theta_c$ with $\theta_c = 0.03$.

In Auel (2014) single particles were recorded by means of a high-speed camera system. The main objective was to investigate the particle transport mode, particle velocities, saltation trajectories and the particle impact energy when a particle impinges the bed at saltation motion. The experiments were conducted at supercritical hydraulic flow conditions for a wide range of aspect ratios and Froude numbers implying in total 264 parameter variations using both natural sediment and glass spheres. The following relations were found:

$$\frac{H_P}{D} = 5.9\theta \qquad\qquad R^2 = 0.85 \qquad [13]$$

Note that in Eq. (13), H_p is defined from particle center to particle center and not from bed to center (Figure 1). The hop length follows:

$$\frac{L_P}{D} = 251\theta \qquad\qquad R^2 = 0.94 \qquad [14]$$
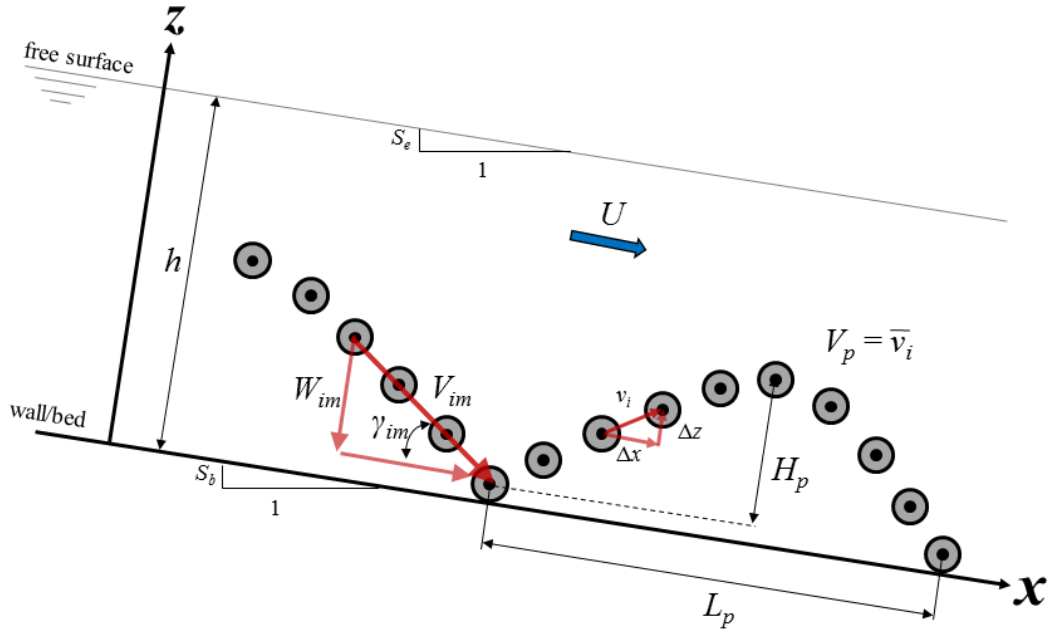
Figure 1: Sketch of saltating particle

The particle velocity V_p, defined as the average downstream travelling velocity (Figure 1), is determined by analyzing data from Auel (2014) as:

$$\frac{V_p}{\left((s-1)gD\right)^{0.5}} = 20 \cdot \theta^{0.5} \qquad\qquad R^2 = 0.98 \qquad [15]$$

The fit scales with the square root of θ, thus Eq. (15) can be simplified to

$$V_p = 20 \cdot U_* \qquad\qquad [16]$$

revealing that the particle velocity is directly related to the friction velocity by the factor 20. Applying Eqs. (13), (14) and (15) to Eq. (12) leads to the simple correlation

$$W_{im} = 1.4 \cdot U_* \qquad\qquad [17]$$

Auel (2014) obtained the particle impact velocity directly from the experimental data by averaging the particle velocities v_i over three consecutive recorded images before impact as:

$$V_{im} = \frac{v_{i-3} + v_{i-2} + v_{i-1}}{3} \qquad\qquad [18]$$

The vertical particle velocity W_{im} is identically calculated. Figure 2 shows W_{im} as a function of θ and reveals that W_{im} scales with the square root of the Shields parameter. The fit follows:

$$\frac{W_{im}}{\left(\left(s-1\right)gD\right)^{0.5}} = \theta^{0.5} \qquad\qquad R^2 = 0.75 \qquad [19]$$

and may be simplified to:

$$W_{im} = U_* \qquad\qquad [20]$$

Hence, two expressions to describe the vertical impact velocity are proposed. It is revealed that the approximation of the vertical impact velocity proposed by Sklar and Dietrich (2004) in Eq. (12) overestimates the measured data in Eq. (20) by a factor of 1.4. Carefully consider that the derivation of both vertical velocities is based on the saltation trajectory analysis in supercritical flows described in Auel (2014). Sklar and Dietrich (2004) proposed different assumptions for the saltation height, length and particle velocity. Applying these fits must not necessarily lead to the same factor of 1.4. However, as no direct W_{im} measurements are available for the data sets used in Sklar and Dietrich (2004), this cannot be definitively clarified.

It is recommended not to neglect the deviation in both derivations due to the fact that the impact velocity scales quadratically with the saltation-abrasion model. For supercritical flows, it is recommended to use the expression found in Eq. (20) to calculate the vertical impact velocity W_{im}.
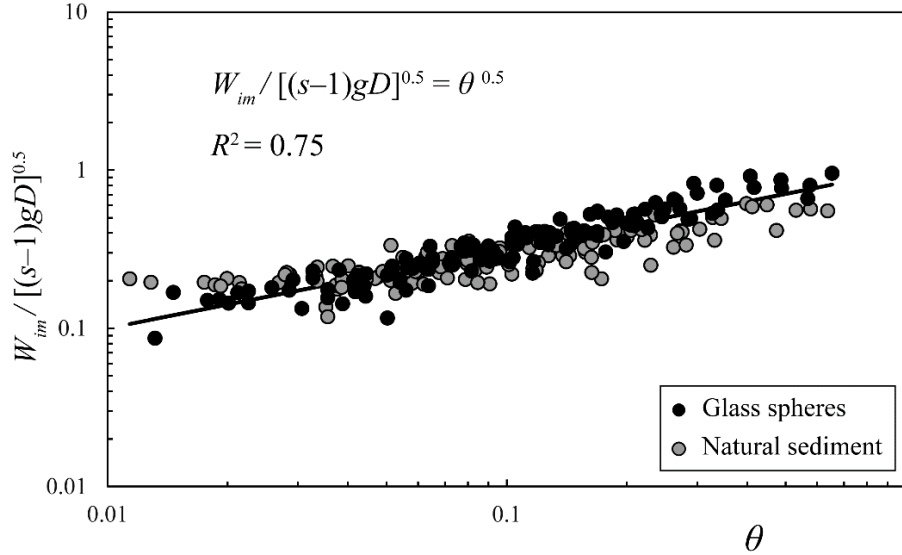
Figure 2: Vertical impact velocity W_{im} as a function of Shields parameter θ based on 264 data points from Auel (2014)

3.3 Correlation between abrasion rate and bed material properties

Sklar and Dietrich (2001) proposed a direct correlation between the material strength and the gravimetric material abrasion rate (Figure 3a). They conducted abrasion exper-

iments in an in-house-developed water-filled abrasion mill. The mill bottom was covered with the probed material. A constant amount of sediment gravel particles was added (M = 150 g, D = 6 mm) using a constant propeller stirring velocity (1000 rpm). In total, 22 rock and six concrete disc samples were tested. Due to the fact that rock exposed to saltating particle impacts fails in tension, Sklar and Dietrich (2001) selected the tensile strength as the decisive parameter. The tensile strength was obtained using the Brazilian test method, thus their values refer to the splitting tensile strength f_{tsp} (Rocco *et al.* 1999). Sklar and Dietrich (2001) proposed the following correlation (Figure 3a):

$$A_{rg} = 7.7(\pm 1.4) f_{tsp}^{-2(\pm 0.1)} \qquad \text{[g/h]} \qquad [21]$$

Additionally they conducted single grain experiments with 70 g quartzite gravel and proposed based on 6 rock samples:

$$A_{rg} = 18(\pm 4.0) f_{tsp}^{-2(\pm 0.6)} \qquad \text{[g/h]} \qquad [22]$$

Sklar and Dietrich (2004) used 9 single grain data sets from Sklar and Dietrich (2001) to quantify the rock resistance coefficient k_v by rearranging Eq. (8) to:

$$k_v = \left(\frac{0.08(s-1)gY_m}{f_{tsp}^2} \right) \frac{q_s}{A_r} \left(\frac{\theta}{\theta_c} - 1 \right)^{-0.5} \left(1 - \left(\frac{U_*}{V_s} \right)^2 \right)^{1.5} \qquad [23]$$

Additionally they analyzed 6 data sets from single particle drop tests. Considering both, the abrasion mill and particle drop tests, they found an average value of

- $k_v = 3.0 \times 10^6$ in a range of 1.0 to 9.0×10^6
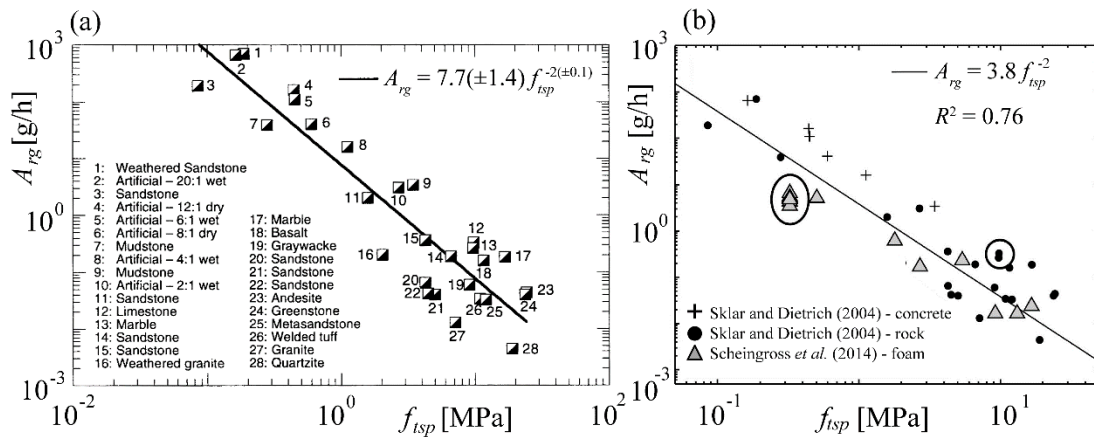
Figure 3: Abrasion mill experiments. Gravimetric abrasion rate Arg as function of splitting tensile strength ftsp from (a) Sklar and Dietrich (2001), and (b) Scheingross et al. (2014)

For application of the saltation abrasion model, they proposed to use the following estimate:

- $k_v \sim 10^6$ (Sklar and Dietrich 2004, 2012)

In order to reproduce these stated values, the abrasion mill experiment data used in Sklar and Dietrich (2004) are listed in Table 2. The average k_v value calculated from this data set is:

- $k_v = 3.6(\pm 2.5) \times 10^6$ (Table 2, Column 6)

This value slightly deviates by 0.6×10^6 from the above stated mean value given by Sklar and Dietrich (2004) due to the fact that the single particle drop tests are not considered in this calculation. Recalculation of the data, using the parameters given in Sklar and Dietrich (2004, Section 5.1: $q_s = 1.08$ kg/(sm), $\theta/\theta_c = 1.2$, $U_*/V_s = 0.19$, $Y_M = 5 \times 10^4$ MPa), reveals the following value:

- $k_v = 5.1(\pm 3.9) \times 10^6$ (Table 2, Column 7)

Comparing this newly calculated k_v value with the original data set reveals a disagreement of 1.5×10^6. This deviation is unclear and not completely comprehensible.

Table 2: k_v calibration from single-grain abrasion mill tests (Sklar and Dietrich 2004, Table 4b)

	Sklar and Dietrich (2004)					New calculation		
1	2	3	4	5	6	7	8	9
Rock type	f_t	ρ_s	A_{rg}	A_r [1]	k_v	k_v [2]	k_v [3]	k_v [4]
	[MPa]	[kg/m^3]	[g/h]	[m/s]	10^6	10^6	10^6	10^6
Concrete (20:1)	0.163	2300	215	8.69×10^{-7}	4.07	5.0	3.9	1.7
Concrete (6:1)	0.448	2300	71	2.87×10^{-7}	1.63	2.0	3.9	1.7
Concrete (4:1)	1.12	2300	5.1	2.06×10^{-8}	3.63	4.5	3.9	1.7
Sandstone	1.583	2450	2.9	1.11×10^{-8}	3.37	4.7	4.6	2.0
Graywacke	9.1	2500	0.22	8.18×10^{-10}	1.38	2.0	4.9	2.1
Limestone	9.78	2600	0.21	7.51×10^{-10}	1.30	2.0	5.4	2.3
Welded tuff	10.9	2600	0.036	1.26×10^{-10}	6.23	9.6	5.4	2.3
Quarzite	19	2600	0.008	2.86×10^{-11}	9.09	13.9	5.4	2.3
Andesite	24.4	2600	0.030	1.06×10^{-10}	1.47	2.3	5.4	2.3
Average					3.6	5.1	4.8	2.0
Standard dev.					2.5	3.9	0.7	0.3

[1] Divided by disc area of $A = 0.03$ m^2, [2] recalculated, [3] Eq. (21), [4] Eq. (22)

Despite the above described approach (use of single data sets), it is also reasonable to directly apply the abrasion rate – material strength fits from Sklar and Dietrich (2001) given in Eqs. (21) and (22) to Eq. (23). This attempt was not done in Sklar and Dietrich (2004), but is carried out herein. Application of Eq. (21) representing the multi-grain abrasion mill experiments leads to

- $k_v = 4.8(\pm 0.7) \times 10^6$ (Table 2, Column 8).

Application of Eq. (22), representing the single particle abrasion mill experiments, leads to

- $k_v = 2.0(\pm 0.3) \times 10^6$ (Table 2, Column 9).

From the single values listed in Table 2 (Columns 8 and 9) it is obvious that k_v only varies with the sediment particle density ρ_s as the other parameters (sediment rate, friction velocity, and Shields parameter) are not varied. Considering all above listed k_v values leads to the conclusion that the deviation is high, varying almost in one order of magnitude ($1 \times 10^6 < k_v < 9 \times 10^6$) with average values of $k_v \approx 2\text{-}5 \times 10^6$ depending on the calculation method. This conclusion confirms the parameter range already stated by Sklar and Dietrich (2004).

Scheingross *et al.* (2014) conducted similar experiments in the same device using artificial foam as a bedrock substitute but varying the particle diameter in a wide range from $D = 0.5$ to 44 mm while keeping the sediment mass constant with 70 g (Figure 3b). They added their data to Sklar and Dietrich (2001) and found

$$A_{rg} = 3.8 f_{tsp}^{-2} \qquad R^2 = 0.76 \qquad\qquad \text{[g/h]} \qquad [24]$$

A_{rg} scales with the inverse of the square of f_{tsp}, being consistent with the findings of Sklar and Dietrich (2001). Note that the satisfying coefficient of determination was obtained converting the data to log-transformed values prior to fitting and not from a direct power-law fitting.

Recent experiments on concrete abrasion in an abrasion drum were performed by Mechtcherine *et al.* (2012) and Helbig *et al.* (2012). Tests were conducted using concrete plate samples exposed to a water-particle mixture at the drum base. The two-phase mixture was composed of equal parts of solid and fluid, and the drum rotated in three different velocities. Typical flow conditions in a lower, middle and upper river reach were simulated using the particle diameter/flow velocity combinations R1: $D = 4.4$ mm and $\omega = 10$ rev/min, R2: $D = 5.0$ mm and $\omega = 13.5$ rev/min, and R3: $D = 8.0$ mm and $\omega = 17$ rev/min. The abrasion rates are calculated from the provided data and given in Table 3. Helbig *et al.* (2012) stated that the abrasion depth linearly scales with time, thus data are averaged and additionally multiplied by the sample area $A = 0.09$ m^2 and concrete density to obtain a gravimetric abrasion rate.

In order to validate and compare the abrasion coefficient k_v, the data from Helbig *et al.* (2012) and Auel (2014) have been added to the data sets from Sklar and Dietrich (2001) and Scheingross *et al.* (2014) presented in Figure 3. The two latter sets are divided by the abrasion mill sample area $A = 0.031$ m^2 to allow for comparison. Furthermore, all data are expressed per meter length to allow for comparison between the abrasion mill, drum and the straight model flume experiments.

Table 3: Gravimetric abrasion rate A_{rg} obtained from drum experiments in Helbig *et al.* (2012)

Concrete No		1	2	3	4	5	6
$f_{c,cube}$	[MPa]	53	54.4	58.6	56.6	77.7	69.5
ρ_c (*)	[kg/m^3]	2299	2588	2408	2494	2389	2416
A_{rg} R1	[g/h]	154.2	100.9	104.2	100.9	121.1	91.7
A_{rg} R2	[g/h]	435.6	260.9	365.3	255.0	271.6	210.7
A_{rg} R3	[g/h]	837.6	649.2	531.2	572.1	577.8	509.1

* the concrete densities are not published in the papers but directly given by the authors

According to Setunge *et al.* (1993) the *rock strength criterion* by Johnston (1985) describing the correlation of rock material constants to the ratio of compression to tensile strength are equally valid for high strength concrete. Consequently, the conclusion may be drawn that a conversion from tensile to compression strength and vice versa is applicable for both materials, rock and concrete. Hence, the compression strength $f_{c,cube}$ values used in Helbig *et al.* (2012) and Auel (2014) are transferred to f_{tsp} values using Eqs. (5) and (6). In Figure 4 the gravimetric abrasion rate A_{rg} is given as a function of the splitting tensile strength f_{tsp}. Auel's data adequately fit in the data range of Sklar and Dietrich (2001) and Scheingross *et al.* (2014), whereas Helbig's data deviate. The fit, excluding Helbig's data, follows:

$$A_{rg} = 316 f_{tsp}^{-2} \qquad R^2 = 0.85 \qquad\qquad \text{[g/(hm')]} \qquad [25]$$

Identically to Scheingross *et al.* (2014) the coefficient of determination is obtained converting the data to log-transformed values prior to fitting. Direct power-law fitting leads to lower values.

Data from Helbig *et al.* (2012) and Auel (2014) show a quasi-vertical alignment in Figure 4 due to the fact that material strength variation is low ($f_{c,cube}$ = 53 to 69.5 MPa for the former and $f_{c,cube}$ = 3.7 to 6.8 MPa for the latter) compared to the wide range of the tested materials. Consider that these data sets are obtained from different test setup conditions, widely varying the flow conditions and sediment parameters. The varying abrasion rate for identical strength is therefore caused by changes in sediment supply rate, particle diameter and flow velocity. These effects cannot be adequately represented by a simple correlation between the material strength and the abrasion rate as given in Figure 4.

However, the data of Auel (2014) satisfactorily fits into the sets by Sklar and Dietrich (2001) and Scheingross *et al.* (2014) and the entire data set reveals a clear correlation of the material strength to the abrasion rate. Eq. (25) may be applied to Eq. (23) to allow for comparison with the k_v values described above. Using the hydraulic parameters given by Sklar and Dietrich (2004) leads to:

- $k_v = 3.7(\pm 0.5) \times 10^6$

This value lies in the range of the above described values derived from data provided by Sklar and Dietrich (2004). Remind that k_v varies from $1{\times}10^6 < k_v < 9{\times}10^6$. All in all, the proposed first order estimate value by Sklar and Dietrich (2004) of $k_v = 10^6$ is widely accepted and used in bedrock abrasion research (Sklar and Dietrich 2006, Lamb *et al.* 2008, Huda and Small 2014, Scheingross *et al.* 2014). Furthermore, Turowski *et al.* (2007) confirmed this value reanalyzing the data from Sklar and Dietrich (2001). Thus, the authors propose to similarly use this value in the saltation abrasion model for concrete structures while keeping in mind the large variation of the abrasion coefficient.
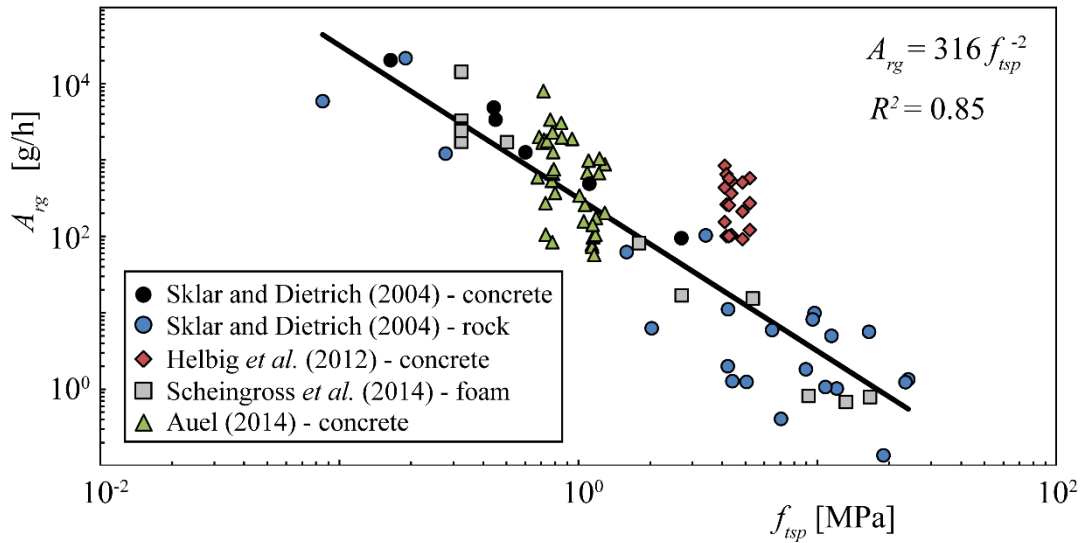
Figure 4: Gravimetric abrasion rate A_{rg} as a function of splitting tensile strength f_{tsp}. Data from Helbig *et al.* (2012) excluded from fit

4 Discussion

4.1 Sensitivity analysis

The effect of the abrasion coefficient and the vertical impact velocity on the abrasion rate given in Eq. (10) is shown in a sensitivity analysis exemplarily applying the prototype data of the Asahi sediment bypass tunnel in Japan. According to Auel (2014), the 2384 m long tunnel is $b = 3.80$ m wide and operated with a design discharge of $Q_d = 140$ m^3/s. The tunnel slope is $S_b = 0.029$, and the concrete invert roughness height is assumed to be $k_s = 3$ mm leading to a supercritical uniform flow velocity of $U = 12.0$ m/s and flow depth of $h = 3.18$ m ($R_h = 1.12$ m). The sediment transport rate $Q_s = 1000$ kg/s is randomly selected.

Figure 5 shows the abrasion rate A_r as a function of k_v, keeping all other parameters constant. For comparison, the vertical particle impact velocity is plotted as $W_{im} = 1.4\,U_*$ (Eq. 17) and $W_{im} = U_*$ (Eq. 20), the former representing the approach by Sklar and Dietrich (2004), the latter the direct data analysis, respectively (Section 3.2).

The abrasion coefficient k_v is a crucial parameter in the saltation-abrasion model. A large change of some orders of magnitude in A_r is revealed in Figure 5. Sklar and Dietrich (2004) stated that k_v is a constant based on Engel (1976), whereas Turowski *et al.* (2013) expected the parameter to be site-dependent, as it subsumes details of particle impact and rebound as well as energy-delivery processes. As discussed in Section 3.3, the coefficient varies around $k_v = 5(\pm 4) \times 10^6$. This variation causes a variation in A_r of almost one order of magnitude. Furthermore, by means of a scaling analysis, Chatanantavet and Parker (2009) stated values ranging from 10^4 for weak rocks such as weathered sandstone to 10^6 for hard rocks such as quartzite or andesite. Hence, the variation in A_r increases to some orders of magnitude leading to the conclusion that further research using standardized abrasion drum/mill facilities (Sklar and Dietrich 2001, Helbig *et al.* 2012, Scheingross *et al.* 2014) is needed to analyze in detail the effect of different bed materials such as concrete, and the effect of varying impact parameters such as flow velocity, sediment transport rate, grain size, and grain hardness.

The variation of A_r due to W_{im} is additionally presented in Figure 5. The comparison reveals that Sklar's assumption ($W_{im} = 1.4\ U_*$) almost doubles A_r. This deviation is evident as the impact velocity scales quadratically, i.e. $1.4^2 = 1.96 \approx 2$.
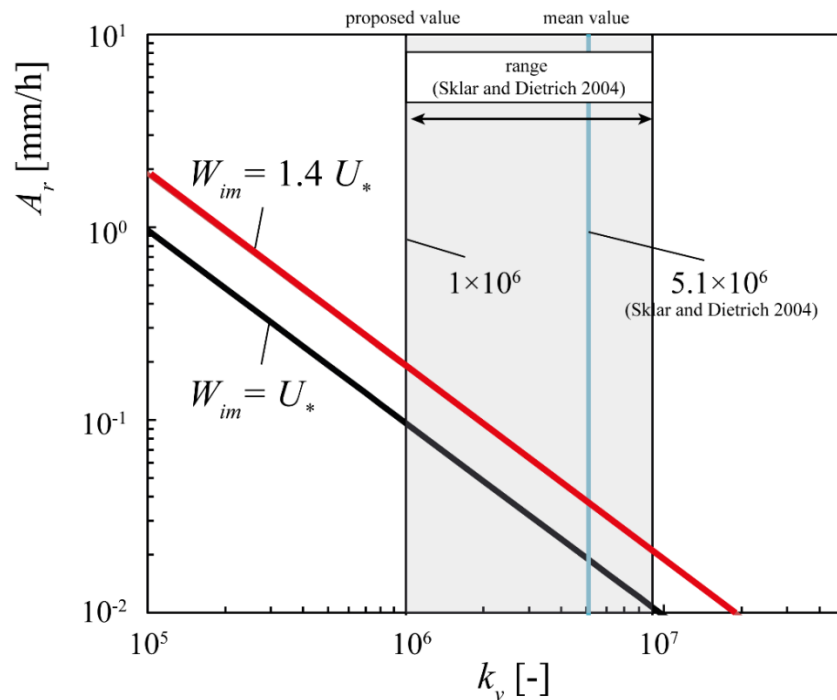

Figure 5: Vertical abrasion rate A_r based on Eq. (10) as a function of abrasion coefficient k_v. Exemplary calculation based on data of Asahi sediment bypass tunnel

4.2 Young's modulus

Based on Clark (1966), Sklar and Dietrich (2004) state that the variation in Young's modulus Y_M of rock is limited and can be treated to first order as a constant value.

Hence in bedrock abrasion related studies a constant value of $Y_M = 5 \times 10^4$ MPa is widely applied (Sklar and Dietrich 2004, Turowski 2007, Lamb *et al.* 2008, Huda and Small 2014). In case of concrete, the Young's modulus is not constant, but varies depending on the compression strength and particularly on the concrete density as shown for example by Noguchi *et al.* (2009) in Eq. (9). Consequently, the Young's modulus has to be studied in more detail in order to estimate its effect on the abrasion rate.

4.3 Resultant impact velocity

Auel (2014) proposed a slightly different abrasion model compared to Eq. (10) using the resultant impact velocity V_{im} instead of the vertical velocity W_{im}. Due to that change, additionally the abrasion coefficient k_v was renamed as C_A since it did not represent the value given by Sklar and Dietrich (2004).

A main advantage of using V_{im} is the excellent correlation of both the particle velocity V_p to the Shields parameter given in Eq. (15) and to the particle impact velocity V_{im}. The latter correlation is given in Figure 6 as:

$$\frac{V_{im}}{(gh)^{0.5}} = 1.0 \frac{V_p}{(gh)^{0.5}} \qquad\qquad R^2 = 1.0 \qquad [26]$$

This reveals, that the impact velocity equals the particle velocity in case of supercritical flows as analyzed in Auel (2014). Consequently, the impact velocity follows in its simplified form using Eq. (16) as:

$$V_p = V_{im} = 20 \cdot U_* \qquad\qquad\qquad \text{[m/s]} \qquad [27]$$

Comparing Eqs. (27) and (20) reveals that the magnitude of the vertical particle impact velocity is 5% of the resultant impact velocity, resulting in an impact angle $\gamma =$ arcsin(0.05) = 2.9°. Whether applying V_{im} or W_{im} in Eq. (10) consequently leads to quite different results of A_r, if the abrasion coefficient is not adapted accordingly.

A further advantage using the resultant velocity is the different effect of the vertical and horizontal component of the impact velocity. According to Bitter (1963a, b) the vertical component causes the so called *deformation wear*, which is related to the particle impact, whereas the horizontal component causes *cutting wear*, which is related to grinding stress. Engel (1976) stated that erosion depends on the sine of the impact angle because the magnitude of the peak tensile stress varies with the normal component of the impact velocity, i.e. the vertical velocity component is the driving factor. Sklar and Dietrich (2004) stated that cutting wear caused by the horizontal velocity component is only important in ductile materials and in case of highly angular impacting particles, but is not significant when brittle materials are impacted by rounded grains as present in river systems. These statements are confirmed by Auel (2014) stating that the maximum the-

oretical threshold for the energy transferred by sliding and rolling motion is only about 10 and 0.1% of the saltation impact energy, respectively.
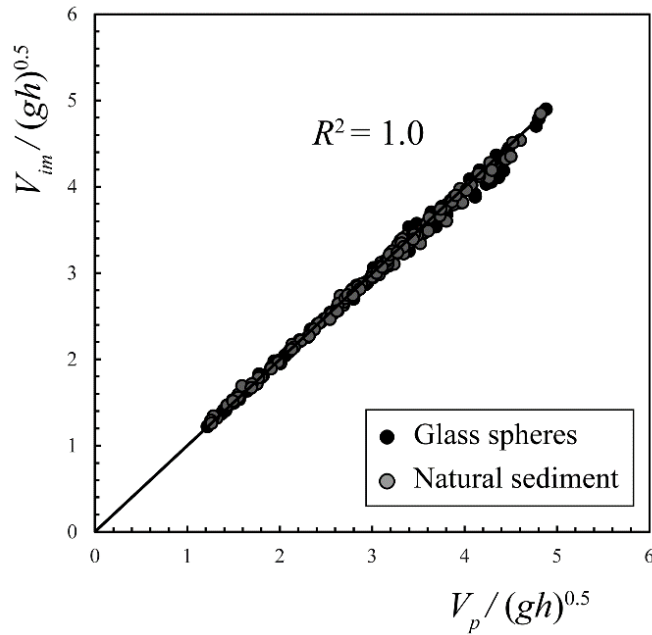
Figure 6: Normalized particle impact velocity V_{im} as a function of normalized particle velocity V_p

Using the resultant impact velocity does not differentiate *deformation* and *cutting* wears but simplifies the applicability of an abrasion model. However, merging these different effects may be also seen as a disadvantage from a physical point of view, as the effects are mixed up. Regardless of the above given explanations, it is proposed to use W_{im} in the saltation-abrasion model given in Eq. (10), for the reasons given hereafter.

The abrasion rate is sensitive to the abrasion coefficient k_v as shown in Section 4.1. Auel (2014) found a linear relation of the measured abraded mass to the supplied sediment mass. However, his proposed abrasion coefficient C_A is only valid in the conducted model study due to the use of the weak mortar (Table 1). The abraded mass of high-performance concrete is expected to be orders of magnitude lower.

So far, the use of the abrasion resistance coefficient k_v as described in Section 3.3 seems to be most adequate. As Sklar and Dietrich (2004) use W_{im} to calculate k_v, the use of W_{im} should be continued as the effect of a slight variation in k_v is already large as described in Section 4.1. An application of V_{im} instead of W_{im} imposes further uncertainties in the estimation of the abrasion rate as V_{im} is 20 times larger than W_{im}. Hence, the use of V_{im} is not meaningful without more knowledge on the underlying abrasion processes resulting from further research on concrete abrasion using standardized abrasion drum/mill facilities as described above.

5 Conclusions

In this contribution the *state of the art* saltation-abrasion model by Sklar and Dietrich (2004) is applied to hydraulic structures exposed to supercritical sediment-laden flows. The proposed model, given in Eq. (10), bases on the particle saltation trajectory, and vertical impact velocity in supercritical flows as well as the invert material properties and the abrasion coefficient k_v. It is shown that

(1) the vertical particle impact velocity equals to the friction velocity and

(2) the abrasion coefficient can be approximated as a first order estimate with a value of $k_v = 10^6$.

The abrasion coefficient k_v is derived from an abrasion rate vs. bed material strength correlation based on standardized abrasion mill experiments. A sensitivity analysis reveals a large effect of k_v on the abrasion rate. Further research is needed to analyze the effects of the parameters i.e. flow velocity, sediment transport rate, particle size, particle hardness, and bed material properties on k_v. Auel (2014) found that the abrasion rate decreases with increasing material strength, but increases with flow velocity and sediment transport rate, and showed that medium-sized particles caused the highest abrasion compared to the smallest and largest particles for the same sediment supply rate. Thus, other parameters directly affect the abrasion, which are not adequately considered by the presented derivation of k_v. Research is currently conducted to quantify a possible correlation between the hydraulic operation conditions, sediment load, invert material properties and measured hydro-abrasion for a wide range of high performance concretes in prototype hydraulic structures (Hagmann *et al.* 2014, 2015). These findings together with data from Mechtcherine *et al.* (2012) and Helbig *et al.* (2012) will enhance the knowledge in concrete abrasion and may be used to find an adequate abrasion coefficient k_v.

Acknowledgments

Notation

A	area	[m^2]
b	width	[m]
A_r	vertical abrasion rate	[m/s]
A_{rv}	volumetric abrasion rate	[m^3/(sm')]
A_{rg}	gravimetric abrasion rate	[kg/(sm')]

117

D	particle diameter	[m]
f_c	compression strength	[Pa]
$f_{c,cube}$	compression strength using cubed sample	[Pa]
$f_{c,cyl}$	compression strength using cylindrical sample	[Pa]
f_t	direct tensile strength	[Pa]
f_{tf}	flexure tensile strength	[Pa]
f_{tsp}	splitting tensile strength	[Pa]
g	gravitational acceleration	[m/s^2]
h	flow depth	[m]
H_p	particle saltation height	[m]
I	number of particle impacts per unit length	[1/m].
k_s	equivalent bed roughness height	[m]
k_v	rock resistance coefficient	[-]
L_p	particle saltation length	[m]
P_R	rolling probability	[-]
Q_s	gravimetric bedload rate	[kg/s]
q_s	specific gravimetric bedload rate	[kg/(sm)]
q_s^*	specific gravimetric bedload transport capacity	[kg/(sm)]
R_h	hydraulic radius	[m]
s	density ratio $s = \rho_s/\rho$	[-]
S	energy line slope	[-]
S_b	bed slope	[-]
T^*	transport stage $T^* = \theta/\theta_c$	[-]
U	uniform flow velocity	[m/s]
U_*	friction velocity $U_* = (gR_hS)^{0.5}$	[m/s]
V_p	mean particle velocity	[m/s]
V_S	particle settling velocity	[m/s]
V_{im}	mean resultant particle impact velocity	[m/s]
v_i	particle velocity between two recorded particles	[m/s]
W_{im}	mean vertical particle impact velocity	[m/s]
Y_M	Young's Modulus of elasticity	[Pa]
γ_{im}	particle impact angle	[°]

θ	Shields parameter $\theta = U_*^2/[(s\text{-}1)gD]$	[-]
θ_c	critical Shields parameter	[-]
ρ	fluid density	[kg/m^3]
ρ_c	invert material density	[kg/m^3]
ρ_s	particle density	[kg/m^3]
ω	rotational drum velocity	[rev/min]

References

Auel, C., Albayrak, I., Boes, R.M. (2014a). Turbulence characteristics in supercritical open channel flows: Effects of Froude number and aspect ratio. *Journal of Hydraulic Engineering* 140(4), 04014004, 16p.

Auel, C., Albayrak, I., Boes, R.M. (2014b). Bedload particle velocity in supercritical open channel flows. *Proc. River Flow* (Schleiss et al. eds.), Taylor and Francis, 923-931.

Auel, C. (2014). Flow characteristics, particle motion and invert abrasion in sediment bypass tunnels. *PhD thesis* 22008, also published as *VAW-Mitteilung* 229 (R. Boes, ed.), ETH Zurich, Switzerland.

Auel, C. Boes, R.M. (2011): Sediment bypass tunnel design – review and outlook. *Proc. ICOLD Symposium „Dams under changing challenges"* (A.J. Schleiss & R.M. Boes, eds.), 79th Annual Meeting, Lucerne. Taylor & Francis, London, UK, 403-412.

Arioglu, N., Canan Girin, Z., Arioglu, E. (2006). Evaluation of ratio between splitting tensile strength and compressive strength for concretes up to 120 MPa and its application in strength criterion. *ACI Materials Journal* 103(1), 18–24.

Bitter, J. G. A. (1963a). A study of erosion phenomena, part I. *Wear* 6, 5–1.

Bitter, J. G. A. (1963b). A study of erosion phenomena, part II. *Wear* 6, 169–190.

Boes, R.M., Auel, C., Hagmann, M., Albayrak, I. (2014). Sediment bypass tunnels to mitigate reservoir sedimentation and restore sediment continuity. *Reservoir Sedimentation* (Schleiss, A.J., De Cesare, G., Franca, M.J., Pfister, M., eds.), ISBN 978-1-138-02675-9, Taylor & Francis, London, UK, 221-228.

CEB-FIB (1991). Evaluation of the time dependent behaviour of concrete. *Bulletin d'Information No.* 199, Comité Européen du Béton/Fédération Internationale de la Précontrainte, Lausanne, Switzerland, 201 p.

Chatanantavet, P., Parker, G. (2009). Physically based modeling of bedrock incision by abrasion, plucking, and macroabrasion. *Journal of Geophysical Research: Earth Surface* 114(F04018), 22p.

Clark, S. P. (1966). Handbook of physical constants. *The Geological Society of America*, Memoir 97, 587 p.

Dietrich, W.E. (1982). Settling Velocity of Natural Particles. *Water Resources Research* 18(6), 1615–1626.

EN 1992-1-1 (2004). Eurocode 2: Design of concrete structures - Part 1-1: General rules and rules for buildings. *The European Union per Regulation* 305/2011, Directive 98/34/EC, Directive 2004/18/EC. European Committee for Standardization, Brussels, Belgium.

Engel, P. A. (1976). Impact wear of materials (Tribology). *Elsevier Science Ltd.*, New York.

Ferguson, R.I., Church, M. (2004). A simple universal equation for grain settling velocity. *Journal of Sedimentary Research* 74(6), 933–937.

Hagmann, M., Albayrak, I., Boes, R.M. (2015). Field research: Invert material resistance and sediment transport measurements. Proc. First Int. Workshop on Sediment Bypass Tunnels, *VAW-Mitteilung* 232 (R. Boes, ed.), ETH Zurich, Switzerland.

Hagmann, M., Albayrak, I., Boes, R.M. (2014). Untersuchung verschleissfester Materialien im Wasserbau mit in-situ-Geschiebetransportmessung ('Investigation on wear-resistant materials at hydraulic structures: in-situ measurements of sediment transport and invert abrasion'). Proc. Symposium „Wasserbau und Flussbau im Alpenraum", *VAW-Mitteilung* 227 (R. Boes, ed.), ETH Zürich, Switzerland, 97-106.

Hannant, D. J., Buckley, K. J., Croft, J. (1973). The effect of aggregate size on the use of the cylinder splitting test as a measure of tensile strength. *Materials and Structures* 6(31), 15–21.

Helbig, U., Horlacher, H.-B., Stamm, J., Bellmann, C., Butler, M., Mechtcherine, V. (2012). Nachbildung der Hydroabrasionsbeanspruchung im Laborversuch, Teil 2 – Korrelation mit Verschleiβwerten und Prognoseansätze (Modeling hydroabrasive stress in the laboratory experiment, Part 2 – Correlation with wear values and prognosis approaches). *Bautechnik* 89(5), 320–330 (in German).

Helbig, U., Horlacher, H.-B. (2007). Ein Approximationsverfahren zur rechnerischen Bestimmung des Hydroabrasionsverschleiβes an überströmten Betonoberflächen (An approximation method for the determination of hydroabrasive wear on overflown concrete surfaces). *Bautechnik* 84(12), 854–861 (in German).

Huda, S.A., Small, E.E. (2014). Modeling the effects of bed topography on fluvial bedrock erosion by saltating bed load. *Journal of Geophysical Research: Earth Surface* 119, 1222–1239.

Ishibashi, T. (1983). Hydraulic study on protection for erosion of sediment flush equipments of dams. *Civil Society Proc*. 334(6), 103–112 (in Japanese).

Jacobs, F., Winkler, K., Hunkeler, F., Volkart, P. (2001). Betonabrasion im Wasserbau (Concrete abrasion in hydraulic structures). *VAW-Mitteilung* 168 (H.-E. Minor, ed.), ETH Zurich, Switzerland (in German).

Johnston, I. W. (1985). Strength of intact geomechanical materials. *Journal of Geotechnical Engineering ASCE* 111(6) 730–748.

Lamb, M.P., Dietrich, W.E., Sklar, L.S. (2008). A model for fluvial bedrock incision by impacting suspended and bed load sediment. *Journal of Geophysical Research* 113(F03025), 18p.

Mechtcherine, V., Bellmann, C., Helbig, U., Horlacher, H.-B., Stamm, J. (2012). Nachbildung der Hydroabrasionsbeanspruchung im Laborversuch, Teil 1 – Experimentelle Untersuchungen zu Schädigungsmechanismen im Beton (Modeling hydroabrasive stress in the laboratory experiment, Part 1 – experimental investigations of damage mechanisms in concrete). *Bautechnik* 89(5), 309–319 (in German).

Noguchi, T., Tomosawa, F., Nemati, K.M., Chiaia, B.M., Fantilli, A.P. (2009). A practical equation for elastic modulus of concrete. *ACI Structural Journal* 106(5), 690–696.

Rocco, C., Guinea, G.V., Planas, J., Elices, M. (1999). Size effect and boundary conditions in the Brazilian test: theoretical analysis. *Materials and Structures* 32, 437–444.

Scheingross, J.S., Brun, F., Lo, D.Y., Omerdin, K., Lamb, M.P. (2014). Experimental evidence for fluvial bedrock incision by suspended and bedload sediment. *Geology* 42(6), 523–526.

Setunge, S., Attard, M.M., Darvall, P.P. (1993). Ultimate strength of confined very high-strength concretes. *ACI Structural Journal* 90(6) 632–641.

Sklar, L.S., Dietrich, W.E. (2012). Correction to "A mechanistic model for river incision into bedrock by saltating bed load". *Water Resources Research* 48(W06902), 2p.

Sklar, L.S., Dietrich, W.E. (2006). The role of sediment in controlling steady-state bedrock channel slope: Implications of the saltation–abrasion incision model. *Geomorphology* 82, 58–83.

Sklar, L.S., Dietrich, W.E. (2004). A mechanistic model for river incision into bedrock by saltating bed load. *Water Resources Research* 40(W06301), 21p.

Sklar, L.S., Dietrich, W.E. (2001). Sediment and rock strength controls on river incision into bedrock. *Geology* 29(12), 1087–1090.

Sklar, L.S., Dietrich, W.E. (1998). River longitudinal profiles and bedrock incision models: Stream power and the influence of sediment supply. *Geophysical Monograph* 107, American Geophysical Union, 237–260.

Sumi, T., Okano, M., Takata, Y. (2004). Reservoir sedimentation management with bypass tunnels in Japan. *Proc. 9th International Symposium on River Sedimentation*, Yichang, China, 1036–1043.

Turowski, J.M., Böckli, M., Rickenmann, D., Beer A.R. (2013). Field measurements of the energy delivered to the channel bed by moving bed load and links to bedrock erosion. *Journal of Geophysical Research: Earth Surface* 118, 2438–2450.

Turowski, J.M. (2009). Stochastic modeling of the cover effect and bedrock abrasion. *Water Resources Research* 45(W03422), 13p.

Turowski, J.M., Lague, D., Hovius, N. (2007). Cover effect in bedrock abrasion: A new derivation and its implications for the modeling of bedrock channel morphology. *Journal of Geophysical Research: Earth Surface* 112, F04006, 16p.

Authors

Dr. Christian Auel (corresponding Author)*
Prof. Dr. Tetsuya Sumi
Water Resources Research Center, Disaster Prevention Research Institute, Kyoto University, Japan
Email: christian.auel@alumni.ethz.ch

Dr. Ismail Albayrak
Prof. Dr. Robert M. Boes
Laboratory of Hydraulics, Hydrology and Glaciology (VAW), ETH Zurich, Switzerland

* formerly VAW, ETH Zurich, Switzerland

Field research: Invert material resistance and sediment transport measurements

Michelle Hagmann, Ismail Albayrak, Robert M. Boes

Abstract

Reservoir sedimentation is a global issue affecting water supply, energy production and flood protection. For a sustainable and safe reservoir operation sediment management is mandatory. Sediment Bypass Tunnels (SBTs) are an efficient and ecological favorable measure by diverting sediment-laden inflows around reservoirs. They may prevent reservoir sedimentation and restore the downstream river reach suffering from sediment deficit. However, high flow velocities and high sediment loads cause substantial hydroabrasion wear. In the project presented herein, the abrasion resistance of different materials is investigated under field operating conditions and compared to life cycle costs by means of *in-situ* experiments. Furthermore, supplementary laboratory experiments are conducted to determine abrasion resistance of investigated materials under controlled conditions and to check and investigate upscaling from laboratory results to field applications. The abrasion resistance of materials increases with their strength. However, since hydroabrasion is a self-intensifying process starting at vulnerabilities and irregularities, implementation and curing is as important as the choice of the material itself.

1   Introduction

SBTs are an effective measure against reservoir sedimentation and contribute to a sustainable use of storage capacity for water supply, energy production and flood control. They divert sediment-laden inflows around dams and thus may restore the natural sediment continuity that is disturbed by dam construction. Due to climate change and population growth sustainable sediment management at reservoirs gained increasing importance and SBTs have recently attracted growing attention, especially in mountainous regions in Asia and South America. However, SBTs are subjected to strong abrasion due to high flow velocities and sediment transport rates causing high annual maintenance expenses in the range of 1% of the investment costs (Auel 2014). An impressive example showing massive damages is the Palagnedra SBT in southern Switzerland (Vischer *et al.* 1997). After a flood event in 1978 the corresponding hydropower plant was shut down and the Melazza River was diverted through the SBT during the refurbishment period of 10 months (Delley 1988). The concrete invert was destroyed and the incision channel depth reached up to 2.7 m into the bedrock (Figure

1). In order to enhance the cost-effectiveness of SBTs suitable invert materials are indispensable.

Therefore a research project was initiated at the Laboratory of Hydraulics, Hydrology and Glaciology (VAW) of ETH Zurich (Hagmann *et al.* 2012, Boes *et al.* 2014, Hagmann *et al.* 2014). The main objectives are to quantify the correlations between the hydraulic operation conditions, sediment load, invert material properties and measured hydroabrasion. To achieve this goal, *in-situ* experiments in Solis, Pfaffensprung and Runcahez SBTs are conducted.

Figure 1: Invert damages at the Palagnedra SBT (Canton Ticino, Switzerland) after an exceptional flood event in 1978 (IM Maggia Engineering AG)

Furthermore, the transferability of laboratory results to field scale is investigated in collaboration with the Institute of Construction Materials of TU Dresden, Germany. Therefore specimens of invert materials from Solis and Pfaffensprung SBTs have been tested in the laboratory and compared to their *in-situ* performance (Bellmann and Mechtcherine 2012, Mechtcherine *et al.* 2012). Finally, outputs of this project together with results of a precedent study on sediment transport and abrasion processes in SBTs (Auel 2014) will help operators of hydraulic systems facing abrasion problems by giving recommendations of SBT design, economical invert materials and their implementation. Herein, the experimental setups, the sediment transport monitoring system, and the recently obtained results are presented.

2 Instrumentation

2.1 Monitoring of hydraulic conditions

To adequately estimate the discharge in the tunnel, precise knowledge of the flow velocity and flow depth is needed. Pressure sensors are popular, competitive and robust devices for the determination of water depth under subcritical flow conditions. However, under the supercritical flow conditions prevailing in SBT, it is difficult to soundly mount these devices in tunnels without disturbing the measurements.

Another commonly used method for continuous and real-time monitoring of hydraulic operating conditions is the radar technique. This is a contact-free technique applicable also under supercritical flow conditions. It determines water levels by measuring time between sent and received pulses. Furthermore, it also measures surface flow velocity using the Doppler Effect. Finally, the discharge is determined based on the continuity equation and a site specific conversion factor adapted from water depth, cross section and surface flow velocity.

2.2 Sediment monitoring

Sediment load is divided into bed load and suspended load. For bedload monitoring there are various techniques available (Bogen and Møen 2001, Gottesfeld and Tunnicliffe 2003, Rickenmann and McArdell 2007, Møen *et al.* 2010). For the present research project, a robust, accurate and continuous real-time measurement technique is needed to monitor sediment load in SBTs. The Swiss plate geophone developed at the Swiss Federal Institute for Forest, Snow and Landscape Research (WSL) fulfills these requirements (Rickenmann and McArdell 2007, Rickenmann *et al.* 2012, Wyss *et al.* 2014). The device consist of an elastically bedded (elastic polymer type "CR/SBR Standard 65±5", manufactured by Angst + Pfister, Zurich, Switzerland) steel plate (S235; l=492 mm, w=358 mm, t=15 mm) mounted by a steel profile (S235, UPE400) flush to the channel invert (Figure 3). Bedload particles impinging the plate cause oscillations which are registered by a geophone sensor (Geospace GS-20DX, manufactured by Geospace Technologies, Houston, Texas) attached on the rear side of the plate within a waterproof casing. The sampling rate is 10 kHz and thus allows sampling of the plate oscillations.

When the signal voltage exceeds a certain threshold value corresponding to vibrations due to clear water background noise, an impulse is registered. The number of impulses correlates linearly with the sediment transport rate whereas the grain size distribution can be estimated based on the maximal amplitude value (Rickenmann *et al.* 2012, Wyss *et al.* 2014). However, correlation between registered signals and sediment transport rate, is strongly site-dependent. Hydraulic flow conditions, particle size distribution and particle shape affect the measurement signal. Therefore a calibration, in best case *in-situ*, is required for every single geophone system. Under controlled laboratory

conditions (mean flow velocity of 4 m/s, water depth of 10 cm) the threshold for detected grain was determined being between 2 and 3 cm for the horizontal arrangement of a geophone system. Furthermore, threshold grain size was significantly lowered by inclining the geophone 10° against the channel bottom slope (Morach 2011).

Turbidimeters are a popular and commonly used optical device for suspended sediment measurements at rivers, lakes, desilting basins and power plants (Grasso *et al.* 2005, Habersack *et al.* 2008). The devices register either the backscatter or the transmission of the emitted visible or infrared light. The signal output is turbidity and has to be converted to suspended sediment concentration using a calibration curve. Therefore, bottle samples are taken regularly from the river. Their calibration is affected by particle shape, size and color (Felix *et al.* 2013). Depending on particle properties the measurement range varies from several milligram per liter up to hundred grams per liter (Black and Rosenberg 1994, Wren *et al.* 2000).

2.3 Abrasion measurement

Abrasion can be measured either by hand using a leveling rule or by use of 3D-laser-technique. Jacobs *et al.* (2001) used the former to measure the abrasion in the Runcahez SBT. Also the abrasion at Asahi SBT, Japan and the abrasion in the Runcahez SBT is measured similarly (Jacobs and Hagmann 2015, Nakajima *et al.* 2015).

However, the advantage of a 3D-laser technique is the provision of high resolution surface maps. Furthermore the measurement process is much less time consuming compared to the leveling rule method. Maps obtained at different stages are used to evaluate temporal and spatial development of abrasion occurring on the surface. Depending on the specifications, 3D–lasers are applicable up to 100 m distance measurements with measurement errors around ± 2 mm. In order to obtain a surface map with high resolution and minimal errors around ± 1 mm, the measurements distance is kept in the range of 1.5 to 10 m.

3 Experimental setups and methodology

3.1 Solis SBT

The Solis SBT located in the Swiss Alps was commissioned in 2012 (Oertli 2009, Auel *et al.* 2011, Oertli and Auel 2015). The SBT intake is located 804.5 m asl. For SBT operation the reservoir level partially lowered (active storage volume: 823.75 and 816 m asl, target SBT operation level: 816 and 814.5 m asl) resulting in pressurized flow conditions at the intake. After the intake flow conditions change to supercritical free surface flow with flow velocities up to 11 m/s.

The SBT houses six test fields, each 10 m long, with different abrasion-resistant materials. Four concretes with different compressive strengths and mixtures, cast basalt tiles and steel plates were implemented directly upstream of the right bend (Hagmann *et*

al. 2012) (Figure 2). In combination with the high-performance concrete invert of Solis SBT, a total of seven different invert materials are tested. For separation of the single trial fields and for proper implementation, steel beams were installed at the end of every field.
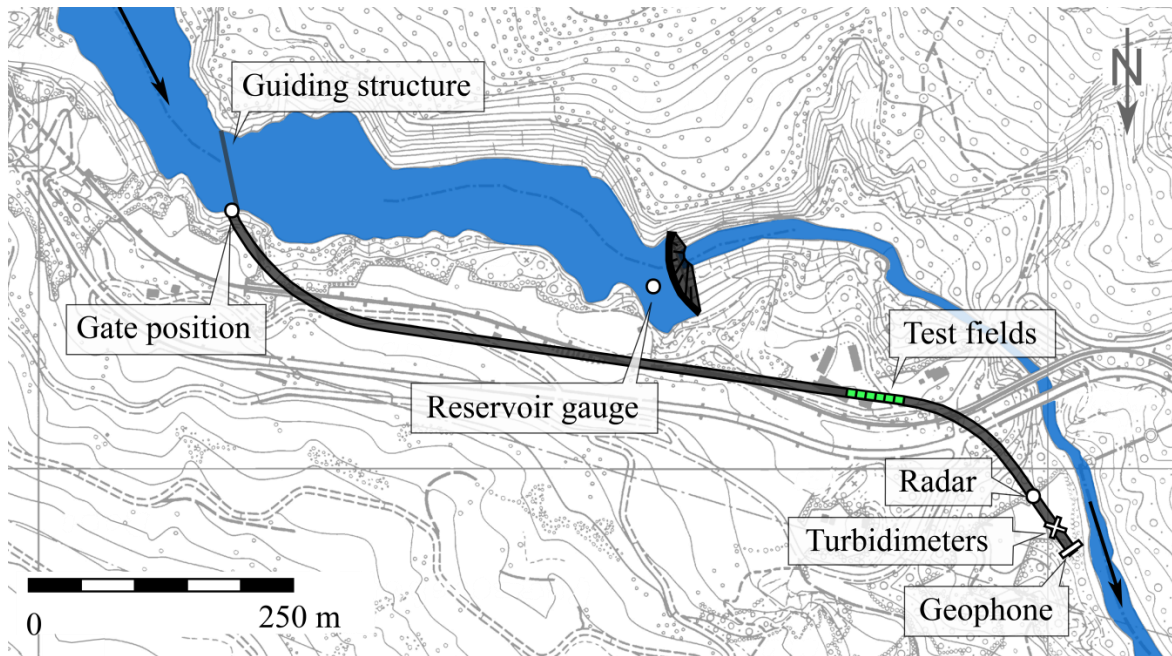

Figure 2: Overview of the Solis SBT with test fields and the instrumentation

Hydraulic conditions in the tunnel and reservoir are monitored using a radar system mounted on the tunnel ceiling (RQ-30, manufactured by Sommer Messtechnik, Koblach, Austria), two pressure sensors installed at both tunnel walls (Probe 26 W, manufactured by Keller AG, Winterthur, Switzerland), and a pressure transmitter measuring the reservoir level (MPA, manufactured by Rittmeyer, Baar, Switzerland), respectively. Furthermore, the position of the intake gate is observed by displacement transducers.

Both, the gate position and the reservoir water level are used in combination with hydraulic model test results (Auel *et al.* 2011) to estimate the discharge. These results can be compared to the measurements using the radar and pressure sensors in the tunnel. The sediment transport is monitored by two turbidimeters installed next to the pressure sensors in the side wall recesses (TubiMax W CUS41, manufactured by Endress+Hauser, Reinach, Switzerland) and by an in-house-constructed geophone system consisting of eight units at the SBT outlet (Figure 3). Generally, the sampling rate is 1/60 Hz, except for the geophones, where it is 10 kHz. The data acquisition is triggered by the SBT intake gate opening.
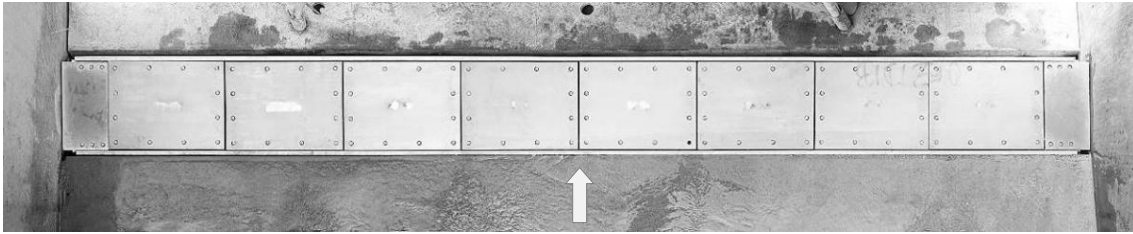
Figure 3: Picture of the geophone system consisting of eight units across the tunnel width, installed at the outlet of Solis SBT; flow direction from bottom to top

The surface of the tunnel invert is mapped by a laser scanner (FARO Focus 3D, manufactured by FARO, Lake Mary, United States). The first measurement was performed in 2012 after implementation. After every significant event provoking invert abrasion further scans are conducted.

3.2 Pfaffensprung SBT

The Pfaffensprung SBT located in the Swiss Alps was commissioned 1922 together with the Pfaffensprung reservoir erected for hydropower generation (SBZ 1943, Vischer *et al.* 1997, Müller 2015). The tunnel is in operation for over 100 days per year when the inflow exceeds the threshold discharge for bedload transport. The operating flow velocities lay between 15 and 17 m/s.
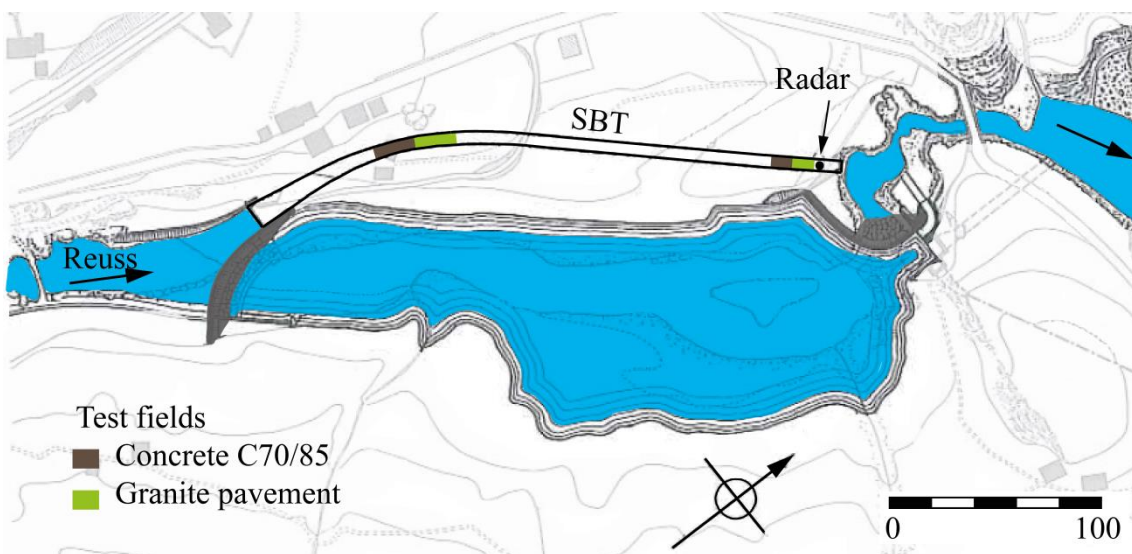
Figure 4: Overview of the Solis SBT with location of test fields and instrumentation

In the winter season 2011/12 and 2012/13 10 m long tests fields were implemented near the outlet and in the tunnel bend (Figure 4). They consist of a granite pavement and high-strength concrete with and without steel fibers. The original layer thickness was 30 cm. Compression strengths of granite and concretes are f_c = 180 MPa, 75 and 79 MPa, respectively. The hydraulic operating conditions are monitored by a radar mounted on the ceiling near the outlet (Vegaplus 54K, manufactured by Vega,

128

Pfäffikon, Switzerland) while the invert abrasion is determined based on measurements taken every winter season by a 3D-laser scanner (Z+F Imager 5006h, manufactured by Zoller + Fröhlich, Wangen im Allgäu, Germany).

3.3 Laboratory tests

To simulate hydroabrasion in the laboratory at controllable conditions a rotating drum developed at the Technical University of Dresden is used (Bellmann 2012, Mechtcherine *et al.* 2012). It consists of an octagonal rotating drum, feed with an abrasive charge and equipped with slab shaped specimens (300 mm × 300 mm × 50 mm). By changing abrasive particle size and rotation velocity, different flow and sediment load regimes are simulated (Bellmann 2012, Mechtcherine *et al.* 2012). The abrasion is determined both by weighing and laser scans providing the parameters abrasion rate, mass loss, and abrasion depth, respectively.

4 Results

4.1 Solis SBT

Since the commissioning, the Solis SBT was in operation four times. It was found that the sediment transport rate changed as a function of the reservoir level, corresponding to an increasing energy head, and suspended sediment rate scattered larger than bed load (Figure 5a and Figure 5b). With increasing reservoir level the bed shear stress upstream of the intake decreases due to the low flow velocity, and reduces the sediment transport capacity leading to lower sediment transport rates in the reservoir and thus in bypass tunnel itself. Reasons for the fluctuations are assumed to be generated by local erosions of the aggradation body.
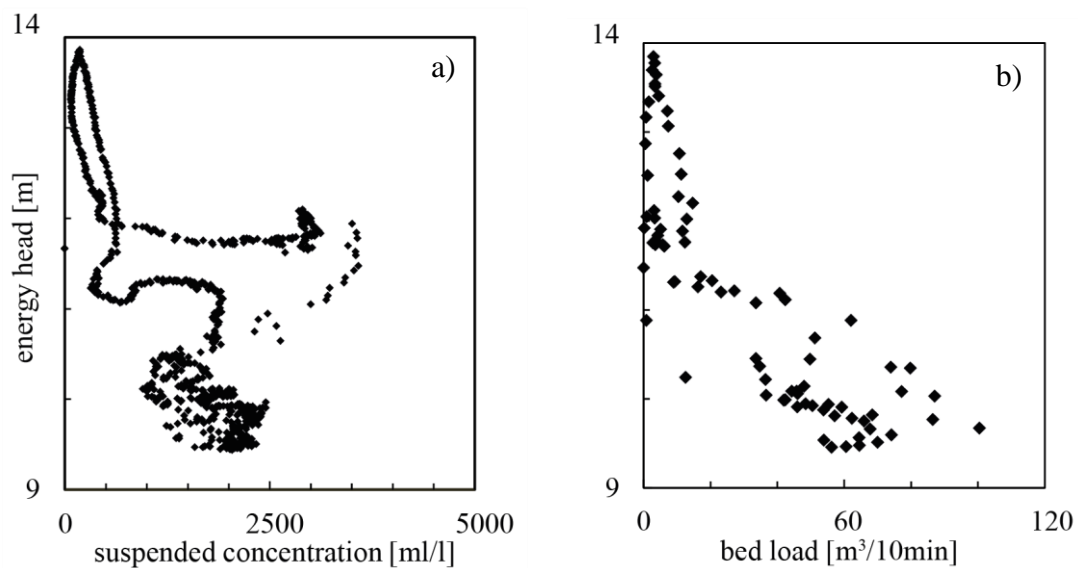

Figure 5: a) Suspended sediment concentration, and b) bed load transport rate depending on energy head during operation on 13th August 2014

Furthermore, the geophone system registered unevenly distributed bedload transport in the spanwise direction. Over 90% of the triggered bed load was transported on the orographic right tunnel side and showed an exponential distribution increasing towards the tunnel wall. This phenomenon resulted from the effect of the bend located 100 m upstream. It induces secondary flow currents causing sediment concentration at the inner side of the bend.

During the first three operations the measured bypassed sediment volume varied between 20'000 and 80'000 m^3, but the portion of bed load was insignificant. Consequently, no abrasion was observed. However, during the operation in August 2014 the suspended and the bed load transport mass were considerable and first abrasion traces were observed. Although an abrasion measurement is yet to be done, visual inspections already showed that cast basalt plates suffered from abrasion at the upstream edges while the concrete fields generally experienced comprehensive abrasion following an undulating pattern. However, at the test fields equipped with high alumina cement concrete and ultra-high-performance fiber-reinforced concrete no abrasions were visible.

4.2   Pfaffensprung SBT

In 2012 and 2013 the Pfaffensprung SBT was in operation for 113 and 131 days, respectively and let all test fields suffer from hydroabrasion. Due to the tunnel bend, abrasion occurred more intensely on the orographic right side, especially for the older concrete near the outlet. Furthermore, comparison of the abrasion topography between 2012 and 2013 revealed that the abrasion pattern stayed similar but amplified and damages grew in streamwise direction (Figure 6a and Figure 6b).

The abrasion on the concrete test fields showed an undulating pattern, whereas the abrasion on the granite test fields were concentrated at the lateral joints and upstream edges of the tiles (Hagmann *et al.* 2014). The mean abrasion rates were 2 mm and 14 mm per year while the maximal abrasion rates were 15 and 35 mm per year for granite and concrete, respectively. Note that the maximal abrasion rates are decisive for SBB to define the refurbishment intervals.

130
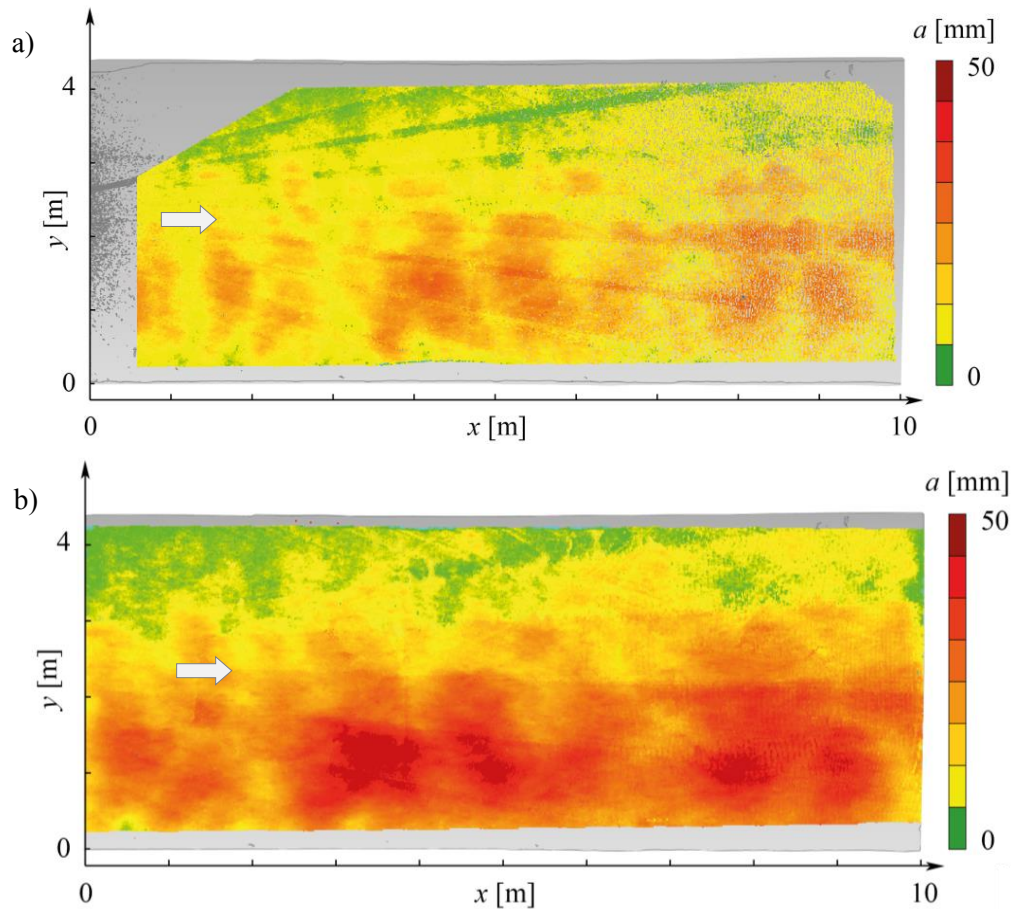
Figure 6: Abrasion of a high strength concrete test field in the Pfaffensprung SBT, a) after one year and b) after two year of operation, flow direction from left to right

4.3 Hydroabrasion drum

The concrete specimens taken from Pfaffensprung SBT were tested using the test drum described in Section 3.3. The tests were done using a mixture of 10 kg of water and 10 kg of steel spheres with a mean diameter of 5 mm. The rotation speed was 17 rotations per minute. Thereby the samples were stressed for 0.5454 s per rotation. The test duration was 58.8 h and the stress duration per sample was 9.09 h causing an abrasion rate of 1.1 mm/h (Figure 7). During the laboratory test a linear correlation between abrasion depth and stress duration was observed confirming former results (Auel 2014). Since the field abrasion was 14 mm per year, this laboratory test was able to reproduce the *in-situ* abrasion depth of a whole season in fast motion within less than 59 hours. Thus this testing procedure seems to be suitable for cross-comparison and determination of hydroabrasion resistance of different materials in respect of future applications. However, this promising result must be confirmed by further investigations.

Figure 7: Hydroabrasion drum test results of high-strength concrete implemented in Pfaffensprung SBT; Abrasion as a function of both, stress duration and total number of rotations

5 Design recommendations

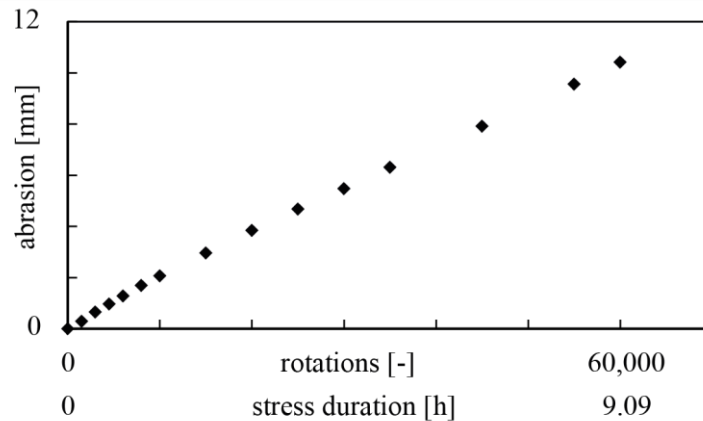Since hydroabrasion is a self-intensifying process, invert irregularities and vulnerabilities or imprecise uneven invert implementation should be avoided or at least minimized in the design and implementation stages. Curves in plan-view should be avoided as sediment transport always occurs on the inner side of the curve due to the development of additional secondary currents. If they are inevitable, invert strengthening along the inner curve should be considered to cope with the increased specific sediment transport rates. Additionally, proper implementation and curing are preconditions for high resistant invert materials. At most sites the grain size distribution covers a large range resulting in a combination of two different particle size-dependent abrasion processes, grinding or impinging. Therefore, it is not possible to equip a facility with an optimum material persisting all operating conditions. Whenever damages appear and surface shows highly irregular pattern and protruding edges, refurbishment should be conducted in order to hinder fast growing damages. Further recommendations may be found in Boes *et al.* (2014).

6 Conclusions

Although hydroabrasion is an omnipresent issue in hydraulic engineering, only few standards or guidelines are available. The operators of facilities facing hydroabrasion wear often test the performance of different materials *in-situ*. However, in many cases even after decades of testing, the optimum lining material is not found. Recent investigations show that laboratory tests using a hydroabrasion drum are suitable to determine the hydroabrasion resistance of lining materials. These results confirm findings of other scientists (Jacobs *et al.* 2001, Kryžanowski *et al.* 2012). However, only a few investigations have been done, thus leaving a knowledge gap concerning the correct simulation of field conditions as well as the transferability of laboratory results to field scale. This requires further experiments.

The present field investigations reveal that monolithic materials exhibit undulating abrasion pattern which sometimes lead to incision channels or pot holes whereas modular materials have weak spots at the joints suffering the highest abrasion rates. Further it is found that hard materials persist suspended sediment. If the dominating abrasion process is caused by saltating particles, materials with high tensile strengths perform better than hard materials prone to brittle fracturing by absorbing the kinetic energy of the impacts. However, force-locked mounting and higher board thickness reduces the risk of fracturing significantly.

Acknowledgement

References

Auel C. (2014). Flow charachteristics, particle motion and invert abrasion in sediment bypass tunnels. *VAW-Mitteilungen* 229 (R. M. Boes, ed.), ETH Zurich, Switzerland.

Auel C., Boes R., Ziegler T., Oertli C. (2011). Design and construction of the sediment bypass tunnel at Solis. *Hydropower and Dams* (3): 62-66.

Bellmann C. (2012). Deterioration of concrete subjected to hydro-abrasion. *Proc. 9th International PhD Symposium in Civil Engineering*, Karlsruhe Institute of Technology (KIT), Germany.

Bellmann C., Mechtcherine V. (2012). Experimental investigation into the deterioration of ordinary concrete subjected to hydro-abrasion. *Proc. MicroDurability*, PRO83, Amsterdam, Netherland.

Black K., Rosenberg M. (1994). Suspended sand measurements in a turbulent environment: field comparison of optical and pump sampling techniques. *Coastal Engineering* 24 (1): 137-150.

Boes R. M., Auel C., Hagmann M., Albayrak I. (2014). Sediment bypass tunnels to mitigate reservoir sedimentation and restore sediment continuity. *Proc. International Riverflow Conference* (A. J. Schleiss *et al.*, eds.), Lausanne, Switzerland: 221-228.

Bogen J., Møen K. (2001). Bed load measurements with a new passive ultrasonic sensor. *Erosion and Sediment Transport Measurement: Technological and Methodological Advances, International Association of Hydrological Sciences*: 19-21.

Delley P. (1988). Erosionsschäden am Umleitstollen Palagnedra und deren Sanierung ('Erosion damages at bypass tunnel Palagnedra and its rehabilitation'). *Proc. Internationales Symposium über Erosion, Abrasion und Kavitation im Wasserbau*, VAW-Mitteilung 99 (D. Vischer, ed.), VAW, ETH Zurich, Switzerland: 329-352.

Felix D., Albayrak I., Boes R. M. (2013). Laboratory investigation on measuring suspended sediment by portable laser diffractometer (LISST) focusing on particle shape. *Geo-Marine Letters* 33 (6): 485-498.

Gottesfeld A. S., Tunnicliffe J. (2003). Bed load measurements with a passive magnetic induction device. *IAHS-Publication*: 211-221.

Grasso D. A., Jakob A., Spreafico M. (2005). Abschätzung der Schwebstofffrachten mittels zweier Methoden. *Wasser Energie Luft* 99 (3): 273-280.

Habersack H., Haimann M., Kerschbaumsteiner W., Lalk P. (2008). Schwebstoffe im Fließgewässer: Leitfaden zur Erfassung des Schwebstofftransportes ('Suspended sediment in waterscourse: guidline for registration of suspended sediment transport'), Bundesministerium für Land- und Forstwirtschaft, Umwelt und Wasserwirtschaft, Vienna, Austria.

Hagmann M., Albayrak I., Boes R. M. (2012). Reduktion der Hydroabrasion bei Sedimentumleitstollen - In-situ-Verusche zur Optimierung der Abrasionsresistenz ('Reduction of hydroabrasion at sediment bypass tunnels - In-situ experiments to optimize the abrasion resistance'). *Proc. Wasserbausymposium "Wasser - Energie, global denken - lokal handeln"* (G. Zenz, ed.), TU Graz, Austria: 91-97.

Hagmann M., Albayrak I., Boes R. M. (2014). Untersuchung verschleissfester Materialien im Wasserbau mit einer Geschiebtransportüberwachung ('Investigation abrasion resistant materials at hydraulic structures with a bed load monitoring'). *Proc. Internationales Symposium „Wasser- und Flussbau im Alpenraum"*, VAW-Mitteilung 227 (R. M. Boes, ed.), ETH Zurich, Switzerland: 97-106.

Jacobs F., Hagmann M. (2015). Sediment Bypass Tunnel Runcahez: Invert Abrasion 1995-2014. *Proc. First International Workshop on Sediment Bypass Tunnels*, VAW-Mitteilungen 232 (R. M. Boes, ed.), Zurich, Switzerland.

Jacobs F., Winkeler W., Hinkeler F., Volkart P. (2001). Betonabrasion im Wasserbau ('Concrete abrasion at hydraulic structures'). *VAW-Mitteilung* (H.-E. Minor, ed.), ETH Zurich, Switzerland.

Kryžanowski A., Mikoš M., Šušteršič J., Ukrainczyk V., Planinc I. (2012). Testing of concrete abrasion resistance in hydraulic htructures on the Lower Sava River. *Strojniški vestnik-Journal of Mechanical Engineering* 58 (4): 245-254.

Mechtcherine V., Bellmann C., Helbig U., Horlacher H. B., Stamm J. (2012). Nachbildung der Hydroabrasionsbeanspruchung im Laborversuch Teil 1 - Experimentelle Untersuchung zu Schädigungsmechanismen im Beton ('Modeling hydroabrasive stress in the laboratory experiment, part 1 - experimental investigations of damage mechanisms in concrete'). *Bautechnik* 89 (5): 309-319.

Møen K., Bogen J., Zuta J., Ade P., Esbensen K. (2010). Bedload measurement in rivers using passive acoustic sensors. *US Geological Survey Scientific Investigations Report* 5091: 336-351.

Morach S. (2011). Geschiebemessung mittels Geophonen bei hohen Fliessgeschwindigkeiten - Hydraulische Modellversuche ('Bedload transport measurement at high flow velocities - hydraulic model tests'). *Master Thesis*, VAW, ETH Zurich, Switzerland, (unpublished).

Müller B., Walker M. (2015). The Pfaffensprung sediment bypass tunnel: 95 years of experience. *Proc. First International Workshop on Sediment Bypass Tunnels*, VAW-Mitteilungen 231 (R. Boes, ed.), VAW, ETH Zurich, Switzerland.

Nakajima H., Otsubo Y., Omoto Y. (2015). Abrasion and corrective measurement of a sediment bypass system at Asahi Dam. *Proc. First international Workshop on Sediment Bypass Tunnels*, VAW Mitteilungen 232 (R. M. Boes, ed.), ETH Zurich, Switzerland.

Oertli C. (2009). Entlandung des Stausees Solis durch einen Geschiebeumleitstollen. *Wasser Energie Luft* 101. Jahrgang, Heft 1: 5-9.

Oertli C., Auel C. (2015). Solis sediment bypass tunnel: First operation experiences. *Proc. First International Workshop on Sediment Bypass Tunnels*, VAW-Mitteilungen 232 (R. Boes, ed.), VAW, ETH Zurich, Switzerland.

Rickenmann D., McArdell B. W. (2007). Continuous measurement of sediment transport in the Erlenbach stream using piezoelectric bedload impact sensors. *Earth Surface Processes and Landforms* 32 (9): 1362-1378.

Rickenmann D., Turowski J. M., Fritschi B., Klaiber A., Ludwig A. (2012). Bedload transport measurements at the Erlenbach stream with geophones and automated basket samplers. *Earth Surface Processes and Landforms* 37 (9): 1000-1011.

SBZ (1943). Rekonstruktion des Umleittunnels am Pfaffensprung des Kraftwerks Amsteg der SBB. *Schweizerische Bauzeitung* 121: 41-42.

Vischer D., Hager W. H., Casanova C., Joos B., Lier P., Martini O. (1997). Bypass tunnels to prevent reservoir sedimentation. *Proc. 19th ICOLD Congress* Q74 R37, Florence: 605-624.

Wren D., Barkdoll B., Kuhnle R., Derrow R. (2000). Field techniques for suspended-sediment measurement. *Journal of Hydraulic Engineering* 126 (2): 97-104.

Wyss C. R., Rickenmann D., Fritschi B., Weitbrecht V., Boes R. M. (2014). Bedload grain size estimation from the indirect monitoring of bedload transport with Swiss plate geophones at the Erlenbach stream. *Proc. River Flow 2014* (A. Schleiss *et al.*, eds.), Lausanne: 1907-1912.

Authors

Michelle Hagmann (corresponding Author)
Laboratory of Hydraulics, Hydrology and Glaciology (VAW), ETH Zurich
Email: hagmann@vaw.baug.ethz.ch

Dr. Ismail Albayrak
Prof. Dr. R.M. Boes
Laboratory of Hydraulics, Hydrology and Glaciology (VAW), ETH Zurich

Downstream morphological impact of a sediment bypass tunnel – preliminary results and forthcoming actions

Matteo Facchini, Annunziato Siviglia, Robert M. Boes

Abstract

Re-establishing the sediment continuum in a river is one of the purposes of sediment bypass tunnels (SBTs). They convey sediments (bed and suspended load) from the upstream river and reservoir to the downstream reach having the potential to modify river morphology. This in turn may affect the river ecosystem altering the habitat conditions for the biota (e.g. fishes, macroinvertebrates). Understanding the effects of SBTs on river morphology is of paramount relevance for both reservoir sediment and river management purposes and is the main objective of an ongoing PhD project at the Laboratory of Hydraulics, Hydrology and Glaciology (VAW) of ETH Zurich. This project focuses on the SBT built at Solis Dam in the canton of Grisons, Switzerland, in 2012. The Solis SBT starts to effectively operate during the flood event of August 13, 2014 when about 80'000 m^3 of sediments pass through the tunnel. In this work we analyze the change in morphology that occurred during this event through a comparison between data collected in the pre-flood period (2012-2014) and those collected after the flood event. Preliminary analyses concerning cross-sectional variations and sediment grain size distributions show that changes occurred in different places downstream of the dam. Ongoing monitoring activities will provide more details on morphological changes and they serve as basis for the development of mathematical modelling aiming to predict future morphological changes and possible ecological effects, assessing different water and sediment release scenarios.

1 Introduction

Rivers are complex and dynamic systems, which are quite reactive to changes of water and/or sediment discharge regime. These changes in turn have the potential to induce dramatic morphological modifications with possible severe effects on stream ecology. The most emblematic and common anthropic cause inducing such changes is the construction of a reservoir (Graf, 2006). In most of the cases, the presence of a dam may reduce the availability of both water discharge and sediments, which in turn affect morphodynamics at a large variety of spatial scales, from the reach- to the cross-sectional scale. Rivers may change the planimetric pattern, e.g. from braided to single

thread (Surian 1999, Surian and Rinaldi 2003), or from sinuous with alternate bars to braided (Rinaldi 2003). They also can modify river cross sections in terms of bed aggradations or degradations and narrowing processes (e.g. Surian and Rinaldi 2003).

Construction of sediment bypass tunnels in dammed rivers changes the sediment discharge regime in the downstream reach, possibly inverting the morphological evolution induced by the construction of the dam (Fukuda *et al.* 2012). Effectively managing a SBT in order to both reduce the amount of sediments deposited in the reservoir and at the same time improving the ecological conditions of the downstream reach is an important task in such changing environment. In this framework, the Swiss Federal Office of Environment (FOEN) co-financed a PhD project entitled "*Re-establishment of the sediment continuum at an alpine reservoir – influence on river morphology, ecology and flood prevention*". The dammed river considered in this project is the Albula in the canton of Grisons, where a SBT has been built at Solis Dam in 2012. In August 2014, a flood with about a twenty-years return period carried approximately 80'000 m^3 of sediment through the tunnel.

The aim of this contribution is twofold. First, we present some preliminary results in which we compare different cross sections measured in the years 2012-2013 and after the 2014 flood. We also compare the sediment grain size distributions in different locations. Second, we describe field measurements and mathematical modelling activities we have planned in order to increase the knowledge about the morphological variations and the possible ecological consequences induced by SBTs.

2   Study site characteristics

The Albula River flows from the Albula pass to the Hinterrhine, draining a 950 km^2 basin. Its total length is almost 40 km. The Solis dam is located along the Albula river just downstream of Tiefencastel in the canton of Grisons (see Figure 1). It is operated by the electric power company of Zurich (ewz) and was built in 1986. It is a 61 m high arch dam with a crest length of 75 m. The catchment area at the dam amounts to 900 km^2. The Albula river reach under investigation is about 8 km long and stretches from the SBT outlet to the river mouth into the Hinterrhine (see Figure 1).

The Solis SBT was built in 2012 with a design capacity of 170 m^3/s corresponding to a five-years return period flood. The total length of the bypass tunnel is 968 m with a slope of 1.9%, except for the inflow section, which is 50 m long with a slope of 1%. The tunnel cross section has an archway shape with a width of 4.40 m and a height of 4.68 m. More details about the Solis SBT can be found in Oertli and Auel (2015).

3   The August 2014 flood

On August 13, 2014, an intense meteorological event occurred in the Albula river basin. The discharge has been measured at two gauges upstream of the SBT, on the Albula and

its major tributary, the Julia River. The gauged station located on the Albula river registered a peak discharge of 130 m^3/s (return period of about 100 years), while the gauged station on the Julia measured a peak discharge of 118 m^3/s (return period of 20 years). As a first approximation, since the two stations are close to the reservoir head and the two peaks are almost simultaneous, the two hydrographs can be summed up in order to get the inflow hydrograph ($Q_{upstream}$ in Figure 2). The peak discharge of 248 m^3/s had a return period between 20 years (HQ_{20} = 226 m^3/s) and 100 years (HQ_{100} = 282 m^3/s) (VAW 2010). During this event, water has been continuously conveyed through the SBT (Q_{SBT} in Figure 3) for about 13 hours. The total Albula discharge downstream of the bypass tunnel outlet ($Q_{downstream}$ in Figure 2) is the sum of Q_{SBT}, and both the bottom outlet discharge Q_{bo} and the spillway discharge Q_{spill} released from the dam, i.e. $Q_{downstream} = Q_{SBT} + Q_{bo} + Q_{spill}$.

Hagmann *et al.* (2015), using geophones mounted at the tunnel outlet estimated the total volume of bed load transported through the tunnel during the entire event to be about 80'000 m^3.

Figure 1: Study site: outlet of Solis SBT near Alvaschein, canton of Grisons, Switzerland (downstream view, photo by M. Facchini)

4 Morphological changes induced by the first SBT operation: Preliminary results

Field measurements have been carried out in three different locations along the 8 km river reach of the Albula River under investigations (see Figure 3): in the upper (cross sections 16-17-18), middle (cross sections 13-14-15) and downstream parts (cross sections 10-11-12) located a few hundreds of meters, 3 km and 6 km downstream of the SBT outlet, respectively. All cross sections have been measured in 2012 and 2013 and after the August 2014 flood, while the grain size distribution has been measured just in the middle and downstream parts in the same years.

The cross sections temporal evolution is given in Figures. 4a, 4b and 4c. In the upper part (Figure 4a, cross section 16) there is a trend of erosion. In the middle part (Figure 4b, cross section 13) aggradation occurred, while in the downstream part (Figure 4c, cross section 10) aggradation is evident. From these preliminary results it seems that a "sediment pulse" dynamics (Cui *et al.*, 2003, Sklar *et al.*, 2009, Venditti *et al.*, 2010, Humphries *et al.*, 2012) can be identified: once the sediments are released from the SBT, they are transported downstream as a sediment wave interacting with the pre-pulse bed material.
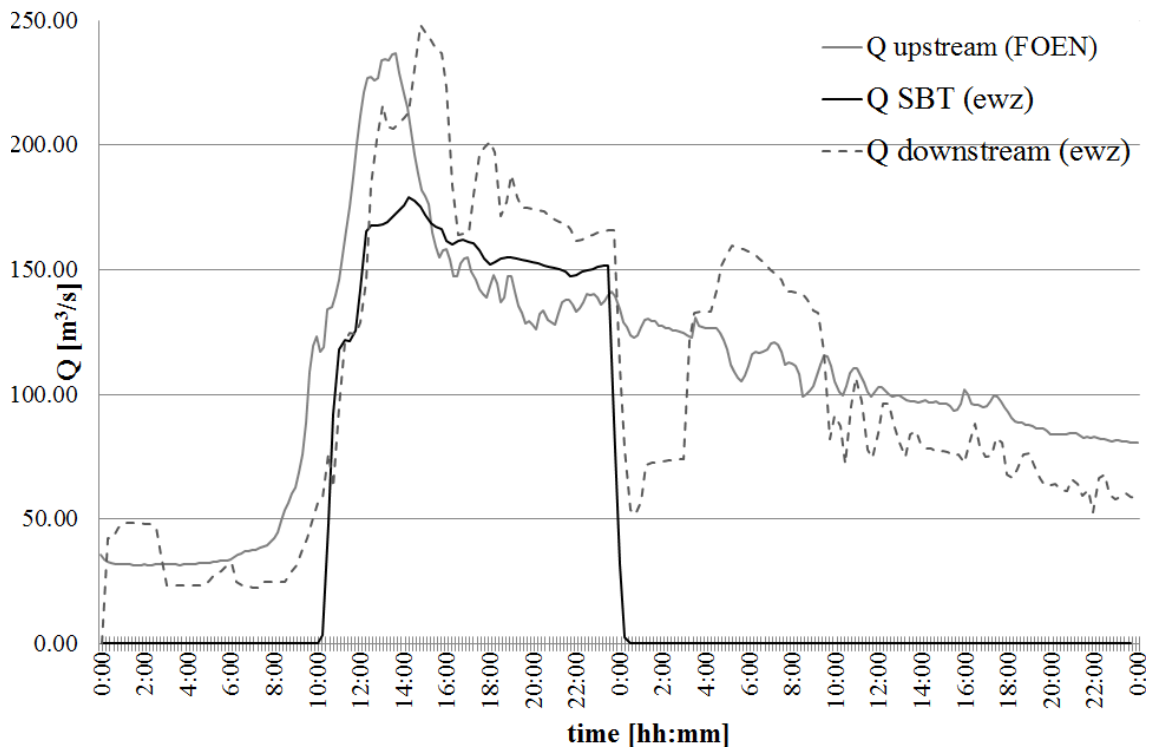
Figure 2: Hydrograph of the August 13, 2014 flood; $Q_{upstream}$ is the sum of the Albula River and Julia River discharge measured upstream of the reservoir (courtesy of FOEN), while $Q_{downstream} = Q_{SBT} + Q_{bo} + Q_{spill}$ (courtesy of ewz)

140

The grain size distribution is compared just in the middle and downstream areas (i.e. in cross sections 13 and 10). The results are shown in Figure 4d where we notice a coarsening trend in cross section 13 and a fining tendency in cross section 10. These results suggest that the coarse part of the sediments released by the SBT has been carried out by the flow up to the middle part of the river reach under investigation, while the finest part has been carried out for a longer distance depositing mainly in the downstream part.

Figure 3: Cross sections measurement sites (source www.swisstopo.ch).

Figure 4: Cross sections 16 (a), 13 (b) and 10 (c): annual comparison (courtesy of Meisser Vermessungen AG); (d) grain size distribution comparison in 2012, 2013 and 2014 (courtesy of Hunziker, Zarn und Partner).

5 Forthcoming activities and expected outcomes

New field monitoring and mathematical modelling activities will be implemented next. Essentially the idea is to have a more d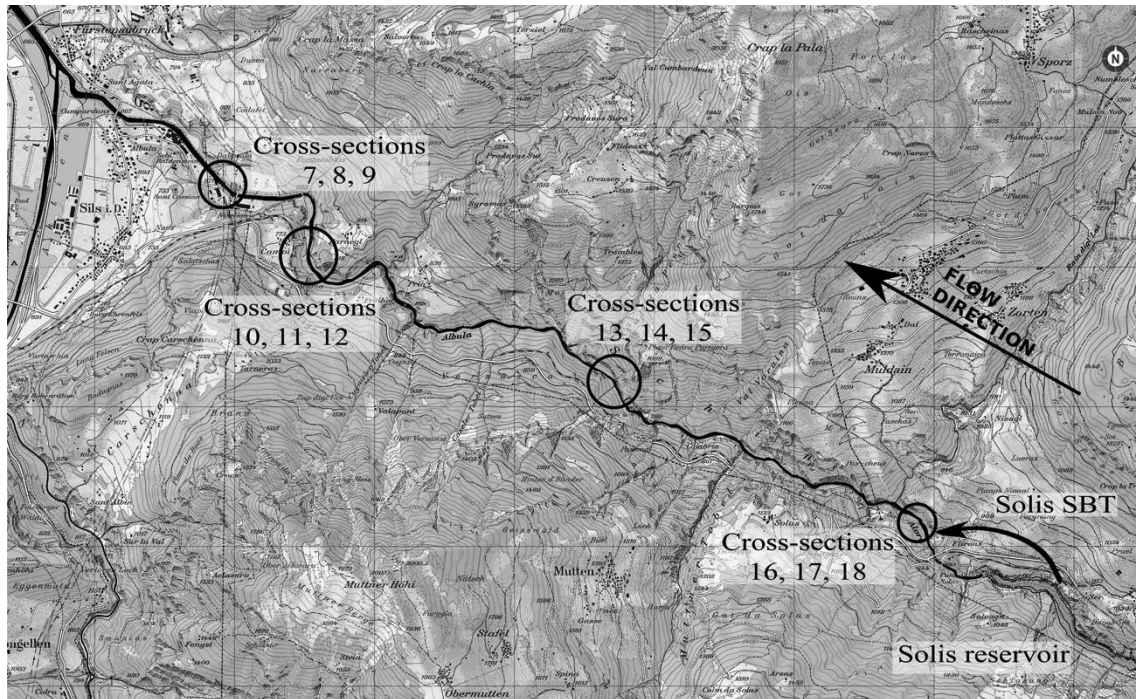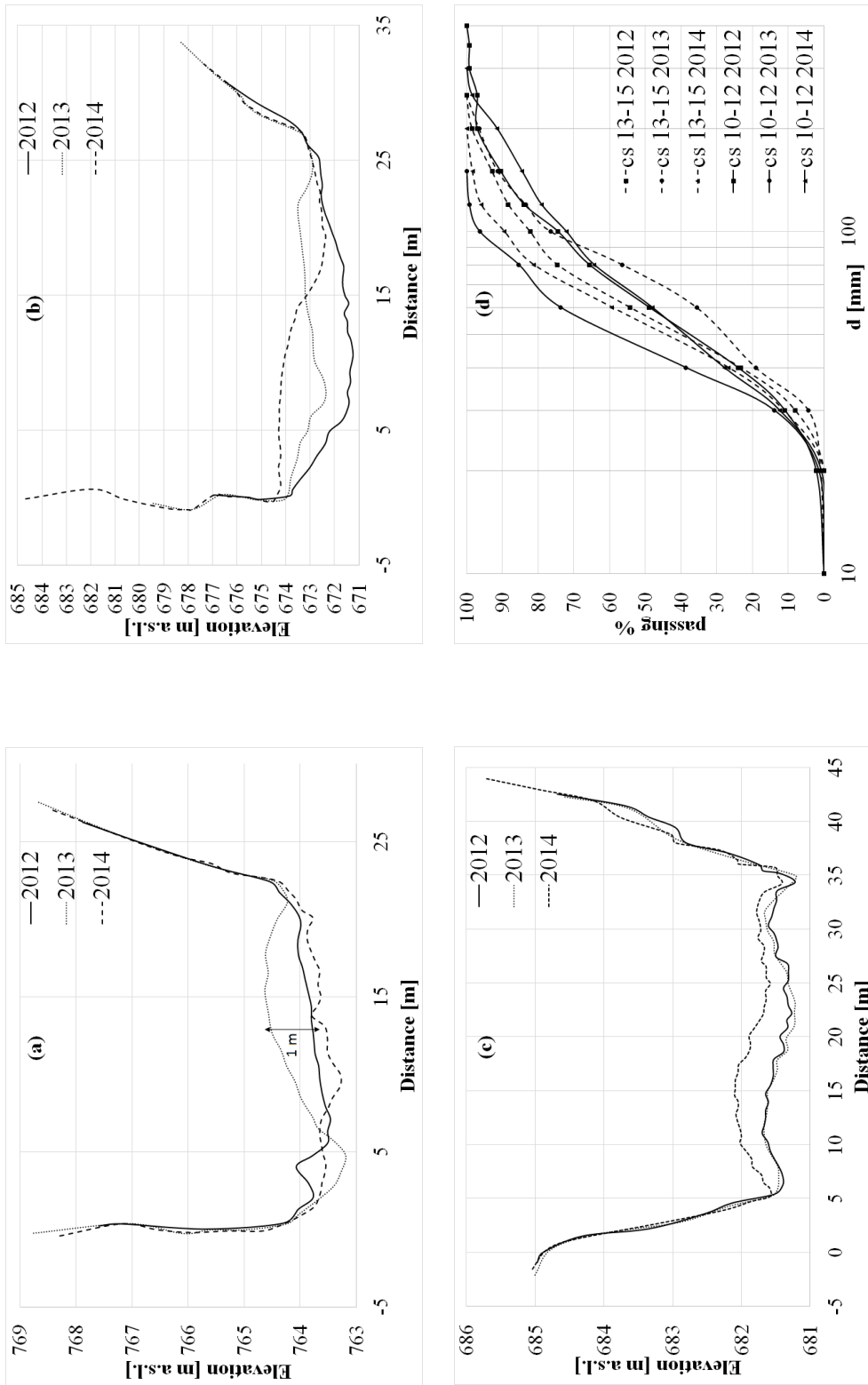etailed description of the topography in order to describe more accurately the morphological changes. These data will be used as a calibration reference for implementing mathematical modelling in order to describe future morphological changes on short (single event) and long time scale and for assessing water and sediment release management strategies. This will also allow us to use meso-habitat modelling in order to estimate the ecological consequences of morphological variations on fish habitat.

In the following we give details on single actions and tasks either planned or already in execution.

5.1 Green LiDAR survey

The green LiDAR survey is essential to have a more complete topographic representation of the river reach under investigation. A first flight has been already carried out on October 18, 2014. A second one is planned after a possible future flood, which will trigger the opening of the SBT. These data can be used for multiple purposes. First, we can analyze both the planimetric and altimetric pattern variations occurring during and between two consecutive SBT operations by comparing the Digital Elevation Models (DEM) that will be extracted from the two LIDAR flights. This allows us also to quantify the morphodynamic variations induced by the sediments introduced in the downstream reach. Second, using the aerial pictures taken during the flights we try to analyze the grain size distribution of the emerged riverbed areas with aerial photosieving: using the texture of the airborne picture we can recognize the size of the top layer particles (Dugdale *et al.* 2010) possibly identifying the grain size distribution variations.

Finally, from the LiDAR data a numerical grid will be extracted in order to run 2D numerical simulations with the software BASEMENT (Vetsch *et al.* 2014), which is able to describe morphodynamic changes in rivers. Once the morphology changes between the situations described by the two DEM will be correctly modelled, i.e. the model will be calibrated, future morphology scenarios will be numerically predicted (e.g. Brestolani *et al.* 2014) possibly including different SBT operation and reservoir management release scenarios.

5.2 Meso-habitat modification analysis

Morphological changes may in turn induce also ecosystem modifications. We will focus mainly on fish and try to quantify habitat changes adopting a reach scale approach, i.e. a meso-habitat analysis (Parasiewicz 2011, Vezza *et al.* 2014). Meso-habitats are areas inside the channel identified by different values of flow velocity, water depth and

substrate grain size. These will be measured during different field surveys to be carried out immediately afterwards the two LIDAR flights. Comparison between the two surveys allows us to quantify the meso-habitat changes induced by the SBT operations whereas two-dimensional numerical simulations will enable us to predict the evolution of the meso-habitat and to assess the effect of different release scenarios (water and sediment) on the fish habitat.

5.3 Long-term morphodynamic predictions

The aim of this task is twofold. First, from the analysis of historical airborne picture pre- and post-dam construction, we try to estimate some simple morphological evolution patterns (mainly concerning the channel width and possibly the river bed level), identifying the effect of the dam on the downstream morphology.

Second, starting from the work by Tealdi *et al.* (2011) we will try to develop a simple, lumped morphodynamic model that describes fluvial cross section dynamics consequent to changes in discharge and sediment transport induced by the SBT. The model will provide the long-term temporal dynamics of the river width and bed level. These dynamics are far from being trivial and can exhibit non-monotonic behavior, with aggradations and degradations, as well as narrowing and widening.

6   Conclusions

The analysis of the SBT operation of August 2014 shows that cross section and grain size distribution variations occurred in different places downstream of the Solis dam, along the entire river reach under investigation. Future field campaigns have been planned with the aim of accurately evaluating the morphological changes induced by SBT operations and possible ecological consequences. Finally, using numerical modelling, future release scenarios (water and sediments) will be evaluated with the aim of increasing the ecological quality of the entire river reach.

References

Brestolani, F., Solari, L., Rinaldi, M., Lollino, G. (2014). On the Morphological Impacts of Gravel Mining: The Case of the Orco River, *Engineering Geology for Society and Territory – Volume 3(66)*, Springer International Publishing Switzerland.

Cui Y., Parker G., Lisle T. E., Gott J., Hansler-Ball M. E., Pizzuto J. E., Allmendinger N. E., Reed J. M. (2003). Sediment pulses in mountain rivers: 1. Experiments, *Water Resources Research*, 39(9): 1239.

Dugdale, S. J., Carbonneau, P. E., Campbell, D. (2010). Aerial photosieving of exposed gravel bars for the rapid calibration of airborne grain size maps, *Earth Surface Processes and Landforms*, 35(6): 627-639.

Fukuda, T., Yamashita, K., Osada, K., Fukuoka, S. (2012). Study on flushing mechanism of dam reservoir sedimentation and recovery of riffle-pool in downstream reach by a flushing bypass tunnel, *Proc. Intl. Symp. on Dams for a Changing World*, Kyoto, Japan.

Graf WL. (2006). Downstream hydrologic and geomorphic effects of large dams on American rivers, *Geomorphology*, 79(3–4, Sp. Iss. SI):336–360.

Hagmann M., Albayrak I., Boes R.M. (2015). Field research: Invert material resistance and sediment transport measurements. Proc. First Intl. Workshop on sediment bypass tunnels, *VAW-Mitteilung* 232 (R. Boes, ed.), Laboratory of Hydraulics, Hydrology and Glaciology, ETH Zurich, Switzerland.

Humphries, R.J., Venditti, J. G., Sklar, L. S., Wooster, J. K. (2012). Experimental evidence for the effect of hydrographs on sediment pulse dynamics in gravel-bedded rivers, *Water Resources Research*, 48(1): W01533.

Oertli C., Auel C. (2015). Solis sediment bypass tunnel: First operation experiences. Proc. First Intl. Workshop on sediment bypass tunnels, *VAW-Mitteilung* 232 (R. Boes, ed.), Laboratory of Hydraulics, Hydrology and Glaciology, ETH Zurich, Switzerland.

Parasiewicz, P. (2011). MesoHABSIM: A concept for application of instream flow models in river restoration planning, *Fisheries*, 26(9): 6-13.

Rinaldi M. (2003). Recent channel adjustments in alluvial rivers of Tuscany, central Italy. *Earth Surface Process Landforms*, 28(6):587–608.

Sklar, L. S., Fadde, J., Venditti, J. G., Nelson, P. A., Wydzga, M. A., Cui, Y., Dietrich, W. E. (2009). Translation and dispersion of sediment pulses in flume experiments simulating gravel augmentation below dams, *Water Resources Research*, 45(8): W08439.

Surian N. (1999). Channel changes due to river regulation: the case of the Piave River, Italy. *Earth Surface Process Landforms*, 24(12):1135–51.

Surian, N., Rinaldi, M. (2003). Morphological response to river engineering and management in alluvial channels in Italy, *Geomorphology*, 50(2003): 307-326.

Tealdi, S., Camporeale, C., Ridolfi, L. (2011). Long-term morphological river response to hydrological changes, *Advances in Water Resources*, 34(12):1643-1655.

VAW (2010). Geschiebeumleitstollen Solis - Hydraulische Modellversuche ('Solis SBT – hydraulic model experiments'), *Bericht* 4269, Laboratory of Hydraulics, Hydrology and Glaciology, ETH Zurich, Switzerland (unpublished).

Venditti, J. G., Dietrich, W. E., Nelson, P. A., Wydzga, M. A., Fadde, J., Sklar, L. S. (2010). Effect of sediment pulse grain size on sediment transport rates and bed mobility in gravel bed rivers, *Journal of Geophysical Research*, 115(F3): W07506.

Vetsch, D. F., Ehrbar, D. Gerber, M. Peter, S. Rousselot, P. Volz, C. Vonwiller, L. Faeh, R. Farshi, D. Mueller, R. Veprek, R. (2014). System Manuals of BASEMENT v. 2.4

Vezza, P., Parasiewicz, P., Spairani, M., Comoglio, C. (2014). Habitat modeling in high-gradient streams: the mesoscale approach and application, *Ecological applications*, 24(4): 844-861.

Authors

Matteo Facchini (corresponding Author)
Laboratory of Hydraulics, Hydrology and Glaciology (VAW), ETH Zurich
Email: facchini@vaw.baug.ethz.ch.

Dr. Annunziato Siviglia
Prof. Dr. Robert M. Boes
Laboratory of Hydraulics, Hydrology and Glaciology (VAW), ETH Zurich

Ecological effects of sediment bypass tunnels

Eduardo J. Martín, Michael Doering, Christopher T. Robinson

Abstract

Different techniques, including Sediment Bypass Tunnels (SBTs), are used to re-establish sediment regimes downstream of dams. Our goal was to evaluate the ecological effects of a new SBT in an alpine stream in Switzerland. Sediment respiration (SR), fine particulate organic matter (FPOM), periphyton biomass and macroinvertebrate density and richness were analysed along a 5 km stretch of the river. Sampling was conducted upstream and downstream of sediment input sources, including the SBT and major tributaries, to determine the ecological impact of SBT high flow events. Our results showed that SR, periphyton biomass and macroinvertebrate density and richness decreased after SBT events due to water and sediment scouring/deposition. These results suggest SBT events act as short-term disturbances, but may potentially enhance sediment regimes downstream of dams in the long term.

1   Introduction

Sediment dynamics are an important feature of rivers and floodplains, maintaining habitat heterogeneity and turnover, and organic matter dynamics (Yarnell *et al,.* 2006). However, anthropogenic alterations have modified, and even eliminated, natural sediment regimes of rivers and floodplains, leading to ecosystem degradation via river-bed colmation, habitat loss and homogenization, and organic matter accumulation (Williams *et al.,* 1984; Brandt, 2000). One of the greatest man-made modifications of river ecosystems is through dams. Nilsson *et al.* (2005) documented that over 50,000 large dams (>15 meters in height) exist in the world, trapping up to 99% of upstream sediment delivery in reservoirs (Williams *et al.*, 1984). Besides the ecological effects, sediment accumulation in reservoirs can cause technical problems in reservoir operation. According to Sumi *et al.* (2004), worldwide reservoir storage capacity decreases around 570 km^3 annually. To overcome ecological and technical problems caused by sediment regime changes from dam operations, different techniques such as flushing or sluicing of reservoirs are used to reduce sediment accumulation in reservoirs and to re-establish sediment regimes below dams. However, these techniques also can harm various ecological properties of river ecosystems. Brandt (2000) showed how sediment additions by flushing can affect river geomorphology and Rabení *et al.* (2005)

and Crosa *et al.* (2010) documented how sediment deposition can affect riverine fish and invertebrates.

An alternative technology to sediment flushing by opening dams are Sediment Bypass Tunnels (SBTs) in hydrologically and topographically suitable systems. SBTs connect reservoirs with the stream below the dam. SBTs are operated during flood events, when water and suspended sediment from upstream enter the reservoir. In combination with an earlier lowering of the water level in the reservoir, the high flow event mobilizes accumulated sediments and transports them through the SBT. In countries such as Switzerland and Japan, SBTs are increasingly used despite the lack of knowledge on the ecological consequences to river and floodplain ecosystems below such structures. This study investigated the ecological effects of SBT events in a Swiss alpine river during one year. Sediment respiration, periphyton biomass and macroinvertebrates were used as ecological indicators to examine SBT events in the river since they respond rapidly to flow and sediment alterations and are used to evaluate and define the ecological conditions of stream ecosystems (Niemi *et al.,* 2004).

Sediment respiration is an ecosystem function property that refers to organic matter oxidation by microbial heterotrophs, e.g. bacteria, in the hyporheic zone of rivers, regulating carbon cycling and CO_2 fluxes into the atmosphere, among other ecosystem processes (Andrews *et al.*, 2001). It is mainly driven by temperature and organic matter content (Doering *et al.,* 2011). Periphyton includes bacteria, fungi and archaea that comprise biofilms covering streambed stones. Biofilms can influence nutrient uptake and the retention of suspended particles (Battin *et al.,* 2003). Macroinvertebrates are aquatic organisms such as insects that inhabit streambeds and provide resources for higher trophic levels in riverine/floodplain food webs. Periphyton and invertebrates in most alpine streams show peaks of growth in autumn, due to the lack of flow events, warm temperatures, light availability and constant discharge (Uehlinger *et al,.* 2010). The specific goals of the study were to:

- Identify and quantify the effects of SBT events to river floodplain structure and function using sediment respiration, periphyton biomass and macroinvertebrates as ecological indicators.

- Study temporal patterns in the ecology of the system following SBT events using the above ecological indicators.

2 Methods

2.1 Study Site and field sampling

The study was conducted on the Albula River, Canton Grisons (SE Switzerland) in the Rhein basin. The Albula is 40-km long and drains a 950 m^2 catchment with an average elevation of 2300 m a.s.l. Average discharge is ca. 35 m^3/s with natural peaks in summer due to snowmelt and precipitation events resulting in discharges >130 m^3/s

(HQ100). The Albula is regulated at the Solis reservoir located just downstream of Tiefencastel. Downstream, the river flows through a narrow canyon for about 7 km until the town of Sils. The canyon causes a heterogeneous stream morphology due to its curved longitudinal profile and the presence of large rocks and wood accumulations that generate riffles, runs, pools and backwaters. A Sediment Bypass Tunnel was built in 2012 about 500 m upriver of the dam to reduce sediment accumulation in the reservoir.
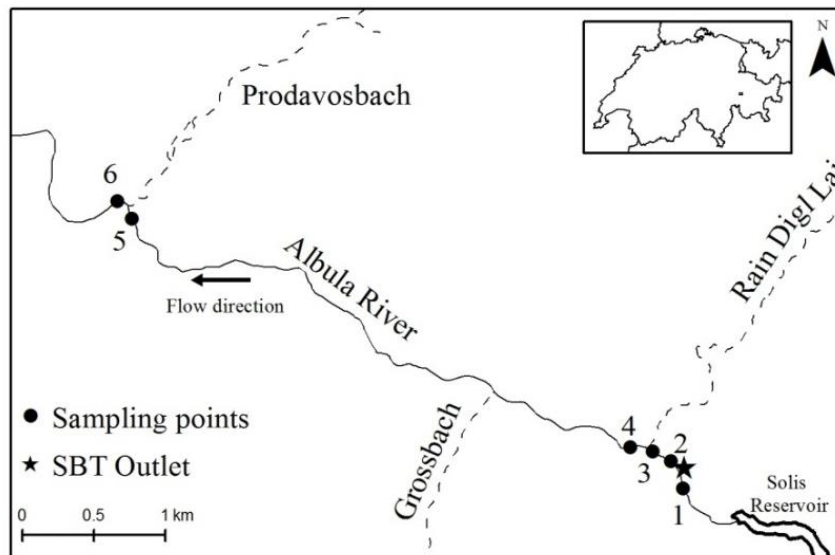
Figure 1: Map of the study stretch below Solis reservoir showing the study sites

The 5-km long study section is located between the dam and a downstream power plant at Sils (Figure 1). Three small tributaries enter the study section: Rain Digl Lai, Grossbach and Prodavosbach located at 350, 1500 and 5000 m downstream of the SBT outlet, respectively. Six sampling sites were established along the study section. The first site was located 50 m upstream of the SBT outlet, and the others downstream of the SBT outlet (100, 400, 500, 4900 and 5000 m; and placed above and below potential sediment input sources such as tributaries) (Figure 1). Three SBT events occurred in 2014 with discharges of 84 (May 23), 114 (June 29) and 160 m^3/s (August 13). Sampling campaigns took place before the first event (May 13), after the first event (June 5) and after the third event on August 28, September 22 and November 11. In between SBT events, spill water had a constant release except for a period in October (Figure 2).

Figure 2: Discharge of the Albula River as bottom outlet flow, spill water flow and SBT flow. Triangles indicate sampling campaign dates and stars show SBT events

2.2 Sediment respiration

Hyporheic sediment respiration (SR, n = 3 per site and date) was measured at each site as the change in O_2 concentration over time using Plexiglas® tubes (5.2 cm diameter, 32 cm long) to incubate hyporheic sediments (after methods in Uehlinger *et al.,* 2002). To avoid the respira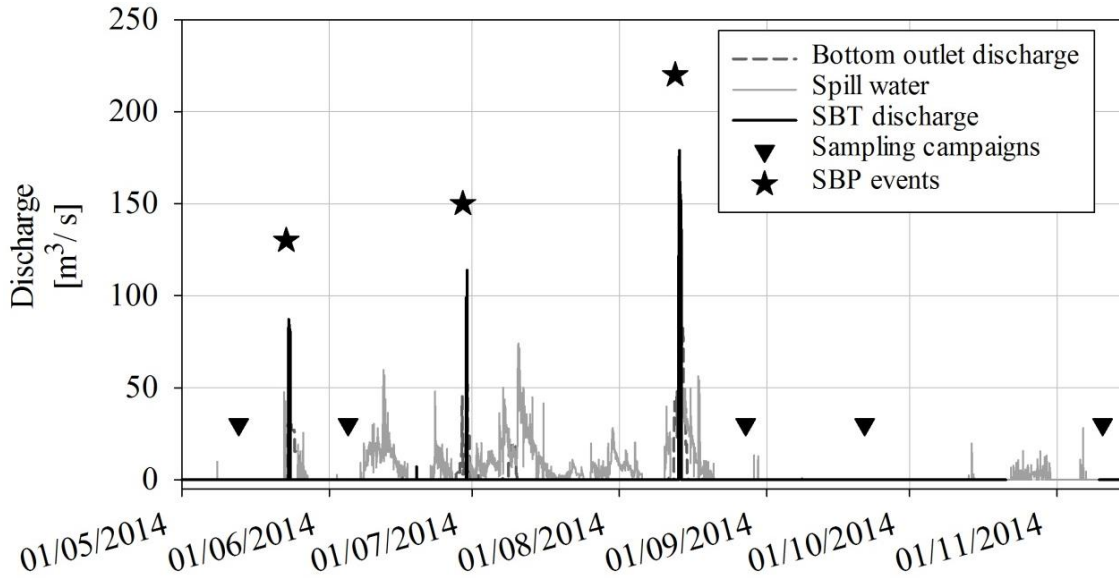tory effect of epilithic algae, ~10 cm of the sediment surface layer was removed. Hyporheic sediments were pre-sieved to 8 mm to exclude metabolically inactive large sediments: i.e. large stones (Doering *et al.,* 2011). Tubes half-filled with sediments and half with water were sealed with rubber stoppers and buried into the sediment for 3 to 4 hours for incubation. Temperature and oxygen concentration were measured before and after incubation with a portable oxygen meter (Hach HQ40d connected to a LD0101 oxygen probe). After incubation, samples were stored at -20°C until analysed. Calculations of respiration were based on O_2 consumption in the tube water (r; g O_2 m^{-3} h^{-1}) and then recalculated as respiration per kg sediment (R, g O_2 kg^{-1} h^{-1}) as follows:

$$R = r\, Vw\, /\, Gw \tag{1}$$

where Vw is water volume in the tube (m^3) and Gw is sediment dry weight (kg). Respiration rates were normalized by a reference temperature of 20°C to minimize seasonal variations due to temperature changes using the Arrhenius equation:

$$R_{20°C} = R_T\, /\, 1.072^{\,T-T20°C} \tag{2}$$

where $R_{20°C}$ is respiration rate at 20°C and T is the water temperature in the tube at the end of the incubation as described in Naegeli *et al.* (1997). In the laboratory, coarse particulate organic matter (CPOM, > 2 mm) was separated from sediments. CPOM samples were dried at 60°C for 48 h, weighed, combusted at 450°C for 4 h and

150

reweighed. Sediments and organic particles <2 mm were dried at 60°C for 48 h, combusted at 450°C for 4 h and reweighed to determine fine particulate organic matter (FPOM). CPOM and FPOM were expressed as g of ash-free dry mass (AFMD)/kg sediment. Only the FPOM data are presented in this paper.

2.3 Periphyton

Five rocks were randomly collected from each site on each date, stored in plastic bags, and kept frozen at -20°C until analysed. In the laboratory, periphyton was removed from the surface of stones using a metal brush and rinsed with deionized water. Subsamples of the suspension were filtered through Whatman GF/F filters. Filters were dried at 60°C for 24 h, weighed, combusted at 450°C for 4 h and reweighed. The rock surface area was calculated by wrapping rocks with aluminium foil and using a weight-to-area relationship. Periphyton biomass was expressed as g AFDM/m^2.

2.4 Macroinvertebrates

Three benthic samples were collected using a Hess sampler (250-um mesh, 0.04 m^2 area) from each site on each visit and preserved with 70% ethanol. In the laboratory, macroinvertebrates from each sample were handpicked and identified to family level (Ephemeroptera, Plecoptera, Trichoptera, Diptera, Crustacea) or order level (Oligochaeta) and counted. Density and taxa richness were calculated for each sample.

2.5 Data analysis

The open-source program R 3.0.1 (R Development Core Team 2010) was used for all statistical analyses. All data were log(x+1) transformed to give a normal distribution (Sokal *et al,*. 1995). To evaluate temporal effects in the stretch, data were pooled by date. ANOVA was used to test for temporal differences between campaigns for each measured variable: SR, FPOM, periphyton, macroinvertebrate density and taxa richness. Tukey's HSD was used as a post-hoc test when differences were significant.

3   Results

3.1   Sediment respiration and FPOM

Sediment respiration differed between dates (ANOVA: $F_{(4,73)} = 5.08$, $p = 0.001$) (Figure 3). $R_{20°C}$ decreased from 1.7 to 1.2 mg O$_2$ (32% decrease) after SBT event 1 (June) and to 0.9 mg O$_2$ (47% decrease) after events 2 (July) and 3 (September) (Tukey's test, $p < 0.05$). About one month after event 3, $R_{20°C}$ increased to 1.4 mg O$_2$ (48% increase) and remained similar in November. Variability in respiration in this later period was higher compared to June (coefficients of variation (CVs) = 68% and 33%, respectively). FPOM did not differ among dates (ANOVA: $F_{(4,73)} = 2.03$, $p = 0.1$) and no correlation was found between FPOM and SR ($r^2 = 0.04$) (Figure 3).
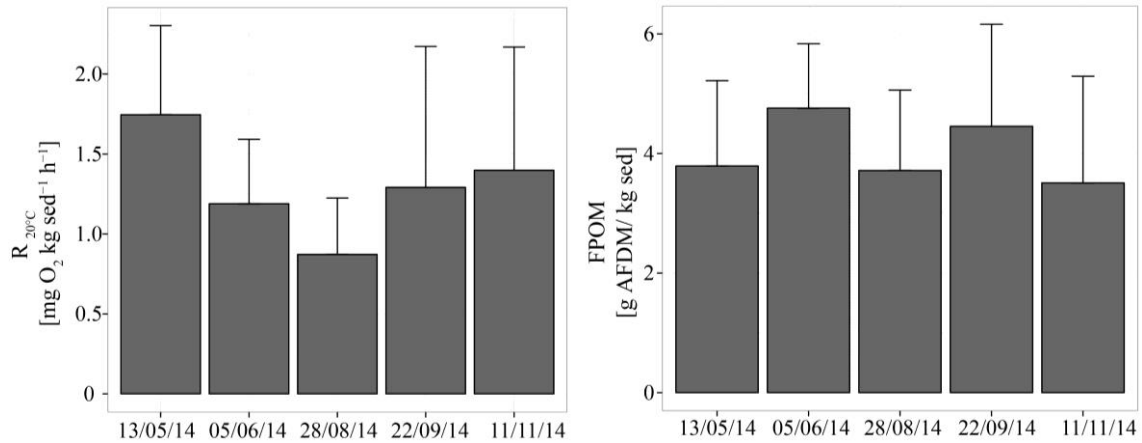
Figure 3: Mean sediment respiration at 20°C ($R_{20°C}$) and FPOM (mean ±1SD, n = 18 per date) using data from all sites per date

3.2 Periphyton

Periphyton showed a similar pattern as sediment respiration with biomass being different between dates (ANOVA: $F_{(4,125)}$ = 10.54, $p < 0.0001$). After the first event, periphyton biomass decreased 47% compared to the first date and decreased 83% after SBT events 2 and 3 (Tukey's test, $p < 0.05$). One month after event 3, biomass significantly increased by 300% (Tukey's test, $p < 0.05$) with another increase of 84% after 2 months (Tukey's test, $p < 0.05$). Variation was substantially higher in November than in September (CVs = 230% and 64%, respectively) (Figure 4).

Figure 4: Mean periphyton biomass (mean ±1SD, n = 30 per date) using all sites combined for each date

3.3 Macroinvertebrates

There were significant flood effects on macroinvertebrate density (ANOVA: $F_{(4,73)}$ = 33.39, $p < 0.0001$) and taxa richness (ANOVA: $F_{(4,73)}$ = 10.19, $p < 0.0001$) (Figure 5).

Macroinvertebrate density decreased from 4618 ind/m^2 in the first campaign to 1287 ind/m^2 after event 1, and decreased to 90 ind/m^2 after events 2 and 3 (Tukey's test, $p < 0.05$). One month after event 3, density increased again to 1786 ind/m^2 (Tukey's test, $p < 0.05$) and remained relatively stable after that. Taxa richness had a similar trend as density, except for a significant increase in taxa richness two months (November) after the last event (Tukey's test, $p < 0.05$) (Figure 5).

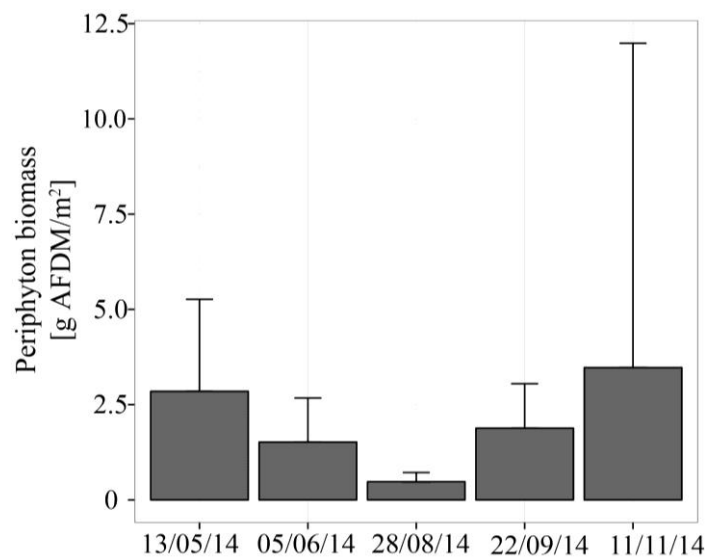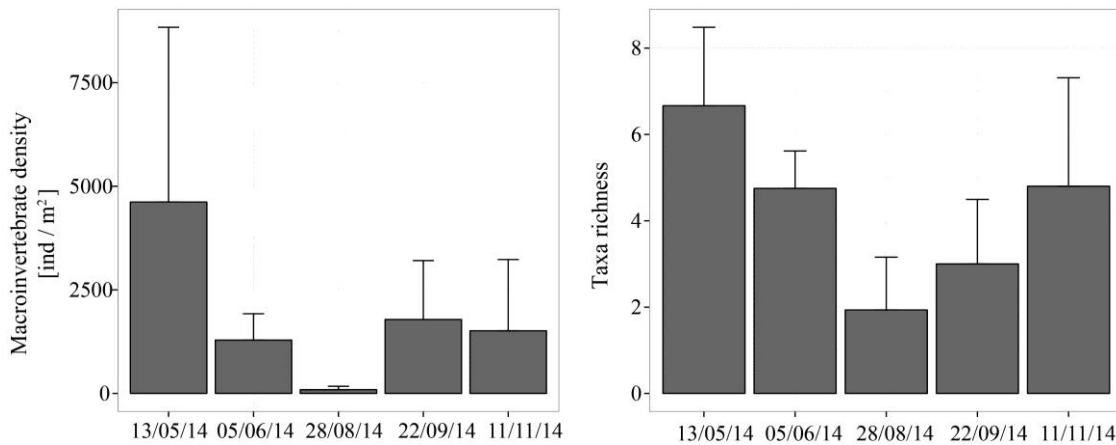Figure 5: Macroinvertebrate density and taxa richness (mean ±1SD; n = 18) using data from all sites per date

4   Discussion

The results suggest that Sediment Bypass Tunnel events affected the structure and function of the Albula River downstream of the dam. Sediment respiration, as an indicator of ecosystem function, was reduced after each event. Further, the decrease in respiration appeared to be related to event intensity. Apparently, water and sediments delivered by the SBT had enough force to mobilize or scour the top 30 cm (at least) of the river bed where the sediment samples were collected. Heterotrophic microbes (e.g., bacteria) were likely disturbed or scoured from bed sediments, thereby decreasing respiration rates after events. In addition, suspended sediments from SBT events may have been deposited during each event, thus decreasing respiration rates due to their low metabolic activity. The reduction in ecosystem respiration is likely a combination of these two factors.

According to Wei *et al.* (2008) and Aristi *et al.* (2014), spill waters from dams can be sources of dissolved and suspended particulate organic matter, which may enhance the concentration of organic matter in streambeds and increase respiration processes after SBT events. The lack of a clear pattern following SBT events in organic matter could indicate patchiness in the scouring and accumulation of (scoured/deposited) sediments due to the morphological heterogeneity of the channel. High CV values found in the last campaigns (September and November) in sediment respiration and FPOM suggest high

spatial heterogeneity in the study stretch in terms of the distribution and abundance of organic matter and in respect to erosion and deposition areas.

Periphyton biomass also was affected strongly by the SBT events, being reduced by 83% after the three SBT events. These results are similar to those found in previous studies by Uehlinger *et al.* (1998) and Robinson *et al.* (2004) in which periphyton was reduced following experimental floods. In this study, abrasion potential was likely high due to the high sediment load during an SBT event. Following SBT events, periphyton also showed rather quick recovery, although being quite variable due to site differences.

Macroinvertebrate density and taxa richness showed a clear reduction after the SBT events. Such a reduction in macroinvertebrate abundance to high flows has been shown in various systems (e.g., Lytle, 2000; Bruno *et al.,* 2009; Robinson *et al.,* 2012). Both medium and high SBT events decreased taxa richness and density due to the high discharge through the canyon (> 75 m^3 in all cases). Further, spill water releases from the dam at the beginning of November also appeared to decrease macroinvertebrate density, as November densities were lower than in October. Taxa richness, in contrast, showed a recovery in November with values close to pre-SBT event values. This recovery may indicate a rapid recolonization by individuals of different taxa that were not affected by a SBT event or by adult insect oviposition of eggs in the study section. The presence of tributaries in the study section can have a positive effect on macroinvertebrate recovery, as suggested by Robinson *et al.* (2003). Seasonality may also affect the recovery of macroinvertebrates and determine which organisms will recover more rapidly than others depending on when a SBT event happens.

In summary, high flows from SBT events seem to have enough power to modify habitat conditions along the study stretch, thereby affecting different key ecosystem variables such as sediment respiration, periphyton biomass and macroinvertebrate abundance and richness. Regardless of these short-term effects, the system seems to recover quite quickly, in a matter of weeks to months. SBT events could be used as experimental flows (Olden *et al.,* 2014), activating erosion and deposition processes that were lost due to regulatory actions of the dam. The potential high impact of SBT events, which are close to unusual high flow events (HQ100) and in frequency, likely have long-term implications on river ecosystems below SBTs. Further studies are needed to understand the long-term effects of SBT events on river/floodplain ecosystems.

Acknowledgements

References

Andrews, J. A. and Schlesinger, W. H., (2001). Soil CO_2 dynamics, acidification, and chemical weathering in a temperate forest with experimental CO_2 enrichment. *Global Biogeochemical Cycles*, 15: 149-162.

Aristi, I., Arroita, M., Larrañaga, A., Ponsatí, L., Sabater, S., von Schiller, D., Elosegi, A. and Acuña, V., (2014). Flow regulation by dams affects ecosystem metabolism in Mediterranean rivers. *Freshwater Biology*, 59: 1816-1829.

Battin, T. J., Kaplan , L. A., Newbold, J. D. and E. Hansen, C. M., (2003). Contributions of microbial biofilms to ecosystem processes in stream mesocosms. *Nature*, 426: 439-442.

Brandt, S. A., (2000). Classification of geomorphological effects downstream of dams. *CATENA*, 40: 375-401.

Bruno, M. C., Maiolini, B., Carolli, M. and Silveri, L., (2009). Impact of hydropeaking on hyporheic invertebrates in an Alpine stream (Trentino, Italy). *Annales de Limnologie - International Journal of Limnologie*, 45: 157-170.

Crosa, G., Castelli, E., Gentili, G. and Espa, P., (2010). Effects of suspended sediments from a reservoir flushing on fish and macroinvertebrates in an alpine stream. *Aquatic Sciences*, 72: 85-95.

Doering, M., Uehlinger, U., Ackermann, T., Woodtle, M. and Tockner, K., (2011). Spatiotemporal heterogeneity of soil and sediment respiration in a river-floodplain mosaic (Tagliamento, NE Italy). *Freshwater Biology*, 56: 1297-1311.

Lytle, D.A., (2000) Biotic and abiotic effects of flash floodings in a montane desert stream. *Archiv für Hydrologie,* 150: 85-100.

Naegeli, M. W. and Uehlinger, U., (1997). Contribution of the hyporheic zone to ecosystem metabolism in a prealpine gravel-bed river. *Journal of the North American Benthological Society*, 16: 794-804.

Niemi, G. J. and McDonald, M. E., (2004). Application of ecological indicators. *Annual Review of Ecology, Evolution, and Systematics*, 35: 89-111.

Nilsson, C., Reidy, C. A., Dynesius, M. and Revenga, C., (2005). Fragmentation and flow regulation of the world's large river systems. *Science*, 308: 405-408.

Olden, J. D., Konrad, C. P., Melis, T. S., Kennard, M. J., Freeman, M. C., Mims, M. C., Bray, E. N., Gido, K. B., Hemphill, N. P., Lytle, D. A., McMullen, L. E., Pyron, M., Robinson, C. T., Schmidt, J. C. and Williams, J. G., (2014). Are large-scale flow experiments informing the science and management of freshwater ecosystems? *Frontiers in Ecology and the Environment*, 12: 176-185.

R Development Core Team, (2010). *R Foundation for Statistical Computing*. Retrieved from htpp://www.R-project.org, Vienna, Austria.

Rabení, C. F., Doisy, K. and Zweig, L. D., (2005). Stream invertebrate community functional responses to deposited sediment. *Aquatic Sciences*, 67: 395-402.

Robinson, C. T. and Doering, M., (2012). Spatial patterns in macroinvertebrate assemblages in surface-flowing waters of a glacially-influenced floodplain. *Aquatic Sciences*, 75: 373-384.

Robinson, C. T., Uehlinger, U. and Monaghan, M. T., (2003). Effects of a multi-year experimental flood regime on macroinvertebrates downstream of a reservoir. *Aquatic Sciences*, 65: 210-222.

Robinson, C. T., Uehlinger, U. and Monaghan, M. T., (2004). Stream ecosystem response to multiple experimental floods from a reservoir. *River Research and Applications*, 20: 359-377.

Sokal, R. R. and Rohlf, F. J.,(1995). *Biometry: the principles and practice of statistics in biological research*. Freeman, New York, 3rd Edition.

Uehlinger, U. and Naegeli, M. W., (1998). Ecosystem metabolism, disturbance, and stability in a prealpine gravel bed river. *Journal of the North American Benthological Society*, 17: 165-178.

Uehlinger, U., Naegeli, M. W. and Fisher, S. G., (2002). A heterotrophic desert stream? The role of sediment stability. *Western North American Naturalist*, 62: 466-473.

Uehlinger, U., Robinson, C. T., Hieber, M. and Zah, R., (2010). The physico-chemical habitat template for periphyton in alpine glacial streams under a changing climate. *Hydrobiologia*, 657 107-121.

Sumi, T., Okano, M. and Takata, Y. (2004). *Reservoir sedimentation management with bypass tunnels in Japan*. 9th International Symposium on River Sedimentation, Yichang.

Wei, Q., Feng, C., Wang, D., Shi, B., Zhang, L., Wei, Q. and Tang, H., (2008). Seasonal variations of chemical and physical characteristics of dissolved organic matter and trihalomethane precursors in a reservoir: a case study. *Journal of Hazardous Materials*, 150: 257-264.

Williams, G. P. and Wolman, M. G.,(1984). *Downstream effects of dams on alluvial rivers*. Geological Survey Professional Paper 1286, U.S. Government Printing Office, Washington, DC.

Yarnell, S. M., Mount, J. F. and Larsen, E. W., (2006). The influence of relative sediment supply on riverine habitat heterogeneity. *Geomorphology*, 80: 310-324.

Authors

Eduardo J. Martín (corresponding Author)
EAWAG, Swiss Federal Institute of Aquatic Science and Technology
8600 Dübendorf, Switzerland.
Email: eduardo.martin@eawag.ch

Michael Doering
ZHAW, Zurich University of Applied Sciences
Grüental
8820 Wädenswil, Switzerland.

Christopher T. Robinson
EAWAG, Swiss Federal Institute of Aquatic Science and Technology
8600 Dübendorf, Switzerland

Current sedimentation research at VAW

Ismail Albayrak, Robert M. Boes

Abstract

This paper gives an overview on research projects related to reservoir sedimentation and engineering problems resulting from significant sediment load at hydropower plants (HPPs) conducted at the Laboratory of Hydraulics, Hydrology and Glaciology (VAW) of ETH Zurich. Research methods and approaches applied in the projects are also presented. Improving performance and efficiency of hydropower and reducing its negative effects on the ecosystem are key targets of the Swiss energy strategy 2050 and of the revised Swiss Water Protection Act, respectively. The overarching goal of a sustainable and flexible operation of HPPs and storage reservoirs leads to a number of challenges and research topics. Among them, reservoir sedimentation, handling of increased sediment yield, hydro-abrasion at turbines and Sediment Bypass Tunnels (SBT), and the potential for future development of HPP are of prime importance, particularly considering the strong impact of climate change. At VAW, we conduct investigations on these topics to provide expert solutions in a holistic and interdisciplinary approach including numerical and physical modellings and field data collection.

Zusammenfassung

Dieser Artikel gibt einen Überblick zu Forschungsprojekten der Versuchsanstalt für Wasserbau, Hydrologie und Glaziologie (VAW) der ETH Zürich im Zusammenhang mit Speicherverlandung und der Sedimentproblematik an Wasserkraftwerken. Die dabei verwendeten Forschungsmethoden werden ebenfalls beschrieben. Wesentliche Ziele der Schweizerischen Energiestrategie 2050 bzw. des revidierten Gewässerschutzgesetzes sind die Effizienzsteigerung bzw. die Sanierung der negativen Auswirkungen der Wasserkraft. Das übergeordnete Ziel einer nachhaltigen und flexiblen Betriebsweise von Wasserkraftanlagen und Speicherseen bietet Platz für herausfordernde Forschungsthemen. Dazu zählen vor allem die Speicherverlandung, der Umgang mit zunehmenden Sedimentfrachten, Hydroabrasion an Turbinen und Sedimentumleitstollen und das zukünftig verfügbare Wasserkraftpotential, nicht zuletzt infolge des Klimawandels. An der VAW werden Untersuchungen zu diesen Themen durchgeführt, um mit ganzheitlichen und interdisziplinären Ansätzen Expertenlösungen zu entwickeln unter Verwendung von numerischen und wasserbaulichen Modellen sowie Felddatenerhebungen.

1 Introduction

VAW as one of the leading international research and consulting institute in hydraulic engineering and glaciology provides exceptional facilities and instrumentation for large-scale laboratory and field researches. The research foci are depicted in Figure 1. The typical research methods applied are physical and numerical models and a combination of both, which is also termed 'hybrid' or 'composite' modelling. Moreover, field and prototype investigations are regularly conducted to collect data on the 1:1 scale as a basis for the calibration and validation of numerical models. Hybrid modelling allows to draw even more precise conclusions and to optimize the model results compared to mere physical or numerical modelling.
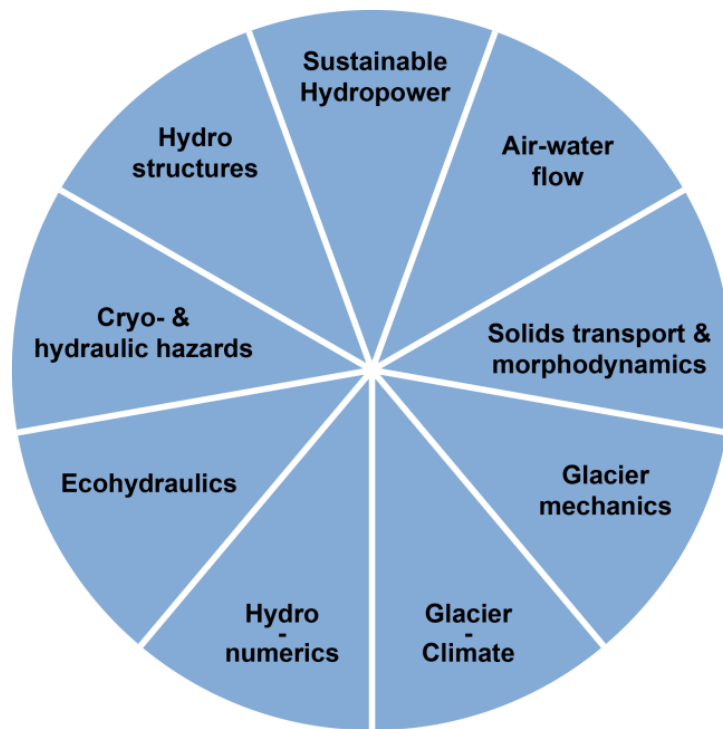
Figure 1: Research foci at VAW

Current research topics in relation to sedimentation include:

- Potential for future hydropower plants in Switzerland: A systematic analysis in the periglacial environment (PHP)

- Sediment transport in super-critical open-channel flow

- Adequate sediment handling at high-head hydropower plants to increase scheme efficiency

- Sediment-induced hydroabrasion at hydraulic structures (e.g. SBT, spillways, stilling basins) and at turbines

- Design and ecological effects of SBTs

2 Current research on sedimentation

2.1 Efficiency increase and flexible usage of hydropower

Better efficiency and increased availability of hydropower are reasonable options to reduce greenhouse gas emissions. An important approach is to invest in improving performance and capacity of hydropower through innovation as well as to abate negative effects of HPP operation on the ecosystem. This leads to a number of challenges tackled in the frame of research topics. Increasing reservoir sedimentation in glacierized areas due to strong impact of climate change is one of the alarming challenges for the hydropower industry. Nevertheless, glacier retreat also offers opportunities to the industry such as potential for future development of HPPs. In the following, the research project on these two topics at VAW is presented.

2.2 Impact of climate change on present and potential future hydropower exploitation in glacierized basins

Glaciers are an important source of water in Switzerland. There is still some 2.3% of the Swiss territory covered by glaciers (940 km^2). Glacier retreat caused by global warming affects many sectors that depend on glacier melt water, like hydropower, fresh water supply, irrigation and tourism. Particularly, the Alpine hydropower industry is concerned by the impacts of climate change. The fact that many basins exploited for hydropower production are partly glacierized and that glacier retreat is accelerating in the last decades contributes to these concerns. Glaciers are known to produce prodigious quantities of sediment ranging from large boulders to fine silt. For the Alps the sediment yields from glacierized basins range from 50 to 7'000 m³/km²/a (Bogen 1989; Hinderer *et al.* 2013). For Swiss glacierized catchments recent sediment discharges up to 400'000 m³/a were reported (Boes and Hagmann 2015)

These data clearly show that the rate of sediment production has recently increased in these glacierized catchments. There is an urgent need for an improved understanding of sediment yield and transport dynamics in connection with ongoing changes in the alpine environment. For improved future runoff projections, glacier evolution under climate change and its consequences on the hydrology and sediment production needs to be experimentally and numerically investigated. This requires an improved data base of the present ice volume and the bed topography of the Swiss glaciers. Also for planning of future potential HP production sites (e.g. new natural lakes due to glacier retreat and potential new reservoirs) and for mitigation measures to reduce the sediment transport due to deglaciation and consequent increased debris availability the aforementioned data base is mandatory.

The Swiss National Science Foundation (SNSF) launched two National Research Programmes (NRPs) to explore scientific and technological as well as social and economic aspects of Swiss Energy Strategy 2050. The 'Energy Turnaround' (NRP 70)

as one of two programmes will generate scientific and technological knowledge which can sustainably contribute to a successful realization of this strategy. VAW participates to this program with three doctoral research projects presented below (see also section 2.4).

Hydraulic structures, applied numerics and glaciology divisions of VAW initiated an interdisciplinary research project to address the above-mentioned challenges hydropower industry faces now and in the future. The present project aims at (1) exploring new potential sites for HPPs in the periglacial environment (PGE) and (2) improving knowledge of sediment yield, transport and reservoir sedimentation at the scale of single glacierized catchments.

A large body of literature exists on reservoir sedimentation and particularly the book of Morris & Fan (2010) gives an excellent overview. The concept of reservoir sediment trap efficiency, E, applies in a simple hydrological approach for reservoir sedimentation. E is the ratio of the deposited sediment to the total sediment inflow. Churchill (1948) and Brune (1953) developed two different empirical formulae to estimate E. Empirical formulae can deliver a first estimation of reservoir sedimentation in a quick way, being affected with large uncertainties, however. Prediction of delta formation and non-uniform sedimentation along the reservoir, and effects of changing reservoir operating rules, for example, involve a detailed analysis of fluid-sediment interactions in the reservoir. This is typically performed with physical or numerical models. The main disadvantages of physical modelling are (I) high cost, (II) long time periods required to run extended simulations, (III) immobility and (IV) scaling problem of cohesive sediment behavior (Morris & Fan 2010). However, physical modelling may be necessary where the flow fields are too complex for mathematical modelling and for analysis of bed topography. From an economic point of view, numerical modelling of reservoir sedimentation is favored over physical modelling provided that all relevant processes are adequately simulated.

Considering pros and cons of both modeling techniques, in this project we aim at developing a numerical model for the simulation of reservoir sedimentation considering river morphodynamics, delta formation and turbidity currents in the PGE. The model will be able to model sediment transport as suspended and bed loads for mixed size sediments on arbitrary topography for varying boundary conditions, e.g. during floods and for normal reservoir operation. The modelling software BASEMENT developed at VAW will be extended to simulate turbidity currents by an appropriate approach. In a first step, the capabilities and performance of the new model will be tested for sedimentation of a simple rectangular reservoir at varying boundary conditions. Based on the corresponding results, the model will be optimized if necessary.

In addition to numerical modelling, field campaigns for selected proglacial lakes and reservoirs will be carried out to obtain suspended sediment concentration (SCC),

160

sediment properties, e.g. hardness (abrasive capacity), particle size distribution (PSD) and flow velocity data. These data will be later used to calibrate and validate the model.

Finally, the model will be used to simulate HPP operation and reservoir sedimentation over decades for existing reservoir and new potential sites and to estimate the reservoir service life. Additionally, the results from the model will be compared with empirical estimates and further improvement of existing equations or a new equation will be proposed. Depending on the reservoir service life and the abrasive capacity of glaciers, different sediment management concepts (e.g. periodic flushing or venting) will be proposed and implemented in the numerical model.

2.3 Sediment bypass tunnels as countermeasure against reservoir sedimentation

The following list shows various severe problems caused by sedimentation:

I. decrease of the active reservoir volume leading to less available water for energy production, drinking water supply and irrigation
II. reduction of retention volume during floods
III. endangerment of operating safety due to blockage of the outlet structures
IV. increased abrasion at hydraulic structures
V. negative impact on the downstream river morphology and ecology, e.g. river bed incision
VI. increased turbine abrasion due to increased suspended load concentrations

If no countermeasures are considered, then reservoir sedimentation will progress and the above mentioned problems will intensify (Auel & Boes 2011). Annandale (1987) and Sumi *et al.* (2004) reviewed in-depth a variety of countermeasures to minimize aggradation in reservoirs. Hereafter, we focus on SBTs, which is one of the effective measure against reservoir sedimentation, mainly for small- to medium-sized reservoirs in terms of their capacity-inflow ratio (CIR), i.e. the ratio of reservoir volume to the mean annual inflow volume.

At VAW, a holistic and interdisciplinary approach has been applied to mitigate sedimentation causing most of the above listed problems (I-V) at the Solis reservoir in the Swiss Alps (canton of Grisons) operated by the Electric Power Company of Zurich (ewz).

The Solis reservoir has been filled up by half of its original reservoir volume due to high sediment input from upstream torrents since its commissioning in 1986, thereby having negatively impacted power production and economic lifespan. Based on a feasibility study ewz selected the SBT solution and mandated VAW to perform physical hydraulic model tests of the planned Solis SBT. Model tests and optimization of design were carried out in a small-scale hydraulic model with a scaling factor of 45 in 2010 (Figure

2). A comprehensive overview of the hydraulic model tests is given by Auel *et al.* (2011). The Solis SBT was commissioned in 2012.
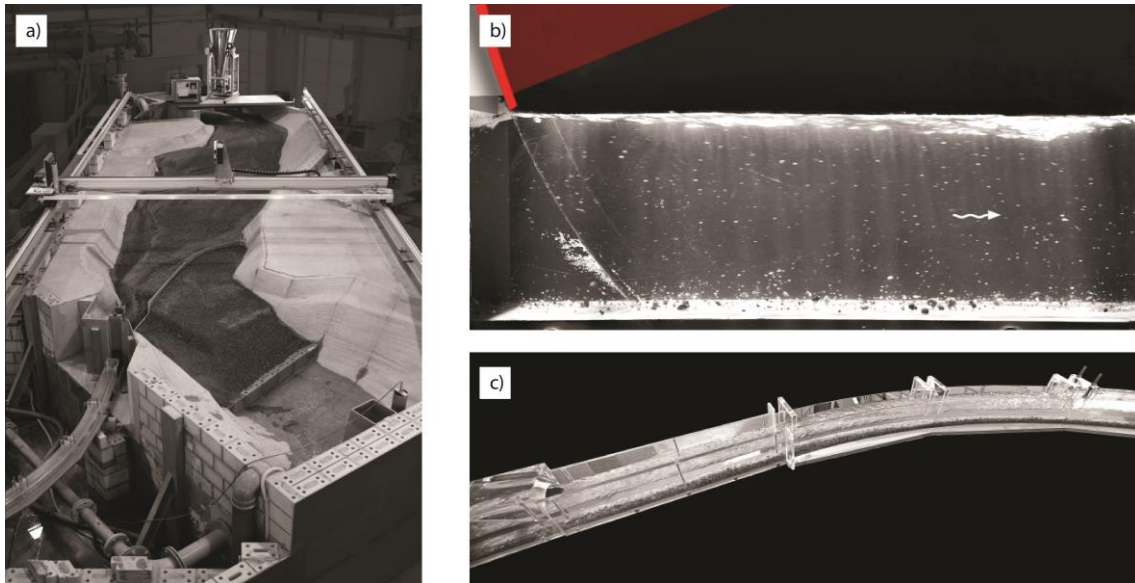

Figure 2: Hydraulic model overview (a), free surface flow behind the tainter gate (b) and sediment transport in the SBT (c) (courtesy of VAW)

Although SBTs are an effective measure against reservoir sedimentation, they are subjected to strong abrasion problem due to both high flow velocities and sediment transport rates causing considerable annual maintenance expenses in the range of 1% of the investment costs (Auel 2014). In order to enhance the cost-effectiveness of SBTs suitable abrasive-resistant invert materials are indispensable. Knowing this fact, VAW in collaboration with ewz initiated a field research study to address hydro-abrasion problems at SBTs and other hydraulic structures by testing various invert materials, their durability and economy (Hagmann *et al.* 2012, 2014 & 2015). At the construction stage of Solis SBT, six test fields with different abrasion-resistant materials, i.e. four concretes of different compressive strengths and mixtures, basalt and steel plates were implemented (Hagmann *et al.* 2012). Together with the high performance concrete invert of Solis SBT, a total of seven different invert materials is being tested. This investigation includes continuous and real-time monitoring of suspended sediment (SS) and bed load in the SBT together with discharge measurements and additionally monitoring of SSC in the upstream and downstream reaches of the reservoir.

In addition to the Solis SBT, *in-situ* experiments are also conducted in the Pfaffensprung and Runcahez SBTs to enlarge the data base with additional invert material tests and different sediment mineralogy. Furthermore, our collaboration is extended with participation of the Institute of Construction Materials (IfB) of TU Dresden. This collaboration enables us to test specimens of the invert materials from the Solis and Pfaffensprung SBTs under laboratory conditions and compare them with their

162

in-situ performance (Bellmann 2012, Bellmann & Mechtcherine 2012;). The outcome of this comparison will allow checking the transferability of simplified laboratory results to the field scale.

In parallel to this field investigation, VAW has conducted another research on the same topic by means of hydraulic laboratory investigation to advance understanding of the fundamental physical processes present in SBTs (Auel 2014). In this project small and large scale turbulence structures of 2D and 3D high speed flows, the particle motion on fixed beds, and the abrasion development in space and time caused by transported sediment has been investigated in a hydraulic flume (Figure 3). The experiments were conducted under varying geometrical and hydraulic conditions for a range of sediment properties and invert lining materials. Densely spaced velocity measurements were carried out using 2D- Laser Doppler Anemometer (LDA). The project mainly focused on the development of an abrasion model and of design criteria for SBTs to mitigate negative effects of abrasion (Auel 2014 and Auel *et al.* 2015).

These two parallel projects, i.e. field and laboratory studies, complement each other. The findings from both projects will help (I) to develop an abrasion model to forecast hydroabrasion of the tunnel invert, (II) to optimize both the channel hydraulics and the tunnel invert materials to minimize hydroabrasion as well as their implementation.
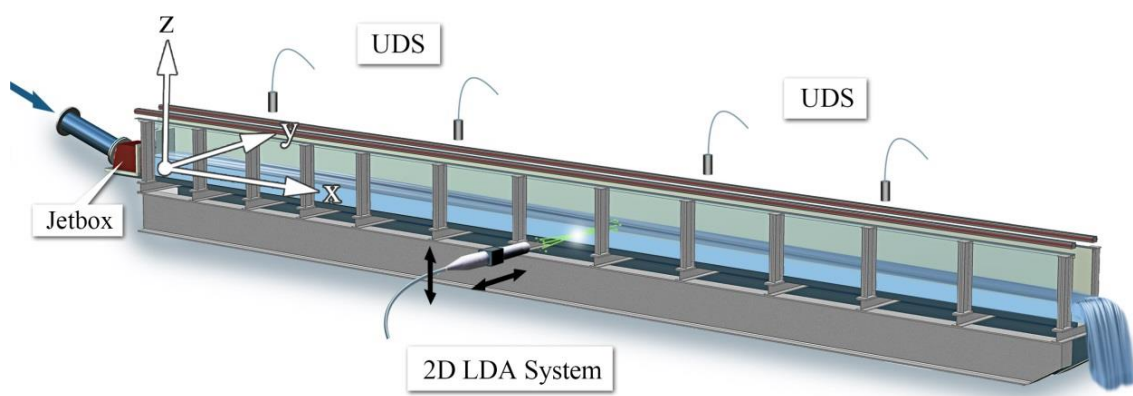
Figure 3: Hydraulic model flume for SBT investigation (Auel 2014)

VAW has moved the research on SBTs a step further by initiating another research project entitled 'Re-establishment of the sediment continuum at an alpine reservoir – influence on river morphology, ecology and flood prevention' (Facchini *et al.* 2015). This research seeks answers to the following research questions by means of numerical and field investigations at the river reach downstream of Solis SBT: (I) How does a SBT affect sediment dynamics and morphology in the downstream reach of a dam? (II) What are the time and spatial scales over which the sediments propagate? (III) Can the development of the new morphology be predicted? (IV) How does extra sediment load from the SBT improve ecological conditions of the downstream reach? (V) Can this improvement be managed by controlled flushing releases through the SBT?

The research includes monitoring activities, which will provide details on morphological changes and serve as a basis for the development of mathematical modelling aiming to predict future morphological changes and possible ecological effects, assessing different water and sediment release scenarios.

2.4   Sediment transport and turbine wear monitoring program

Hydro-abrasive wear at turbines (Figure 4) or other hydraulic parts due to hard suspended mineral particles, e.g. quartz, in the water or due to reservoir siltation may cause substantial maintenance costs and significant negative impact on power generation and revenue at HPPs. For optimized design and operation of hydraulic structures as well as for environmental concerns, there is an increasing need for continuous monitoring of SSC and PSD in rivers and lakes These data can be used as a basis for economically optimized operation in which actual wear of hydraulic turbines is mitigated with the option of temporary switch-offs of HPPs during suspended sediment peaks.

The turbine abrasion problem has been experimentally investigated with an interdisciplinary approach in the scope of doctoral research project entitled 'Effects of suspended sediment on Pelton turbine wear and efficiency'. This project aims at a continuous and real-time monitoring of SSC and PSD and at the quantification of turbine abrasion and resulting efficiency loss at the Fieschertal HPP in the canton of Valais, Switzerland. In this project, VAW has gained a broad experience on sediment monitoring systems by testing the latest technology instruments both in the laboratory and in the field. Felix *et al.* (2013a) reported the measuring capabilities of various turbidimeters, a portable laser diffractometer (LISST) and an ultrasonic system by testing in suspensions made of quartz fine sand, feldspar and mica powders in a mixing tank. These particles are mainly found in the turbine water of the studied HPP. The *LISST* has the advantage to provide not only SSC, but also PSD data, so that SSC results are less affected by the varying size of suspended particles, as was confirmed by field experiments (Felix *et. al*. 2013b, 2013c).
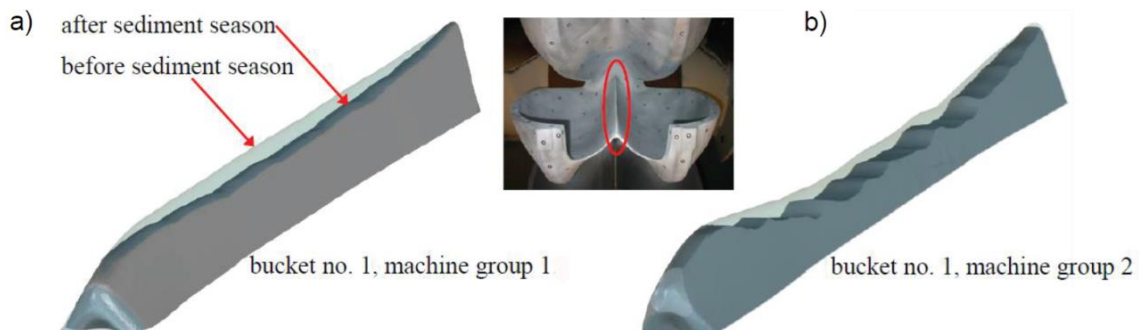

Figure 4: 3D views of the digitized main splitters (red ellipse): Comparison between the splitter geometries before (transparent) and after the sediment season (grey) of buckets no. 1 of machine groups 1 and 2 (Abgottspon *et al.* 2014)

2.4 Design improvement of desilting facilities to increase scheme efficiency

Similar to the project described in section 2.3, the present project deals with the mitigation of hydroabrasion at turbines and steel hydraulic parts by focusing on design improvement of desilting facilities at HPPs (Figure 5). It is a part of the above-mentioned NRP 70 'Energy turnaround'.

Hydro-abrasive wear at turbines and steel hydraulics parts is directly related to the efficiency of desilting facilities (less efficiency, more sediment transport to turbines and hence more abrasion), representing a key factor for sustainable and improved HPP operation under severe sediment conditions such as in Alpine regions. Operational experience indicates that desilting facilities are often not working properly.

The project goal is to provide an improved hydraulic design guideline for desilting facilities at HPPs with an emphasis on the effects of different headwork arrangements such as intake type or the use of tranquilizing rakes. To achieve this goal, numerical and field experimental approaches are chosen as an efficient approach, since physical modeling of sediment particles in the silt range is strongly affected by scale effects and a systematic investigation of all parameters would be time-consuming and costly. These approaches will allow to systematically investigate the effect of the approach flow conditions on the behavior of particle settling and the trap efficiency of desilting basins. The outputs of this investigation will help to advance in the understanding of flow-sediment interactions in desilting basins under field conditions, and to provide a numerical tool to simulate and optimize desilting facilities to increase the overall scheme efficiency.
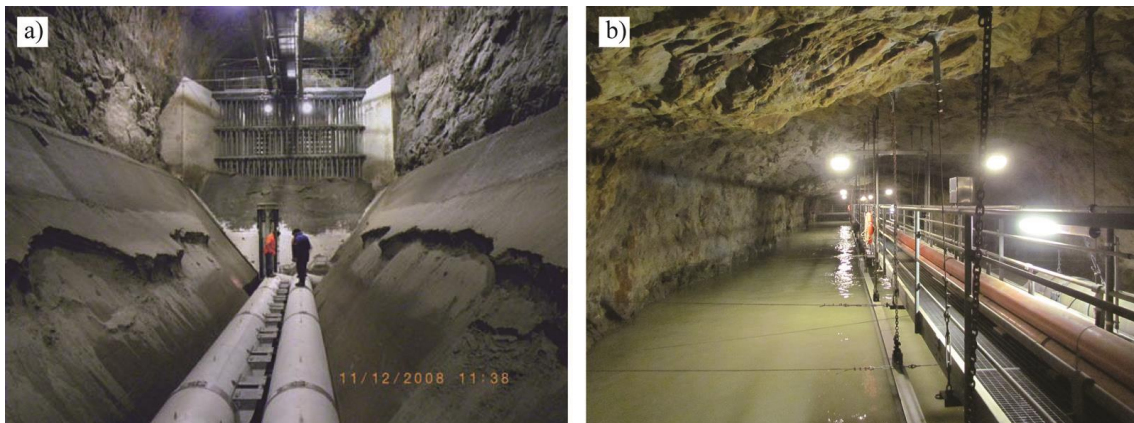

Figure 5: Desilting facility of Fieschertal HPP after sediment flushing (a) (Truffer *et al.* 2009) and in operation (b) (courtesy of VAW)

3   Conclusions

This paper gives an overview on research projects related to reservoir sedimentation and engineering problems resulting from significant sediment load at HPPs carried out at

VAW of ETH Zurich, and on research methods and approaches applied in these projects.

Increasing reservoir sedimentation under the strong impact of climate change is one of the challenges. To address this problem, the hydraulic structures, applied numerics and glaciology divisions of VAW have teamed up in the framework of NRP 70 'Energy Turnaround'. In the scope of two doctoral research projects, past, present and future run-off, and sediment discharge in glacierized catchments of the Swiss Alps, their abrasion capacity, reservoir sedimentation and countermeasures, and exploitation of potential for future HPP development are investigated by means of field experimental campaign and numerical simulation.

The on-going and one completed projects on SBTs at VAW present a holistic approach (section 2.2) for a sustainable use of present and future SBTs. Moreover, this approach will give insight into better understanding of (I) supercritical flow, (II) particle motion, (III) mechanism of hydroabrasion, (IV) abrasion resistance of invert materials, (V) design of SBTs and (VI) ecological effect of SBTs; and also create a data base for numerical models. In these projects, physical and numerical modelling methods are used. The data are collected from laboratory and field experiments. The outputs of the projects are innovative and will contribute to better sedimentation management via SBTs without compromising environmental impacts.

Turbine abrasion at high- and medium-head HPPs and countermeasures are investigated in another two doctoral research projects. While the first project investigating continuous and real-time monitoring of sediment loads, turbine efficiency and abrasion will allow to develop predictive models for hydro-abrasive wear, and optimizing the operation of high-pressure water turbines, the second project (NRP 70) deals with the topic of desilting facilities for design and efficiency improvements using a numerical tool. Both projects will provide innovative solutions for optimized design and operation of HPPs.

4   Acknowledgements

5   References

Abgottspon, A., Staubli, T., Felix D., Albayrak, I., Boes, R.M. (2014). Monitoring Suspended Sediment and Turbine Efficiency. *Hydro Review Worldwide*, 22(4): 28-36.

Annandale, G.W. (1987). *Reservoir sedimentation*. Developments in Water Science 29. Elsevier Science Publishers B.V., Amsterdam, The Netherlands.

Auel, C., Albayrak, I., Sumi, T., Boes, R.M. (2015). Saltation-abrasion model for hydraulic structures. Proc. First Intl. Workshop on Sediment Bypass Tunnels, *VAW-Mitteilungen* 232 (R.M. Boes, ed), ETH Zürich, Switzerland: in press.

Auel, C. (2014). Flow characteristics, particle motion and invert abrasion in sediment bypass tunnels. PhD Thesis 22008, also published as *VAW-Mitteilungen* 229 (R.M. Boes, ed.), ETH Zurich, Switzerland.

Auel, C., Boes, R.M. (2011): Sediment bypass tunnel design – review and outlook. *Proc. ICOLD Symposium „Dams under changing challenges"* (A.J. Schleiss & R.M. Boes, eds.), 79th Annual Meeting, Lucerne. Taylor & Francis, London, UK, 403-412.

Auel, C., Boes, R., Ziegler, T., Oertli, C. (2011). Design and construction of the sediment bypass tunnel at Solis. *Hydropower and Dams*, 18(3), 62–66.

Bellmann, C. (2012). Deterioration of concrete subjected to hydro-abrasion. *Proc. 9th International PhD Symposium in Civil Engineering*, Karlsruhe Institute of Technology (KIT), Germany.

Bellmann, C., Mechtcherine, V. (2012). Experimental investigation into the deterioration of ordinary concrete subjected to hydro-abrasion. *Proc. MicroDurability Amsterdam*, Netherland. Rilem Proceedings PRO83.

Bogen, J. (1989). Glacial sediment production and development of hydro-electric power in glacierized areas. *Ann. Glaciol.*, 13: 6–11.

Boes, R.M. & Hagmann, M. (2015). Sedimentation countermeasures – examples from Switzerland. Proc. First Intl. Workshop on Sediment Bypass Tunnels, *VAW-Mitteilung* 232 (R.M. Boes, ed.), ETH Zürich, Switzerland, 193-210.

Brune, G.M. (1953). Trap efficiency of reservoirs. *Trans. Am. Geophys. Union* 34(3): 407-418.

Churchill, M.A. (1948). Discussion of "Analysis and use of reservoir sedimentation data," by L.C. Gottschalk, *Proc. Federal lnteragency Sedimentation Conf.*, Denver, USA, 139-140.

Facchini, M., Siviglia, A., Boes, R.M. (2015). Downstream morphological impact of a sediment bypass tunnel – preliminary results and forthcoming actions. Proc. First Intl. Workshop on Sediment Bypass Tunnels, *VAW-Mitteilungen* 232 (R.M. Boes, ed), ETH Zürich, Switzerland: in press.

Felix, D., Albayrak, I., Boes, R.M. (2013a). Monitoring of Suspended Sediment – Laboratory Tests and Case Study in the Swiss Alps. *Advances in River Sediment Research*, (Fukuoka S., Nakagawa H., Sumi T., Zhang H., eds), Taylor & Francis, London: 1757-1766.

Felix, D., Albayrak, I., Boes, R.M., Abgottspon, A., Deschwanden, F., Gruber, P. (2013b). Measuring Suspended Sediment: Results of the first Year of the Case Study at HPP Fieschertal in the Swiss Alps. *Proc. Hydro 2013 Conference*, Innsbruck, Austria: paper 18.03.

Felix, D., Albayrak, I., Boes, R.M. (2013c). Laboratory investigation on measuring suspended sediment by portable laser diffractometer (LISST) focusing on particle shape. *Geo-marine Letters*, 33(6): 485-498.

Hagmann, M., Albayrak, I., Boes, R.M. (2015). Field research: Invert material resistance and sediment transport measurements. Proc. First Intl. Workshop on Sediment Bypass Tunnels, *VAW-Mitteilungen* 232 (R.M. Boes, ed), ETH Zürich, Switzerland: in press.

Hagmann, M., Albayrak, I., Boes, R.M. (2014). Untersuchung verschleissfester Materialien im Wasserbau mit in-situ-Geschiebetransportmessung ('Investigation on wear-resistant materials at hydraulic structures: in-situ measurements of sediment transport and invert abrasion'). Proc. Symposium „Wasserbau und Flussbau im Alpenraum", *VAW-Mitteilungen* 227 (R. Boes, ed.), ETH Zürich, Switzerland, 97-106.

Hagmann, M., Albayrak, I., Boes, R.M. (2012). Reduktion der Hydroabrasion bei Sedimentumleitstollen - In-situ-Verusche zur Optimierung der Abrasionsresistenz ('Reduction of hydroabrasion at sediment bypass tunnels - In-situ experiments to optimize the abrasion resistance'). *Proc. Wasserbausymposium "Wasser - Energie, global denken - lokal handeln",* (G. Zenz, ed.), TU Graz. 91-97.

Hinderer, M., Kastowski, M., Kamelger, A., Bartolini, C., Schlunegger, F. (2013). River loads and modern denudation of the Alps: A review. *Earth-Sci. Rev.*, 118: 11–44.

Morris, G.L., Fan, J. (2010). Reservoir sedimentation handbook: Design and management of dams, reservoirs, and watersheds for sustainable use. McGraw-Hill, New York.

Sumi, T., Okano, M., Takata, Y. (2004). Reservoir sedimentation management with bypass tunnels in Japan. *Proc. 9th International Sympo*sium on River Sedimentation, Yichang, China, 1036–1043.

Truffer, B., Küttel, M., Meier J. (2009). Wasserfassung Titer der GKW –Entsanderabzüge System HSR in grossen Entsanderanlagen ('Intake Titer of GKW – Sand removal system HSR for large desilting facilities'). *Wasser Energie Luft* 101(3): 207-208.

Authors

Ismail Albayrak (corresponding Author)
Email: albayrak@vaw.baug.ethz.ch.
Prof. Dr. R.M. Boes
Laboratory of Hydraulics, Hydrology and Glaciology (VAW), ETH Zurich

Laboratory research: Bed load guidance into sediment bypass tunnel inlet

Giovanni De Cesare, Pedro Manso, Milad Daneshvari, Anton J. Schleiss

Abstract

Sediment management in reservoirs situated in mountainous regions is a critical operational concern with direct implications in live storage sustainability and therefore in production revenues. The paper presents the main results of a physical model study of a sediment evacuation system foreseen for a large hydropower scheme in Ecuador, carried out at the Laboratory of Hydraulic Constructions (LCH) of the Ecole Polytechnique Fédérale de Lausanne (EPFL). The system comprises a sediment bypass tunnel (SBT) and a submerged weir nearby the gated tunnel inlet, conceived mainly to bypass bed load sediments. Four operation modes were identified and documented. The final sediment bypass efficiency is almost 100% for frequent floods under upstream drawdown, reducing to 20% for larger flood events above the capacity limit of the bypass tunnel. The tests resulted in an improved configuration of the system in all operational modes, including reverse flushing. Guidelines for prototype operation were proposed to consider, among others, the sequential combination of high and low reservoir levels and different gate openings, during and after floods events, in order to improve the overall sediment bypass efficiency.

Zusammenfassung

Das Management der Stauseeverlandung im Berggebiet ist von grosser Bedeutung, es hat direkten Einfluss auf das Nutzvolumen, den nachhaltigen Betrieb und somit auf den wirtschaftlichen Ertrag. Es werden die wichtigsten Resultate einer physikalischen Modellstudie aufgezeigt, bei welcher der Eingangsbereich eines Sedimentumleitstollens einer grossen Wasserkraftanlage mit Stausee nachgebildet und dessen Effizienz getestet wurde. Die Versuche wurden am Laboratoire de Constructions Hydrauliques (LCH) der Ecole Polytechnique Fédérale de Lausanne (EPFL) durchgeführt. Vier Betriebsarten können identifiziert und dokumentiert werden. Die am Schluss erhaltene Sediment Bypass Effizienz erreicht beinahe 100% für häufige Hochwasser dank Absenkung im Oberwasser, dieser Wert reduziert sich auf 20% bei Abflüssen im Bereich der Kapazität des Sedimentumleitstollens. Die Versuche führten zu einer optimalen Auslegung der Anlage für allen Betriebsarten, inklusive der Umkehrspülung. Es konnten Richtlinien für den effizienten Prototypbetrieb erarbeitet werden, welche unter anderem den

variablen Seestand und verschiedene Schützenöffnungen während und nach einem Hochwasserereignis berücksichtigen.

1 Introduction

Maintaining the operational live storage of hydroelectric reservoirs in high sediment-yield river catchments is a challenge for operators wishing to guarantee yearly energy production, revenues and debt reimbursement. Failing to convey downstream part of the sediment inflow may lead to progressive aggradation of the reservoir bathymetry, increased sediment loading on dams and increased entrainment of sediment in hydraulic structures such as power intakes and clogged bottom outlets. Equipment wear and damage increase the operational expenditures and the risk of production stoppage and loss of revenues. Therefore, active management of sediment bed load inflows has become common practice in some alpine catchments and power schemes, namely for storage dams with short reservoirs and large annual drawdown ranges, as well as for low-head dams with shallow reservoirs.

Some experiences have been gained in terms of bed load transit from upstream to downstream by carrying out regular flushing operations through the bottom outlets (typically for dams higher than 15 m) and through the spillway gates (for low-head dams). Operations without lowering the reservoir level have local impact, whilst operations with reservoir drawdown may allow for larger sediment outflows. The former is done with small operational impact whereas the later implies stopping production for at least some days. The sediment concentration flowing downstream must respect environmental constraints and regular purging operations must be scheduled with and authorized by the public authorities. However, purging operations are not only cumbersome and costly, but also often not concomitant with natural floods and therefore not reproducing the original river regime. The present legal framework in Switzerland requires the partial reestablishment of bed load transit as part of a policy to maintain riverbed morphology and ecology. Therefore, the present challenge is to develop sediment transit concepts that not only extend the lifetime of reservoirs at minimum cost but also contribute to the reestablishment of the morphological diversity downstream. One solution is the construction of sediment bypass tunnels (Vischer et al. 1997, Morris 1997). However, most developments answer specific project needs as no general design rules or operational guidelines exist yet (Sumi et al. 2004). Optimization of such tunnels should consider conveying bed load downstream during natural floods, reducing the impact of sediment flushing operations on hydropower production and positively contributing to maintaining the live storage.

The work presented in this paper contributes to the achievement of these goals by presenting a case study in Equator for which a new operational concept using a

sediment bypass tunnel was developed and then tested, validated and optimized through physical modelling.

2 Background on sediment bypass tunnels

The first BPTs were built in the early 20th century in Japan and Switzerland (Vischer et al. 1997; Sumi et al. 2004), construction rate reducing to an average of about one per decade until the early 2010's. These tunnels are designed for free-flow operation, with design velocities between 7 and 15 m/s, hydraulic sections between 20 and 30 m^2, general slopes from 1 to 4%, design discharges from roughly 40 to 400 m^3/s, most of them being operated less than 30 days per year. A typical layout includes a tainter gate as regulating device at the inlet, leading to a flow accelerating reach followed by the typical cross section reach with the general slope until the outlet and energy dissipating structure.

SBTs are becoming more popular due to increased concern about the sustainability of live storage (and revenues) and of growing public interest to reduce reservoir trap efficiency and guarantee sufficient sediment transfer to downstream river reaches and maritime coastlines. Kondolf et al. (2014) present an overall balance of live storage depletion worldwide due to sediment trapping, which inevitably reduces mankind's ability to supply water & electricity to a growing population. Sediment trapping simultaneously aggravates the deficit of sediment replenishment vital for territorial security and biodiversity downstream. Not surprisingly, a larger number of countries has been adopting policy measures to reinforce monitoring of sediment bed load within river basin management.

Recent research on SBTs focuses on the resistance of the tunnel invert to hydroabrasion (Boes et al. 2014) and well as the SBTs' efficiency combining fieldwork and numerical modeling. Kantoush et al. (2012) measured at prototype scale the flow characteristics and suspended sediment concentration (SSC) in a SBT in Japan during flood seasons, which revealed to be instrumental to calibrate previous numerical model studies. However, other sediment management solutions are being developed in parallel that could be combined with SBTs to increase the overall bypass efficiency (BE), such as venting of suspended sediment (SS) through bottom outlets, turbining SS, flushing with drawdown and so forth. As an example, Jenzer-Althaus (2011) developed an original system that mobilizes fine settled material allowing for its easier flushing. The system is composed of water sprinklers disposed such as to generate cyclonic motion in areas where main flow velocities would be high enough to push the SS downstream (through the SBT or another device). However, no information was found on the damage incurred further downstream at the SBT outlets or of any specific design criteria adopted for the energy dissipation structures with regard to clear-water structures from spillways or river diversion tunnels (which are temporary by definition).

3 Chespí dam and hydroelectric power plant

The Chespí-Palma Real hydro power plant is located in the northwestern part of Ecuador on Guayllabamba River, about 30 km north of the capital, Quito. The project is developed on behalf of HidroEquinoccio in Quito. The plant consists of a double curved arch dam, 68 m height, with a reservoir capacity of 4.4 x 10^6 m³ and an active storage capacity of 2.3 x 10^6 m³. The reservoir gathers the water of an approximate 4'500 km² large basin. The hydroelectric power plant, located in a cavern downstream of the dam, consists of four Pelton units with 470 MW installed capacity (For more information, see Grimaldi et al. 2015).

Sediment management is a fundamental aspect of this project. The estimated mean annual sediment flux is some 820'000 m³. If no action is taken, the reservoir would be filled-up within some years. To avoid regular drawdown flushing of the reservoir and subsequently the plant shutdown, a sediment bypass structure is planned upstream of the reservoir. An underwater sill, located immediately downstream of the inlet structure is used as an obstacle in the main river course, preventing excessive sedimentation of the reservoir. Two alternatives sill locations were defined during the design stage; the first one (called hereafter "upstream sill") is situated right next to the inlet structure and the second one (called hereafter "downstream sill") is placed further downstream.

4 Sediment bypass concept

The sediment bypass concept with four main stages, outlined by Lombardi and further developed by the LCH (De Cesare et al. 2012) is explained hereafter (Figure 1):

a) **Normal reservoir and hydropower plant operation;** the SBT remains closed, the mainly clear (with negligible suspended sediment) upstream inflow passes over the sill into the reservoir. Latent bed load is retained upstream. There is no limitation on hydropower exploitation.

b) **Upstream drawdown flushing and transfer**. When the upstream discharge reaches a level that triggers bedload, SBT can be partially opened to transfer bedload (to ensure transport capacity in the SBT); lowering the water level upstream will accelerate bedload flushing, keeping the inlet structure free of deposits.

c) **SBT use under full load.** When the inflow discharge exceeds the SBT capacity, water level rises, the excess discharge flows over the sill into the reservoir and may require spillway operation. Bedload is continuously evacuated through the SBT. Suspended load is split, partially being evacuated through the SBT and the remainder settling close to the dam

172

d) **Reverse flushing with drawdown.** At the end of a flood event, water flowing back from the reservoir is evacuated through the SBT, keeping the zone between the sill and the inlet structure free of deposits.

During all above-mentioned stages, hydropower operation over the useful capacity of the reservoir can continue.
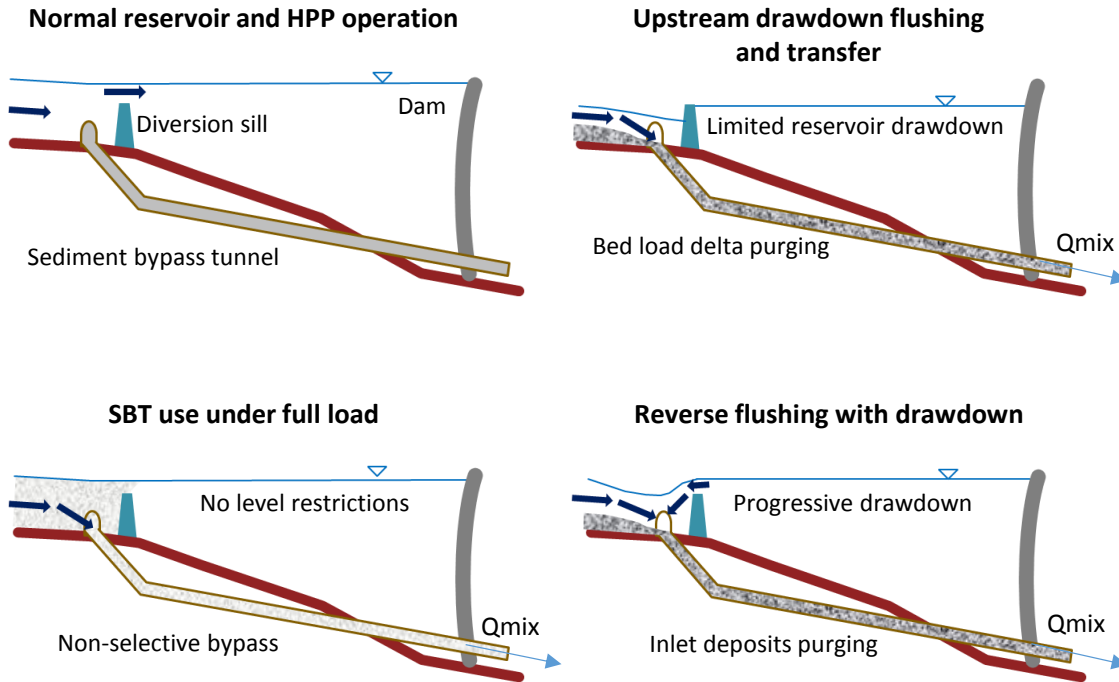

Figure 1: Schematic drawing illustrating the sediment bypass concept for the Chespí-Palma Real reservoir

5 Laboratory model

The objectives of the model tests are to validate and optimize the following aspects:

a) the performance of the sediment bypass in the established configuration;

b) the identification of potential deposit zones in the river; and,

c) the sediment flushing procedure for proper evacuation during floods.

The physical model was built in the Laboratory of Hydraulic Constructions (LCH) of the Ecole Polytechnique Fédérale de Lausanne (EPFL) (LCH 2011). Based on the dimensions, the discharge as well as the grain sizes, a scale of 1:38 was used. The model was operated according to the Froude similarity. The grain size distribution considered for the study was a $d_{50} = 20$ mm, the maximum reaching some 130 mm. Bedload transport capacity similarity between prototype and physical model has been evaluated using the critical Shields parameter. Taking into account the hydraulic parameters of the considered upstream river reach, a model "bedload" consisting of washed fine sand 0/4 mm was chosen.
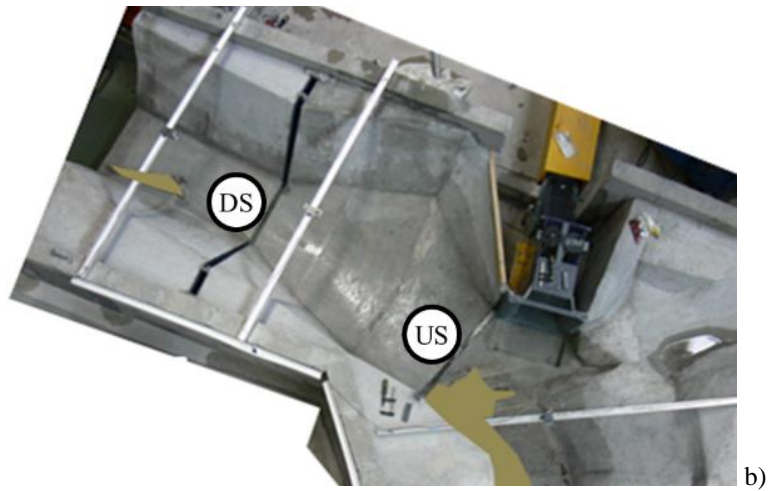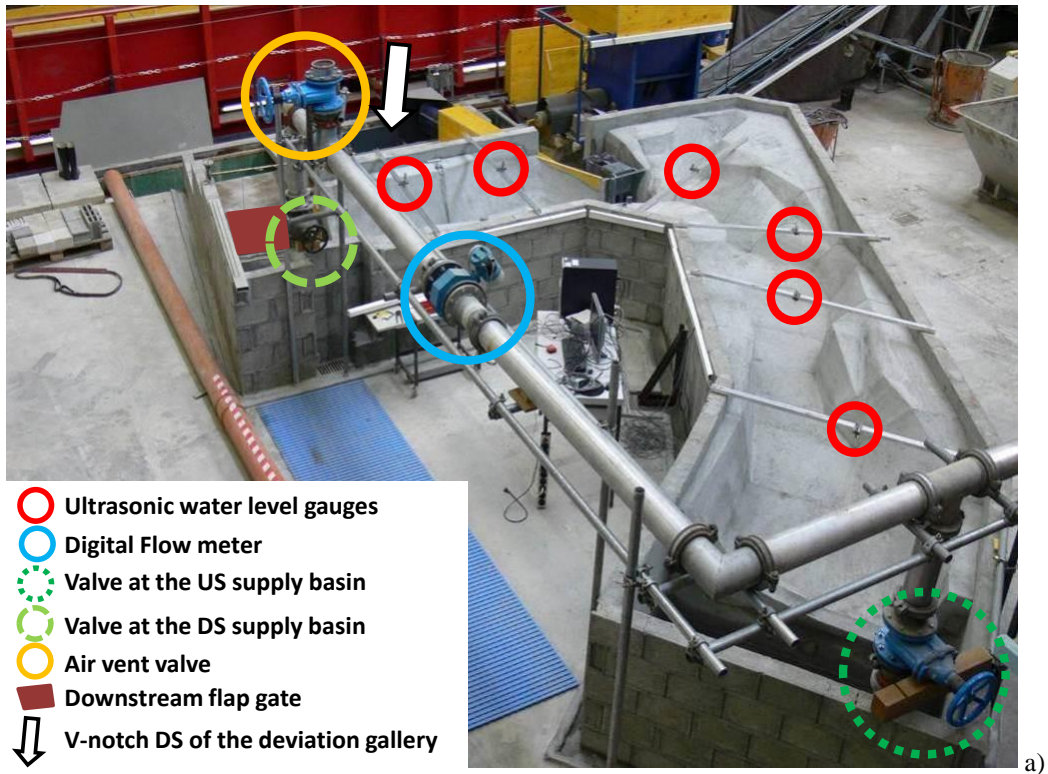
Figure 2: Picture of the physical model constructed at the LCH with its main operational elements (a), the two sill positions (b) as well as the adjustable downstream DS (c) and upstream US sill (d)

Two distinct sill positions were tested; the upstream (US) sill touches the right bank limit of the intake structure, whereas the downstream (DS) sill is located some 68 m downstream, perpendicular to the river axis. Both sills have two distinct crest levels, the right one (in river flow direction at outer bank in the bend, side of the SBT intake) is always 2 m higher, the elevation changes at the central axis of the sill.

6 Validation and optimization

6.1 Test runs

6.1.1 Clear water tests with sill

In a first step, clear water tests were performed to validate the discharge capacity, to obtain water level profiles as well as local velocity measurement for all potential operational modes. The test variables were the gate openings, two different sill positions and two sill elevations, different upstream river discharges (50, 100, 200 and 400 m^3/s, the last one corresponds to a 5-year return period flood), and two different reservoir water surface levels (1'445 and 1'450 m asl). Hydraulically the intake operates as expected from desk design and rating curves for all operational modes could be established. The approach flow conditions were investigated, with and without sill at both positions.

6.1.2 Run with bed load, no SBT operation, nor sill

In order to reproduce the natural behavior of the river in the model (e.g. during reservoir drawdown), the inlet gates were completely closed and there were no sills in the river. The potential deposition zones in the river were identified. Around 50 kg of sediment (model scale) were introduced at the upstream of the river with a discharge slightly higher than the one required for bed load transport initiation. After about one hour (model scale) the river found its equilibrium (no more erosion or deposition). Apart from minor deposits at the end of the model and inside the bend, there is practically no deposit downstream of the inlet structure. This observation is in accordance with the river slope, flow regime, grain size distribution and critical shear stress.

6.1.3 Run with bed load, SBT operation, with sill

Tests with sediment were performed for two different incoming discharges to verify the system efficiency for floods with different return periods. Both sill positions at two different sill levels were tested. Sediment was fed continuously. Once the sediment level attained approximately the lower elevation of the sill, the SBT inlet gates were completely opened. The reservoir water level was kept at 1'445 m asl by introducing an additional discharge from downstream to compensate the outgoing discharge through the bypass. The test duration was about 4 to 5 hours at model scale, which corresponds to one day at prototype scale.

6.2 Test results for SBT operation

After each simulated flood events, sediment samples from the model were assessed: volume evacuated through the SBT, volume deposited downstream of the sill (i.e. the potential inflow to the reservoir) and volume of the deposits upstream of the sill. This allows estimating the efficiency of the sediment bypass structure (Figure 3).
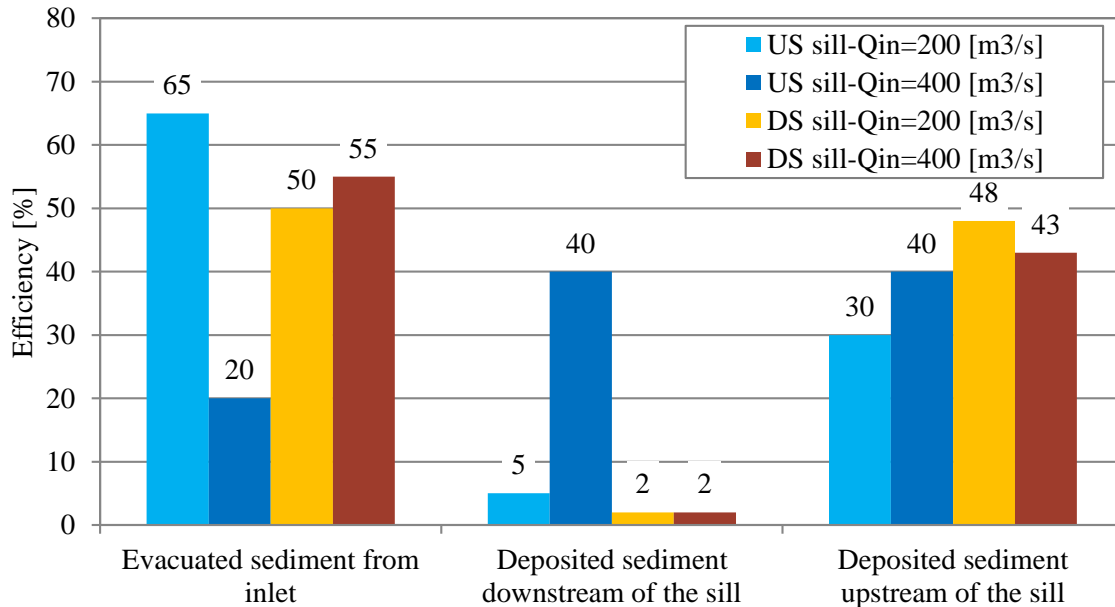

Figure 3: Efficiency for downstream sediment transfer corresponding to the four tested configurations. Ratio of deposited volumes regarding total sediment input for given test configurations

For the lower chosen discharge (200 m^3/s), the US sill performed best, bypassing some 65% of all incoming bed load downstream. When doubling the discharge, this value drops to 20%; in fact, most of the bed load passes the sill entering therefore into the reservoir. The DS sill performs generally much better and independently of the discharge. For all tested configurations, the amount of sediment retained upstream of the sill is similar for both sill locations, the DS sill having more space for deposits between the SBT intake and the sill. For lower discharges, that are getting close to the bed load motion limit, upstream drawdown flushing is required to transfer the sediment.

6.3 Final retained geometry

In conclusion, the sill at the downstream position allows for at least a 50% flushing efficiency whatever the discharge tested. On the other hand, the sill at the upstream position functions at 70% efficiency for a 200 m^3/s flood event. It should be reminded that the flushing efficiency term is used to assess the amount of the evacuated sediment by the bypass gallery. However, the upstream sill plays a significant role in preventing reservoir sedimentation. As the flushing process should be efficient for frequent flood events and not necessarily for extreme flood events, and taking into account the possibility of using the reservoir water for cleaning the area in front of the SBT inlet,

the upstream sill works better than the downstream one. Therefore, based on the obtained results the retained configuration would be the upstream sill with a crest level at 1'444-1'442 m asl (variable across the valley width, see Figure 2c and 2d). This configuration leads to better sediment flushing and less deposition in front of the bypass inlet. To prevent the remaining sediment to enter the reservoir, reverse flushing from the reservoir should be performed.

6.4 Principles for future SBT planning, design and operation

For future operations as well as for studies on similar schemes with SBT leading to some Best Practice Guide, among others, the main following procedures should be considered:

- Selection of inlet location, elevation and orientation by respecting the river geometry, past and future rating curves and the reservoir storage curve;

- Evaluation of the need for a weir separating the SBT inlet from the reservoir, design, position, orientation and elevation of the structure;

- Choice of hydraulic design and operating regimes, for target bypassing capacity and operation frequency;

- Evaluation of target sediment grain size distribution and volumes (bed load and suspended load) with regard to total sediment yield, acceptable reservoir storage loss and sediment flushing and venting capacity of other hydraulic structures such as bottom outlets and power intakes;

- Review of tunnel design respecting topography, hydraulics, sediment transport capacity, lining material (mainly for invert and side walls) and outlet design (e.g. position, elevation, orientation, geometry with regards to the downstream river reach, rating curves and location of other infrastructure such as the powerhouse or bridges);

- Planning of a operation follow-up, instrumentation and monitoring to guarantee proper collection of operation data, efficiency rating, damage observation, etc.;

- Assessment of economic feasibility and continuous need, as well as of the corresponding ecological benefits derived from limiting the reservoir's trap effect on the river ecosystem bed load budget.

7 Conclusions

A physical model at a scale of 1:38 has been built at the Laboratory of Hydraulic Constructions (LCH) of the Ecole Polytechnique Fédérale de Lausanne (EPFL). The hydraulic design was validated by the laboratory experiments. The sediment bypass

concept was optimized by selecting the best position of the sill. The upstream sill position was retained as it works satisfactory for most flood discharges.

7.1   Contribution of the bypass system

Without the bypass system the reservoir would be filled up within less than 10 years of operation. To mitigate such process, flushing operations through the bottom outlet of the dam with a reservoir drawdown could be carried out, leading to plant stoppage and loss of water and revenues. The sediment bypass system is an incremental project cost (capex) but avoids future expenses (opex) or production losses (reduced revenues). It guarantees the long-term availability of the live storage and production, thus liberating future cash flows for debt reimbursement and investment remuneration. The cost of the bypass system (including interests) is estimated as being approximately one order of magnitude lower than the total costs for palliative sediment flushing with reservoir drawdown over the expected project lifetime (considering the water losses and provision of replacement energy).

7.2   Contribution of the physical model tests

The physical model tests allowed validating the preliminary desk design, as well as optimizing the structures and the operational concept. First, the hydraulic conditions and by pass relations were validated for varying reservoir water levels. The location of the submerged diversion weir was revised, increasing the flushing efficiency for the most important operational scenarios. The foreseen operational guidelines were optimized, leading to the establishment of four different modes of operation, each with specific constraints and operational principles. In summary, the goals to improve sediment flushing efficiency while reducing production stoppage time and water losses has been achieved in laboratory conditions, allowing facing the reality of prototype implementation and scheme operation with reduced uncertainty regarding the reduction of live storage and production revenues.

Acknowledgement

References

Boes R.M., Auel C., Hagmann M. and Albayrak I. (2014). Sediment bypass tunnels to mitigate reservoir sedimentation and restore sediment continuity. *Reservoir Sedimentation* by Schleiss A., De Cesare G., Franca M., Pfister M. (Eds.), Taylor & Francis Group, London, ISBN 978-1-138-02675-9, pp: 221-228

Boillat J.-L., Martinerie R., Garcia J. and De Cesare G. (2008). La gestion sédimentaire en milieu alpin. *La Houille Blanche*, vol. 63, num. 4, p. 122-129

De Cesare G., Pfister M., Daneshvari M. und Bieri M. (2012). Herausforderungen des heutigen wasserbaulichen Versuchswesens mit drei Beispielen, Wasserwirtschaft 7-8, 2012, pp. 71-75

Grimaldi C., Micheli F. and Bremen R. (2015). Sediment Management in Andean Region: Chespí-Palma Real project, *Proceeding of First International Workshop on Sediment Bypass Tunnels*, Zurich, Switzerland

Jenzer-Althaus J. (2011). Sediment evacuation from reservoirs through intakes by jet induced flow, *EPFL PhD thesis N°4927 / LCH Communication N° 45* (eds. Schleiss A, De Cesare G.)

Kantoush S., Sumi T., Murasaki M. (2012). Evaluation of sediment bypass efficiency by flow field and sediment concentration monitoring techniques. *Journal of Japan Society of Civil Engineers, Ser. B1 (Hydraulic Engineering)*, Volume 67, Issue 4: 169-174 (2012). DOI: 10.2208/jscejhe.67.I_169

Kondolf, G. M. et al. (2014). Sustainable sediment management in reservoirs and regulated rivers: Experiences from five continents. *Earth's Future*, 2: 256–280, doi:10.1002/2013EF000184

LCH (2011). Chespí-Palma Real, Ecuador - Physical hydraulic model tests for flood and sediment bypass. LCH report 09/2011, EPFL Lausanne (unpublished project report)

Lei, C. (2008). Sediment management in the Three Gorges Reservoir. *Journal of Hydropower & Dams*, Issue Six: 115-122

Morris G. L. and Fan J. (1997). Reservoir Sedimentation handbook – design and management of dams, reservoirs, and watersheds for sustainable use. *McGraw-Hill*

Sumi T., Okano M. and Takata Y. (2004). Reservoir sedimentation management with bypass tunnels in Japan. *Proc. 9th Int. Symp. on River Sedimentation*, Oct. 18 – 21, 2004, Yichang, China, 1036-1043

Vischer D., Hager W. H., Casanova C., Joos B., Lier P. and Martini O. (1997). Bypass tunnels to prevent reservoir sedimentation, Q74-R37, in Proceeding of the 19th ICOLD Congress, Florence, Italy

Authors

Dr. Giovanni De Cesare (corresponding Author)
Laboratory of Hydraulic Constructions (LCH), EPFL, Lausanne
Email: giovanni.decesare@epfl.ch

Dr. Pedro Manso
Prof. Dr. Anton J. Schleiss
Laboratory of Hydraulic Constructions (LCH), EPFL, Lausanne

Milad Daneshvari
SGI Consulting SA, Châtelaine - Genève

180

Management alternatives to combat reservoir sedimentation

Gregory L. Morris

Abstract

Many techniques are available to actively manage reservoir sedimentation, and an equally important suite of adaptive strategies are available for managing the impacts of sedimentation without manipulating the sediment. Successful reservoir management to combat the effects of sedimentation may employ a combination of active plus adaptive strategies. This paper describes both active and adaptive strategies to manage reservoir sedimentation, and may be useful as a checklist of options to consider in addressing a sedimentation problem. Widespread application of both active and adaptive strategies will be required to successfully address the growing sedimentation problem worldwide.

1 Introduction

Sedimentation reduces reservoir storage and the benefits derived therefrom. Sustainable reservoir management seeks to retard sedimentation and reduce its adverse impacts, ultimately achieving an equilibrium between sediment inflow and outflow that sustains storage capacity while maximizing project benefits.

Successful sedimentation management may employ a combination of strategies which may change over time as sedimentation advances. The classification of "active" management techniques presented by Morris (2014) has been modified and expanded in **Error! Reference source not found.** to include "adaptive" strategies which do not manipulate sediment, yet which are essential management options. Both active and adaptive options should be considered as integral components of the management strategy, and a combination of both approaches may represent the best overall response.

2 Reduce sediment yield

Two types of strategies may be used to reduce sediment yield: control of either surface or channel erosion at its source, or trapping eroded sediment upstream of the reservoir.

2.1 Surface erosion

Soil surface erosion is initiated by raindrop impact which dislodges soil particles to initiate transport. Control of soil erosion generally focus on establishing and sustaining a protective vegetative cover. Leaves and vegetative detritus covering the soil intercept raindrops and protect the surface from direct impact.

1 – Reduce Sediment Yield from Upstream

- Sediment Trapping Above Reservoir
  - Large Dams
  - Dispersed structures (check dams, farm ponds)
- Reduce Sediment Production
  - Channel Erosion Control
    - Gully Stabilization
    - Stream Channel Stabilization & Restoration
  - Soil Erosion Control, Revegetation
    - Forests
    - Rangeland
    - Farms
    - Construction Sites and Developed Areas

2 – Route Sediments
(maintain transport, minimize deposition)

- Sediment Pass-Through
  - Reservoir Drawdown & Sluicing
    - Flood Event
    - Seasonal
  - Vent Turbid Density Currents
- Sediment Bypass
  - Flood Bypass Channel
  - Bypass Tunnel
    - High Level (no drawdown)
    - Low Level (drawdown)
  - Offstream Reservoirs

3 – Focus or Remove Sediment Deposits

- Modify Operating Rule (focus or redistribute sediment)
  - Hydraulic Scour
    - Pressure Flushing
    - Empty Flushing
  - River Flushing Below Dam
    - Discharge Beolw dam
    - Discharge Off-Channel
- Mechanical Excavation
  - Dredging
  - Dry Excavation
    - Hydraulic Dredge (slurry pump)
    - Hydrosuction (siphon) Dredge
    - Air Lift Dredge
    - Mechanical-lift (bucket, clamshell, dragline, backhoe)
    - Agitation Dredge

4- Adaptive Strategies
(sediments not manipulated)

- Reallocate Storage, Improve Operational Efficiency
- Modify Intakes or Other Structures to Avoid Sediment
- Raise Dam to Increase Volume
- Water Loss Control & Conservation
- Decommission Infrastructure

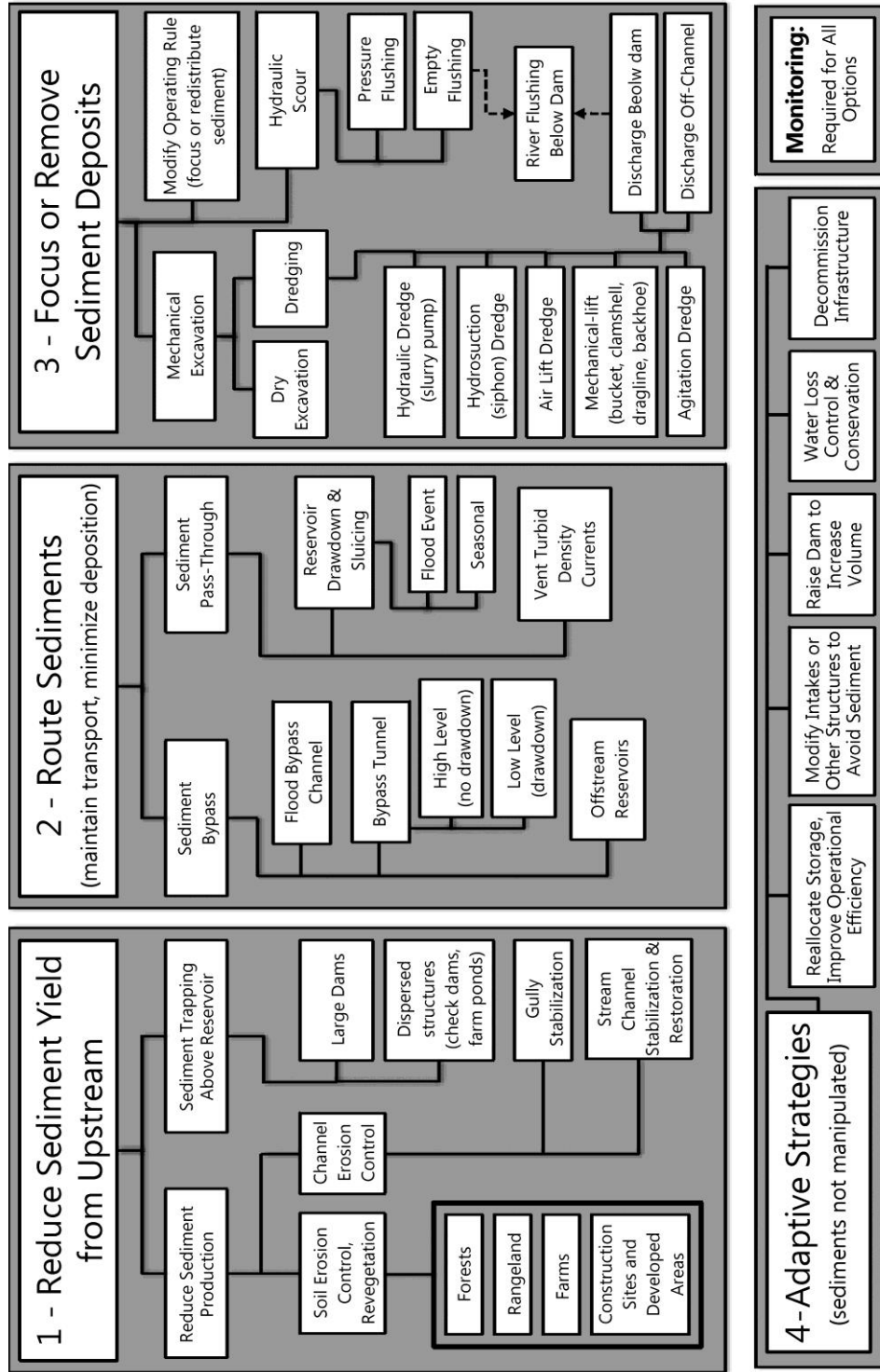**Monitoring:**
Required for All Options

Figure 1: Classification system for sedimentation management outlining the four major types of activities that can be undertaken to combat sedimentation and its consequences.

Organic material gives structure to the soil, providing both physical and chemical binding agents in the form of plant roots, mycorrhizal fungi threads and microorganisms. Plant material also provides food and habitat for burrowing fauna (earthworms, for example), which further improves soil structure, porosity and permeability. Through these vegetation-linked processes the soil develops a self-sustaining structure that resists erosion. Even if surface runoff is initiated, the plant material on the soil surface including grass stems, fallen leaves and twigs, creates small obstacles which impede shallow surface flow and helps trap sediment after it travels only a few centimeters.

2.2 Channel erosion

Once surface runoff flows coalesce to form channels the resulting concentrated flow can be highly erosive. However, the bank erosion frequently apparent on the exterior of stream meanders only represents a significant source of sediment export when the channel is incising and widening. Bank erosion associated with the natural meandering of rivers, with an eroding bank on one side and a growing point bar on the opposite side, does not export significant sediment downstream as long as the river's longitudinal profile and cross-section do not change (the stream simply moves laterally across its floodplain, eroding one bank and filling the other). Prior to attempting channel erosion control it is important to distinguish between the natural meandering of a stable channel and accelerated erosion from a growing channel cross-section. Attempts to stabilize a naturally meandering stream of stable cross-section will not reduce sediment yield. Gullies, on the other hand, represent an extreme case of channel incision and widening, frequently associated with intermittent flow.

2.3 Sediment trapping

Not all sediment that enters a channel will reach a downstream reservoir. Sediment trapping naturally occurs when a river overflows its channel and flows more slowly across its floodplain, depositing part of the sediment load. Large dams act as highly effective sediment traps, but a large number of small structures such as check dams and farm ponds can also be very effective in trapping sediment. For example, at least 2.6 million small farm ponds capture runoff from 21% of the total drainage area of the conterminous USA, representing 25% of total sheet and rill erosion (Renwick *et al.* 2005).

3 Route sediments

Sediment routing techniques maintain inflowing sediment in motion, either passing sediment-laden floods around (bypass) or though (pass-through) the storage zone.

3.1 Sediment bypass strategies

3.1.1 *Offstream reservoir*

Offstream reservoir storage is constructed outside the natural river channel by impounding a side tributary having a small watershed or constructing the impoundment on an upland area. Clear water is diverted into the offstream reservoir by a river intake, but large sediment-laden flows are passed beyond the intake and are not diverted into storage. Offstream reservoirs have been used for municipal supply and as daily regulation storage for run-of-river hydropower. Although highly effective in reducing sedimentation, provision should be made for their eventual cleanout.

3.1.2 *Sediment bypass tunnel*

A sediment bypass tunnel (SBT) has its entrance upstream of the storage volume to be protected from sedimentation. It diverts either suspended sediment or bed load around the storage, discharging below the dam. They are sized to pass flood flows. Although outlet works at earthen dams often use tunnels through the abutments, these do not qualify as SBTs because they do not intercept sediment upstream of the storage zone. SBTs normally operate for extended or multiple periods each year, reducing environmental impact compared to the larger and more concentrated sediment releases characteristic of reservoir emptying and flushing.

SBT systems may be classed as either "high-level" or a "low-level" depending on the placement of the tunnel intake and whether it is required to draw down the reservoir to flush bed material through the tunnel. A high-level SBT system can flush bed material without reservoir drawdown, the low-level system cannot. However, a low-level SBT system can still bypass suspended material around the dam without drawdown.

The entrance to a high-level SBT is installed at the upstream limit of the reservoir so that water and sediment can be bypassed around the impoundment without reservoir drawdown. The typical arrangement involves a low check dam to trap and divert sediment into the bypass tunnel located immediately upstream of the check dam (Figure 2A). At high flood flows the tunnel entrance will become submerged by backwater from the check dam and create orifice flow. The low velocity in front of the submerged SBT entrance will not transport coarse sediment into the tunnel, which now acts in a pressure flushing mode. When flow rate and water level diminish and free flow again occurs at the tunnel entrance, the higher velocity shallow flow will again transport coarse material into the tunnel. This sequence is illustrated in Figure 2(B).
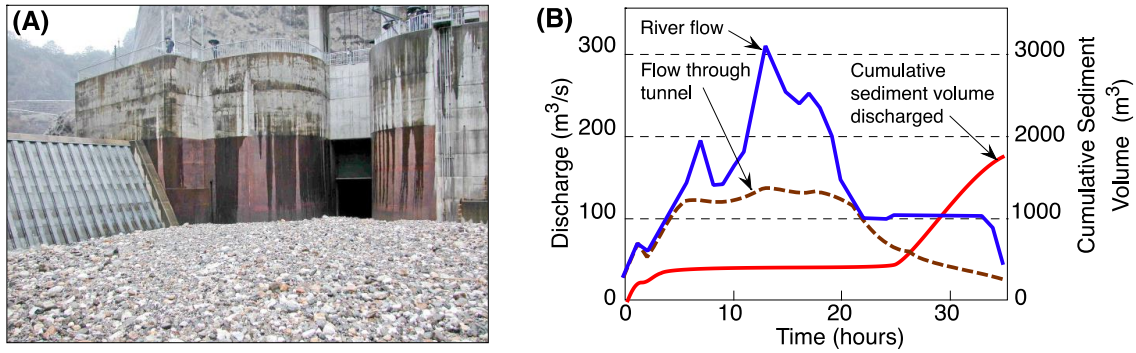
184

Figure 2: (A) Photo of the entrance to the bypass tunnel at Asahi pumped storage reservoir, Japan, with check dam on left. (B) Sediment bypass tunnel behavior at Asahi reservoir showing that bed material sediment is discharged only at lower rates of flood flow when the tunnel entrance is not submerged (after Fukuda *et al*. 2012).

The 30 Mm^3 multi-purpose Miwa dam in Japan (Umeda *et al*. 2004, I.E.A. 2006) provides an example of a high-level SBT designed for suspended sediment bypass. It uses the arrangement outlined in Figure 3 incorporating two separate upstream dams. A check dam traps bed load and suspended sand, which are removed mechanically, and further downstream a weir diverts flood flows and their suspended sediment into the SBT. This arrangement eliminates most of the abrasion damage in the tunnel and the trapped bed material can be excavated for use as construction material.
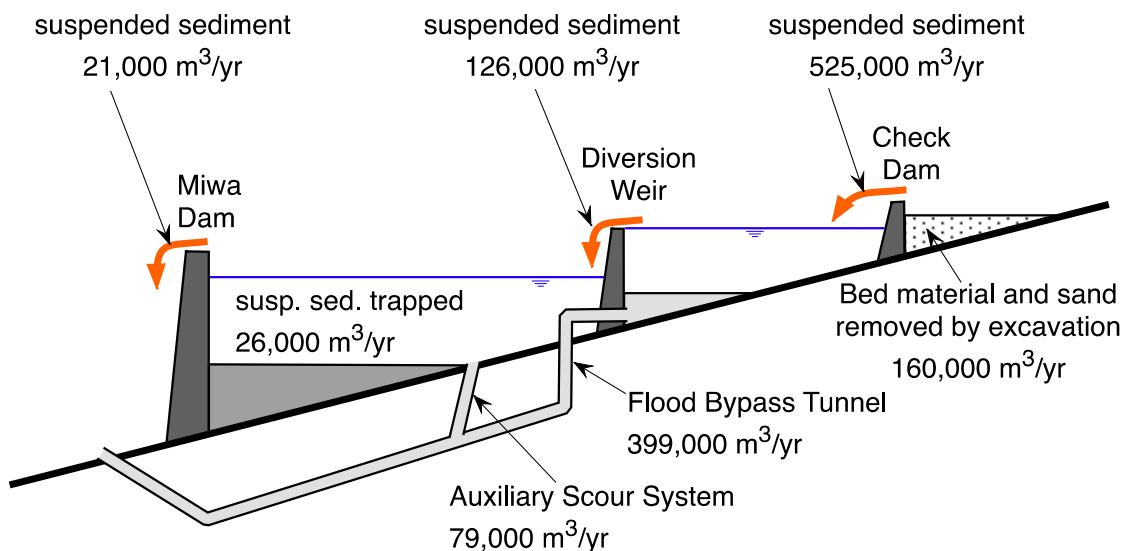

Figure 3: Sediment bypass arrangement for Miwa dam, Japan (after I.E.A. 2006)

In longer reservoirs a low-level SBT may be used with the tunnel entrance located near the dam and below normal pool level. The submerged SBT can bypass suspended load including turbidity currents without reservoir drawdown, but to control the advancing delta the reservoir is drawn down for empty flushing. The flushing discharge may be passed through the SBT or through low level outlets at the dam.

The Solis reservoir in Switzerland is an example of SBT flushing designed to maintain storage for daily hydropower regulation. Bed load from the advancing delta is directed into the tunnel entrance by a low guide wall, designed to emerge above the water surface only when the reservoir is drawn down to the flushing level (Auel *et al* 2010).

At a run-of-river project under evaluation in Nepal a SBT is being considered to maximize the bypass of suspended sand, minimizing both sediment and hydraulic loading (maximize sedimentation efficiency) in the regulating storage volume between the SBT and the intake, and avoiding costly underground sedimentation basins for a design flow of 675 m^3/s. This operational strategy is shown in Table 1. The reservoir will be periodically flushed by opening high-capacity low-level gates at the dam.

Table 1: Operational Strategy, Suspended Sediment Bypass Tunnel at Run-of-River Hydropower Dam.

Inflow	Operation
Inflow < Design Flow	All inflow to power + environmental flow
Design Flow < Inflow < Flushing Flow	Inflow exceeding Design Power is bypassed
Inflow > Flushing Flow Threshold	Gates at dam opened for empty flushing of reservoir

3.2 Reservoir drawdown and sediment sluicing

Sediment *sluicing* involves temporary reservoir drawdown during events with high sediment inflow to reduce residence time and enhance sediment discharge. Even in a shallow and nearly circular reservoir having poor geometry for sediment release, limited drawdown which reduces flood detention time can increase the discharge of fine sediment (Lee *et al.* 2013). More aggressive drawdown, reducing reservoir level to create riverine flow along the impounded reach during a flood, may even scour and release a portion of the previously deposited sediment. Drawdown sluicing can be performed on a seasonal basis, as practiced during the monsoon at some Himalayan run-of-river hydropower dams to preserve peaking capacity, or it may be event-based with reservoir operated guided by real-time reporting gages and hydrologic forecast models.

Because previously deposited sediment can be removed by both sluicing and flushing, in some cases the differentiation between these techniques may be ambiguous. The parameters in Table 2 may help to distinguish between the two processes.

Sluicing passes the natural hydrograph and its associated sediment through the reservoir with as little attenuation as possible, maintaining natural patterns of flow and sediment transport below the dam. This minimizes downstream environmental impacts. On the other hand, flushing can release very high peak sediment concentrations (e.g. >100,000 mg/l) and may require complex environmental mitigation measures. It is important that sites where sluicing is planned be properly designated to avoid being characterized as having the adverse downstream impacts normally associated with empty flushing.

Table 2: Differentiation between sluicing and flushing

Parameter	Sluicing	Flushing
Timing	Always coincides with natural flood flows	May not coincide with natural floods
Reservoir intakes	Can usually be operated during sluicing periods	Cannot operate (concentration too high, water level too low)
Outlet capacity	Can pass large floods with minimum backwater	Discharge may be limited by low level outlet capacity
Sediment discharge	Sediment Outflow ≈ Inflow	Sediment Outflow > Inflow
Erosion pattern	No retrogressive erosion	Retrogressive erosion may occur
Gate placement	Set and operated to achieve desired hydraulic profile during drawdown	Set gates at lowest possible level to maximize erosion in empty reservoir

3.3 Turbidity Current Venting

Turbid density currents are sediment-laden flows that plunge beneath the impounded water. Under favorable conditions they can travel along the submerged thalweg to the dam where they either accumulate as a submerged "muddy lake" or are released (Figure 4). Turbidity currents usually transport fine sediment that can pass hydropower turbines with minimal abrasion. Although occurring frequently, turbidity currents do not always transport significant amounts of sediment to the dam. Bathymetric surveys revealing horizontal sediment beds extending upstream from the dam (Figure 4) indicate that large amounts of sediment are transported to the dam but not released.

Turbidity current motion is facilitated when the submerged current flows along a defined channel, but as the submerged channel is infilled with sediment deposited by successive turbidity currents the reservoir thalweg becomes flat and wide. The turbidity current then spreads out, becoming wide and shallow with larger top and bottom surface areas. This increases frictional resistance, and also facilitates both sediment deposition plus dilution from above with clear water. Both processes lower the current's density and velocity, allowing more sediment to deposit, and eventually causing the current to stall. Thus, turbidity currents which reach the dam by following the original river channel during the first years of impounding, may dissipate after the bottom configuration becomes flat as a result of sedimentation from repeated turbidity flows. Empty flushing can scour out and maintain a submerged channel which will help sustain turbidity current motion.
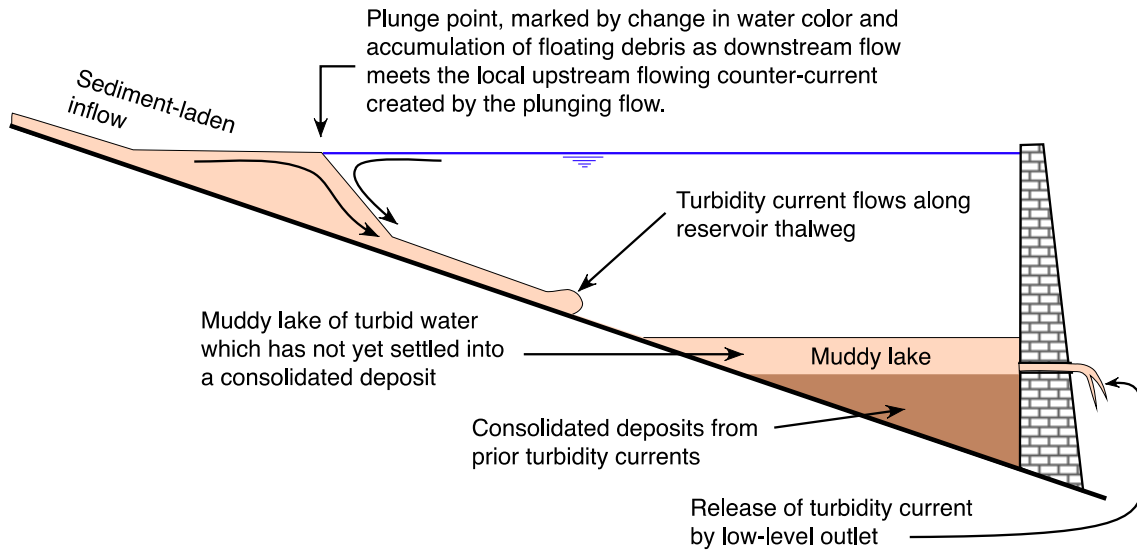
Figure 4: Passage of turbid density current through a reservoir and the deposit of a horizontal bed of fine sediment due to sedimentation from the submerged muddy lake.

4 Sediment Deposits: Focus, Redistribute, Remove

4.1 Focus or Redistribute Sediment

Reservoir delta profiles are influenced by the operating rule. When a reservoir is drawn down to a consistent minimum elevation each year the delta will establish a relatively stable profile and most inflowing sediment will be deposited on the delta face, which will advance as shown in Figure 5A. Sand in reservoir deltas is highly abrasive and cannot be allowed to encroach on a hydropower intake. To retard delta advance the reservoir's minimum operating level may be gradually raised, focusing delta deposition into the upper portion of the reservoir per Figure 5B. Conversely, a reservoir may be drawn down during floods to scour and move the delta deposits deeper into the impoundment, for example, to reduce backwater and upstream flood levels.
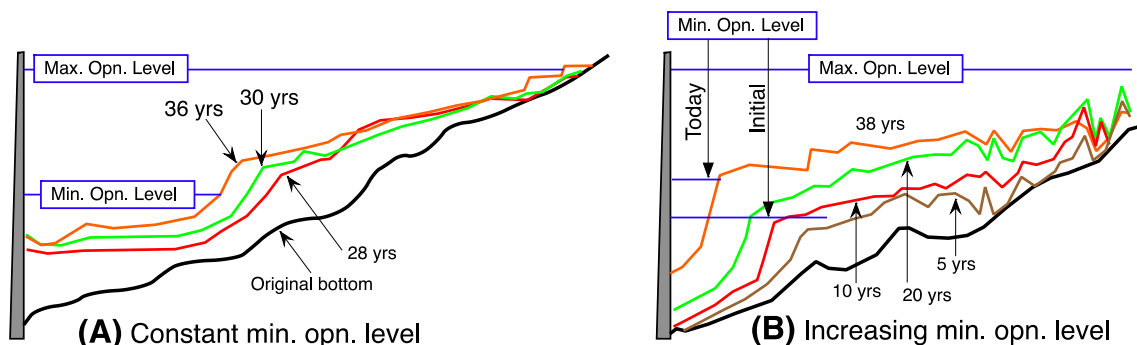

Figure 5: Advancement of reservoir delta: (A) with constant minimum operating level and (B) with an increasing minimum operating level.

188

4.2 Remove Sediment

Sediment may be mechanically excavated conventional excavation when the reservoir is drawn down, and is frequently used to recover coarse sediment from the delta for commercial purposes. Construction of a check dam to trap coarse sediment into a zone to facilitate mechanical removal was previously shown for Miwa dam (Figure 3).

Dredging of submerged sediments is generally the least costly and most feasible method of excavating large volumes from reservoirs; it does not require the reservoir to be emptied, and a slurry pipeline is a clean and efficient method of transporting sediment. Permanent dredging may be feasible at hydropower sites which have less costly self-supplied energy. For example, the intake at the Bajo Anchicayá run-of-river dam in Colombia has been maintained by continuous dredging since 1962.

Siphon or *hydrosuction* dredging is a special case of hydraulic dredging in which the motive force for transporting slurry through the pipeline is provided by the head differential between the reservoir level and the foot of the dam. Since the maximum head available for slurry transport is limited by the dam height, operation of a hydrosuction dredge will typically be limited to within a few kilometers of the dam.

4.3 Flushing

Pressure flushing occurs when a submerged low level outlet is opened to release sediment while the reservoir level is high. It will produce a localized scour cone immediately above the pressure flushing outlet. An intake located above this low-level flushing outlet can be maintained free of sediment, but this operation will not remove sediment beyond its immediate area of influence.

Empty flushing entails opening a low-level outlet to completely empty the reservoir to scour sediment deposits. Differences between sluicing and flushing have already been summarized in Table 2. Maximum flushing effectiveness is achieved by placing the outlet at the lowest level possible to maximize the erosional energy, and by using the highest discharge that can pass through the bottom outlet without backwater. For reservoirs in series, when the lower reservoir is empty a high-flow may be released from the upper reservoir to maximize downstream scour. *Sequential flushing* occurs when two or more reservoirs in series are flushed simultaneously, passing eroded sediment from upstream reservoirs through the downstream reservoirs with minimal redeposition.

While empty flushing may achieve a sediment balance for the fine fraction of the inflowing load, the coarse fraction may continue to accumulate in the reservoir. For example, Sumi *et al.* (2010) reported that flushing at the Unazuki dam in Japan removed 73% of the total sediment inflow but only 10% of the coarse sediment >2 mm. Thus, even with flushing a sediment balance may not be obtained across a reservoir.

4.4 River flushing

Both empty flushing and dredging may release high-concentration flow below the dam, and sediment accumulation in the river channel can have adverse consequences to the environment, flood control, navigation etc. An essential consideration in these strategies is to provide sufficient clear water releases to flush the released sediment downstream in an acceptable manner.

5 Adaptive strategies

Adaptive strategies are actions to combat sedimentation impacts which do not involve handling sediment. They may be used with or instead of active sediment management.

5.1 Reallocate storage and improve operational efficiency

Reservoir pools are normally established based on specific water levels, such as a flood control pool that occupies the upper portion of a multi-purpose reservoir. Sedimentation does not affect all pools equally, and the higher pool(s) typically experience much less sedimentation than the lower pool(s) used for water supply. The pool limits may be modified to reallocate the storage loss in a more equitable manner among users.

In many reservoirs operating rules were established >50 years ago, before the advent of real-time hydrologic monitoring and forecast tools. These tools make it possible to improve the hydrologic efficiency of the available storage. For example, a buffer pool (within the flood control pool for example), may be either filled for water supply or emptied for flood control, depending on existing and forecast hydrologic conditions. By improving the system's operational efficiency it may be possible to sustain benefits to all users for an interim period, despite sedimentation, and thereafter to partially mitigate storage loss impacts. Improvements in operational efficiency are typically very inexpensive compared to any type of active sediment management.

5.2 Modify structures to avoid sediment

Sediment will eventually reach critical structures: intakes, spillways, and hydropower equipment. To manage higher sediment loads, modify structures, provide protective coatings to hydro-mechanical equipment, etc.

5.3 Raise dam to increase volume

Storage may be increased by raising the dam, and even a relatively small increase in dam height can provide significant additional storage since the additional volume will be added to the top of the reservoir where surface area is greatest. The additional height may also be achieved constructing a higher dam just downstream of the existing dam, which will then be submerged.

5.4 Water loss control and conservation

As water supply declines due to storage loss, it becomes increasingly important to use the available water more efficiently. This includes reduction of physical water losses as well as conservation by users (such as more efficient irrigation). It may also entail economic transitions into activities that are inherently more water efficient. Given the large differences in the economic benefits of water use among different activities, significant reductions in water use may have only modest economic consequences. For example, Hanak (2012) noted that, "*California's economy has become less reliant on water intensive activities. For instance, agriculture and related manufacturing account for nearly four-fifths of all business and residential water use, but make up just 2 percent of state GDP and 4 percent of all jobs*".

5.5 Decommission Infrastructure

The long term sustainable use of all reservoirs is not justified, and a dam may be decommissioned when sedimentation renders it no longer economic to operate. For example, the 32 m San Clemente dam in California is currently being removed at a cost of $80 million due to obsolescence by sedimentation (www.sanclementedamremoval.org). Acceptable end-of-life strategies should be developed at any dam for which sustainable use is not considered feasible.

6 CONCLUSION

Reservoir storage is critical for sustaining our society. A variety of active and adaptive strategies exists to combat sedimentation, and will need to be implemented on an increasingly widespread scale to sustain economic activity and living standards.

References

Auel, C., Berchtold, T., and Boes, R. (2010). Sediment Management in the Solis Reservoir Using A Bypass Tunnel. *8th ICOLD European Club Symposium*, Innsbruck: 1–6.

Fukuda, Tomoo, Yamashita, K., Osada, K., Fukuoka, S. (2012). Study on Flushing Mechanism of Dam Reservoir Sedimentation and Recovery of Riffle-Pool in Downstream Reach by a Flushing Bypass Tunnel. *Proc. Intl. Symp. on Dams for A Changing World*. Kyoto, Japan.

Hanak, E. ed. (2012). *Water and the California Economy*. San Francisco: Public Policy Institute of California.

IEA. (2006). *Case Study 04-01: Reservoir Sedimentation - Dashidaira Dam, Japan*. IEA Hydropower Implementing Agreement Annex VIII, Hydropower Good Practices. http://www.ieahydro.org/Case_Studies.html.

Lee, C., Foster, G. (2013). Assessing the Potential of Reservoir Outflow Management to Reduce Sedimentation Using Continuous Turbidity Monitoring and Reservoir Modelling. *Hydrological Processes* 27 (10): 1426–39. doi:10.1002/hyp.9284.

Morris, G.L. (2014). Sediment Management and Sustainable Use of Reservoirs. *Modern Water Resources Engineering*, edited by Lawrence K. Wang and Chih Ted Yang, 279–337. Totowa, NJ: Humana Press. http://link.springer.com/10.1007/978-1-62703-595-8_5.

Renwick, W.H., Smith, S.V., Bartley, J.D., Buddemeier, R.W. (2005). The Role of Impoundments in the Sediment Budget of the Conterminous United States. *Geomorphology* 71 (1-2): 99–111. doi:10.1016/j.geomorph.2004.01.010.

Sumi T., Kantoush, S.A. (2010). Integrated Management of Reservoir Sediment Routing by Flushing Replenishing, and Bypassing Sediments in Japanese River Basins. *International Symposium on Ecohydrology*, Kyoto. pp 831–838.

Umeda, M., Okano, M., Yokomori, G. (2004). Application of Fine Sediment Behavior to Sedimentation Management in Miwa Dam, Japan. *ydraulics of Dams and River* Structures. London: A.A. Balkema.

Author

Gregory L. Morris
GLM Engineering COOP, San Juan, Puerto Rico, USA.
Email: gmorris@glmengineers.com

Sedimentation countermeasures – examples from Switzerland

Robert M. Boes, Michelle Hagmann

Abstract

The situation and extent of reservoir sedimentation in Switzerland as well as its negative effects are briefly presented and typical concepts and measures to counter sedimentation are given. Although, on average, sedimentation of Swiss reservoirs is not yet very pronounced, there is a clear trend of increasing sediment production and yield in alpine regions, particularly in glaciated catchments due to glacier melt and retreat of permafrost. Four Swiss examples, where sedimentation has become critical, are presented. Thereby different measures are taken to counter negative reservoir sedimentation effects by a) increasing dead storage, b) reducing sediment yield, c) routing or d) removing sediment. The selected concept in each case agrees well with Japanese classifications and experience.

Zusammenfassung

Nach der Vorstellung des Problems und des Ausmasses der Stauraumverlandung in der Schweiz werden klassische Konzepte und Gegenmassnahmen präsentiert. Wenngleich Stauraumverlandung in der Schweiz im Mittel noch nicht sehr ausgeprägt ist, so ist doch ein klarer Trend hin zu verstärktem Sedimentabtrag im Alpenraum im Allgemeinen und in vergletscherten Einzugsgebieten im Speziellen zu beobachten. Es werden vier Beispiele von Schweizer Talsperren vorgestellt, an denen die Verlandungssituation kritische Ausmasse angenommen hat. Dort wurden jeweils unterschiedliche Massnahmen getroffen, nämlich a) zur Vergrösserung des Totvolumens, b) zur Reduktion des Sedimenteintrags, c) zum Durchleiten und d) zum Austrag von Sedimenten. Die jeweils gewählten Konzepte stimmen gut mit japanischen Empfehlungen und Einstufungen überein.

1 Introduction

1.1 Reservoir sedimentation in Switzerland and worldwide

Like natural lakes, artificial reservoirs impounded by dams are prone to sedimentation. Depending on local conditions including size, topography, relief and geology of the catchment, hydrological boundary conditions, and size and shape of the reservoir, this process can last between a few and several thousand years. The Koorawatha Reservoir in Australia, for instance, has silted up so quickly after its commissioning in 1911 that it

could soon no longer fulfill its function (Figure 1a). Although this extent of siltation is hardly found in Central European countries like Switzerland, Alpine reservoirs may also exhibit significant sedimentation rates leading to operational problems after a few decades or even less. For instance, the Tourtemagne Reservoir in the canton of Valais, Switzerland, built from 1957 to 1958, is heavily silted by now (Figure 1b).
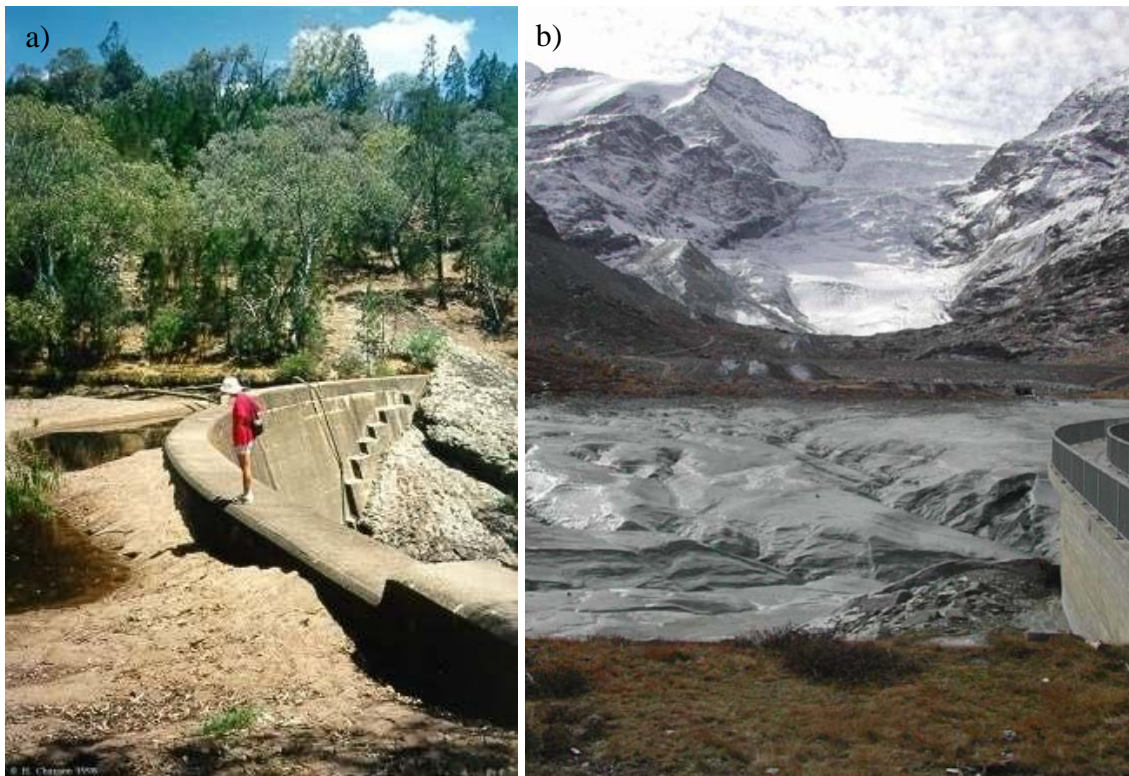

Figure 1: a) Fully-silted Koorawatha Reservoir in Australia (Chanson 1998), b) Tourtemagne Reservoir in Valais, Switzerland, with glacier in the background (Hauenstein 2005)

On a global level more reservoir volume is currently lost due to sedimentation than is created by new dam construction and enhancement of existing reservoirs. Without adapting reservoir sediment management it would just be a matter of time until no more storage volume were available. Figure 2 shows that the gradient of the sedimentation curve is higher than that of the storage capacity, so that the useful or active reservoir volume is gradually decreasing with time. Despite comparatively small average sedimentation rates, this also holds for Alpine countries like Austria and Switzerland, where construction of new reservoirs is only marginal nowadays. Compared to worldwide sedimentation rates, European rates are sub-average (Table 1). In the literature, rates of 1-2%, i.e. higher than those given by Basson (2009) may also be found (Schleiss & Oehy 2002). Due to human impacts (deforestation, agriculture) and climate change (accumulation and increasing intensity of rainstorms, retreat of glaciers and permafrost), this value is supposed to increase (Walling and Webb 1996, Syvitski 2003, KOHS 2007, Schleiss *et al.* 2010, Wisser *et al.* 2013).

194

In Austria and Switzerland mean sedimentation rates are 0.8% per year and only slightly exceed the European average (Basson 2009). That does not seem critical at first sight, but sediment supply from high Alpine catchments has recently increased significantly, causing severe sedimentation and hydroabrasive wear problems at reservoirs and hydroelectric facilities. In the scope of climate change and significant glacier retreat, easily erodible moraine material is left behind in large quantities and washed into downstream reservoirs (Figure 1b). The following specific sediment yields from glacierized Swiss catchments were reported recently:

- Gries Reservoir (catchment area of 10 km^2), canton Valais: 1800 m^3/km^2/a until 2010, followed by a rapid increase to 7000 m^3/km^2/a since then (A. Baumer, OFIMA). This recent sediment yield exceeds all known values.

- Unterer Grindelwaldgletscher (catchment area of 25 km^2), canton Berne: up to 1'000 m^3/km^2/a until 2005, and 800-1600 m^3/km^2/a since then (N. Hählen, Abt. Naturgefahren, Interlaken).

- Gebidem Reservoir, Aletschgletscher (catchment area of 198 km^2), canton Valais: 1000-2000 m^3/km^2/a in the 1990s and 1500-2500 m^3/km^2/a in the last decade (HYDRO-Exploitation).
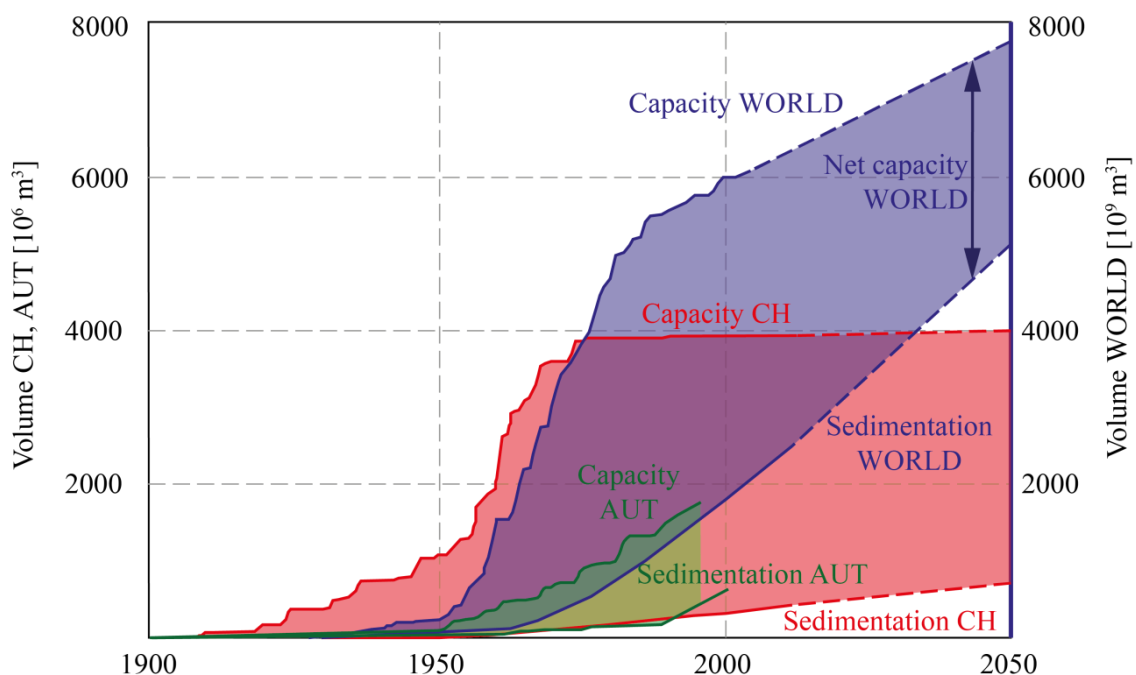

Figure 2: Increase of both reservoir sedimentation and storage volume in the Alpine countries Austria and Switzerland as well as worldwide between 1900 and 2050 (extrapolated) (adapted from Schleiss & Oehy, 2002 and Boes & Reindl, 2006)

To counter the decrease of reservoir volume due to sedimentation processes, a total investment of 13 to 19 billion US$ would be required for storage replacement, equaling

about 20-30% of the yearly global budgets for reservoir operation and maintenance (Schleiss *et al.* 2010). The measures effectively taken to counter reservoir sedimentation are by far smaller than required for a sustainable long-term reservoir management.

Table 1: Mean sedimentation rates on a continental level and worldwide (from Basson 2009)

Region	Annual sedimentation rate [%]
Africa	0.85
Asia	0.79
Australia & Oceania	0.94
Central America	0.74
Europe	0.73
Middle East	1.02
North America	0.68
South America	0.75
Global	0.8

1.2 Negative effects of reservoir sedimentation

The sedimentation processes in a reservoir have multiple negative consequences. The relative reservoir size, particularly its Capacity-Inflow Ratio (CIR), i.e. the ratio of reservoir volume to the mean annual runoff, greatly affects the reservoir trap efficiency. The longer the residence time of stored water, the finer sediments may settle, and the more the sediment transport capacity of the formerly natural stream is reduced. This interruption of the sediment continuity has negative effects in the tailwater of a dam, e.g. river bed degradation (bedrock exposure), change in river bed morphology such as fixed river channel and armor coating (coarsening of bed material), sea shore erosion, hydrological regime smoothing (tractive force decrease, decrease of disturbances due to peak flow reduction), reduction of the dynamics of rapids and pools in rivers, and loss of biodiversity due to habitat deterioration (Cajot *et al.* 2012, Sakurai & Hakoishi 2012, Facchini *et al.* 2015).

A common approach distinguishes between delta formation at the upper reach of a reservoir caused by coarse sediments (bed load) and the aggradation of fines in the deeper water zone further downstream which is often highly affected by density currents for rather narrow and elongated reservoirs of steep bottom slope (Schleiss *et al.* 2010, Boes 2011). Depending on this type of sedimentation process the active reservoir storage decreases in two different ways (Figure 3). While for the first type the original stage-volume curve rotates about the origin as a delta is formed (Figure 3a), whereas for the second type the aggradation of the deeper reservoir water zone by fines causes a parallel shift, so that the active storage reduction is more pronounced at low reservoir levels for the latter (Figure 3b). From an operational point of view it is essential to keep the total active storage for small compensation basins over the reservoir's life time, while for seasonal or multi-seasonal storage reservoirs it is a question of economic optimization to what extent sedimentation is allowed. Generally, the reduction of the

reservoir's active storage due to sedimentation leads to a reduction of water availability to serve the reservoir's purposes, such as power production or water for irrigation, domestic and industrial use. Moreover, the reduction of the reservoir's stage-volume (Figure 3) and stage-surface relations due to sedimentation leads to a reduced flood retention capacity.
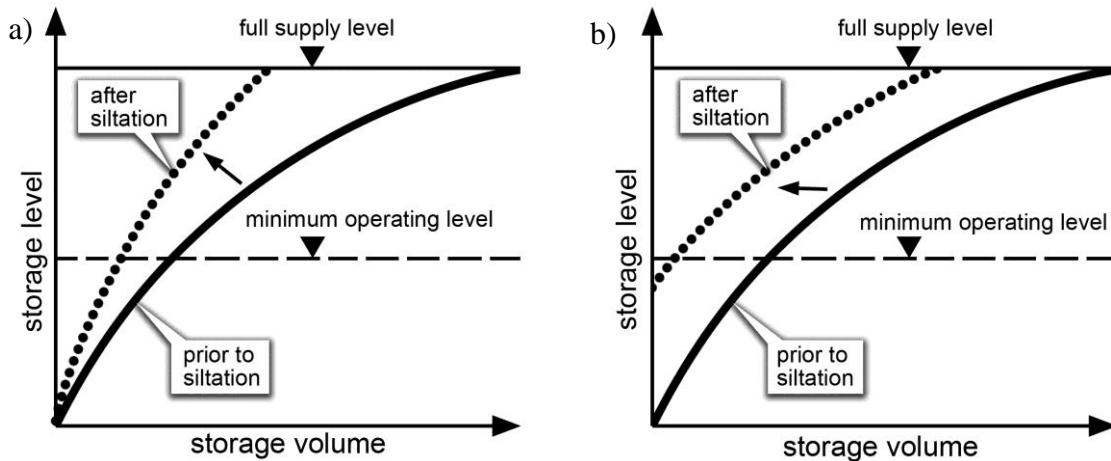

Figure 3: Reduction of reservoir volume due to a) delta formation, b) deep level aggradation (adapted from Vischer 1981)

At the dam, sedimentation may endanger the safe operation of low-level dam outlets such as bottom outlets on the one hand and water intakes on the other. The former are important safety elements to be operational at any time. If the sediment transport through bottom outlets exceeds their transport capacity, flow choking may occur which would greatly endanger their safe operation. Moreover, if low-level outlets are used regularly to flush coarse sediment, hydro-abrasive erosion of the invert lining must be taken into account (similar to sediment bypass tunnels, see e.g. Auel & Boes 2011, Sumi & Kantoush 2011 and Boes *et al.* 2014) to avoid negative secondary effects such as leakage at the gate or cavitation damage induced by the uneven invert surface. Furthermore, if the sediment concentration in the waterways is too high, severe wear of hydraulic structures (turbines, steel hydraulic parts) may occur (Boes 2013, Abgottspon *et al.* 2014). Therefore, the entrainment of sediment into waterways has to be minimized to serve the reservoir's purposes, e.g. production of hydroelectricity, in an economic and reliable way.

2 Reservoir sedimentation countermeasures

There is a variety of options to counter reservoir sedimentation. State-of-the-art overviews are e.g. given by Annandale (1987), Morris & Fan (1998), and Sumi (2005). If the available reservoir volume is supposed to be kept or (partly) regained, measures to limit the sediment production in the catchment and its input into the reservoir, to avoid the settling of sediment in the reservoir, or to remove sediment already settled have to

be taken. In general, in order to be as efficient as possible, these measures should be considered from the very beginning of the planning phase of an artificial reservoir. The most effective way to counter reservoir sedimentation is certainly an optimized consideration of the location and layout of the dam and reservoir. For instance, if the reservoir has a small direct catchment and is mainly fed by water diversions from neighbouring catchments or is located as an off-stream reservoir, the sediment input can be greatly reduced, provided the intakes are equipped with efficient gravel traps and desilting facilities (Figure 4). In general, preventive measures are preferable, as retroactive desiltation measures for existing reservoirs with significant sediment aggradation are generally considerably more difficult and costly. Particularly the choice of feasible retroactive measures tends to be much more restricted compared to preventive ones (Müller & De Cesare 2009, Boes 2011).
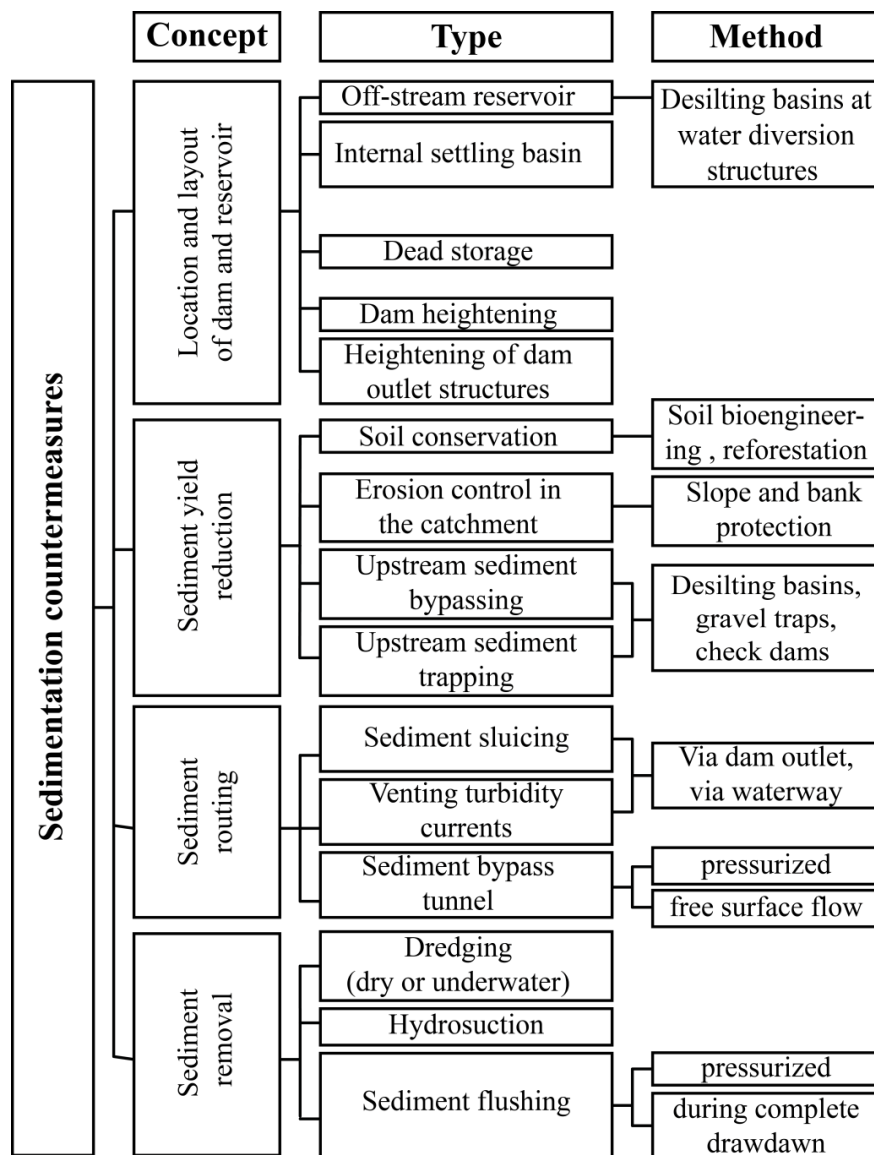
Figure 4: Classification of concepts, types and methods to counter reservoir sedimentation (adapted from Sumi *et al.* 2004 and Boillat *et al.* 2003)

At the conceptual planning stage, various concepts to reduce reservoir sedimentation may be distinguished (Figure 4). On the one hand, as presented above, the careful selection of the location and layout of a reservoir may greatly reduce its service life regarding sedimentation. On the other hand, and particularly for existing reservoirs with severe sedimentation problems, sediment yield reduction, sediment routing and sediment removal may be distinguished. While the former two are mainly preventive to avoid sediment input into a reservoir, the latter two are retroactive, as they demand handling of sediments already washed into or even settled in the reservoir. Despite this classification, guidelines on how to tackle sedimentation issues are typically rather generic. However, as the environmental, technical and economic boundary conditions of reservoirs are highly site-specific, every case has to be treated and optimized individually.

3   Swiss case studies

In the following, a number of cases from Swiss reservoirs are presented covering different types of sedimentation countermeasures. Their location is shown in Figure 5. They give a rough idea on the specific situation and extent of reservoir sedimentation and are grouped according to the selected main concept. More details can be found in the mentioned literature.
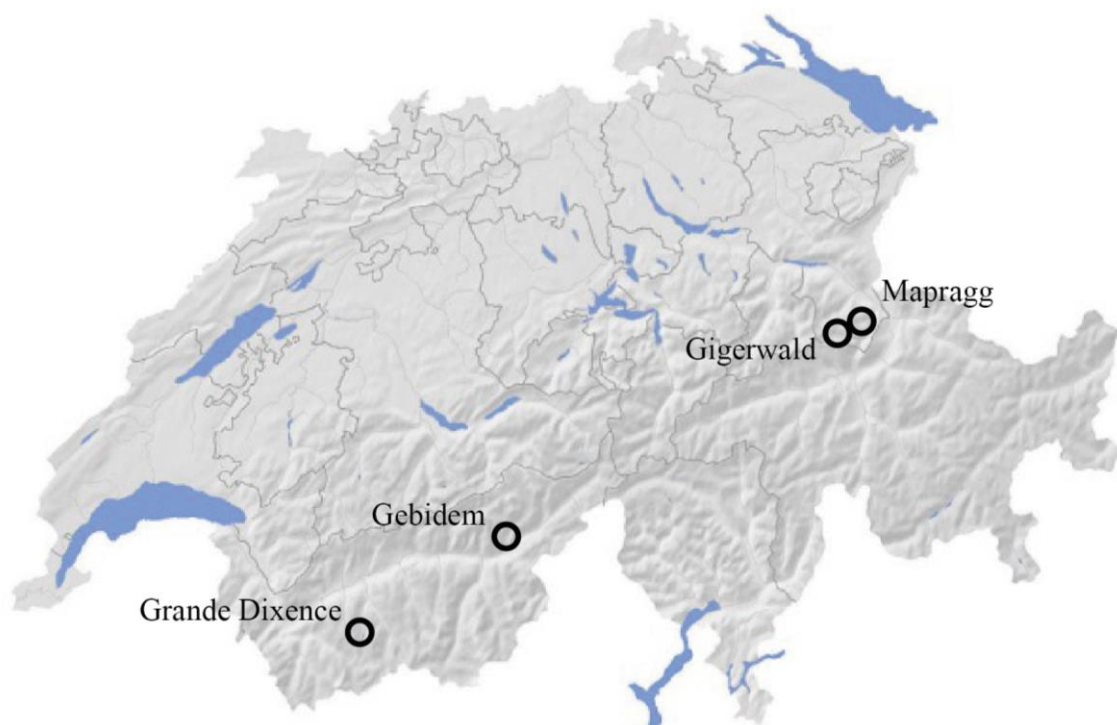

Figure 5: Location of the case studies presented herein

3.1 Location and layout of reservoir and dam

Grande Dixence Reservoir

Grande Dixence is the largest Swiss reservoir with an original volume of 400 hm^3 located on the Dixence River in the Valais Alps at an elevation of 2364 m asl. While its direct catchment is only 46.3 km^2, the total catchment of all water diversions and inflows amounts to 357 km^2. The reservoir is impounded by a 285 m high gravity dam with a volume of almost 6 hm^3, still being the highest gravity dam in the world. The reservoir is mainly filled with considerable summer run-off from 35 glaciers diverted at 75 stream intakes which is collected and pumped into the 100 km long collection galleries at four large pumping stations with heads of up to more than 400 m. Despite desilting of the run-off at the stream water intakes and pumping stations, the Grande Dixence Reservoir has continued to fill up with sediments since its commissioning in 1961, so that additional measures have had to be taken.

In particular, the first Dixence Dam, a hollow gravity masonry dam commissioned in 1935 and located 400 m upstream of the new dam with a crest level of 2241 m asl (i.e. 124 m below the Grande Dixence dam crest), creates an internal settling basin of 50 hm^3 and thus greatly increases the reservoir's dead storage. This dam is submerged for most of the year, while the reservoir level typically falls below its crest from April to May only (Figure 6a), with a multi-annual averaged minimum of some 2230 m asl. However, in this period, the whole discharge flows through two orifices in the upstream and downstream dam faces, entraining fine sediments between the two dams. These sediments settle at an average rate of 50 cm/year and, without adequate countermeasures, would reach the water intake at the Grande Dixence Dam in 2018 (Bretz & Barras 2012).

From a number of concepts investigated, the increase of the dead storage upstream of the Dixence Dam by creating a new upstream orifice located 11 m above the existing one and by plugging the latter was selected (Figure 6b). The new upstream orifice and the extension of the one downstream increase the discharge capacity from 55 to 130 m^3/s, corresponding to the total discharge capacity of the production units and enabling full capacity even at low reservoir levels in spring. The definitive storage upstream of the Dixence Dam is expected to be large enough for more than 100 years (Bretz & Barras 2012).
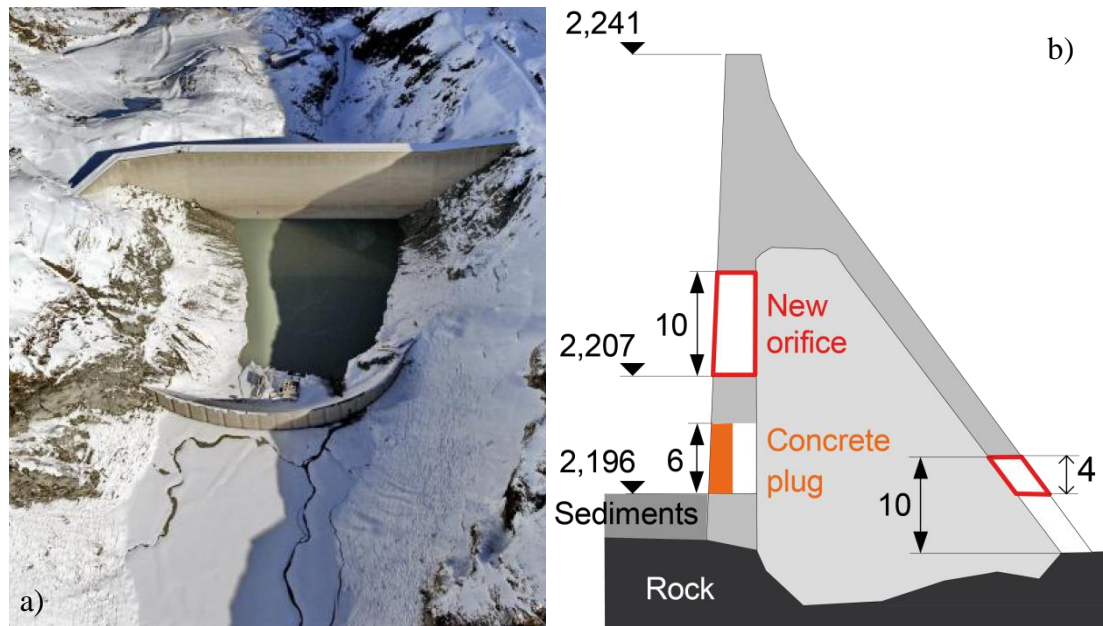
Figure 6: a) Grande Dixence Dam (upper) and Dixence Dam (lower), b) New orifice and concrete plug on the existing orifice at the upstream dam face of Dixence Dam, and extension of downstream orifice; numbers in [m] (adapted from Bretz & Barras 2012)

3.2   Sediment yield reduction

Gigerwald Reservoir

The 147 m high arch dam Gigerwald impounds a reservoir with an initial volume of some 35 hm³ located at 1335 m asl on the Tamina River in the Canton of St. Gallen, Eastern Switzerland. It was commissioned in 1976 by the operator Kraftwerke Sarganserland (KSL), featuring a total catchment area of 97 km^2, 52 km^2 of which come from the direct catchment, while run-off from a 45 km^2 catchment in the neighbouring Weisstannen Valley is diverted at a number of water intakes equipped with desilting facilities (Figure 7). A mean annual sedimentation volume of about 60'000 m^3 or 0.2% of the reservoir volume had been observed, so that the total sedimentation volume had reached 1.7 hm^3 until 2006, representing 5% of the initial volume. Despite the desilting facilities at the Weisstannen Valley intakes, 40 to 50% of the sediment originate from that water diversion, while 60 to 50% stem from the direct Tamina River catchment (Müller & De Cesare 2009). From 2003 the annual bed level increase amounted to 0.75 m, and in 2006 the level was just 5.4 m below the common intake structure of the bottom outlet and the waterway, respectively. It was therefore expected that within only 5 to 15 years the intake invert level would be reached, so that countermeasures had to be implemented.

To reduce the sediment yield it was decided to install turbidimeters at the intakes (Figure 7) enabling continuous sediment monitoring in real-time to detect high sediment concentrations during floods. This allows to automatically switch-off the water

201

diversions once critical threshold values are exceeded, typically during floods. The sediment input can therefore be reduced significantly.

3.3 Sediment routing

Mapragg Reservoir

Mapragg Reservoir is impounded by a 75 m high concrete gravity dam located on the Tamina River downstream of the Gigerwald Reservoir. Together with the latter it is the heart of the pumped storage scheme operated by KSL. Mapragg Reservoir serves as a compensation basin for that scheme and feeds the Sarelli Hydropower Plant (HPP) located on the shore of the Rhine river (Figure 7). The reservoir volume of 5 hm^3 is filled with run-off from a 159 km^2 total catchment, of which 62 km^2 come from the Tamina river catchment downstream of Gigerwald.
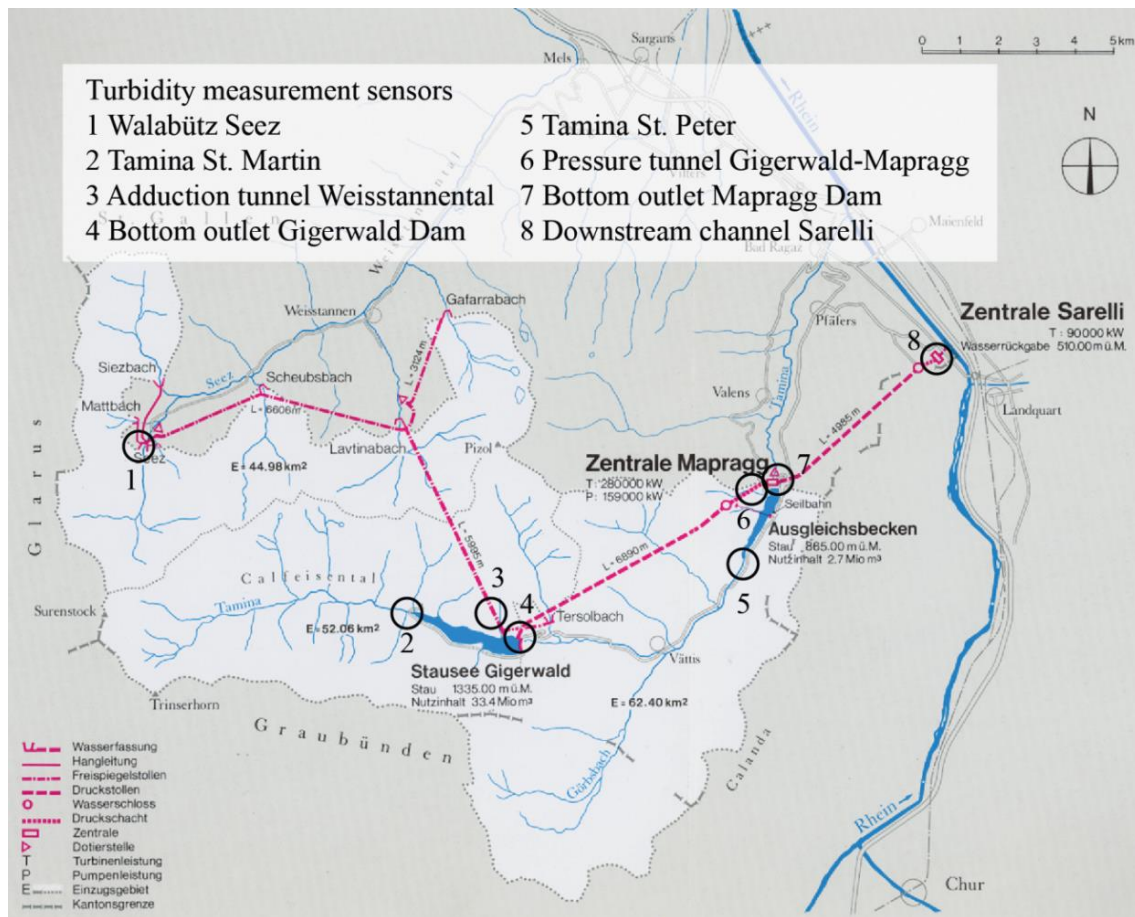
Figure 7: Situation of Gigerwald and Mapragg Reservoirs and the connected hydroelectric schemes of Kraftwerke Sarganserland (KSL) (adapted from Müller & De Cesare 2009)

Bathymetric measurements in the years 2000 to 2007 indicated that the reservoir level was close to the bottom intake invert level. On average, the Mapragg Reservoir had annually silted up by 0.4% of its reservoir volume. A balancing of sediment fluxes in the KSL schemes using turbidimeters showed that 70% of the sediment come from the

202

direct natural catchment, while 30% are diverted through the pressure tunnel from the Gigerwald Reservoir (Müller & De Cesare 2009). In summer 2006, 14% of the total sediment inflow of some 58'000 t into Mapragg Reservoir were pumped back, while 26% were turbined via the Sarelli HPP. Therefore, 35'000 t settled in the reservoir.

A concept study of various countermeasures shown in Figure 4 resulted in the selection of turbidity current venting through the bottom outlets at Mapragg, as large amounts of sediment are transported to the dam by such high-density flows during flood events (Müller & De Cesare 2009). The bottom outlets are opened once suspended sediment concentrations of SSC = 2 g/l are exceeded at the dam; expected maximum SSC values amount up to 14 g/l. According to the permission from the authorities, the maximum outlet discharge is limited to between 5 and 25 m^3/s, and the maximum discharge is attained gradually, thus simulating small to medium natural floods with their rising and falling limbs (Figure 8). After SSC has fallen below 2 g/l, a post-purge is done with gradual discharge reduction and the bottom outlets are closed again (Müller & De Cesare 2009).
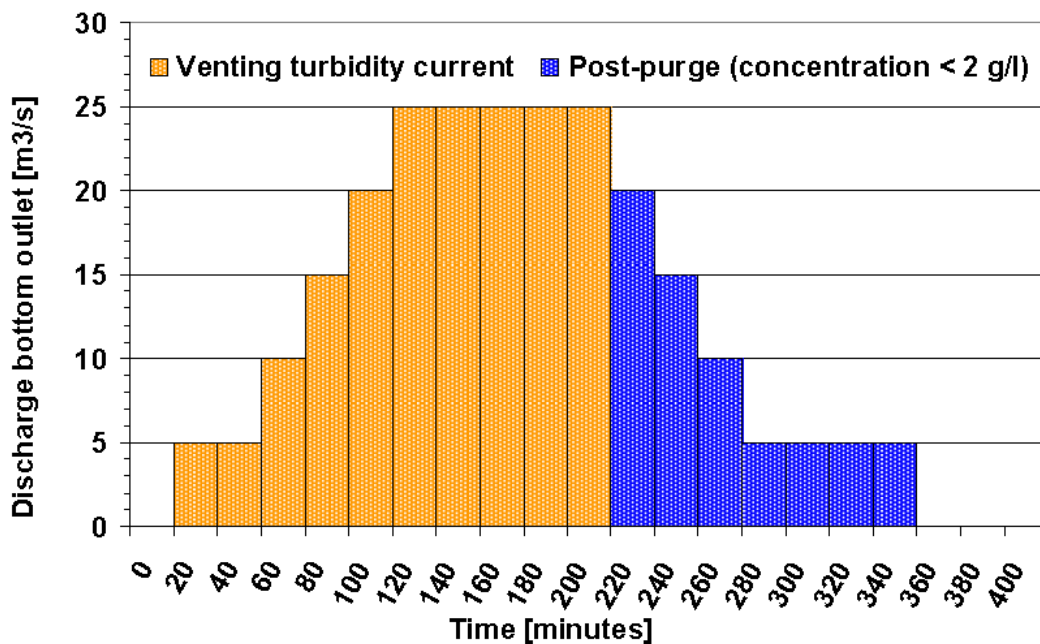

Figure 8: Bottom outlet discharge during and after turbidity current venting for SSC > 11 g/l (from Müller & De Cesare 2009)

3.4 Sediment removal

Gebidem Reservoir

The Gebidem Reservoir located at 1436 m asl on the Massa River in the Valais Alps intercepts annually around 400'000 m^3 of solid material. With a reservoir volume of only some 9.2 hm^3 and an annual runoff of 429 hm^3/a (period 1981 to 2000) from a 198 km^2 catchment (47.7 km^2 of which are partly diverted to another HPP), the

Capacity-Inflow Ratio is CIR = 0.021, and the reservoir life as the ratio of reservoir capacity to mean annual sediment volume amounts to 23 years. According to Sumi (2005) the Gebidem Reservoir is thus suitable for sediment flushing. The catchment mounting to more than 4000 m asl is highly glaciated (64%) as it drains the *Grosser Aletschgletscher*, the largest Alpine glacier 23 km long. Note that the runoff increased to 470 hm³/a during the last 10 years or so due to increased glacier melt (Meile *et al.* 2014).

A HPP with a head of 750 m is fed from the Gebidem Reservoir (Figure 9). As most of the runoff occurs during four months in summer only, the Bitsch HPP is operated by the owner Electra-Massa as a run-off river scheme. At a design discharge of 55 m³/s the turbine water contains between 10 and 13 kg of silt and sand, or an average of almost 40 t/h (www.alpiq.com). Due to the high SSC, the high quartz content of the mineral particles and the remarkable head, all of which decisive parameters as to hydro-abrasive erosion of turbines (Boes 2013, Abgottspon *et al.* 2014), the maintenance effort for the Pelton turbines is significant. This led to a raising of the water intake at the Gebidem Dam in 1996 (corresponding to the first concept of Figure 4) to reduce the abrasiveness of the turbine water due to smaller SSC and reduced mean particle diameter.
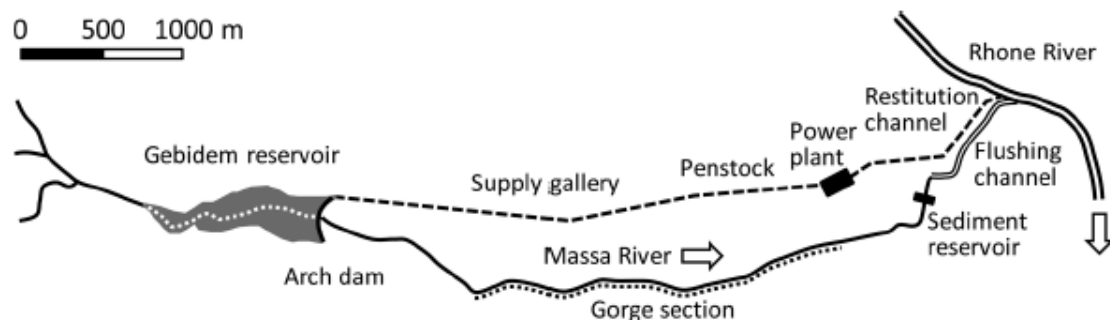

Figure 9: Elements of the hydropower scheme of Electra-Massa (from Meile *et al.* 2014)

The runoff carries some 450'000 m³/a of sediments as an annual mean, of which 10% is conveyed to the Bitsch HPP, while 90% is retained in the Gebidem Reservoir, which quickly fills up. These sediments must therefore be evacuated by annual flushing of the reservoir over 4 to 7 days to enable a sustainable use of the scheme (Meile *et al.* 2014). The flushing flows of 15 to 20 m³/s (Sumi 2005, Meile *et al.* 2014) cross the Massa Gorge, a small sediment retention reservoir with gravel extraction, and an artificial flushing channel before discharging into the Rhone River some 5 km downstream of the dam (Figure 9). Flushing is generally a complex operation for which optimal conditions are required, in particular concerning (Boillat & Pougatsch 2000)

- natural flow conditions in the downstream river(s),
- sediment transport capacity all along the downstream tributary,

- seasonal life cycle conditions of the fauna in the downstream river(s), and

- biochemical properties of the sediments.

In view of these requirements, the Valais cantonal authorities prescribe maximum volumetric sediment concentrations of 10 ml/l (corresponding to SSC values of some 16 to 20 g/l, depending on the sediment bulk density), which are, however, not met during flushing of Gebidem Reservoir (Meile *et al.* 2014). This is admitted in this particular case as the rocky gorge and the flushing channel downstream of Gebidem do not feature particular habitats from an ecological point of view. To account as much as possible for the boundary conditions given above, flushing usually takes place from May to June. Due to snow melt the discharges of the Massa and the downstream Rhone Rivers are then high and enable to increase dilution and limit adverse effects on the environment. To further dilute the sediment-laden flushing flows in the Massa River just upstream from the Rhone confluence with additional discharges of up to 15 m^3/s as well as to minimize the volume of flushing water and therefore production losses, a 500 m long dilution supply tunnel from a neighboring low-head HPP (Figure 10) has been constructed from 2005 to 2006 (Meile *et al.* 2014).
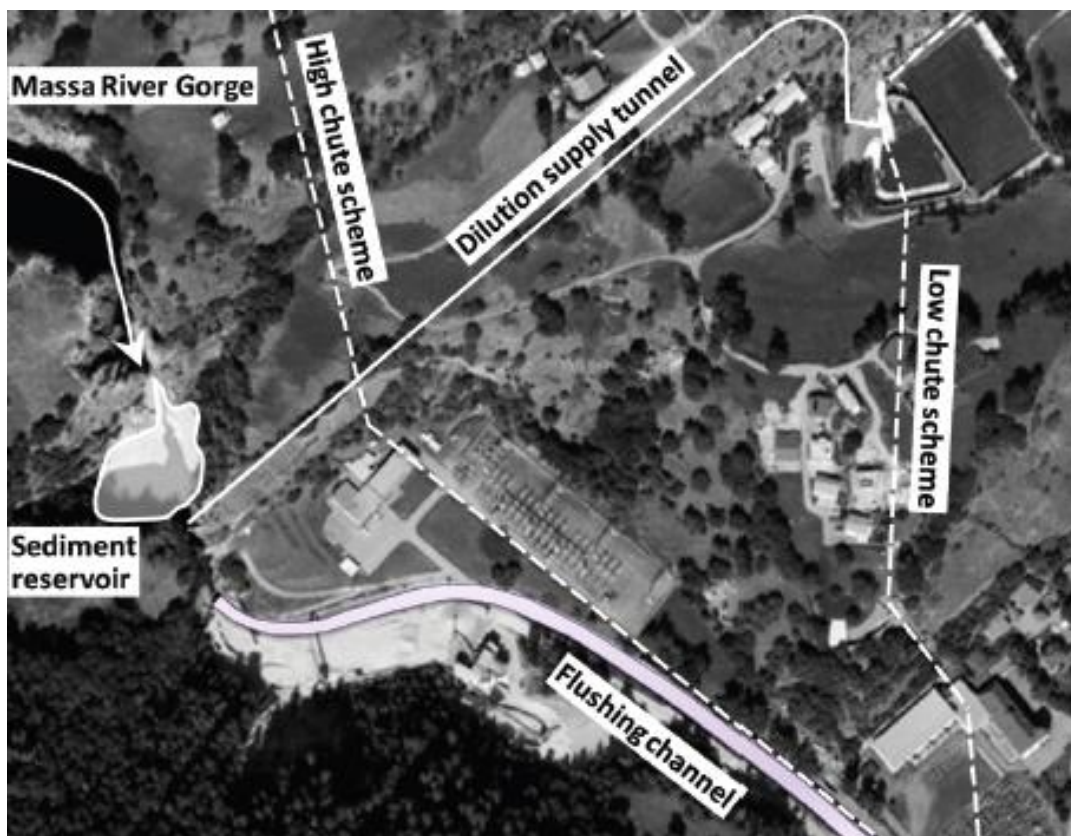

Figure 10: Schematic view of the dilution supply tunnel project (from Meile *et al.* 2014)

4 Discussion of Swiss case studies

The sediment management options given in the examples above are shortly discussed based on charts given by Sumi *et al.* (2005, Figure 11) and Annandale (2013, Figure 12).
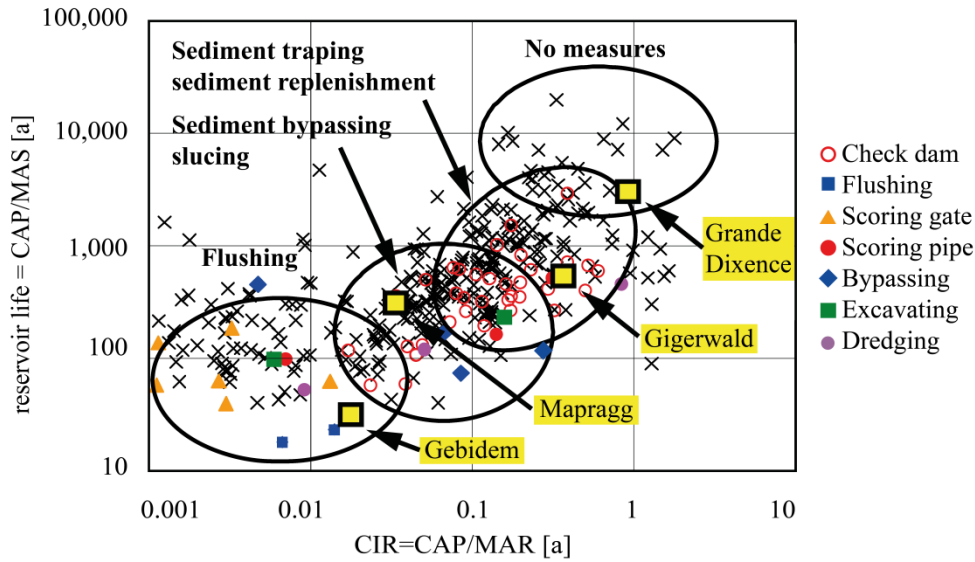

Figure 11: Sediment management options at Japanese reservoirs and of the Swiss case studies presented herein (from Sumi 2005)
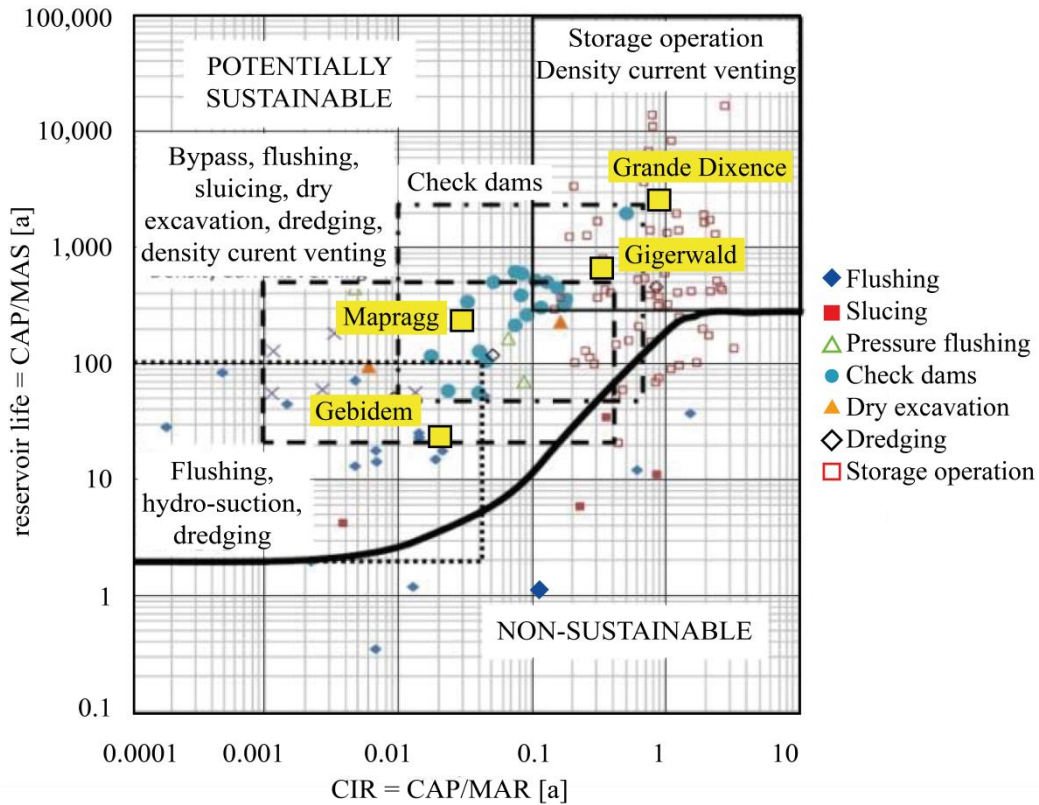

Figure 12: Categorization of reservoir sedimentation countermeasures (adapted from Annandale 2013)

206

According to these, the concept selected to counter sedimentation (see Figure 4) is particularly a function of both the reservoir life and the capacity inflow ratio. As depicted in Figure 11 and Figure 12, the respective concepts selected in the presented case studies agree well with the primary solution to be retained according to both Japanese and international experiences.

In brief, at the large annual storage reservoir Grande Dixence the dead storage is enlarged by taking advantage of the old Dixence Dam for sediment storage. With these methods the design life of the dam and the connected HPPs is expected to reach about a century. In the comparatively smaller Gigerwald Reservoir sediments will be bypassed at water intakes from an indirect catchment with water diversion in times of floods carrying the majority of fines into the reservoir by conducting real-time SSC monitoring at the intakes. Mapragg has a reasonable size for using a sediment bypass tunnel, sluicing or, alternatively, density current venting. The latter has been selected because this phenomenon is the driving factor of sedimentation problems at the dam outlets. Gebidem Reservoir is operated like a large water intake of a run-of-river HPP with annual flushing. Alternatively, according to Annandale (2013), sediment sluicing or bypassing around the dam to the downstream Massa River Gorge appear as viable options (Figure 12). Most importantly, according to Figure 12, all cases presented herein are judged to be potentially sustainable, i.e. above the dividing line separating sustainable and non-sustainable conditions.

5   Conclusions

Reservoir sedimentation reduces the active storage and leads to operational problems sooner or later. Most reservoirs worldwide are affected by sedimentation processes. Despite general knowledge of sedimentation processes, these phenomena were largely underestimated or not adequately taken into account in the past in the design, layout, construction and maintenance of dams and reservoirs. Although hydroelectric power is rightly regarded as a sustainable energy resource and is highly valuable in view of achieving climate protection goals, the sustainable use of storage plants for peak power production would be questionable without applying adequate reservoir sedimentation management techniques.

Although there are no patent remedies to avoid or to minimize reservoir sedimentation, a number of viable concepts and methods exist that have to be assessed individually for each single case due to the site-specific boundary conditions. Besides the technical feasibility, the economic soundness and ecological acceptability have to be considered. Four selected examples from Swiss reservoirs cover the whole spectrum of concepts to counter sedimentation and highlight the appropriateness of the measures taken in every case with respect to the theoretical reservoir life and relative reservoir volume.

References

Abgottspon, A., Staubli, T., Felix, D., Albayrak, I., Boes, R.M. (2014). Monitoring suspended sediment and turbine efficiency. *Hydro Review Worldwide*, 22(4): 28-36.

Annandale, G.W. (1987). Reservoir sedimentation. *Developments in water science* No. 29. Elsevier Science Publishers B.V., The Netherlands.

Annandale, G.W. (2013). Quenching the Thirst: Sustainable Water Supply and Climate Change, *Createspace*, ISBN-10: 1480265152.

Auel, C., Boes, R.M. (2011). Sediment bypass tunnel design – review and outlook. *Dams and reservoirs under changing challenges* (A.J. Schleiss & R.M. Boes, eds.), CRC Press/Balkema, Leiden, The Netherlands: 403-412.

Basson, G.R. (2009). Management of siltation in existing and new reservoirs. General Report Q. 89, *Proc. 23rd ICOLD Congress*, Brasilia, Brazil, 20 pages.

Boes, R.M., Auel, C., Hagmann, M., Albayrak, I. (2014). Sediment bypass tunnels to mitigate reservoir sedimentation and restore sediment continuity. *Reservoir Sedimentation* (Schleiss, A.J., De Cesare, G., Franca, M.J., Pfister, M., eds.), ISBN 978-1-138-02675-9, Taylor & Francis Group, London, UK: 221-228.

Boes, R.M., Felix, D., Albayrak, I. (2013). Schwebstoffmonitoring zum verschleissoptimierten Betrieb von Hochdruck-Wasserkraftanlagen ('Suspended sediment monitoring for wear-optimized operation of high-head hydropower plants'), *Wasser, Energie, Luft* 105(1): 35-42 (in German).

Boes, R. (2011). Nachhaltigkeit von Talsperren angesichts der Stauraumverlandung ('Sustainability of dams in view of reservoirs sedimentation'). *Mitteilung* 164, Lehrstuhl und Institut für Wasserbau und Wasserwirtschaft (H. Schüttrumpf, ed.), RWTH Aachen, Germany, 161-174 (in German).

Boes, R., Reindl, R. (2006). Nachhaltige Maßnahmen gegen Stauraumverlandungen alpiner Speicher ('Sustainable measures to counter sedimentation of Alpine reservoirs'). Proc. Symposium „Stauhaltungen und Speicher - Von der Tradition zur Moderne", *Report* 46/1, Institut für Wasserbau und Wasserwirtschaft, TU Graz, Austria, 179-193 (in German).

Boillat, J.-L., Oehy, C.D., Schleiss, A.J. (2003). Reservoir sedimentation management in Switzerland. *Proc. 3rd World Water Forum "Challenges to the Sedimentation Management for Reservoir Sustainability"*, Kyoto, Japan: 143-160.

Boillat, J.-L., Pougatsch, H. (2000). State of the art of sediment management in Switzerland. *Proc. Intl. Workshop and Symposium on Reservoir Sedimentation Management*, Tokyo, Japan: 143–153.

Bretz, N.-V., Barras, M. (2012). Sediment Management at Grande Dixence Dam. *Proc. Intl. Symposium on Dams for a changing World*, Kyoto, Japan, paper 345, 6 pages.

Cajot, S., Schleiss, A., Sumi, T., Kantoush, S. (2012). Reservoir sediment management using replenishment: A numerical study of Nunome Dam. *Proc. Intl. Symposium on Dams for a changing World*, Kyoto, Japan, paper 224, 6 pages.

Chanson, H. (1998). Extreme reservoir Sedimentation in Australia: a Review. *Intl Jl. of Sediment Research* 13(3), 55-63 (ISSN 1001-6279).

Facchini, M., Siviglia, A., Boes, R.M. (2015). Downstream morphological impact of a sediment bypass tunnel – preliminary results and forthcoming actions. Proc. First Intl. Workshop on Sediment Bypass Tunnels, *VAW-Mitteilung* 232 (R.M. Boes, ed.), ETH Zürich, Switzerland, 137-147.

Hauenstein, W. (2005). Vorstellung des Projektes ALPRESERV ('Introduction into the ALPRESERV project'). Proc. ALPRESERV «Gestion durable des sédiments dans les réservoirs alpins» ('Sustainable sediment management in Alpine reservoirs'), *Comm.* 22 (A. Schleiss, ed.), EPF Lausanne, Switzerland, 11-24 (in German).

KOHS, Kommission Hochwasserschutz im Schweizerischen Wasserwirtschaftsverband (2007). Auswirkungen der Klimaänderung auf den Hochwasserschutz in der Schweiz ('Effects of climate change on flood protection in Switzerland'), *Wasser, Energie, Luft*, 99(1), 55-57 (in German).

Meile, T, Bretz, N.-V., Imboden, B., Boillat, J.-L. (2014). Reservoir sedimentation management at Gebidem Dam (Switzerland). *Reservoir Sedimentation* (Schleiss, A.J., De Cesare, G., Franca, M.J., Pfister, M., eds.), ISBN 978-1-138-02675-9, Taylor & Francis Group, London, UK: 245-255.

Morris, G. L., Fan, J. (1998). *Reservoir sedimentation handbook: Design and management of dams, reservoirs, and watersheds for sustainable use*. McGraw-Hill, New York, USA.

Müller, Ph., De Cesare, G. (2009). Sedimentation problems in the reservoirs of the Sarganserland Kraftwerke - venting of turbidity currents as the essential part of the solution'). *Proc. 23rd ICOLD Congress*, Brasilia, Brazil, Q. 89 – R. 21, 13 pages.

Sakurai, T., Hakoishi, N. (2012). Present conditions and future prospects of sediment supply from reservoirs to downstream rivers. *Proc. 24th ICOLD Congress*, Kyoto, Japan, Q. 92 – R. 34, 22 pages.

Schleiss, A., Oehy, Ch. (2002). Verlandung von Stauseen und Nachhaltigkeit ('Reservoir sedimentation and sustainability'), *Wasser, Energie, Luft,* 94(7/8), 227-234 (in German).

Schleiss, A., De Cesare, G. & Jenzer Althaus, J. (2010). Verlandung der Stauseen gefährdet die nachhaltige Nutzung der Wasserkraft ('Reservoir sedimentation endangers the sustainable use of hydropower'), *Wasser, Energie, Luft*, 102(1), 31-40 (in German).

Sumi, T., Kantoush, S.A. (2011). Comprehensive Sediment Management Strategies in Japan: Sediment bypass tunnels. *Proc. 34th IAHR World Congress*. Brisbane, Australia, 1803–1810.

Sumi, T. (2005). Sediment Flushing Efficiency and Selection of Environmentally Compatible Reservoir Sediment Management Measures, East Asia of ICOLD, *Proc. Intl. Symposium on Sediment Management and Dams*, 2nd EADC Symposium, 9-22.

Sumi, T., Okano, M., Takata, Y. (2004). Reservoir sedimentation management with bypass tunnels in Japan. *Proc. 9th Intl. Symposium on River Sedimentation*. Yichang, China, 1036–1043.

Syvitski, J.P.M. (2003). Supply and flux of sediment along hydrological pathways: research for the 21st century. *Global and Planetary Change* 39(1): 1-11.

Vischer, D. (1981). Verlandung von Flussstauhaltungen und Speicherseen ('Sedimentation of stream ponds and reservoirs'). Proc. Intl. Symposium „Verlandung von Stauhaltungen und Speicherseen im Alpenraum". *VAW-Mitteilung* 53, Laboratory of Hydraulics, Hydrology and Glaciology (D. Vischer, ed.), ETH Zurich, Switzerland, 9-25 (in German).

Walling, D. E., Webb, B. W. (1996). Erosion and sediment yield: A global overview. *Proc. IAHS Publications - Series of Proc. and Reports,* Int. Association Hydrological Sciences 9: 2911-2921.

Wisser, D., Frolkin, S., Hagen, S., Bierkens, M.F. (2013). Beyond peak reservoir storage? A global estimate of declining water storage capacity in large reservoirs. *Water Resources Research* 49 (9): 5732-5739.

Authors

Prof. Dr. Robert M. Boes (corresponding Author)
Laboratory of Hydraulics, Hydrology and Glaciology (VAW), ETH Zurich
Email: boes@vaw.baug.ethz.ch

Michelle Hagmann
Laboratory of Hydraulics, Hydrology and Glaciology (VAW), ETH Zurich

210

Sediment bypass tunnel Runcahez:
Invert abrasion 1995-2014

Frank Jacobs, Michelle Hagmann

Abstract

In 1962 the Sediment Bypass Tunnel (SBT) at the compensation basin Runcahez, located in the Canton of Grisons in the Swiss Alps, went into operation. The invert of the SBT was made partly out of concrete and partly remained the bedrock. Already after a few years the tunnel invert has been severely abraded by the relatively coarse bed load requiring repair work nearly every year. In 1993 a research project was started to evaluate suitable types of concrete for the rehabilitation of the invert. In 1995 five types of special concrete were cast in test fields of 10 m length. The abrasion depths were measured by geodetic measurements and the conditions of the test fields were surveyed by visual inspections. The results showed that suitable types of concrete were abraded approx. 1 mm/year during 20 years.

1   Introduction

The SBT Runcahez is situated in the Canton of Grisons in the Swiss Alps in the valley of the river Somvixer Rhine (Figure 1). The Runcahez compensation basin is part of the Vorderrhein hydropower scheme/cascade operated by *Kraftwerke Vorderrhein AG*. The SBT was constructed at the beginning of the 1960s and went into operation in 1962.

In the inlet section invert was made of normal and special concrete (unreinforced). In the remaining downstream part of the tunnel the excavated rock forms the invert. According to core samples taken in 1995 the cube compressive strength was approx. 70 MPa for the normal and approx. 80 MPa for the special concrete (both approx. 30 years old). The first damages were reported in the late 1960s.The damages continuously occurred and almost yearly repair works were necessary and carried out. During refurbishment works in 1994 and 1995 a part of the tunnel invert, between the intake and the test fields, is paved with cast basalt tiles (Fig. 1).

The Runcahez SBT was on average put in operation 2.3 times per year and the yearly operation duration is approx. 12.3 h (mean data for the period 1962 – 1999). The diameters of the bed load components are typically $d_{50} = 0.16$ m, $d_{mean} = 0.23$ m, $d_{90} = 0.53$ m and $d_{max} = 1.20$ m. This SBT is an outstanding example with relatively short annual operation times and large sizes of bed load material resulting in severe invert abrasion.

2 Concrete test fields placed in 1995

A research work was launched in 1993 to investigate the process of abrasion and suitable materials for various types of hydraulic structures (e.g. weirs, channels, SBTs). The project was funded by the Swiss Association of Producers of Electricity (PSEL, currently called swisselectric) and the Association of the Swiss Cement Manufacturers (VSZKGF, currently called cemsuisse). The work was carried out by TFB (Technik und Forschung im Betonbau, Switzerland) and VAW (Laboratory of Hydraulics, Hydrology and Glaciology of ETH Zurich). The research work comprised mainly in-situ tests at Runcahez SBT and was completed in 2001 with the publication of the report by Jacobs *et al.* (2001).
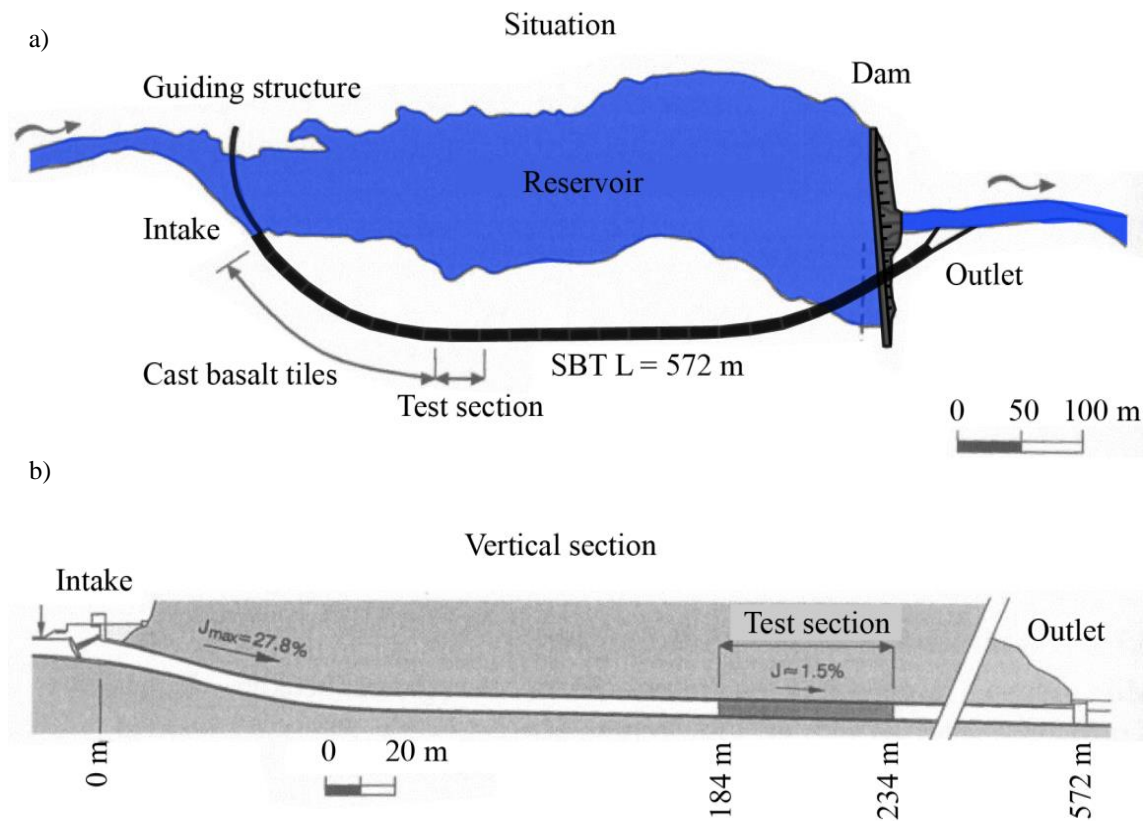
Figure 1: a) Layout and b) vertical section of the SBT Runcahez and location of the test fields (test section) in the bypass tunnel, after Jacobs et al. (2001)

In 1994 it was decided to test several types of concrete in the Runcahez SBT (Table 1). At this time it was not clear which process is the most damaging for the invert:

- Fracturing and breaking of brittle material due to impacting boulders saltating and rolling on the invert

- Abrasion of material with low resistance against grinding (when bed load components slide on the invert)

Therefore, the goal was to investigate the performance of different materials (Table 1). The concrete properties were tested on separately manufactured specimens. It is seen in Table 2 that the target properties were achieved. The roller compacted concrete (RCC) showed as expected generally the largest variability in the properties. This is attributed to the placement and compaction processes.

Table 1: Description and composition of tested types of concrete in the SBT Runcahez, from Jacobs *et al.* (2001); *three component polymer; **rounded river gravel

Concrete type	Concrete containing silica fume	High performance concrete	Steel fiber concrete	Roller compacted concrete	Polymer concrete EMACO APS T 2040
Abbreviation	SC	HPC	SFC	RCC	PC
Target properties	Very high strength, high modulus of elasticity	High strength, not too high modulus of elasticity	Very high strength, high modulus of elasticity, fibres for bridging cracks	Mean strength and modulus of elasticity, for convenient placing on large areas	Mean strength and low modulus of elasticity
Cement [kg/m^3]	450	500	480	400	1060*
Water/cement ratio	0.32	0.30	0.30	0.32	-
Additions [kg/m^3]	Silica fume: 40	-	Silica fume: 24 Steel fibers: 45	-	
River sand 0/4 mm [kg/m^3]	563	565	559	656	250
Basaltic gravel 3/15 mm [kg/m^3]	1505	1432	1405	1452	1250**

Table 2: Properties of the tested types of concrete in the SBT Runcahez; the properties are given for an age of 90 days, from Jacobs *et al.* (2001)

Concrete type	Concrete containing silica fume	High performance concrete	Steel fiber concrete	Roller compacted concrete	Polymer concrete EMACO APS T 2040
Cube compressive strength [N/mm^2]	109 ± 4	94 ± 3	114 ± 2	68 ± 12	68 ± 4
Modulus of elasticity [kN/mm^2]	57 ± 1	56 ± 1	58 ± 1	51 ± 4	13 ± 2
Splitting tensile strength [N/mm^2]	12 ± 1	10 ± 1	12 ± 2	9 ± 2	14 ± 1
Fracture energy [J/m^2]	210 ± 35	209 ± 35	1019 ± 412	143 ± 64	867 ± 93
Density [kg/m^3]	2683 ± 18	2655 ± 58	2726 ± 6	2568 ± 39	2360 ± 17

Each type of concrete was cast in a field of 10 m length and 3.8 m width. Between every test field a steel beam was placed with the intention of limiting the damage propagation from one field to the next. Before casting the concrete, an even underground was prepared (Figure 2): part of the old concrete was removed and the erosion channel in the middle of the tunnel width was levelled out with a normal concrete (approx. 45 MPa cube compressive strength at 28 days). In each field the concrete was cast in a thickness of 30 cm except for the polymer concrete. Due to its high price a thickness of 20 cm was chosen.
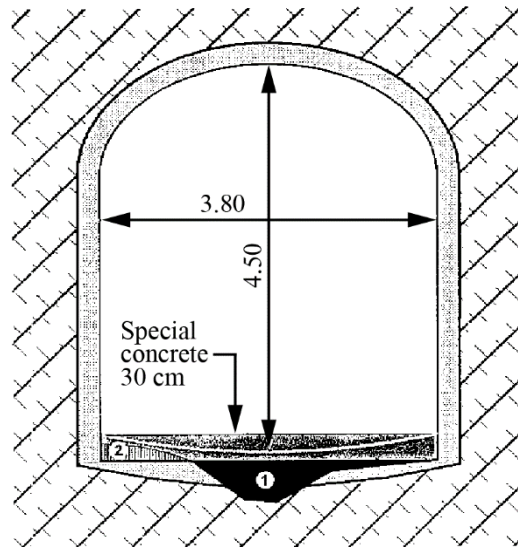
Figure 2: Cross section of the sediment bypass tunnel in Runcahez, ① casting of concrete to level out the underground ② removal of concrete, from Jacobs *et al.* (2001)

After the placement of concrete all fields were visually inspected. In every field cracks were observed (Figure 3). The cracks run more or less perpendicular to the flow direction and had in general widths of maximum 0.1 mm, except for the fields with silica fume containing concrete (up to 0.5 mm) and the polymer concrete (up to 2 mm). The cracks were mainly caused by the hydration heat under restrained conditions.
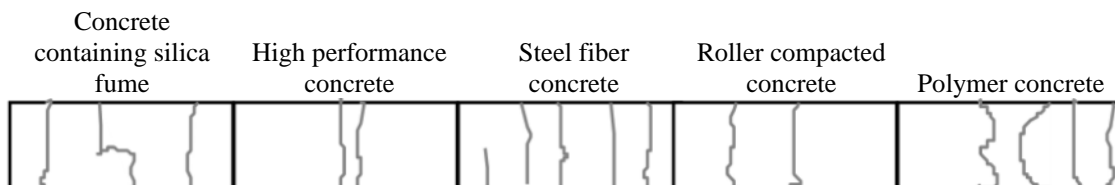

Figure 3: Cracks in the test fields visible some days after casting, the flow direction is from left to right (Jacobs *et al.* 2001)

3   Damages observed over 20 years

From 1995 to 1999, the surfaces of all five test fields were yearly monitored by geodetic measurements and visual inspections. A further inspection and further measurements

were carried out by Hagmann in 2012 and 2014, respectively. The following figures, partially based on data from Jacobs *et al.* (2001) and from Hagmann.

Figure 4 shows the development of the abrasion depths, averaged over each field, for the various types of concrete over the last 20 years. The mean abrasion rate was approx. 1 mm/year, except for the RCC field with a much higher rate. In Figure 5 the same abrasion values are shown as a function of the estimated bed load mass. The mean abrasion rate was approx. 1 mm/10'000 tons of bed load, again except for the RCC. Since no bed load measurements are available at this site, the bed load mass was estimated. From 1995 to 1999 the discharge and operation duration were measured and enabled bed load estimation based on the approach of Smart and Jaeggi (1983) (Jacobs *et al.* 2001). After 1999 mean annual bed load volume determined from 1996 to 1999 is assumed.

In Figure 6 and Figure 7 the local maximum abrasion depth per test field is displayed. The local abrasions were in general twice as deep as the averages per test field except for the RCC. The deep local abrasion in the RCC field is mainly attributed to insufficient compacting near the tunnel walls. As it was not possible to use a road roller close to the tunnel walls, the RCC had been compacted with a hand-held device. After one year of service it was already visible that more material was lost in these areas.
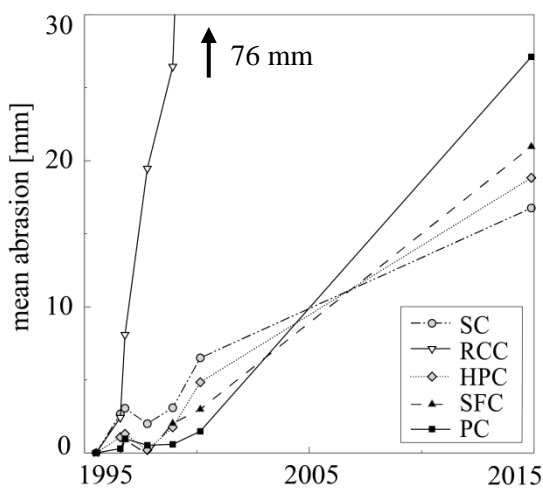

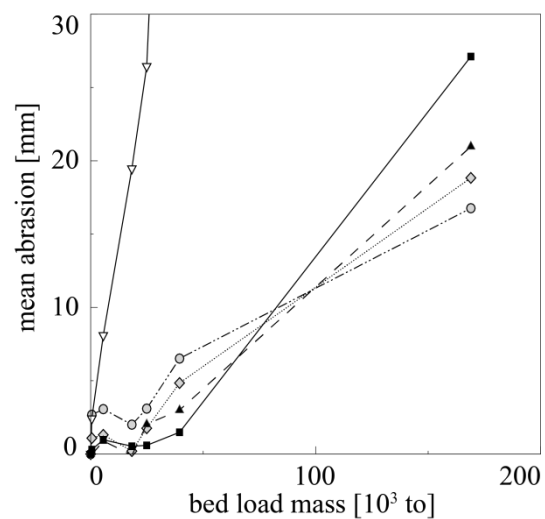Figure 4: Mean abrasion depths (averaged in each test field) over time (years)

Figure 5: Mean abrasion depths (averaged in each test field) as a function of bed load mass
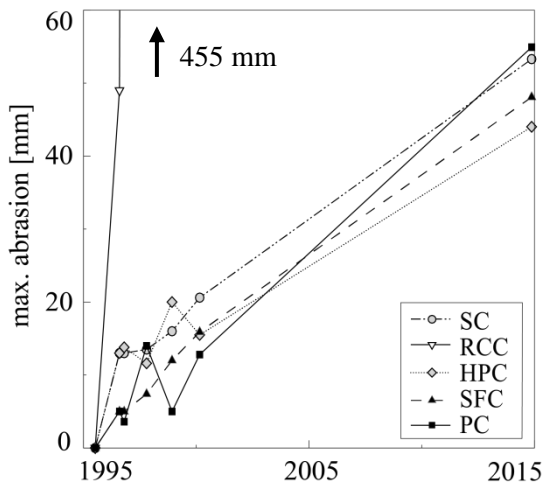
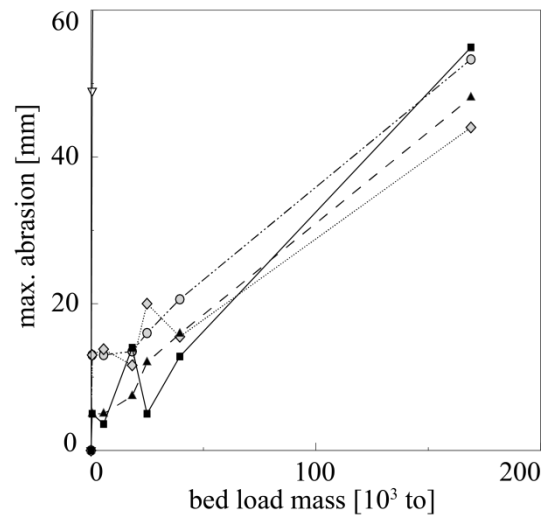Figure 6: Local maximum abrasion depths (per test field) over time (years)

Figure 7: Local maximum abrasion depths (per test field) as a function of bed load mass

A map of erosion depth in the RCC test field 5 years after construction is shown in Figure 8. . The damage along the tunnel walls continuously spreads out. Such spreading of an initial damage is a typical and dangerous process which can also be observed with pavements.

Figure 9 and Figure 10 show the abrasion map in the test field made of silica fume concrete after 5 and 20 years, respectively. It can be seen that the abrasion patterns are similar but amplified. This is typical for a self-intensifying harming process.
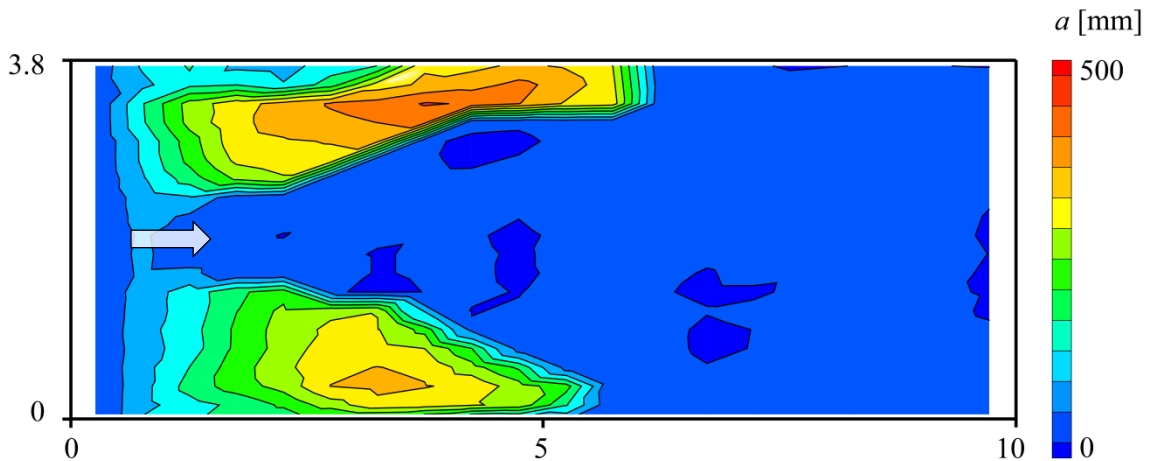

Figure 8: Top view on the RCC test field with erosion depth over 5 years (1995 to 1999), the arrow indicates the main flow direction
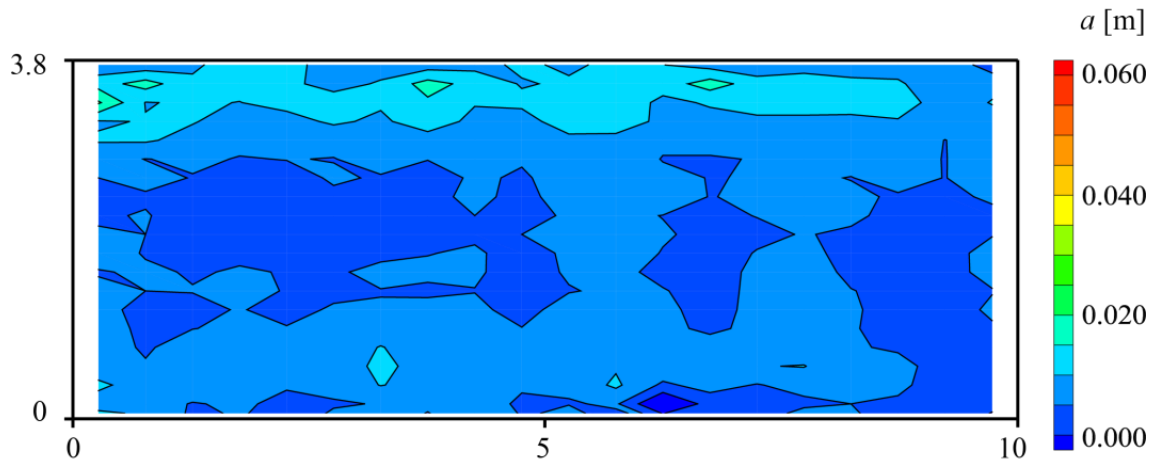
Figure 9: Top view on the test field made of silica fume concrete with abrasion depth over 5 years (1995 to 1999)
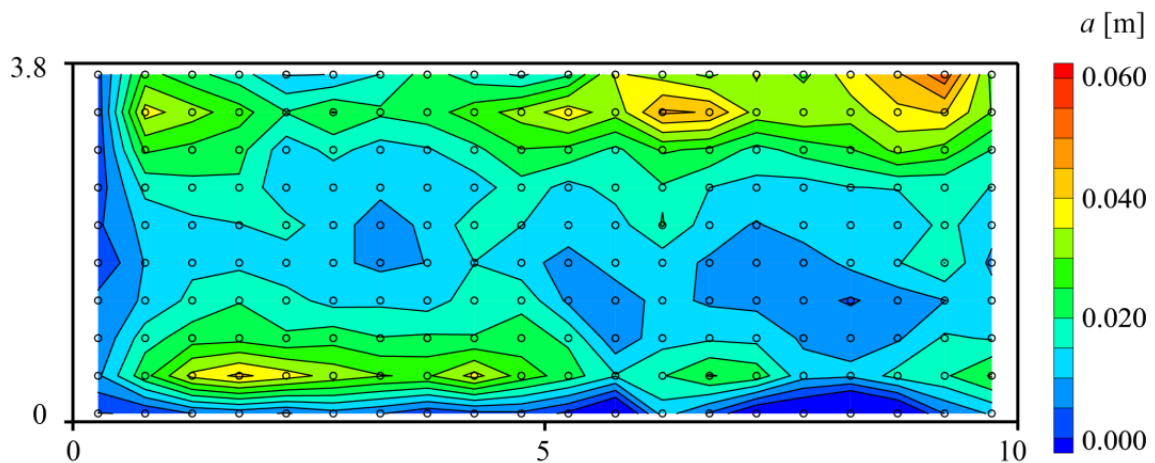

Figure 10: Top view on the test field made of silica fume concrete with abrasion depth over 20 years (1995 to 2014), circles represent measurement points

In 2012, no significant additional damages were observed along the (Figure 11). So far the cracks did not have any negative consequences. Moreover, uneven abrasion patterns on the inverts (Figure 10, Figure 12 and Figure 13) and a severe abrasion on the steel beams (Figure 14) were observed during many inspections.

Due their brittleness many cast basalt tiles got cracks by impacts of boulders (Figure 15). With further action of the bead load and the flow, the tiles fell apart and are swept away. From broken and missing tiles the destruction of the pavement propagates in flow direction.

It is interesting to note that the abrasion occurs mainly on the invert and only to a very small extent on the tunnel walls (Figure 16). At the lower part of the walls only a few millimeters of the normal type of concrete were abraded during 20 years.
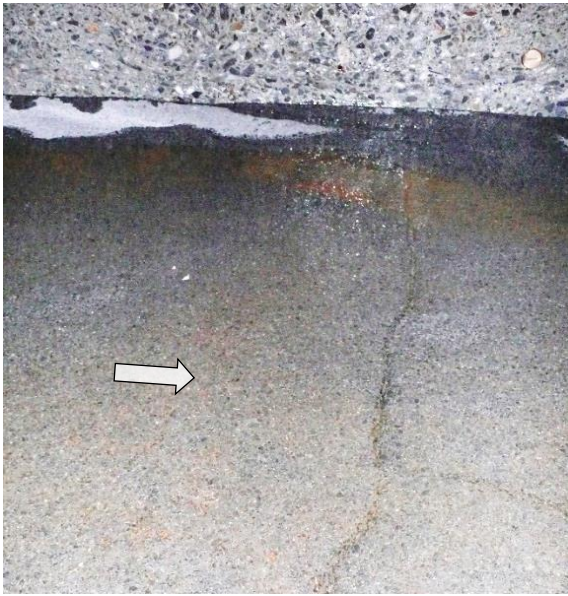
Figure 11: Crack in the HPC test field running perpendicular to the flow direction, picture taken 2012

Figure 12: Erosion channel on the normal tunnel lining, picture taken 2012

Figure 13: damage (uneven surface) in the HPC test field, picture taken 2012

Figure 14: Damage on the steel beam separating the HPC field (right) from the SFC field (left), basaltic aggregates (dark grains) are visible, picture taken 2012

Figure 15: Damage in an area with cast basalt tile paving, picture taken 2012

Figure 16: Minor damage due to abrasion in the PC test field and at the lower part of the wall (normal concrete), picture taken 2012

4   Conclusions

Five types of special concrete were tested on the invert of Runcahez SBT over the past 20 years. The SBT's annual operation time is relatively short, but the bed load components are relatively coarse. Abrasion depths were quantified by repeated geodetic surveys. Annual abrasion rates were calculated and abrasion rates with respect to the estimated transported bed load mass.

Excepting the RCC, for all types of special concretes, surface-averaged erosion rates of approx. 1 mm per year were determined. This corresponds to approx. 1 mm per 10'000 tons of bed load which were transported over the 3.8 m wide tunnel invert. These moderate abrasion rates result at this site in a tolerable maintenance effort and in a reasonable expected life time of a concrete invert with a usual thickness. The tests proved that adequate special concrete can be used under severe exposure conditions and maintain the stability of the tunnel invert as well as the tunnel itself.

For Runcahez SBT it is still not clear which property of the concrete is of utmost importance to reduce the abrasion and to characterize the abrasion resistance.

The proper implementation, especially the compaction of the concrete, is very important since small damages due to insufficient concrete compaction can rapidly spread out. The flatness of the concrete surface is also very important to avoid locally pronounced abrasion damages due to surface irregularities which could lead to larger damages.

It is expected that the invert concrete in this SBT with an original slab thickness of 30 cm will still be suitable for more than another decade if the size and/or quantity of the bed load is not significantly increased.

Acknowledgement

References

Jacobs, F., Winkler, K., Hunkeler, F., Volkart, P.(2001). Betonabrasion im Wasserbau (‚Concrete abrasion in hydraulic structures'), *VAW-Mitteilungen* 168 (H.-E. Minor, ed.), ETH Zurich, Switzerland.

Smart G. M., Jaeggi M. N. R. (1983). Sedimenttransport in steilen Gerinnen ('Sediment transport in steep channels'). VAW-Mitteilungen 64 (D. Vischer, ed.), VAW, ETH Zürich, Switzerland.

Authors

Frank Jacobs (corresponding author)
Technik und Forschung im Betonbau (TFB AG)
Email: jacobs@tfb.ch

Michelle Hagmann
Laboratory of Hydraulics, Hydrology and Glaciology (VAW), ETH Zurich
Email: hagmann@vaw.baug.ethz.ch

Solis sediment bypass tunnel: First operation experiences

Christof Oertli, Christian Auel

Abstract

The Solis dam was built in 1986 by the Electric Power Company of Zurich (ewz). Ever since the construction, large amounts of sediments accumulated in the reservoir and led to severe sediment aggradation. As a consequence, the storage volume was reduced by about 50% till 2012 causing loss of energy production. Additionally, in the near future sediments may have caused severe damage at the dam due to blockage of the bottom outlets. Therefore, in 2011 and 2012 a sediment bypass tunnel was realized in order to redirect the incoming sediments into the tailwater to inhibit sediment aggradation. Since its inauguration, the tunnel was operated four times including a 100-year flood event in August 2014. First operational experiences are described herein.

1 Introduction

The Solis reservoir, built in 1986 by ewz, is located in the canton of Grisons in the south-eastern part of the Swiss Alps. The reservoir is retained by an arch dam of 61 m height with a crown length of 75 m. The reservoir is fed by the turbined water of the upstream power plants Tiefencastel Ost and West as well as the Albula and Julia River. The reservoir itself provides the water supply for the two power plants Sils and Rothenbrunnen taking the function of a daily storage.

The original volume of the reservoir was 4.1 million m^3 with an active storage volume of 1.5 million m^3. The reservoir is operated between the minimum level of 816 m a.s.l. and the full supply level of 823.75 m a.s.l. according to the active volume range.

Due to the large catchment area of 900 km^2, an average annual amount of 80'000 m^3 sediment material accumulated in the reservoir. The narrow topology of the reservoir caused a one-dimensional sediment aggradation process progressing towards the dam. From 1986 to 2008 the sediment aggradation caused a decrease of the active storage of 1.0 million m^3 (Auel *et al.* 2011). Figure 1 illustrates the annual aggradation of the reservoir obtained by echo-sounding surveys. In 2012, about half of the original reservoir volume was filled with sediments.
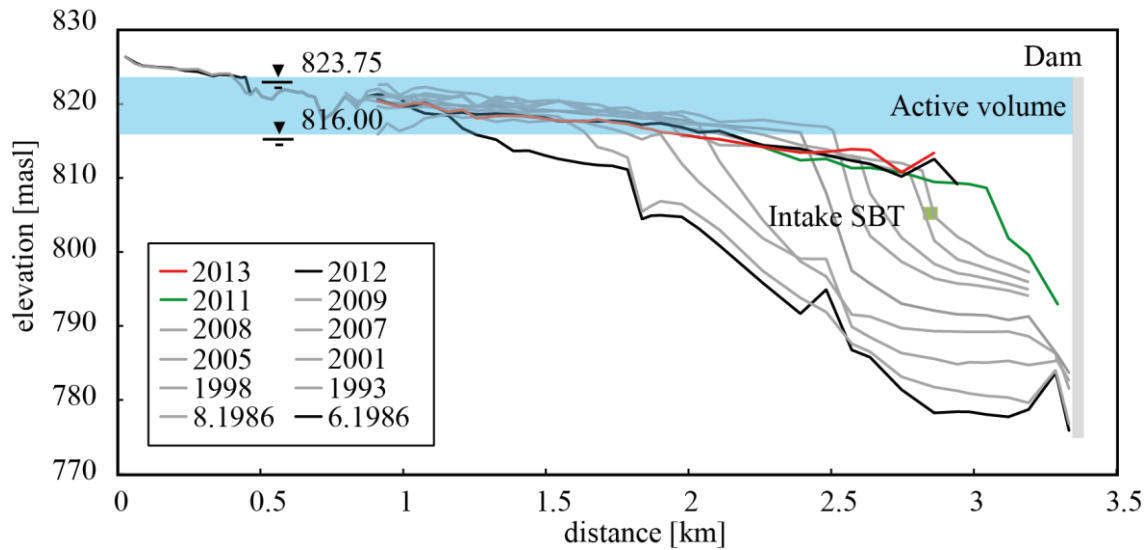
Figure 1: Sedimentation at Solis reservoir (courtesy of M. Hagmann)

2   Feasibility study of countermeasures

The sediment aggradation derogated an economical operation of the hydropower plants and endangered the operational safety of the bottom outlets. Different alternatives were studied in order to avoid these negative impacts and restore the active storage volume. Strategies such as dredging, free surface flushing, sluicing and bypassing through a tunnel were considered (Auel *et al*. 2010, Auel *et al*. 2011). Mechanical dredging turned out to be inappropriate due to both ecological and economic reasons. Flushing sediments through bottom outlets in free surface flow was not considered as an effective countermeasure as well because of the low capacity of the bottom outlets. Another problem was the financial loss due to a complete reservoir drawdown and the resulting plant shutdown. Furthermore having in mind that flushing has to be done during natural flood events emerging rapidly, reaction time would be short for a complete drawdown.

Partial drawdown sluicing and bypassing through a tunnel seemed to be adequate strategies and have been examined in hydraulic model tests at the Laboratory of Hydraulics, Hydrology and Glaciology (VAW) of ETH Zurich (Berchtold and Lais 2008, Auel *et al.* 2010, 2011). Sluicing sediments through the bottom outlets resulted in both a funnel-shaped cone in the bottom outlet vicinity and an entire degradation of the aggregation body throughout the reservoir. The extent of the degradation depended on both the inflow discharge and the level drawdown magnitude. The sluicing process lead to a relocation of the already aggregated sediments towards the dead storage and allowed the newly incoming sediments to be guided through the reservoir into the tailwater. Thus, the model tests showed that sluicing is an effective strategy to keep the active volume free from sedimentation (Berchtold and Lais 2008). However, some drawbacks were emphasized. The bottom outlets are small and likely prone to blockage by driftwood and mudslides of fine sediments. Additionally severe abrasion in the

outlets was expected and safety concerns arose due to the fact that the closing process of the gates could be inhibited by clogging sediment.

Besides the sluicing technique, a sediment bypass tunnel (SBT) was studied to guide the incoming sediments into the tailwater (Auel *et al.* 2010, 2011). The tunnel was not located at the reservoir head as mostly applied worldwide (Auel and Boes 2011), but located about 450 m upstream of the dam. Consequently the bypass only minimizes sedimentation in the lower reservoir part. Similar to the sediment sluicing, the reservoir level is partially lowered to obtain free surface flow conditions at the upper reservoir forcing sediment transport towards the intake. The model results showed that the tunnel bypasses all incoming coarse sediments independent of the flood discharge. However, if the design discharge is exceeded, a surplus flow passes the tunnel intake and leads parts of suspended sediments to the front of the reservoir. Blockage of the tunnel intake was considered as less likely compared to the bottom outlet sluicing as the area of the tunnel was 4.3 times larger. Additionally, blockage due to driftwood was minimized by adequate structural measures guiding the material towards the dam.

For a sound comparison of the two strategies ewz quantified the economic benefits of both methods having in mind that the larger the active volume the higher the benefit. The key parameters to obtain an active volume free from sediment deposition are the incoming discharge and water level drawdown regardless of the routing technique. Hence, sluicing and bypassing are identically considered as an effective measure to keep the active volume free from sediments. In a second step, the risk probability of both strategies, i.e. the blockage of the bottom outlets or the tunnel intake, was quantified and compared with the costs (Oertli 2009). On the one hand sluicing sediments through the bottom outlets caused higher risks but showed better profitability whereas flushing sediments through a bypass tunnel caused lower risks at a lower profitability. Sluicing included a number of high risks which may lead to a complete plant shutdown over a long period, while flushing through a tunnel shifted these risks to a new structure upstream and away from the dam and power intake vicinity.

The total cost of the SBT amounted to 37 million CHF being about 18 million CHF more expensive as estimated. The annual costs for maintenance and repair were estimated to 880'000 CHF. This value seems to be conservative from today's perspective as the invert abrasion is low so far (Hagmann *et al.* 2015). The alternative sluicing strategy through the bottom outlets would have caused investments of only about 2.0 million CHF and annual costs for maintenance and repair of 350'000 CHF. Additionally, the above described high risks of the bottom outlet sluicing were transferred to equivalent monetary costs leading to the situation that both strategy costs were almost identically rated. Moreover, Solis reservoir is an important power hub between other ewz HPPs up- and downstream, so that a shutdown would affect power

production of a number of plants. Therefore, ewz decided to choose the sediment bypass tunnel as countermeasure.

In Europe, energy is traded at the European Energy Exchange in Leipzig, Germany (EEX). The presented economic calculations and decisions were mostly based on energy prices in 2008. As the market-based price for electric power in Europe significantly decreased since then (Figure 2), the comparison would probably lead to a different result today.
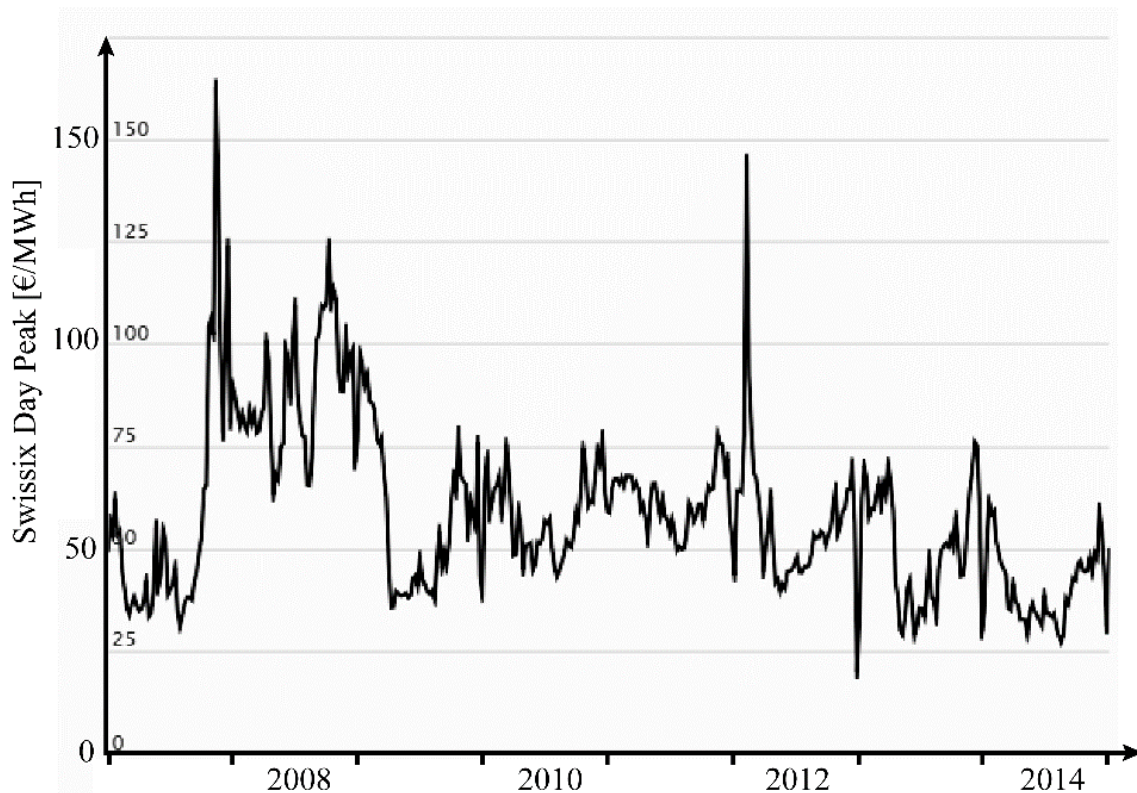

Figure 2: EEX *Swissix Day Peak* price from 2007 to 2014 (www.eex.com)

3   Sediment bypass tunnel design

The SBT design was developed in close collaboration with VAW of ETH Zurich (Auel *et al.* 2010, 2011). The tunnel was constructed from 2011 to 2012 and consists of the components described in the following (Figure 3). A 140 m guiding structure crosses the reservoir from the left to the right bank and leads the sediment laden inflow to the inlet structure. The tunnel intake is located around 450 m upstream of the reservoir on the right bank and not at the reservoir head. Consequently, the water enters in pressurized inflow conditions with a maximum energy head of about 20 m at maximum reservoir level. However, the reservoir is lowered prior a flood event leading to free flow conditions upstream of the intake and provoking the sediment to be transported towards the tunnel. The minimum reservoir level of the active volume (816 m a.s.l.) was defined as the standard for flushing events (Figure 4).
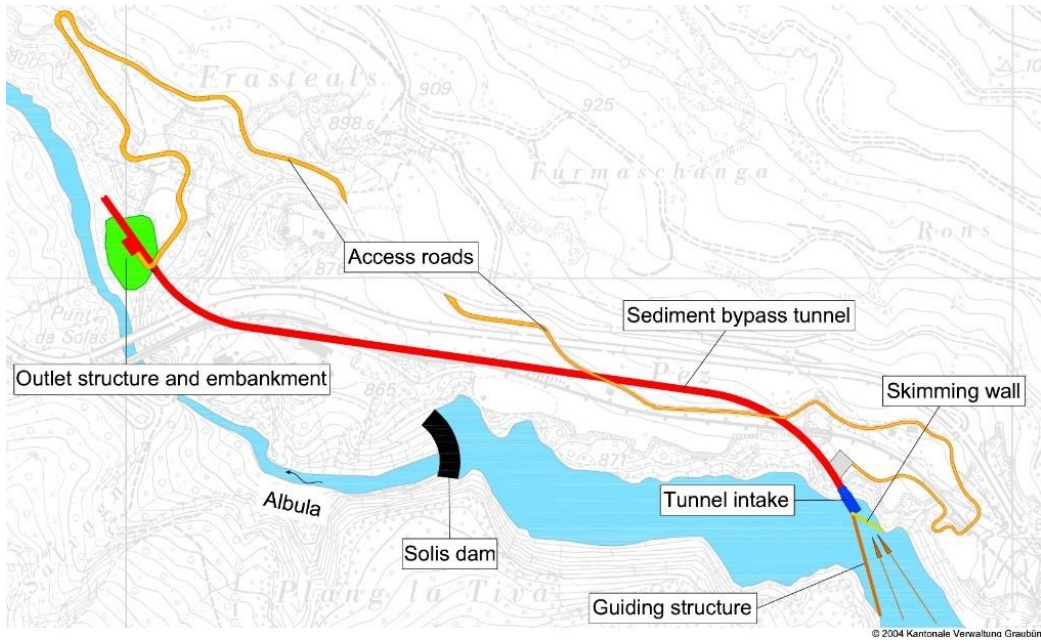
Figure 3: Overview of Solis sediment bypass tunnel (adopted from Auel *et al.* 2011)
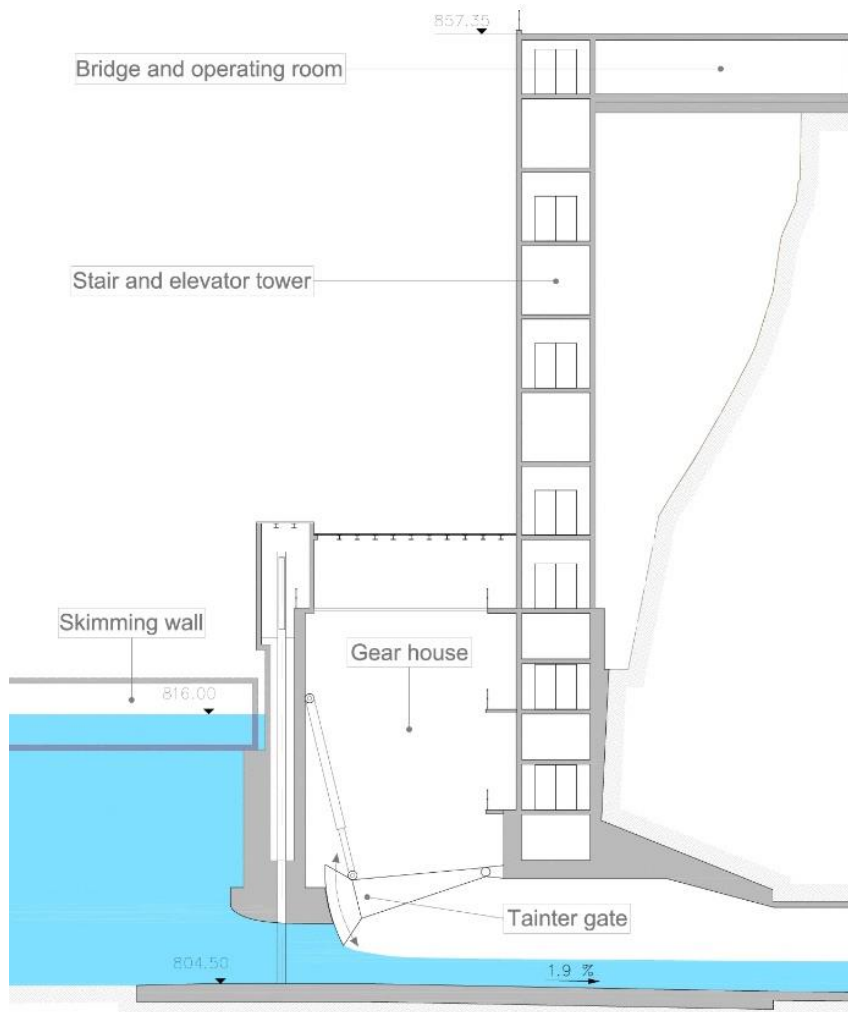

Figure 4: Detail of tunnel intake (adopted from Auel *et al.* 2011)

However, the upstream erosional effect is substantially higher for lower levels. Depending on the future conditions, bypassing with lower levels (e.g. 814.5 m a.s.l.) may be considered. The design capacity of the tunnel is $Q_d = 170$ m³/s (flood event occurring approximately once in 5 years). A tainter gate regulates the inflow into the tunnel. Stop logs located in front of the gate are used for revision.

In case of high floods exceeding the design tunnel discharge, a partial flow is guided towards the dam trough an opening in the guiding structure. Additionally as skimming wall guides incoming driftwood safely towards the dam, where it is mechanically removed or flushed over the spillway (Figure 5). These facilities were optimized in the hydraulic model tests described in Section 2 (Auel *et al.* 2010, 2011).

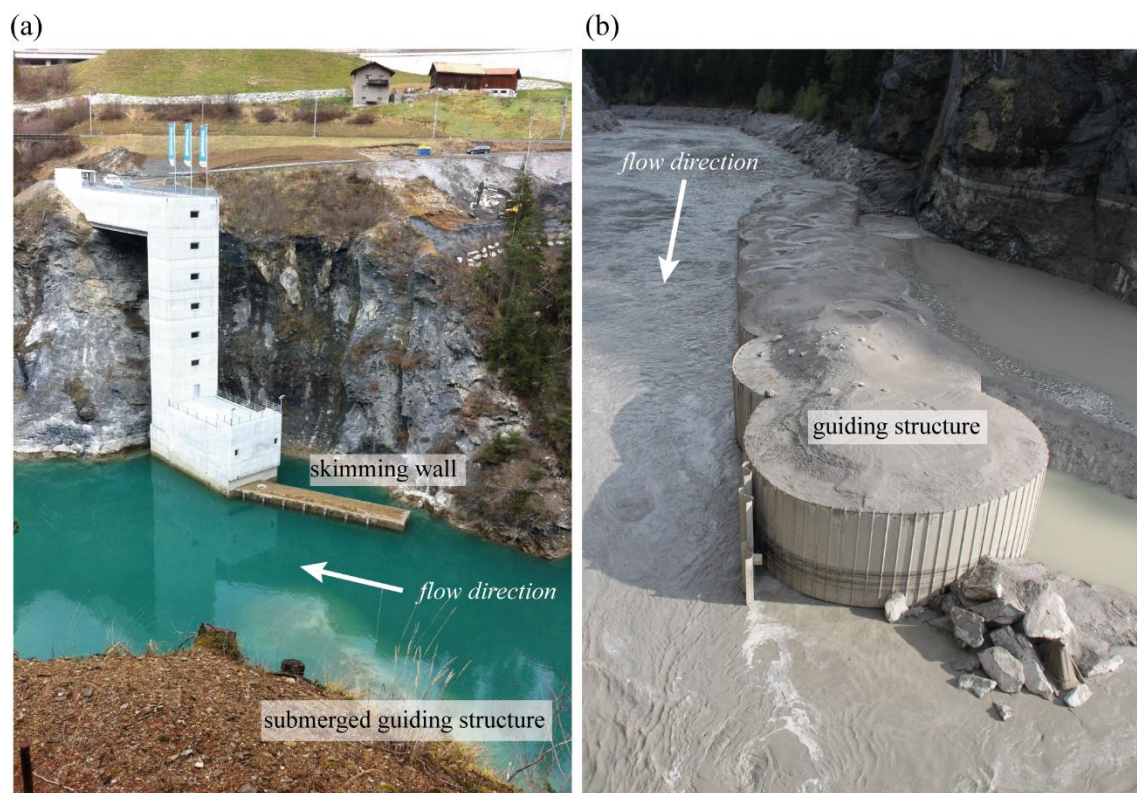(a)   (b)

Figure 5: (a) Tunnel intake with tower in November 2012. View from left bank. Reservoir level at approx. 820 m a.s.l. (b) Detail of guiding structure during bypass operation at May 3rd 2013. Reservoir level at approx. 816 m a.s.l. (courtesy of ewz)

The total length of the tunnel including the intake and outlet is 968 m with a constant bed slope of 1.9%. The cross section is constructed as an archway type with a width of 4.40 m and a height of 4.68 m. The invert is concrete lined using an abrasion-resistant high performance concrete with a compression strength $f_c \geq 70$MPa (Hagmann *et al.* 2015). Downstream of the dam, the water is released through a 100 m long cantilever outlet structure and drops about 8 m into the Albula River (Figure 6).

Figure 6: Cantilevering tunnel outlet during operation on May 23rd 2014 (courtesy of C. Auel)

4   Measurements at Solis reservoir

The Solis reservoir is equipped with a range of devices measuring the in- and outflow as well as the sediment load. Discharge is measured at gauging stations in the Albula and Julia River operated by the Federal Office of the Environment (FOEN). Also the discharge released by the upstream HPP Tiefencastel West and Ost is known, thus the total inflow into Solis reservoir is precisely predictable. The outflow consists of the turbined water at Rothenbrunnen and Sils as well as the bottom outlet, spillway and bypass tunnel discharges in case of flood events. All values are recorded by ewz.

Suspended sediment load is measured using turbidity meter at Albula gauging station upstream of the reservoir and downstream of Sils HPP in the tailrace channel. Additionally, suspended and bedload are measured in the bypass tunnel using geophones for the latter (Hagmann *et al.* 2015).

Finally, reservoir sedimentation is surveyed almost every year using echo sounding (compare Figure 1).

5   First tunnel operation

The sediment bypass tunnel operated for the first time on May 3rd 2013 in order to divert a minor flood during the snowmelt period. A maximum discharge of 110 m³/s was routed through the tunnel during 12 hours runtime in total. As a result, sediment aggradation upstream of the intake was levelled to a homogenous gradient of 3.8‰ and sediment was shifted closer to the inlet structure. The net sedimentation increase

upstream of the intake was about 10'700 m^3 compared to the survey prior the flood event. This increase was expected as the bed level of the upstream reservoir part had to adapt to the new flushing conditions with a low reservoir level.

After a further minor flood in spring 2014, a 100-year flood event occurred on August 13th 2014 in the Albula River. A maximum discharge of 288 m^3/s was recorded, of which 179 m^3/s were routed through the sediment bypass tunnel. Mastering this event with a new bypass facility was a challenge for the task force team. At the same time, a train derailed close to the reservoir head and was in danger to slide into the reservoir. Thus the reservoir level had to be lowered between 814 and 816 m a.s.l. due to police instructions. The tunnel operation lasted 14 hours in total.

Sedimentation in the reservoir increased by approximately 102'000 m^3. At a similar flood event in 1987 with a comparable maximum inflow of 252 m^3/s, sedimentation increased by 248'000 m^3. The comparison between the two flood events in 1987 and 2014 shows that a large amount of sediments was routed through the sediment bypass tunnel. Further details regarding the bypassed sediments are published in Hagmann *et al.* (2015).

6 First operator impressions

So far the sediment bypass tunnel masters the flood events impeccably without any technical problems. The hydraulic system, the abrasion-resistant invert lining and the driftwood diversion function particularly well. Based on the hydraulic model experiments, the intake and guiding structure are designed well. All facilities operate as described in the experiments.

An optimal SBT operation requires a sufficient preliminary lead time. The reservoir level has to be lowered to 816.0 m a.s.l., different operation systems have to be taken into service, sediment concentration measurements have to be installed in the rivers and a number of specialists as well as auxiliary staff needs to be mobilised. Thus, the monitoring of the weather forecast is crucial. However, a reliable forecast is challenging as the effective rainfall in the catchment area is influenced by both the southern and northern meteorological conditions.

The head of operations takes the decision, if SBT operation is initiated. Due to the above-mentioned reasons, this decision needs to be taken as early as possible. However, a premature decision is prone to the risk of a cost-intensive and nerve-stretching operation cancellation in case the flood turns out to be minor. Therefore, a decision support system to simplify and sustain the decision-making process is of utmost interest.

A further important aspect of the tunnel operation is the energy management. If the reservoir is lowered below 816.0 m a.s.l., HPP Sils and Rothenbrunnen have to shut down. A short-term outage of a power plant leads to a considerable economic damage

because alternative energy needs to be acquired on the energy stock exchange leading to high penalties for the operators due to guaranteed system services. Hence, the decision on which level the operation should be conducted also depends on the current market situation.

The current SBT operation is comparable to a *blind flight*. The only information at disposition are the gauging stations in rivers and the reservoir itself as well as the suspended sediment concentration measurements (Section 4). Thus it is very challenging to ensure an optimal operation based on only this information. The head of operations has to estimate both the operation duration and the amount of bypassed water while keeping the reservoir level preferably constant. The level is effected by the opening of the tunnel intake gate as well as the bottom outlet and HPP headrace tunnels. There is a substantial potential to waste water (and money) due to imprecise flushing operation.

It is planned to use the direct sediment transport measurements by geophones (Hagmann *et al*. 2015) as an additional information to provide detailed knowledge if sediment is still transported with the flow. This information is considered as very helpful as the effect of reservoir level variation can be directly correlated to change in sediment transport. So far, the recorded data is used by VAW but not included as a real-time measurement in the operation process.

7   Ecological aspects

The first five years of operation, i.e. until 2017, a concentrated ecological monitoring is conducted. In addition to the direct effects to the habitat in the tailwater, also the long-term and indirect effects of the flushing events will be measured, i.e. the invertebrate, river bed clogging and reproduction of the aquatic fauna. Today's obvious lack of sedimentation will be replenished in the upcoming years. It is assumed that a natural habitat for flora and fauna will develop.

The following aspects directly affect the success of the ecological benefits. On the one hand it has to be ensured that the natural flood hydrograph as well as the sediment concentration can be maintained also downstream of the dam. Especially the sediment concentration of the declining flood has to be monitored considering a subsequent rinsing with clean water. On the other hand attention should be paid to the sediment concentration during reservoir drawdown prior the flushing process. The downstream sediment concentration should be limited and not reach unnaturally high levels: The limit for the average concentration is 40 mg/l, while short peaks can be higher.

In 2017, the results of this ecological monitoring will be analysed and definitive requirements regarding the operation of the sediment bypass tunnel will be elaborated.

8 Conclusion

The Solis sediment bypass tunnel operated well in the first two years after commissioning. However, sediment aggradation increased in the reservoir due to a 100 year flood event in summer 2014 exceeding the design capacity of the tunnel by about 40%. As a result the surplus inflow was diverted to the dam causing sedimentation of suspended load at the dam vicinity.

Certain organisational challenges arose in the first years showing that several more years of experience are still required to ideally operate the tunnel considering ecological, economical and operational aspects.

Moreover, the Solis sediment bypass tunnel is an excellent example for interdisciplinary collaboration. The positive cooperation between the academically-oriented specialists of ETH Zurich, the practice-oriented engineers and qualified HPP staff at ewz led to success of the design, construction and operation of the tunnel.

Acknowledgments

9 References

Auel, C. Boes, R.M. (2011): Sediment bypass tunnel design – review and outlook. *Proc. ICOLD Symposium „Dams under changing challenges"* (A.J. Schleiss & R.M. Boes, eds.), 79th Annual Meeting, Lucerne. Taylor & Francis, London, UK, 403-412.

Auel, C., Boes, R., Ziegler, T., Oertli, C. (2011). Design and construction of the sediment bypass tunnel at Solis. *Hydropower and Dams* 18(3), 62–66.

Auel, C., Berchtold, T., Boes, R. (2010). Sediment management in the Solis reservoir using a bypass tunnel. *Proc. 8th ICOLD European Club Symposium*, Innsbruck, Austria, 438–443.

Berchtold, T., Lais, A. (2008). Entlandung Stausee Solis: Modell- und Naturversuche zur Geschiebeumlagerung (Desilting of Solis reservoir: Model- and nature tests regarding sediment reallocation). Int. Symposium "Neue Anforderungen an den Wasserbau", ETH Zurich, Switzerland, *VAW-Mitteilungen* 207, 305-315 (in German).

Hagmann, M., Albayrak, I., Boes, R.M. (2015). Field research: Invert material resistance and sediment transport measurements. Proc. First Int. Workshop on Sediment Bypass Tunnels, *VAW-Mitteilungen* 232 (R. Boes, ed.), ETH Zurich, Switzerland.

Oertli, C. (2009). Entlandung des Stausees Solis durch einen Geschiebeumleitstollen (Desilting of Solis reservoir using a sediment bypass tunnel). *Wasser Energie Luft* 101(1), 5-9 (in German).

Authors

Christof Oertli (corresponding Author)
Electric Power Company of Zurich (ewz), Switzerland
Email: christof.oertli@ewz.ch

Dr. Christian Auel
Water Resources Research Center, Disaster Prevention Research Institute, Kyoto University, Japan, formerly VAW, ETH Zurich, Switzerland

Rehabilitation of the Palagnedra sediment bypass tunnel (2011-2013)

Andrea Baumer, Riccardo Radogna

Abstract

The sediment bypass tunnel (SBT) at the Palagnedra compensation basin, owned and operated by Maggia Power Plants in southern Switzerland, was completed in 1977. Mainly during and after severe floods in 1978 and the early 1980s, in which the SBT proved to be effective against reservoir sedimentation, the tunnel invert and the underlying Gneiss rock were eroded up to 4 m deep. In three winters from 2011 to 2013, rehabilitation works were carried out on the most downstream 350 m of the SBT. The erosion trenches were filled with compacted gravel in the lower parts and with steel fibres concrete in the upper 1.2 m. On top, a 30 cm thick invert slab was rebuilt using a special concrete with higher resistance against abrasion. In the most downstream 100 m of the SBT erosion is monitored since 2011 by regular theodolite survey and occasional laser scans.

1   Introduction

The Palagnedra compensation basin is part of the Maggia Power Plants, which use the waters of a 750 km^2 catchment area in the southern Swiss Alps. Five hydropower plants (HPPs) with an installed capacity of around 600 MW produce on average over 1'300 GWh/a. The lowest stage of the cascade, between Palagnedra and the Verbano power station located at the Lago Maggiore, contributes with over 500 GWh/a.

The 72m high gravity dam of the Palagnedra compensation basin was completed in 1953. A reservoir of 4.8 Mio m^3 was created along the Melezza River (Figure 1). The capacity of the Verbano HPP is 55 m^3/s. The annual mean turbine discharge is 25 m^3/s of which 5.4 m^3/s come from the direct catchment area of the Melezza River (140 km^2). The rest comes from the upper stages HPPs (capacity 40 m^3/s). The annual mean flow of the Melezza is 7.3 m^3/s. When the inflows exceed the capacity of the Verbano HPP, up to 30% of the Melezza's total annual discharge volume is spilled at the Palagnedra dam during some 10 to 15 days, quite equally distributed during the year except for the period between mid-December and mid-March.

The Melezza flows from West to East, the valley is thus perpendicular to winds blowing from the South, i.e. the Mediterranean Sea. The mountains in the Melezza catchment emerging at the edge of the Padania plain create a first obstacle to such winds with high

humidity. This may cause intense and abundant rainfall: The average annual precipitation reaches 2'200 mm, with extremes of 91 mm per hour (1993) or 414 mm per day (1983). This leads to quick and strong increases in river discharge: in some 4 to 5 hours the flow easily goes from 4 m^3/s to over 200 m^3/s, with peaks over 1'000 m^3/s.

In 1953 the Palagnedra dam was dimensioned for a discharge of 500 m^3/s; this had been estimated to correspond to a flood with a return period of 100 years. No particular attention had been paid to solid transport. Just a few years after completion, problems began with sediment inflows of 70'000 to 130'000 m^3 per year and flood peaks exceeding the spillway design discharge. The first measure against sedimentation was to install a pumping system which was in operation during several winters (from 1968 to 1973) and permitted to keep the power water intake free of sediments. As the active storage capacity was reduced year after year, a long term solution needed to be found quickly. A sediment bypass tunnel (SBT) was chosen. Good conditions for a SBT were present: a narrow valley upstream of the dam where a new auxiliary dam could easily be built, most solid transport into the reservoir occurring during spillage at the dam, and relatively short distance from the upper reservoir reaches to the river downstream of the dam.
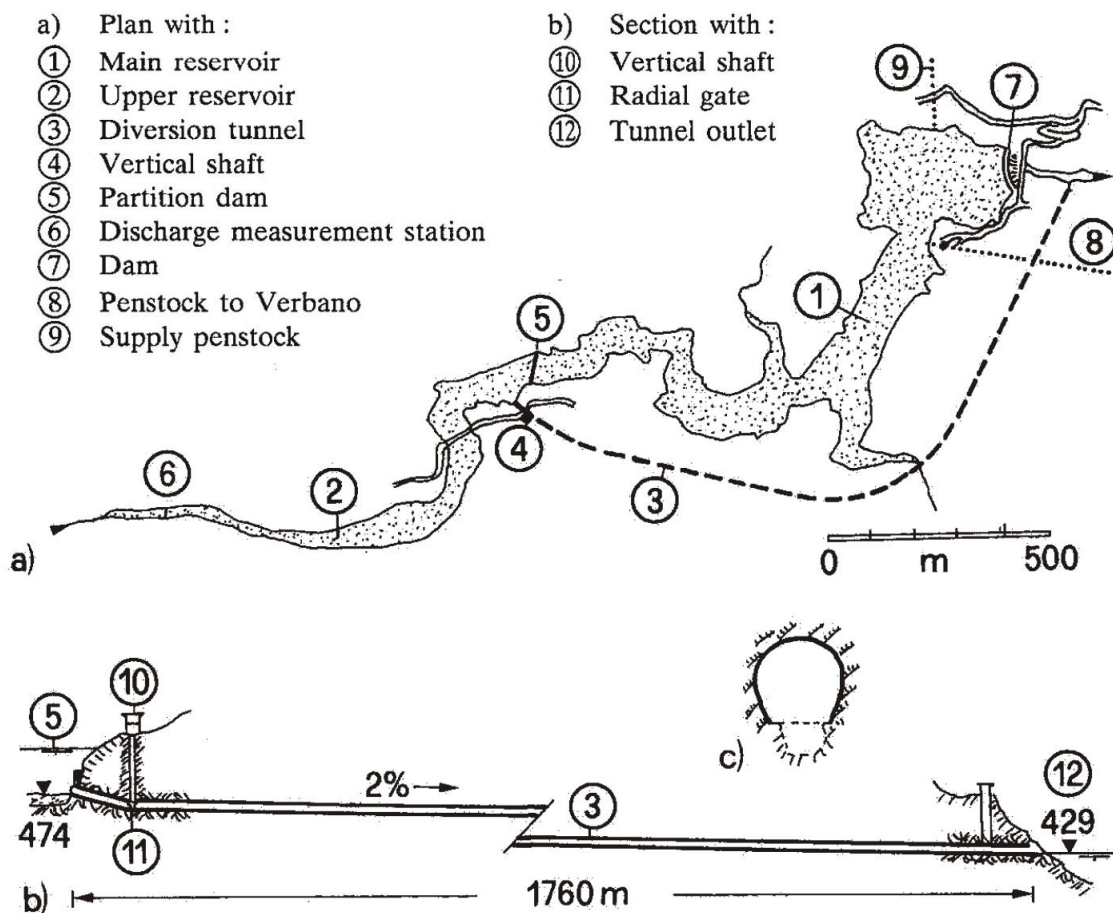

Figure 1: a) Plan view of the Palagnedra compensation basin with the SBT, b) longitudinal section along the SBT (Vischer *et al.* 1997)

236

The SBT was conceived with a length of 1.76 km, a slope of 2% and a horseshoe profile with 6.3 m diameter (cross section of 30 m^2). The discharge capacity of the SBT is 250 m^3/s with free surface flow downstream of the radial gate. The flow velocity at maximum discharge is about 10 m/s.

In the acceleration stretch, i.e. between the intake and the radial gate (no. 11 in Figure 1), basaltic aggregates and Lafarge cement were used to increase the abrasion resistance of the invert concrete of the SBT. In the rest of the tunnel length a "normal" concrete was placed at the invert.

The partition dam (no. 5 in Figure 1) forms an auxiliary reservoir of 140'000 m^3 in the Palagnedra compensation basin. This auxiliary reservoir can be emptied by opening the SBT's radial gate. This allows staying in operation with the main reservoir as it is fed with water from the upper HPPs. The operating rule of the SBT is to gradually open the radial gate when the Melezza discharge reaches 50 m^3/s and then to divert the river water completely through the SBT, avoiding solids entering the main reservoir. Only when the inflow exceeds 250 m^3/s, the upper reservoir fills up and water charged with fine sediments in suspension passes the partition dam. The coarser sediments are still transported through the SBT as bed load (sliding, rolling and saltating) or in suspension. With regular operation, 4 to 5 times a year, an estimated 90% of solid transport is diverted, leaving some 10'000-20'000 m^3 of fine sediments that settle every year in the main reservoir. These fine sediments are evacuated every 10 years through the bottom outlet with drawdown of the whole reservoir and sufficient dilution for environmental reasons.

2 Flood events, invert abrasion and maintenance until 2011

In some severe floods in the first years after completion, the SBT proved to be efficient. In the tragic 1978 flood the tunnel was closed. As a consequence of the extreme 1978 flood event, the HPP stage Verbano was put out of operation during 10 months. During this time, the Melezza's water was diverted through the SBT, causing deep erosion channels in the tunnel (Delley 1988). The sediment transport rate during this period was abnormally high, since up to 8 m high sediment deposits in the upstream part of the reservoir, which had been built up during the flood event, were successively eroded.

After these events, the invert concrete of the tunnel has been gradually eroded and the erosion continued in the underlying rock where it was exposed to the sediment-laden flow. Along the acceleration stretch, the originally placed special invert concrete has been replaced by a steel lining to increase the resistance against abrasion. The rest of the tunnel was let untouched in the sense of letting it develop towards an equilibrium state.

The two most catastrophic flood events since the commissioning of the SBT occurred in 1978 and the early 1980s. Inspections made in those years revealed that the invert had been eroded by up to 4 m deep.

In 1983 local repair works were carried out for safety reasons: Approximately 220 m^3 of normal concrete (BN 300, i.e. with 300 kg cement per m^3 concrete) were put in place and vibrated, also as a foundation for the steel ribs of the tunnel roof support.

Since 1985 until now there has been no further major erosion of the tunnel invert caused by severe floods, but continuous erosion at a low rate.

3 Situation in 2011 before the rehabilitation works

The state of the tunnel invert erosion in the year 2011, i.e. before the beginning of the rehabilitation works described in this paper, is illustrated by photographs in Figure 2 and by typical cross sections in Figure 3. The invert concrete slab has been almost completely eroded. In some cross sections, the flow area has almost doubled due to erosion of concrete and rock!

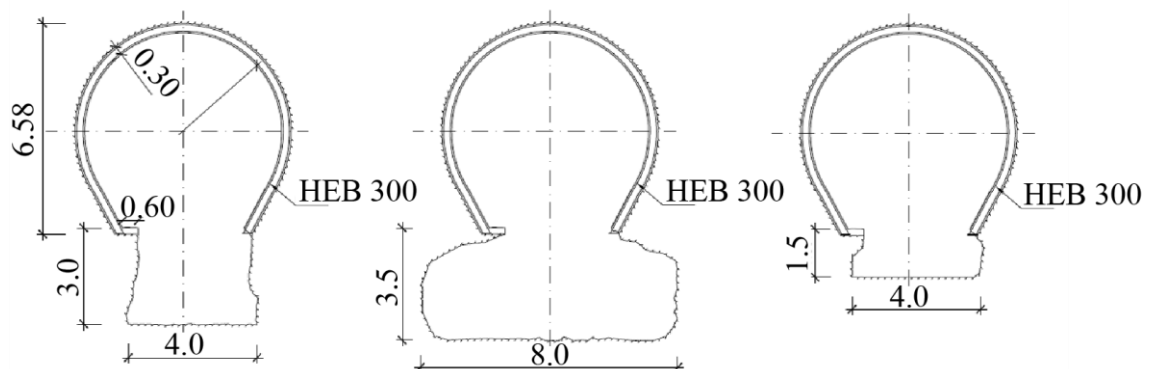Figure 2: Eroded invert concrete and underlying Gneiss rock (2011)

Figure 3: Typical tunnel cross sections before rehabilitation works (2011)

4 Rehabilitation works 2011-2013

4.1 Overview

For technical and economic reasons, it was decided to carry out restoration work on the SBT only on a selected part of its length. The most sensitive area with respect to consequential damages by a potential tunnel collapse is the crossing of the SBT beneath the headrace tunnel to the Verbano HPP with scarcely 8 m coverage (highlighted by the arrow in Figure 4). Restoration works were carried out on the most downstream 350 m of the SBT, corresponding to 20% of its total length. The project envisaged to restore the original tunnel invert elevation by filling the erosion trenches and cavities and to increase the abrasion resistance of the invert by using a special concrete.

The work had to be done in periods when the operation of the SBT was not requested, i.e. in winter. Although the work involved only relatively small quantities of material to put in place, the complex logistics and the short available periods to intervene meant that the work had to be carried out in three stages over three years.
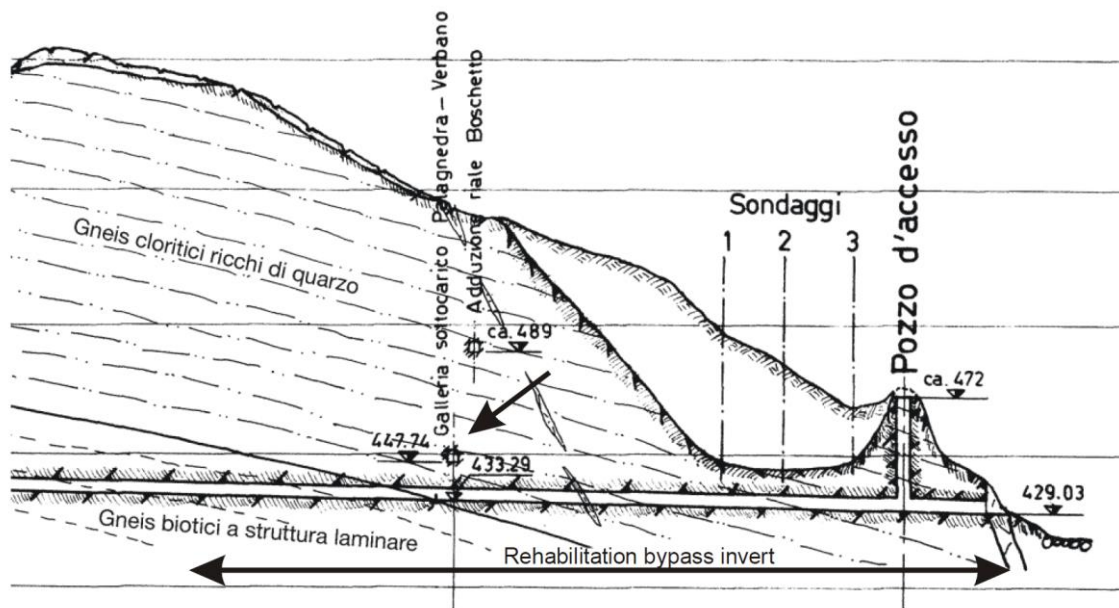

Figure 4: Longitudinal section of the SBT showing its most downstream part (drawing from 19xx, with planned invert level).

4.2 Work sequence

Each stage of the work comprised essentially the following sequence of activities:

- Closing the bypass tunnel with a sector sluice gate and stoplogs
- Setting up the building site with a winch for lowering personnel and materials through the access shaft ("Pozzo d'accesso" in Figure 4, height = 44m) into the tunnel

- Installing lighting and electric supply and implementing a safety programme
- Setting up a system for diverting seepage water with pumps and DN200 piping suspended along the left wall of the tunnel
- Draining water from erosion trenches and cavities
- Removing of sediments and drift wood etc. from the trenches and cavities
- Removing damaged invert concrete
- Cleaning the rock substrate with high pressure water jets
- Filling of the erosion trenches and cavities, as described hereafter
- Placing the top layer of special concrete with high abrasion resistance
- Dismantling the construction site

4.3   Project changes during construction

In the original project of the rehabilitation works and in the contract, it was foreseen to cast "normal" concrete into the erosion trenches and cavities directly on the rock and to cover this by an invert slab made of special concrete with high abrasion resistance with a thickness of at least 30 cm. In the following, the concrete beneath the slab is called substrate concrete.

During the first stage of the work we found out after the cleaning process that some of the erosion trenches were much deeper than expected. To fill these, three times as much substrate concrete would have been required compared to what was originally specified. To limit the costs it was decided to fill the lower parts of the trenches and cavities – until 1.5 m below the top of the invert slab – with gravel from our stocks (Figure 5). Reinforcing fibres were added to the substrate concrete where it was placed on the compacted gravel. Fibres take tensile stresses; this enhances the flexural resistance of the substrate concrete layer. With the gravel fill, higher tensile stresses occur at the bottom side of the substrate concrete since the gravel fill is less rigid than a fill with a binding agent would be. The fibres contribute also to a greater resistance against dynamic loading (fatigue), as caused by boulders rolling and saltating through the tunnel.

However, once the 30 cm top layer of special concrete becomes eroded, the fibres will be exposed and may accelerate the process of degradation of the substrate concrete by causing tear-off. Therefore, monitoring the progress of erosion is an integral part of this technical solution.

4.4   Materials

Since the invert slab is exposed to heavy wear, the type of concrete to be used was studied in detail. The performance objectives for this concrete were a combination of the following properties:

- High impact resistance, aiming for a typical cube compressive strength of 80 MPa

- High resistance to abrasion, using 100% (by mass) siliceous limestone aggregates with 40% coarse gravel 16/32 mm, mixed with quartz sand and silica fume powder

- Low capillary permeability, with a water/binder ratio <0.4 in order to limit saturation of the concrete and to slow down disintegration through freeze/thaw cycles

- Shrinkage compensated, that means a water/binder ratio <0.4; usage of 40% coarse gravel; limiting the amount of binder to 360 kg/m^3 and using a hyperplasticising additive and compensator withdrawal

- High initial resistance using 52.5 type cement, silica fume powder and a water/binder ratio <0.4

The Istituto di Meccanica dei Materiali (Institute of Engineering Materials, IMM) in Grancia (Lugano), involved as consultants on the choice of concrete, proposed the following special high-performance concrete, which was manufactured at a certified (so called 2+) production plant:

- Strength class (SN EN 206-1)   C50/60, $\varnothing$ 32 mm

- Exposure class   XC4, XD3, XF1

- Consistency class   F3

- Cement type   CEM II/AD 52.5 R (Fortico) Holcim

- Cement dosage: 360 kg / m^3

- Water/binder ratio: < 0.40

- Aggregate from 'Hüntwangen':   80%   (40% of 0/4 mm, 40% of 16/32 mm)

- Aggregate from 'Avegno':   20% (8/16 mm)

- Quartz sand 0/1 mm: 75 kg / m^3 (4%)

- Silica fume, type Sikafume HR-TU: 20 kg / m^3

- Fluidising additive (for processability): D-Zero (2.5%) (Concretum AG) or FRG (1%) (Sika AG)

The cube compression tests performed by IMM on specimens of a nominal size of 150 mm yielded the following results for compressive strength over time:

- 7 days   59.5 ± 3.8 N/mm2

- 28 days   80.0 ± 0.9 N/mm2

- 90 days   79.0 ± 2.3 N/mm2

Abrasion resistance was tested according to Böhme (SN EN 13892-3) by the Labor für Prüfung und Materialtechnologie, Wallisellen, on a 200x20x70 mm sample hardened for 28 days. An abrasion of 1.8 mm was obtained, confirming that the invert concrete has "a high resistance to abrasion".

For the substrate concrete we used an ordinary concrete (300 kg cement per m^3) and 1 kg/m^3 of steel fibres (Fibermesh MD Inforce).

4.5   Quantities

The main quantities of materials involved are summarised in the following table:

Table 1: Main material quantities

Item	Stage 1 [m^3]	Stage 2 [m^3]	Stage 3 [m^3]	Total [m^3]
Concrete to be demolished	10	2	3	15
Compacted gravel fill	94	104	489	687
Substrate concrete	303			303
Substrate concrete with fibers	24	478	282	784
Special concrete with high abrasion resistance	154	161	150	465

5   Situation in 2013 after rehabilitation

The result of the tunnel invert rehabilitation is shown in the cross sections in Figure 5 and the photographs in Figure 6.
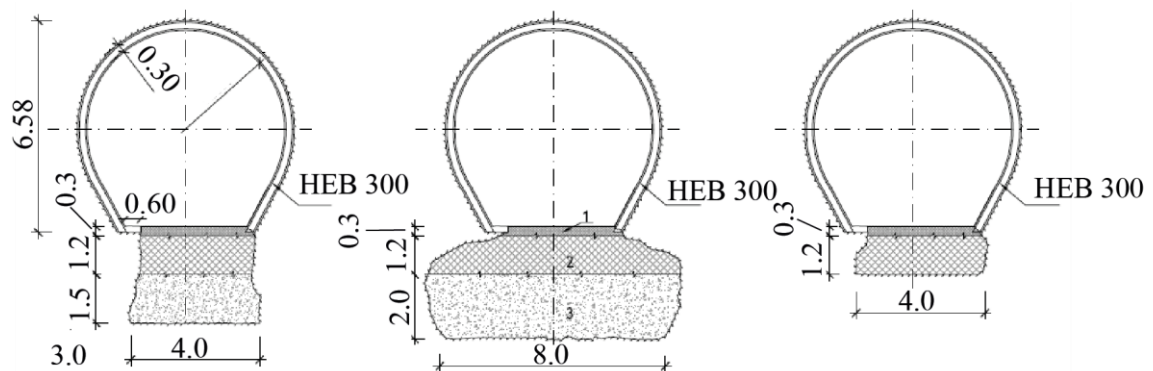

Figure 5: Typical tunnel cross sections after rehabilitation works (2011-2013)   1 Special concrete with high abrasion resistance, 2 Substrate concrete, 3 Compacted gravel

Figure 6: New concrete invert in the most downstream 350 m of the Palagnedra SBT (2013)

6 Monitoring

The erosion depth of the invert is monitored by repeated 3D laser scanning in the most downstream 100 m of the bypass tunnel. The first laser scan was done on the restored surface after the first stage of the work carried out in 2011. This specialized survey task had been contracted to an external company. The theoretical measuring uncertainty of the survey is ± 5 mm. Figures 7 and 8 show exemplary results of the first laser scan.
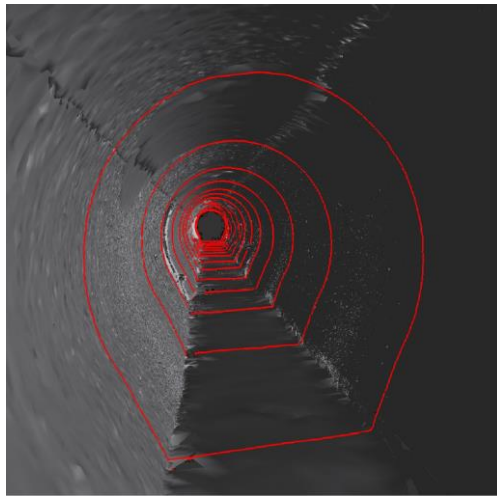

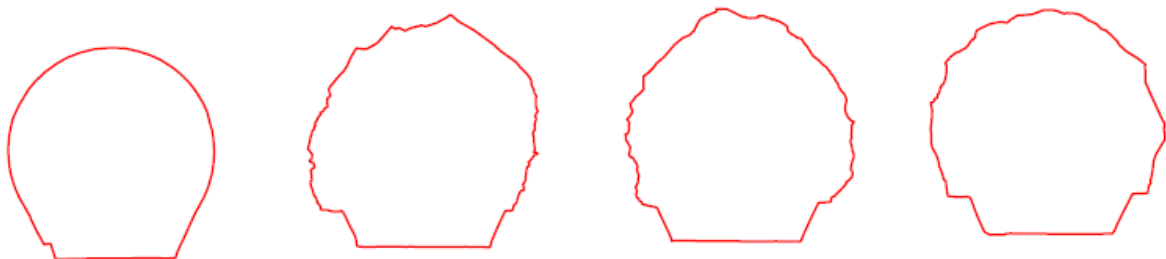Figure 7: 3D output of first laser scan survey (2011)

Figure 8: Examples of tunnel cross sections obtained from 3D laser scanning

The second scan of the tunnel in this stretch was done during the second stage of the work in 2012. The quantity of water that passed through the bypass tunnel over the year was $20 * 10^6$ m^3. The erosion depth was a few millimetres on average, which is barely perceptible with the measuring uncertainty of this method. We further noticed that seepage water flowing along the tunnel with a flow depth of a few centimetres compromised the accuracy of the laser scan measurements.

We decided to use a second monitoring method with a traditional theodolite, which is simpler and cheaper since it can be carried out by our personnel. Since the measurements are made in cross sections, less information is available. Nevertheless, this method allows us to monitor the progress of the erosion and to order the next laser scan at an adequate time.

Besides monitoring the abrasion depth, it is useful to have information on some variables describing the causes of the abrasion, i.e. the water flow and the transported sediment. Discharge data is available from the gauging station on the Melezza River in Camedo just upstream of the reservoir. Since no installations for bed load transport measurements are available at Palagnedra SBT, the water discharge is taken as an indicator for the "load" acting on the invert. This is a rough approximation since e.g. the bed load transport rate is not generally proportional to the discharge (higher sediment concentration during floods). From the discharge, the water volume flowing through the SBT in certain time intervals is calculated. It is intended to correlate the water volumes with the measured abrasion depths.

7 Conclusions

The Palagnedra SBT with a length of 1.76 km, a slope of 2% and a horseshoe-shaped cross section with 6.3 m diameter was commissioned in 1977. The two most catastrophic floods occurred in 1978 and the early 1980s. Inspections in those years revealed that the concrete and the rock at the tunnel invert had been eroded by up to 4 m deep and for safety reasons a local restoration was carried out. Since 1985 there have been no severe flood and no further major erosion of the invert, but rather continuous erosion at a low rate. On long term erosion could cause serious damage not so much to the bypass tunnel itself but to the headrace tunnel of Verbano HPP, which passes less than 8 m above the SBT. Therefore the Maggia Power Plants decided to realize rehabilitation works on the most downstream 350 m of the SBT where the headrace tunnel crosses and rock coverage of the SBT is relatively small.

During the first stage of the work we discovered that some of the trenches and cavities formed by erosion were much deeper than expected. In order to limit the construction cost, a new solution was applied. It consisted of filling the deeper trenches and cavities with compacted gravel up to 1.5 m below the planned invert level. Above this fill a 1.2 m thick layer of concrete was cast. Reinforcing fibres were added to this concrete for

greater resistance to dynamic loading, as caused by boulders rolling along the tunnel. Finally, a 30 cm thick invert slab made of special concrete with high abrasion resistance was cast in place.

The erosion is monitored on the most downstream 100 m of the tunnel. Two laser scans, in 2011 and 2012 respectively, yielded similar geometries. Traditional theodolite surveying in cross sections is also used to monitor the progress of erosion and to decide when the next laser scan will be ordered.

References

Delley, P. (1988). Erosionsschäden im Spülstollen Palagnedra und deren Sanierung. Internationales Symposium über Erosion, Abrasion und Kavitation im Wasserbau. VAW-Mitteilung Nr. 99, D. Vischer (ed.), ETH Zürich, Switzerland: 329-352.

Martini, O. (2000). La galerie de derivation de Palagnedra. Symposium 26-27 October 2000, Tokio, Japan

Vischer, D.L. et al. (1997). Bypass tunnels to prevent sedimentation, ICOLD 1997 Florence, Q.74, R.37, 605-624

Authors

Andrea Baumer
Department of civil engineering Maggia Power Plants (Ofima), Locarno
Email: maggia@ofima.ch

Riccardo Radogna
Department of civil engineering Maggia Power Plants (Ofima), Locarno

The Pfaffensprung sediment bypass tunnel: 95 years of experience

Bärbel Müller, Martin Walker

Abstract

The Pfaffensprung sediment bypass tunnel was commissioned in 1922 and is continuously operative since that time. The sediment bypass tunnel has to be rehabilitated regularly due to high abrasion caused by transported bed load, ranging from grain sizes of some millimeters up to boulders. Since 1961, several repairs with different materials have been carried out nearly every year.

1   History of the Amsteg power plant

After ten years of construction, the Gotthard railway line was put into operation in 1882. The electrification of the railway line was planned already few years later. On the one hand the capacity of the railway, which could hardly manage the constantly increasing passenger and freight transportation rates, had to be enhanced. On the other hand, the air pollution in the 15 kilometer long Gotthard tunnel caused by smut emitted by the steel locomotives, was very high.

The concession to use the hydraulic power of the Reuss between Andermatt and Amsteg, as well as the tributaries of Meienreuss, Fellibach and Chärstelenbach, had been granted by the canton Uri at the 23rd December 1907. The concession contract notably allowed the construction of artificial lakes at suitable locations in the Reuss region and the derivation of water to the canton Ticino.

In 1912 the administrative board of the Swiss Federal Railways SBB decided to electrify the Gotthard railway line between Erstfeld and Bellinzona. However, the start of construction was delayed by the outbreak of World War I.

The Amsteg power plant was constructed between 1918 and 1922 and put into operation in 1922. With the original production of 270 GWh per year the Amsteg power plant was the biggest hydropower station in Switzerland at the time. Since the power plant had been designed as a run-off-river power plant without a large basin, two third of the electric production was generated in the summer months of June to September.

The extensive modernization of the Amsteg power plant from 1993 to 1998 allowed to increase the installed capacity from 56 to 120 MW and to raise the production to 460 GWh per year.

2 Water utilization and characteristics of the catchment area

Between Göschenen and Amsteg, the hydropower of the Reuss and her tributaries is used several times. The power plants and the water inlets are presented in Figure 1 and Table 1.
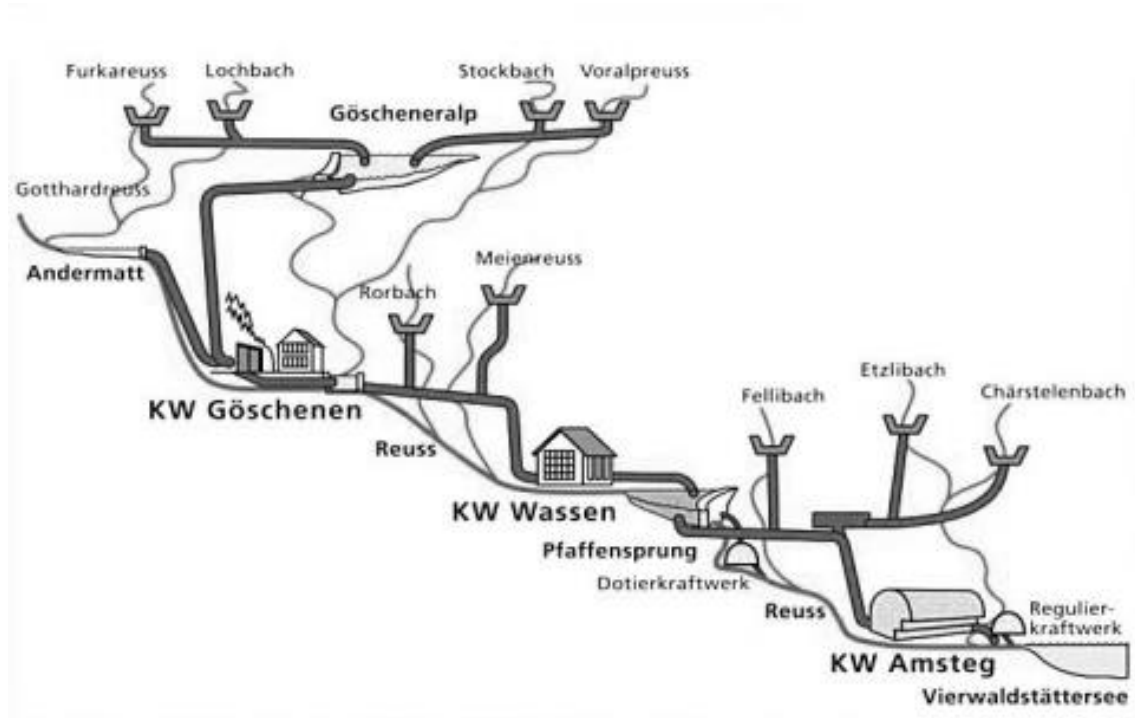

Figure 1: Water utilization of river Reuss: schema of the Reuss cascade

Table 1: Catchment areas and production of the Reuss cascade (internal documents and calculations)

Power plant	Catchment area / tributary	Area [km^2]	Production [Mio kWh/year]
	Göscheneralptal	42.8	
	Voralpreuss	19.3	
	Furkareuss	23.4	
	Lochbach	5.0	
Göscheneralp – Göschenen		90.5	400
	Meienreuss	69.3	
	Rohrbach	7.9	
	Gotthardreuss	28.3	
Göschenen – Wassen		105.5	280
	Reussfassung Pfaffensprung	30.6	
	Fellibach	24.3	
	Chärstelenbach	81.7	
	Etzlibach	28.9	
Wassen – Amsteg		165.5	460

The catchment area of the Reuss cascade covers an area of about 380 km^2. A part of the water is transferred from canton Uri to canton Ticino and feeds the retaining structure of Ritom. The total inflow of the Reuss and the water inlets is used in the Amsteg power plant to produce energy. This corresponds to a mean annual inflow of 600 to 650×10^6 m^3. The one year flood discharge HQ1 is about 220 m^3/s. The ten year flood discharge HQ10 has been calculated by Gilg (1982) to 320 m^3/s, the 100 year flood discharge HQ100 was estimated at 460 m^3/s.

3   Compensation reservoir Pfaffensprung

The natural widening of the Reuss upstream of the so-called „Pfaffensprung" allowed the implantation of a basin for the compensation of short-term peak loads, which should at the same time allow the sediments to be settled to purify the water. The original concept of the retaining structure, which has not substantially been modified since 1922, is presented in Figure 2. The principal parts of the site are the compensation reservoir ① with guiding weir ② and dam③, the water inlet ("Reussfassung") ④, the sediment bypass tunnel at the left bank ⑤, the discharge elements ⑥ and the intake gallery of the Wassen power plant.
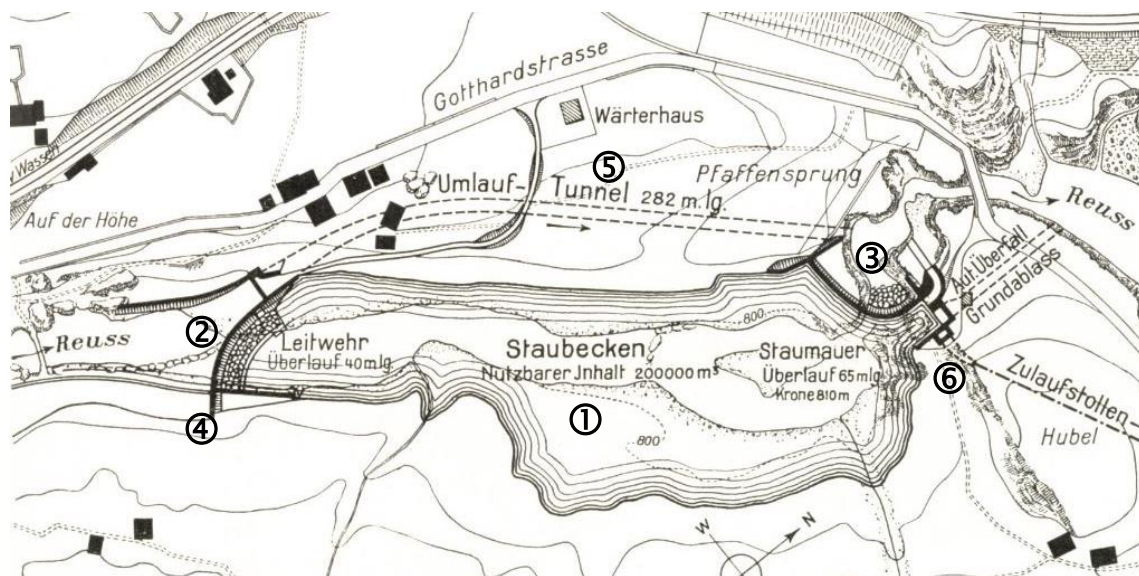

Figure 2: Concept of the retaining structure Pfaffensprung

The narrow canyon of „Pfaffensprung" favored the construction of a 32 m high and 38.5 m wide arch dam built with layered masonry. The layers are 3 to 6 m high and consist of vertically positioned, rectangular granite blocks (Figure 3).
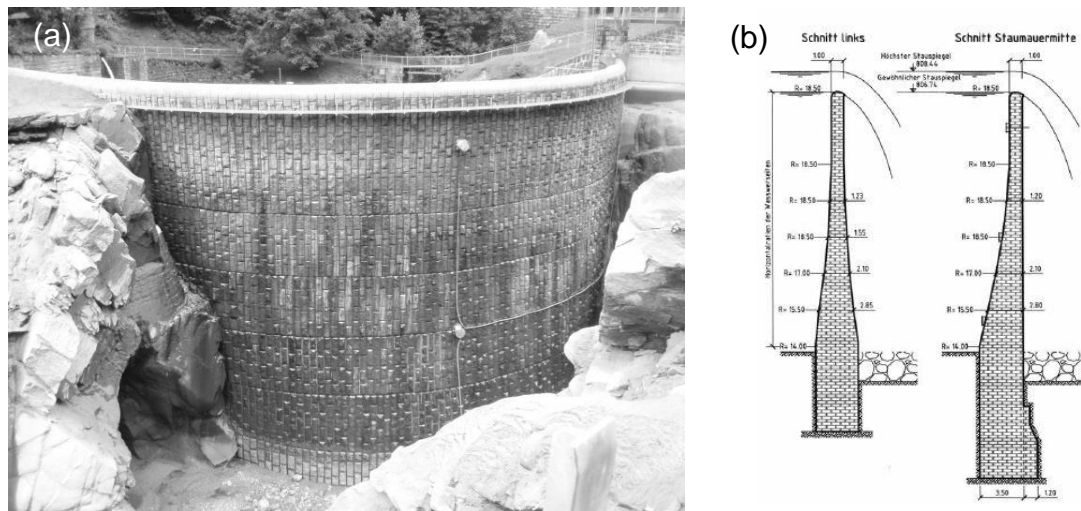
Figure 3: (a) View of the arch dam from upstream and (b) profiles close to the left abutment (left profile) and in the middle of the dam (right profile)

The Pfaffensprung dam is the only arch dam in Switzerland which has completely been built of masonry.

4 Geology

The Pfaffensprung reservoir is located in the Aare granite, which reaches from the Aletsch area in the west to the Oberalpstock area in the east. In the axis of the Reuss valley the Aare granite begins in the canyon of Schöllenen in the south and ends at the altitude of Gurtnellen in the north.

Quartz, plagioclase and orthoclase form one third each as major constituents of the Aare granite, biotite is the dominating accessory constituent with a portion of a few percent. The solid rock in the area of Pfaffensprung can be characterized according to Schneider (1989) as a fibrous to massive, medium to coarse grained biotite-granite, or as a biotite-granite gneiss, respectively.

The geomorphology of the Reuss valley has primarily been shaped by glacial erosion. The newly formed valley was slightly hollowed out after the glacial recession, but it has partially been refilled by both the lateral inflows and rock fall landslide material.

In the geological reports of Schneider (1989, 1990) the actual situation in the area of the Pfaffensprung reservoir is summarized as follows: The slope on the right bank is built from fine- to coarse-grained, partially coarse-blocky gully rock-waste. On the left bank the rock fall landslide material, which can be found above the concrete sidewall, is layered with blocks up to several meters, originating from artificial fill (excavation material). The sediments lying beneath the rock fall land slide material consist exclusively of river rock waste. Clean to silty fine sands can be found apart from coarse-grained, clean to slightly silty sands and gravels. Moraine material is present only in little quantities, the biggest part has been eroded by the Reuss and her tributaries. In the

region of the sediment bypass tunnel the river rock waste is crossed by gully rock-waste with a higher content of silt. At the bottom of the basin coarse-grained river rock waste and mainly fine-grained fluvial sediments have been deposited.

As illustrated in Figure 4, the sediment bypass tunnel traverses solid rock only on the last 50 to 100 m before its outlet. As shown in profile 2, the form of the rock contour line cannot precisely be determined and the bypass tunnel could either cross solid rock or river rock waste. The solid rock is covered with fluvial deposits of variable thickness and with rock fall landslide material.

5   Sediment bypass tunnel

The inflow of the Reuss is directed into the compensation reservoir by means of a water intake, the "Reussfassung" (no. 4 in Figure 2). The water intake has been designed for a discharge of 16 m^3/s. With regard to a water extraction preferably free from bed load, it has been designed as a bypassing intake. Larger inflows and floods are directed into the sediment bypass tunnel by means of an overflow weir. The sediment bypass tunnel with a length of 283 m has been designed hydraulically in such a way, that one year floods of 220 m^3/s can be discharged. On long-term average, the tunnel is operated about 135 days from april to november. Apart from the discharge of floods, the sediment bypass tunnel conveys the bed load transported by the Reuss and therefore prevents a fast aggradation of the compensation reservoir. The hydraulic and economic requirements as well as the previously described geological conditions have defined the design and the construction of the sediment bypass tunnel as described below.

5.1   Geometry and alignment

Alignment and geometry of the sediment bypass tunnel resulted from the demand for both the shortest possible length and an economic masonry thickness considering the topographic, geologic and hydraulic requirements.

On the first 25 meters the tunnel inclines by 6 m resulting in an average slope of S = 0.24, additionally the tunnel cross-section tapers from 66 m^2 at the inlet to 21 m^2. (Figure 5). In the following tunnel sector the bottom slope is S = 0.03. The cross-section of the inlet resulted from the installation of two hydraulic gates with a width of 5 m each. The s-shaped inclination of the bottom acts as an acceleration section and guarantees the hydraulic performance of the sediment bypass tunnel.
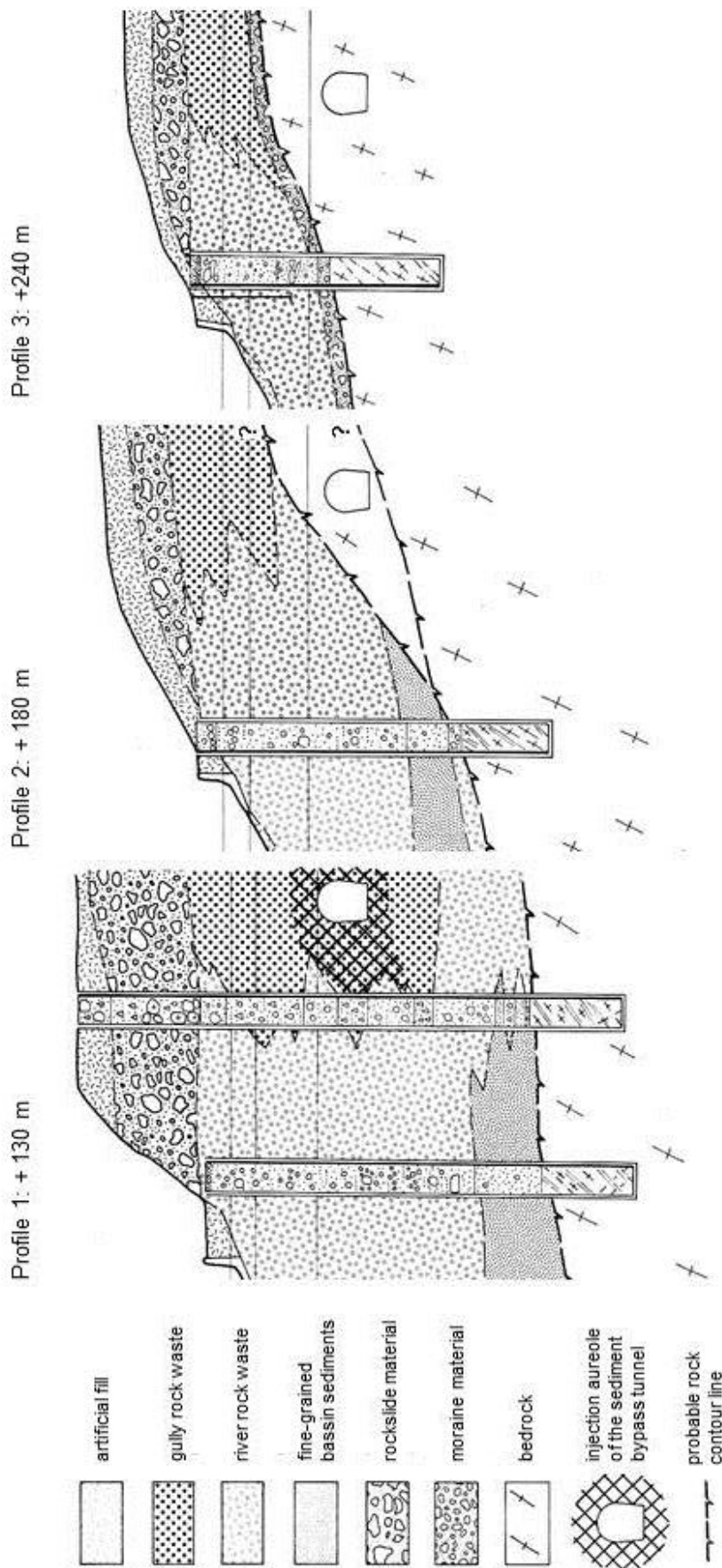
Figure 4: Geological cross-sections (modified after Schneider (1990))As shown in Figure 5, the cross section between the inlet and the passage to the normal profile after 65 m are highly asymmetric. An economic material usage is possible, if the arch follows as far as possible the pressure line and if it is loaded only by compressive stresses. Due to the alignment of the tunnel and the geology, passive earth pressure could not be taken into account for the right abutment. The unilateral earth pressure causes a highly asymmetric pressure line, which would have resulted in disproportionate wall thicknesses, if a symmetric cross section had been chosen. The tunnel sections layout with a highly asymmetric cross section was additionally complicated by the trumpet-like expanding cross-section of the inlet area.
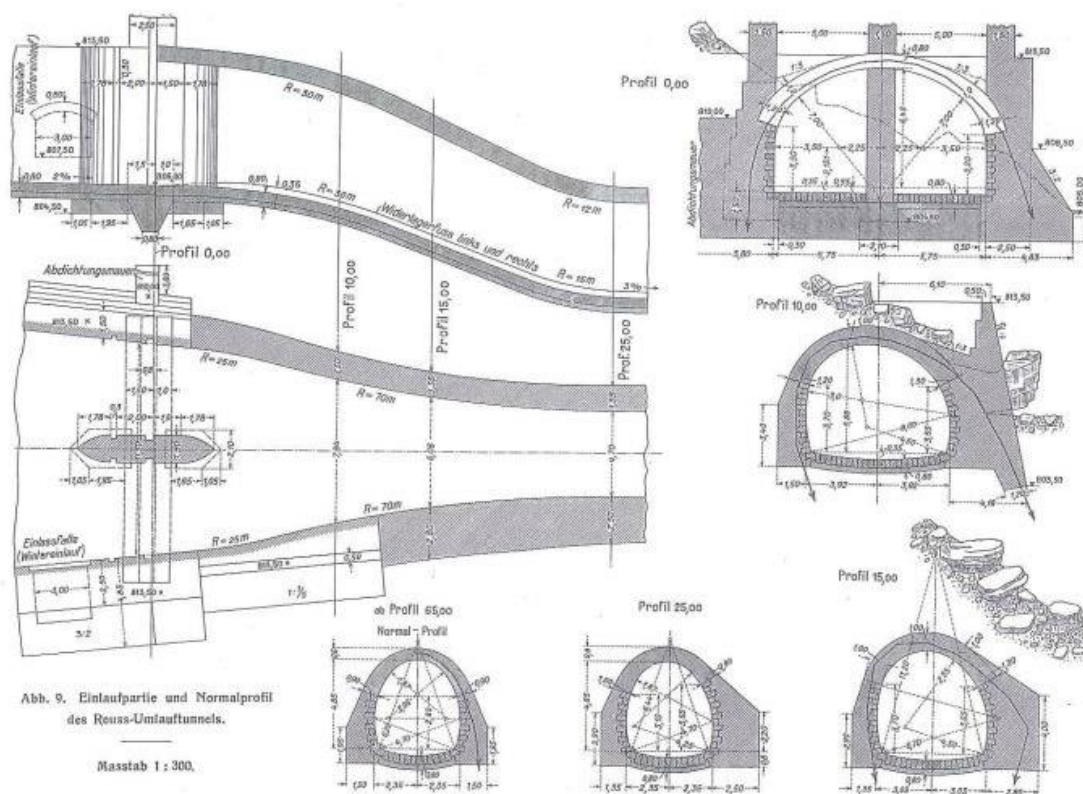
Figure 5: Inlet area and cross sections of the Pfaffensprung sediment bypass tunnel. Bottom left: normal profile

5.2 Construction

The geological conditions described in chapter 4 made the construction of the sediment bypass tunnel complicated. The applied construction method using underpinning (belgian method), which had already been started with the excavation of the pilot tunnel, was continued with extensive preventive measures to underpin the abutments. Sustainable, continuous supports had to be designed in order to underpin the arch in form of 54 cm high concrete girders reinforced with five I-beams, as described by Studer (1925).

6 Maintenance of the Pfaffensprung sediment bypass tunnel

The design of the sediment bypass tunnel generated abrasion problems at the tunnel invert. The hydraulic performance requires a high flow velocity of approximately 15 m/s in order to carry the bed load containing grain sizes in the range of millimeters (like quartz sand) up to large boulders through the tunnel. When planning the sediment bypass tunnel, the engineers were already aware of the associated problems and decided to pave the bottom with jointed, 50 cm thick granite blocks. The first six years of operation revealed, that the mean abrasion of the bottom reached 4 millimeter in the linear sections, whereby in particular the longitudinal joints had been eroded. The

abrasion rate was higher in more intensely charged sectors (mainly at the inner curve) and reached several centimeters (Studer 1925).

6.1 First rehabilitation works in the 1960ies and 70ies

Between 1961 and 1978, extensive rehabilitation works were carried out for the first time. The replacement of the abraded granite blocks could not be realized due to both strong leakage and economic reasons. In 1962 the scoured bottom was provisionally revetted using concrete of normal strength. From 1963 to 1965 construction chemistry products had been tested, which did not show any positive results. In 1966, cast basalt tiles produced by Kalenborn, Germany, were applied for the first time. In fact the cast basalt tiles were able to withstand the abrasion, but unfortunately they were scoured and carried away during flood events in 1966. A larger test field was realized in 1967 using basalt concrete, which showed a good performance during the several operation periods. Lafarge cement was applied as binding agent. The cube compressive strength of the basalt concrete was $f_c = 1'200 \text{ kg/cm}^2$ (118 N/mm^2) after 28 days – a value that satisfied even the requirements of a high-performance concrete. Regular measurements and monitoring carried out by the power plant operator suggested a mean abrasion rate of one millimeter in one year. Unfortunately the test field was partially destroyed and scoured by the bed load composed of quartz sand, stones and boulders carried during a flood event in July 1977. After the event, the bottom was grouted and drained systematically, and the scoured zones were filled with basalt concrete again.

6.2 Rehabilitation works in the 1990ies

Rehabilitation and repair works were carried out periodically in the following years. After the well-proven basalt concrete, fused cast basalt linings (Abresist®) were applied in 1995; until 2000 the sediment bypass tunnel had been revetted completely with this material.

6.3 Rehabilitation works in 2000

Within the scope of the annual repairs of local damages, cast basalt tiles in combination with basalt concrete were implemented on the bottom from 2001 to 2011. In several small test fields the arrangement and the patterns of the tiles were varied as well as the width of the joints. Regular, checkerboard and staggered patterns were applied. The arrangement of the cast basalt tiles could be horizontal or upright in order to increase the material thickness.

6.4 Recent rehabilitation works

The annual repairs, which are usually carried out during the winter months, result in high costs of more than 100 000 CHF per year. A feasibility study was then commissioned in 2010 with the objective to develop solutions for a long-lasting rehabilitation of the bottom (Leu 2010). In this study the installation of a test field with

compact granite blocks without joints (accurately fitting arrangement) was recommended. At the same time, additional test fields for high-performance concretes were designed with the collaboration of TFB AG and VAW, ETH Zurich (Hagmann *et al.* 2015). The test fields were realized during the winter months in 2011/2012 and in 2012/2013.

6.4.1 Test fields with granite blocks

The arrangement of the granite blocks is shown in Figure 6. The 30 cm high and 1 m^2 large granite blocks with cut edges were placed on a concrete underlay without joints and a transversal slope of 1.7% towards the outer curve. The granite originating from the canton Uri („Urner Granit") is characterized by a particular high hardness. In 2011/2012 the first test field with a length of 10 m was realized in the straight zone between 258 and 268 m; a second test field of 20 m length followed in 2012/2013 in the curved section between 70 and 90 m.
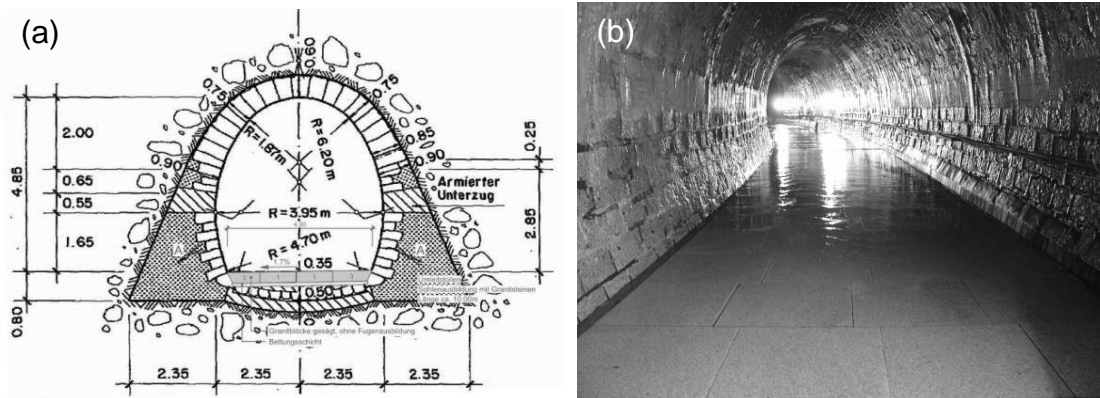

Figure 6: (a) Cross-section of the tunnel profile with granite bottom, and (b) installed test field (2012/2013)

6.4.2 Test fields with high-performance concrete

In march 2012 a test field of 10 m length was installed adjoining the test field with granite blocks. The test field was realized with steel fibre reinforced high-performance concrete and with a thickness of 30 cm. The composition of the concrete had been defined by TFB AG in preliminary tests. The requirements for the high-performance concrete were accomplished by the aggregates of Gasparini AG, Altdorf. The utilized concrete attained a mean compressive strength of $f_c = 115 \pm 8$ N/mm^2 and a bending tensile strength of $f_{tb} = 15.2$ N/mm^2.

A second test field of 20 m length was realized in 2013 adjoining the granite field in the curved section (between 50 and 70 m). Since the steel fibres had not shown any positive effect with respect to the abrasion, TFB and SBB decided to produce the concrete used for the new test field without adding steel fibres. Apart from that, the composition had not been modified. The concrete was easier to handle without the steel fibres. However, the expected compressive strength could not be reached. The considerably lower

compressive strength of only $f_c = 78 \pm 21$ N/mm^2 can probably be attributed to the utilization of recycling water instead of potable water.

The concrete compositions and the results of the material tests are summarized in Jacobs (2013).

6.4.3 Performance of the test fields

After the completion of the test fields with granite and high-performance concrete, two floods with maximal discharges of 178 und 247 m^3/s occurred in 2012. Large damages resulted in the sediment bypass tunnel in consequence of these floods, whereby the two test fields presented few damages and comparably little abrasion. In the granite test field, abrasion was observed mainly in the edges and in the wall connections (Figure 7). Several small spallings were identified, caused by the impact of the transported boulders. The mean abrasion rate of the granite blocks averaged out at approximately 3 mm and up to 10 mm at the edges. The abrasion rate of the concrete test field was clearly higher with 15 mm on average and 30 mm maximum. Local damages could on the contrary not be observed, the abrasive wear took place over the full surface area (Figure 8). The test fields are annually surveyed with laser scanning and evaluated by the Laboratory of Hydraulics, Hydrology and Glaciology (VAW) of ETH Zurich (Hagmann *et al.* 2015).
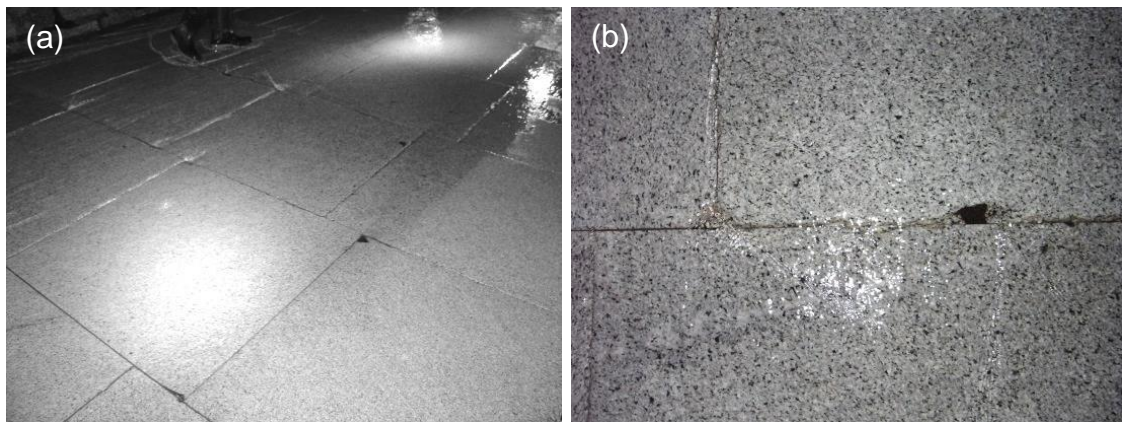

Figure 7: Abrasion of the granite test field after one operating period. (a) Longitudinal abrasion patterns in flow direction, (b) detail of abraded joint
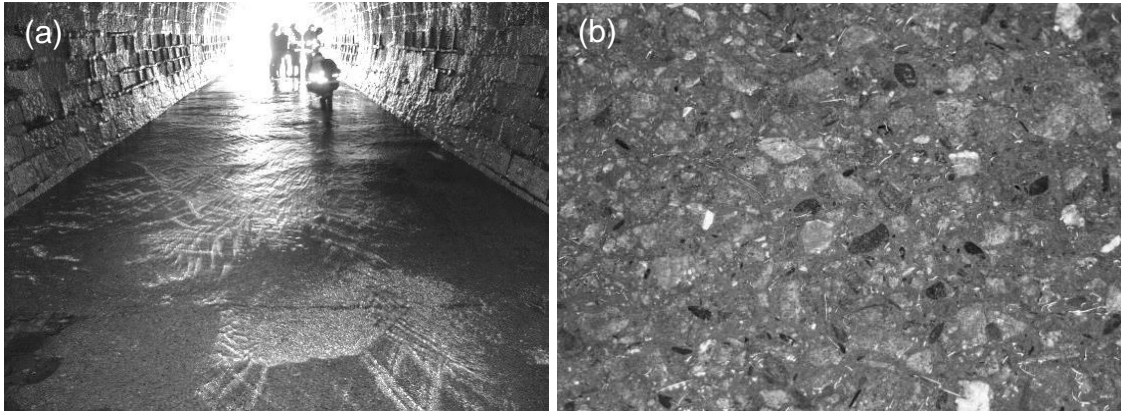
Figure 8: Abrasion of the high-performance concrete test field after one operating period. (a) Straight tunnel section, (b) detail (about 20 to 30 cm)

6.4.4 Performance of the building materials in the remaining sections

The cast basalt tiles used in the remaining tunnel sections can well withstand the abrasive stress probably caused by the transported quartz sand, whereby abrasion mainly occurs in the joints. This is observable particularly well in the case of checkered laying patterns; the abrasive wear in flow direction is clearly visible (Figure 9a). The impact caused by saltating stones and boulders, carried during flood events, provoke damage of the cast basalt tiles. Damaged tiles will subsequently be scoured and washed-out, so that the damaged spots increase rapidly (Figure 9b).

Figure 9: Abrasive wear in flow direction and local damage. (a) Diagonally checkered cast basalt tiles with mortar panels in between, (b) field of subsequently scoured and washed out cast basalt tiles

7 Conclusions

The experience of the last decades and the first practical knowledge with granite and high-performance concrete have persuaded the power plant operator, the Kraftwerk Amsteg AG, to rehabilitate the remaining sections, which are actually revetted with cast basalt tiles, using accurately fitting granite blocks. The test fields with high-performance concrete will temporarily be maintained. This will allow to study and

compare the long-time behavior of the test fields during the next years. The granite blocks are less delicate to saltating particle impact than cast basalt tiles, mainly because of the element thickness of 30 cm and because of the jointless arrangement.

References

Gilg, B. (1989). Bericht über die Stauanlage Pfaffensprung und ihre Nebenanlagen, insbesondere über das Verhalten in den Jahren 1982 – 1987. *Stauanlage Pfaffensprung, 5-Jahreskontrollen,* Bericht vom 1. Juli 1989.

Hagmann, M., Albayrak, I., Boes, R.M. (2015). Field research: Invert material resistance and sediment transport measurements. Proc. First Int. Workshop on Sediment Bypass Tunnels, *VAW-Mitteilungen* 232 (R. M. Boes, ed.), ETH Zurich, Switzerland.

Jacobs, F. (2013). Umleitstollen Pfaffensprung, Feld mit Hochleistungsbeton, Bericht U 123340 TFB AG

Leu, E. (2010). Umleitstollen Pfaffensprung, Schadstellen Sohlenbereich: Studie Massnahmen. Bericht vom 5.10.2010, Bigler AG

Schneider, T.R. (1989). Geologische Grundlagen. *Stauanlage Pfaffensprung, 5-Jahreskontrollen,* Bericht Nr. 407b.

Schneider, T.R. (1990). Ausgleichsbecken Pfaffensprung, Auswertung der Sondierungen 1989/90. *Neubau Kraftwerk Amsteg, geologisch-geotechnische Grundlagen,* Bericht Nr. 317e.

Studer, H. *et al.* (1925/26). Das Kraftwerk Amsteg der Schweizerischen Bundesbahnen. *Sonderdruck der Schweizerischen Bauzeitung* Band 86/87.

Authors

Bärbel Müller (corresponding Author)
Energy operations, Swiss Federal Railways SBB
Email: baerbel.mueller@sbb.ch

Martin Walker
Kraftwerk Amsteg AG, Amsteg